Distinct and common functions of mTORC1 and mTORC2 in Purkinje cells

Inauguraldissertation

zur
Erlangung der Würde eines Doktors der Philosophie
vorgelegt der
Philosophisch-Naturwissenschaftlichen Fakultät
der Universität Basel
von

Nico Angliker

aus Birr (AG)

Basel, 2015

Genehmigt von der Philosophisch-Naturwissenschaftlichen Fakultät

auf Antrag von

Prof. Dr. Markus A. Rüegg

Prof. Dr. Bernhard Bettler

Basel, den 17.02.2015

Prof. Dr. Jörg Schibler

Dekan

Table of Contents

1. Summary

In mammalian cells, the serine/threonine protein kinase mTOR (mammalian target of rapamycin) is present in two complexes, called mTORC1 and mTORC2. While several of the components are common to both complexes, raptor and rictor are only associated with mTORC1 or mTORC2, respectively. Due to differences in their molecular composition mTORC1 and mTORC2 possess distinct functions and properties (Laplante & Sabatini, 2012). For example, mTORC1 but not mTORC2 is sensitive to the immunosuppressive drug rapamycin. mTORC1 integrates various extracellular signals (e.g. growth factors, energy status or amino acid availability) to promote protein synthesis, to regulate lipogenesis and to inhibit autophagy (Shimobayashi & Hall, 2014). In line with these features, mTORC1 was found to be essential for cell growth and proliferation. In contrast, activation and function of mTORC2 is less well understood. It phosphorylates and activates members of the AGC kinase family, including Akt, SGK1 and PKC, suggesting a role in cell survival/metabolism and actin cytoskeleton organization.

In the brain, mTOR signalling has been implicated in several neurodevelopmental and neurodegenerative disorders like autism spectrum disorders (ASD) or Huntington's disease. The availability of approved drugs, such as rapamycin and its analogs (called rapalogs), has made the mTOR signalling pathway an attractive target for the treatment of those diseases. Although rapamycin has been shown to preferentially target mTORC1, prolonged exposure also inhibits mTORC2 (Sarbassov *et al.*, 2006). Thus, it is important to unravel the specific and the common functions of mTORC1 and mTORC2 in the central nervous system.

In this study, the roles of mTORC1 and mTORC2 were analysed in Purkinje cells by conditionally deleting floxed *Rptor* or *Rictor* genes, respectively, using an *L7/Pcp-2*-driven expression of the Cre recombinase. The resulting mouse lines are called RAPuKO or RIPuKO, which stands for raptor or rictor Purkinje knockout, respectively, and allowed to study the functions of mTORC1 and mTORC2 in developing and adult Purkinje cells and to investigate the effect on mouse behaviour.

We found that the phenotypes of RAPuKO and RIPuKO mice only sparsely overlapped but mostly differed, which assigns mTORC1 and mTORC2 distinct functions in these neurons. (I) mTORC1, but not mTORC2 abrogation in Purkinje cells reduced the social interest of mice. (II) Ablation of either mTORC1 or mTORC2 in Purkinje cells was sufficient to cause motor coordination deficits, yet, for RAPuKO mice the onset of these deficits was age-dependent while motor deficits of RIPuKO mice could be detected at any tested age. (III) The motor phenotype of RIPuKO mice was accompanied by developmental aberrations, such as impaired climbing fibre synapse elimination and hampered dendritic self-avoidance, while the age-dependent motor phenotype of RAPuKO mice seemed to be driven by Purkinje cell degeneration that finally led to apoptosis and a loss of these neurons. Vice versa, no signs for deficient climbing fibre elimination or Purkinje cell loss could be

detected for RAPuKO or RIPuKO mice, respectively. (IV) mTORC1 and mTORC2 ablation in Purkinje cells both affected neuron morphology in a similar manner, which included multiple primary dendrites and a reduction of the neuron size, yet, last was more pronounced for raptor-deficient cells.

Altogether, both mTORC1 and mTORC2 ablation in Purkinje cells had a pronounced, yet distinct, effect on these neurons and the mouse behaviour, unlike in other tissues where inactivation of mTORC2 has been reported to result in a minor phenotype in comparison to mTORC1 ablation (Bentzinger *et al.*, 2008; Godel *et al.*, 2011).

While ablation of mTORC1 and mTORC2 in Purkinje cells resulted in mostly distinct phenotypes, we found that sustained mTORC1 activation in these neurons by a TSC1 knockout (TSCPuKO) caused a phenotype that was similar to the one of RAPuKO mice. In both RAPuKO and TSCPuKO mice an age-dependent loss of Purkinje cells due to apoptosis was observed, which was paralleled by reactive gliosis. Moreover, in both cases Purkinje cell apoptosis was preceded by signs of neurodegeneration in form of axonal swellings that accumulated neurofilaments. Also in terms of behaviour similar phenotypes were observed since both knockout mice showed reduced social interest (Tsai *et al.*, 2012). These behavioural phenotypes support the growing notion that the cerebellum is important for non-motor related functions (Schmahmann *et al.*, 2007; Wang *et al.*, 2014) and that mTORC1 plays a role therein. TSC1 knockout in Purkinje cells has been reported to cause also repetitive behaviour in mice in addition to abnormal social behaviour and therefore it has been suggested that these mice show an autism-like phenotype (Tsai *et al.*, 2012).

In summary, this study provides *in vivo* data for the importance of mTORC1 and mTORC2 in developing and adult Purkinje neurons. We find that both complexes are crucial for Purkinje cells, yet, in mostly distinct manners. This finding is in line with the model that mTORC1 and mTORC2 largely feed separate downstream effectors, although they share many molecular components. The knowledge of the function of mTORC1 and mTORC2 in adult neurons is important for the development of treatment options that target the mTOR pathway. This work clearly suggests that such drugs need to be highly selective for the different complexes. Moreover, this work highlights that a complete inhibition of mTORC1 may have detrimental effects on the survival of neurons and that this may also precipitate autism-like pathologies.

2. Abbreviations

Aβ	amyloid β
ADP	adenosine diphosphate
Akt/PKB	protein kinase B
ALS	amyotrophic lateral sclerosis
AMP	adenosine monophosphate
AMPA	α-amino-3-hydroxy-5-methyl-4-isoxazolepropionic acid
AMPK	5'AMP-activated protein kinase
Arc	activity-regulated cytoskeleton-associated protein
ASD	autism spectrum disorders
ATF4	activating transcription factor 4
ATG7/13/14	autophagy-related protein 7/13/14
ATP	adenosine triphosphate
BDNF	brain-derived neurotrophic factor
CamKII	calcium/calmodulin-dependent protein kinase type II
CAD	carbamoyl-phosphate synthetase 2, aspartate transcarbamylase, dihydroorotase
Car8	carbonic anhydrase 8
$Ca_v2.1$	P/Q voltage-dependent calcium channel
CA1/3	cornu ammonis area 1/3
CC3	cleaved caspase-3
CF	climbing fibre
C57/BL6	C57 black 6
DAP1	death-associated protein 1
DCN	deep cerebellar nucleus/nuclei
DEPTOR	DEP domain-containing mTOR-interacting protein
DG	diacylglycerol
DNA	deoxyribonucleic acid
eEF2k	elongation factor 2 kinase
EGF	epidermal growth factor
EGL	external granule layer
eIF4A/B/C/D/E	eukaryotic translation initiation factor 4A/B/C/D/E
E-LTP	early-LTP
EPSC	excitatory postsynaptic current
ER	endoplasmatic reticulum
Erk	extracellular-signal related kinase

E0, 1, 2, 3…	embryonic day 0, 1, 2, 3…
Fbw8	F-box/WD repeat-containing protein 8
FIP200	focal adhesion kinase family-interacting protein of 200 kDa
FJB	Fluoro-Jade B
fMRI	functional magnetic resonance imaging
Fmr1	fragile X mental retardation 1
FMRP	fragile X mental retardation protein
FoxO1/3a	forkhead box O1/3a
GABA	gamma-aminobutyric acid
$GABA_AR$	$GABA_A$ receptor
GABARAP	$GABA_AR$ associated protein
GAD65	glutamic acid decarboxylase 65 kDa
GAP	GTPase-activating protein
GAP-43	growth associated protein 43
GCL	granule cell layer
GEF	guanine nucleotide exchange factor
GFAP	glial fibrillary acidic protein
GluR2	glutamate receptor 2
GlyR	glycine receptor
Grb10	growth factor receptor-bound protein 10
GRIP	glutamate receptor-interacting protein
GSK3α/β	glycogen synthase kinase 3α/β
GTP	guanosine triphosphate
HFS	high frequency stimulation
HIF1α	hypoxia inducible factor 1α
HM	helix motif
IGF1	insulin-like growth factor 1
IGL	internal granular layer
IP3	inositol 1,4,5-trisphosphate
IPSCs	inhibitory postsynaptic currents
IRS1	insulin receptor substrate 1
L	lateral
L-LTP	late-LTP
LTD	long-term depression
LTP	long-term potentiation
M	medial
MAM	mitochondria-associated ER membrane

MAPK	mitogen-activated protein kinase
MAP1B	microtubule-associated protein 1B
MARCKS	myristoylated alanine-rich C-kinase substrate
mEPSC/mIPSC	miniature excitatory/inhibitory postsynaptic currents
mGluRs	metabotropic glutamate receptors
ML	molecular layer
MLIs	molecular layer interneurons
mLST8	mammalian lethal with SEC13 protein 8
MPTP	1-methyl-4-phenyl-1,2,3,6-tetrahydropyridine
mRNA	messenger ribonucleic acid
mSin1	mammalian stress-activated MAP kinase-interacting protein 1
mTOR	mammalian target of rapamycin
mTORC1/mTORC2	mammalian TOR complex 1/2
NDRG1	N-myc downstream regulated 1
Nedd4-2	neural precursor cell expressed developmentally down-regulated gene 4-like
NET	norepinephrine transporter
NMDA	N-methyl-D-aspartate
PA	phosphatidic acid
PCL	Purkinje cell layer
PDK1	phosphoinositide-dependent kinase-1
PF	parallel fibre
PGC1α	PPARγ coactivator 1α
PICK1	protein-interacting with C kinase 1
PIKE	PI3K enhancer
PIKK	phosphatidylinositol-3-kinase-related kinase
PI3K	phosphatidylinositol-3-kinase
PI(3)P	phosphatidylinositol-3-phosphate
$PI(3,4,5)P_3$	phosphatidylinositol-3,4,5-triphosphate
PKC	protein kinase C
PLCβ4	phospholipase C β4
PLD1	phospholipase D1
PPARγ	peroxisome proliferator-activated receptor γ
PP1/2A/2B	protein phosphatase 1/2A/2B
PRAS40	proline-rich Akt substrate 40 kDa
protor1/2	protein observed with rictor 1/2
PTEN	phosphatase and tensin homolog

P0, 1, 2, 3…	postnatal day 0, 1, 2, 3…
RAbKO	raptor brain knockout
Rac1	ras-related C3 botulinum toxin substrate 1
Ras	rat sarcoma
raptor	regulatory-associated protein of mTOR
RAPuKO	raptor Purkinje cell knockout
REDD1	regulated in development and DNA damage response 1
Rheb	ras homolog enriched in brain
rictor	rapamycin-insensitive companion of mTOR
RIPuKO	rictor Purkinje cell knockout
RL	rhombic lip
RNA	ribonucleic acid
Rsk	ribosomal S6 kinase
RTKs	receptor tyrosine kinases
RT-PCR	reverse transcription polymerase chain reaction
SGK1	serum-and glucocorticoid-induced protein kinase 1
SREBP	sterol regulatory element-binding protein
STAT3	signal transducer and activator of transcription 3
STEP	striatal-enriched protein tyrosine phosphatase
S6	ribosomal protein S6
S6K1	S6 kinase 1
TBC1D7	TBC1 (TRE2–BUB2–CDC16) domain family member 7
TFEB	transcription factor EB
Tiam1	T-cell lymphoma invasion and metastasis-inducing protein 1
TM	turn motif
TOR	target of rapamycin
TOR1/2	target of rapamycin 1/2
TSC1/2	tuberous sclerosis complex 1/2
TSCPuKO	TSC1 Purkinje cell knockout
UBCs	unipolar brush cells
ULK1	unc-51-like kinase 1
UPR	unfolded protein response
v-ATPase	vacuolar H^+-ATPase
VGCC	voltage-gated calcium channel
VZ	ventricular zone
WIPI2	WD repeat domain phosphoinositide-interacting protein 2
WM	white matter

YY1	Ying Yang 1
4E-BP1/2	elF4E-binding protein 1/2
5'TOP mRNA	5' terminal oligopyrimidine tract containing mRNA

3. Introduction

In 1991 the research group of Michael N. Hall discovered in a genetic screen two genes that render yeast sensitive to the immunosuppressive and cytostatic compound rapamycin (Heitman *et al.*, 1991). The genes identified back then were named after their targeting compound, *target of rapamycin 1* (*TOR1*) and *2* (*TOR2*). Soon after this discovery, TOR was cloned, purified and characterized in mammalian cells that possess only one TOR ortholog, referred to as mammalian TOR (mTOR) (Brown *et al.*, 1994; Chiu *et al.*, 1994; Sabatini *et al.*, 1994; Sabers *et al.*, 1995). More than two decades after this discovery, a wealth of evidence has accumulated that ascribes (m)TOR a crucial and conserved role in cell growth, i.e. accumulation of mass, of eukaryotes (Wullschleger *et al.*, 2006). Nowadays, mTOR related research is a lively and competitive field given the functions and properties of mTOR that turned out to be relevant for various pathological conditions, thereby offering potential venues for disease treatments (Laplante & Sabatini, 2012). The list of diseases mTOR has been linked to is long and includes cancer, various metabolic diseases such as obesity, fatty liver disease, insulin resistance and diabetes, neurodegenerative diseases like Parkinson's, Alzheimer's, or Huntington's disease and also mental disorders, including schizophrenia or autism spectrum disorders (ASD) (Dazert & Hall, 2011; Lipton & Sahin, 2014).

mTOR belongs to the family of phosphatidylinositol-3-kinase-(PI3K)-related kinases (PIKK) as it contains a carboxy-terminal serine/threonine kinase similar to the lipid kinase PI3K (Keith & Schreiber, 1995). Together with other proteins mTOR associates to two different complexes that are referred to as mTOR complex 1 (mTORC1) or 2 (mTORC2). These two complexes overlap to some part in their protein composition, such as the mLST8 and DEPTOR protein and the Tti1/Tel2 complex. Other proteins are specific for either of them; raptor and PRAS40 are only found at mTORC1 while rictor, mSin1 and protor1/2 are specific for mTORC2 (Fig. 1). As consequence of their different composition, mTORC1 and mTORC2 have distinct properties and downstream targets (Wullschleger *et al.*, 2006; Laplante & Sabatini, 2012). For example, mTORC1 is sensitive to acute treatment with the compound rapamycin while mTORC2 is only affected by a prolonged treatment with this compound (Sarbassov *et al.*, 2006). This difference in rapamycin sensitivity and the fact that mTORC1 inactivation generally results in a more severe phenotype than mTORC2 ablation (Bentzinger *et al.*, 2008; Kumar *et al.*, 2008; Cybulski *et al.*, 2009; Godel *et al.*, 2011) may explain why the mTORC1 signalling is better characterized than the one of mTORC2 as described below.

3.1. The mTORC1 pathway

mTORC1 is known to contribute to cell growth by promoting anabolic processes, such as protein, lipid and nucleotide synthesis. In parallel, mTORC1 diminishes catabolic processes by inhibiting autophagy and lysosome biogenesis (Shimobayashi & Hall, 2014). All these processes are regulated by mTORC1 in response to various stimuli and signals that impinge on this complex, including growth factors, amino acids, stress, energy status and oxygen as depicted in figure 1. The following two sections summarize the downstream targets and upstream regulators of mTORC1.

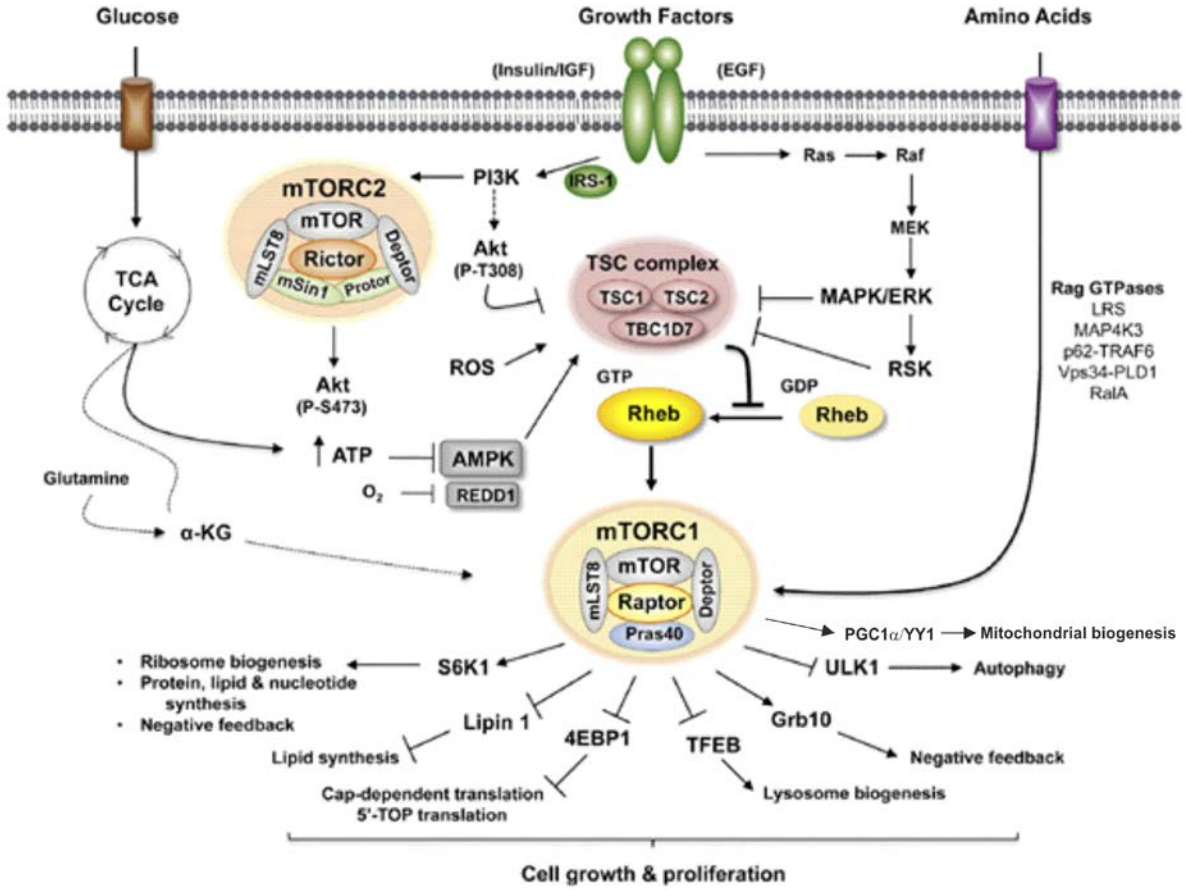

Figure 1: Overview on the mTOR signalling network with focus on mTORC1 (adapted from (Huang & Fingar, 2014)). Growth factor stimulation results in mTORC1 activation either via the PI3K-Akt or Ras/MAPK/Erk/Rsk axis that both converge on the TSC complex. mTORC1 also senses amino acid availability via Rag GTPases and, via the AMPK-TSC complex axis, integrates cues of the energy level. In turn, mTORC1 has the power to influence various processes needed for cell growth and proliferation, such as protein, lipid and nucleotide synthesis as well as mitochondrial biogenesis.

3.1.1. Downstream targets and effects of mTORC1

A great body of evidence supports the role of mTORC1 in protein synthesis. The best studied targets via which mTORC1 controls protein synthesis are the S6 kinase 1 (S6K1) and the elF4E-binding protein 1 (4E-BP1). mTORC1 directly phosphorylates and activates S6K1, which in turn increases ribosome biogenesis via the ribosomal protein S6 and, hence, ultimately promotes protein synthesis (Chauvin *et al.*, 2014) (Fig. 1). Additionally, S6K1 activity increases translational initiation and elongation by targeting various other factors, for example the elongation factor 2 kinase (eEF2k) (Wang *et al.*, 2001; Laplante & Sabatini, 2012). Phosphorylation of 4E-BP1 by mTORC1 also promotes synthesis of proteins by releasing inhibition on the eukaryotic translation initiation factor 4E (eIF4E). This enables eIF4E to assemble with the eIF4F complex that is needed to initiate translation of mRNAs at the 5' cap structure that is possessed by most of the mRNAs (Ma & Blenis, 2009). Next to its influence on global mRNA translation, mTORC1 seems to be particularly important for the translation of 5'TOP mRNAs, a subset of mRNAs that encode for components of the translation machinery (Hsieh *et al.*, 2012). Recently, it has been suggested that this is controlled by mTORC1 via the 4E-BP axis (Thoreen *et al.*, 2012). Altogether, mTORC1 plays a key role in protein synthesis, which classically is considered the major pathway by which this complex contributes to cell growth.

More recent findings indicate that mTORC1 regulates additional processes that are necessary for cellular growth, such as lipid and nucleotide synthesis. mTORC1 has been shown to regulate lipid synthesis by activating the transcription factors SREBPs that are key regulators of lipogenic genes (Porstmann *et al.*, 2008). SREBPs have been reported to be indirectly targeted by mTORC1 either via activation of S6K (Duvel *et al.*, 2010) or inhibition of Lipin-1 (Peterson *et al.*, 2011) that have a positive or negative influence on activation of SREBPs, respectively. Through SREBPs mTORC1 also manages to upregulate expression of genes that are involved in the pentose phosphate pathway, which in turn generates ribose for the synthesis of purine and pyrimidine nucleotides that are needed to produce DNA and RNA (Duvel *et al.*, 2010). Additionally, mTORC1 stimulates *de novo* pyrimidine synthesis via CAD (carbamoyl-phosphate synthetase 2, aspartate transcarbamylase, dihydroorotase) that is phosphorylated and activated by S6K1 (Robitaille *et al.*, 2013).

Anabolic processes controlled by mTORC1 consume energy and, hence, it is not surprising that mTORC1 also positively regulates ATP production and promotes mitochondrial activity (Schieke *et al.*, 2006). mTORC1 contributes to the biogenesis of mitochondria by promoting mitochondrial gene expression (Cunningham *et al.*, 2007). Cunningham and colleagues suggest that mTORC1 controls expression of mitochondrial genes by stimulating association of the transcription factor Ying Yang 1 (YY1) with the PPARγ coactivator 1α (PGC1α).

Next to the anabolic contributions of mTORC1 to cell growth, the same complex is capable of inhibiting catabolic processes to prevent a loss of cell mass. Most importantly, mTORC1 is a key regulator of autophagy, a multistep process that allows to degrade organelles and macromolecules to recover amino acids and other metabolites under starving conditions or to remove damaged and toxic

cell material (Green & Levine, 2014). Autophagy results in the formation of double-membrane structures called autophagosomes that contain cargo to be degraded. Subsequently, autophagosomes fuse with lysosomes to form autolysosomes in which the content is finally degraded (Fig. 2). mTORC1 is a negative regulator of autophagy and intervenes at different points in this process (Dunlop & Tee, 2014).

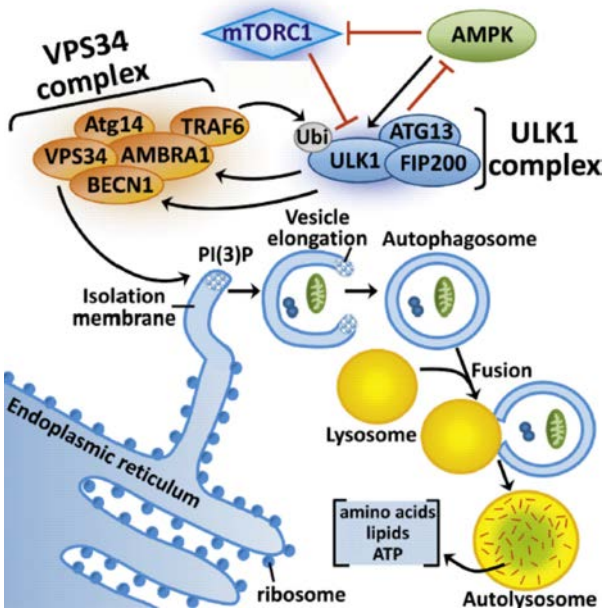

Figure 2: Autophagy and its dependence on mTORC1 (adapted from (Dunlop & Tee, 2014)). In autophagy, organelles and macromolecules are packed in double-membrane structures called autophagosomes that subsequently fuse with lysosomes to form autolysosomes in which the content is degraded. TORC1 inhibits initiation of autophagy by directly phosphorylating ULK1 of the "preinitiation complex".

First and foremost, mTORC1 has been shown to block induction of autophagy by directly phosphorylating and inhibiting ULK1 of the preinitiation complex that contains ATG13 and FIP200 next to ULK1 (Kim *et al.*, 2011; Wirth *et al.*, 2013). mTORC1 also phosphorylates ATG14 of the "initiation complex" that is activated by the "preinitiation complex" upon autophagy induction. The "initiation complex" contains the class III PI3K VPS34 that generates phosphatidylinositol-3-phosphate (PI(3)P) that is essential for the formation of autophagosomes. Phosphorylation of ATG14 by mTORC1 results in an inhibition of PI(3)P production by this complex (Yuan *et al.*, 2013). Moreover, mTORC1 negatively regulates autophagy via other autophagy-related proteins, such as DAP1 (death-associated protein 1), a suppressor of autophagy, (Koren *et al.*, 2010) and WIPI2 (WD repeat domain phosphoinositide-interacting protein 2) that seems to be important for autophagosome formation (Hsu *et al.*, 2011). Growing evidence indicates that mTORC1 controls autophagy also in an indirect manner by influencing biogenesis of lysosomes via a transcription factor termed TFEB that regulates various genes important for lysosomal function. TFEB is directly phosphorylated by mTORC1 at Ser142, which has been suggested to prevent nuclear translocation and, hence, negatively affect lysosome biogenesis. In line with this suggestion, pharmacological inhibition of mTORC1 as well as starving conditions have been observed to cause nuclear translocation of TFEB and to promote lysosome biogenesis (Martina *et al.*, 2012; Settembre *et al.*, 2012).

3.1.2. Activation and negative feedback looping of mTORC1

mTORC1 is responsive to growth factors but also integrates various cues that indicate the nutrient, energy or stress level of a cell. Insulin and IGF1 are classical examples of growth factors that result in mTORC1 activation via the PI3K-PDK1-Akt pathway that is considered the major pathway by which growth factors trigger mTORC1 (Fig. 3) (Sengupta *et al.*, 2010). Binding of insulin to its tyrosine kinase receptor causes a recruitment of IRS1 (insulin receptor substrate 1) to the receptor that goes along with a subsequent activation of the phosphatidylinositol-3-kinase (PI3K). The $PI(3,4,5)P_3$ generated by PI3K recruits Akt to the plasma membrane where Akt becomes activated by phosphorylation at Thr308 by the phosphoinositide-dependent kinase-1 (PDK1) (Alessi *et al.*, 1996; Alessi *et al.*, 1997; Dangelmaier *et al.*, 2014). Finally, activated Akt promotes mTORC1 activation by phosphorylating and inhibiting PRAS40, an mTORC1 inhibitor (Sancak *et al.*, 2007; Vander Haar *et al.*, 2007), and by suppressing the TSC complex that excerpts an inhibitory effect on mTORC1 as well. Akt phosphorylates TSC2 at several residues, which results in an inhibition of the TSC complex that consists of TSC1 (hamartin), TSC2 (tuberin) and TBC1D7 (TBC1 (TRE2–BUB2–CDC16) domain family member 7) (Inoki *et al.*, 2002; Manning *et al.*, 2002; Tee *et al.*, 2002; Dibble *et al.*, 2012). The TSC complex is a key upstream regulator of mTORC1 and not only responds to growth factors that signal via PI3K-Akt-PDK1 but also to such ones that signal via Ras/MAPK/Erk/Rsk, like the epidermal growth factor (EGF) (Mendoza *et al.*, 2011). Erk (Ma *et al.*, 2005) and Rsk (Roux *et al.*, 2004) both target TSC2 at sites that differ from each other (and largely the ones of Akt) (Dibble & Manning, 2013) but have in common that they cause an inhibition of the TSC complex in their phosphorylated state (Fig. 3). Next to this indirect effect via the TSC complex, Erk and Rsk have more recently been shown to directly phosphorylate mTORC1 at raptor, which also promotes mTORC1 activity (Carriere *et al.*, 2008; Carriere *et al.*, 2011).

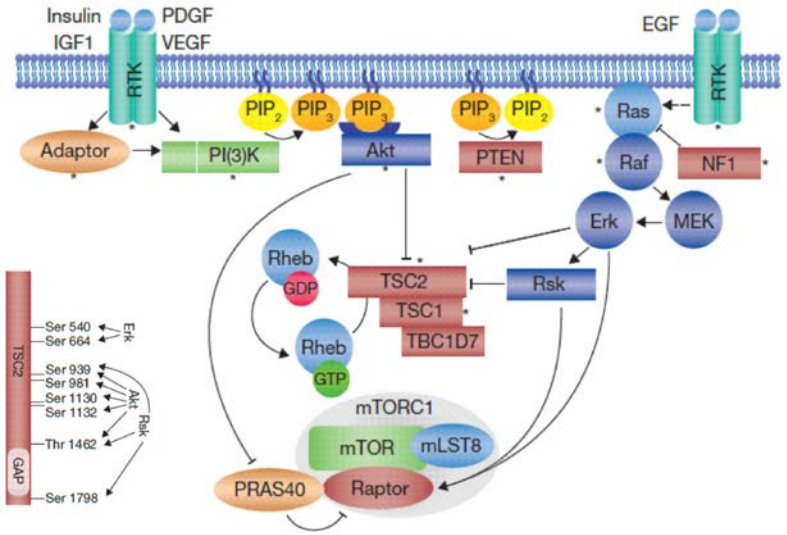

Figure 3: Activation of mTORC1 by growth factors (adapted from (Dibble & Manning, 2013)). Growth factors triggering receptor tyrosine kinases (RTKs) can activate mTORC1 via the PI3K-Akt or Ras/Erk/Rsk axis. In both cases this leads to an inhibition of the TSC complex by a phosphorylation of TSC2, which releases inhibition on mTORC1 and causes its activation. TSC2 is phosphorylated by Akt, Erk and Rsk at sites that largely differ from each other.

The TSC complex influences mTORC1 activity by acting as a GTPase-activating protein (GAP) for the small GTPase Rheb that is crucial for activation of mTORC1 by all upstream pathways (Tee *et al.*, 2003; Dibble & Manning, 2013). Consequently, inhibition of the TSC complex increases activated, GTP-loaded Rheb that activates mTORC1. Although Rheb binds mTORC1 directly, the mechanism of activation is unknown (Long *et al.*, 2005). Rheb may activate mTORC1 by binding phospholipase D1 (PLD1) and promoting its activity (Sun *et al.*, 2008). PLD1 generates phosphatidic acid (PA), which is required for activation of mTORC1 (Fang *et al.*, 2001; Yoon *et al.*, 2011).

Growth factor activation of mTORC1 fails in the absence of amino acids, which demonstrates that amino acid sensing of mTORC1 dominates over its stimulation by growth factors (Hara *et al.*, 1998). Lysosomes turned out to be a crucial platform for amino acid sensing of mTORC1 as well as for integration of growth factor signalling. Amino acid stimulation results in a translocation of mTORC1 from the cytosol to the surface of lysosomes where mTORC1 binds Rag proteins that are small GTPases like Rheb (Sancak *et al.*, 2008; Sancak *et al.*, 2010) (Fig. 4).

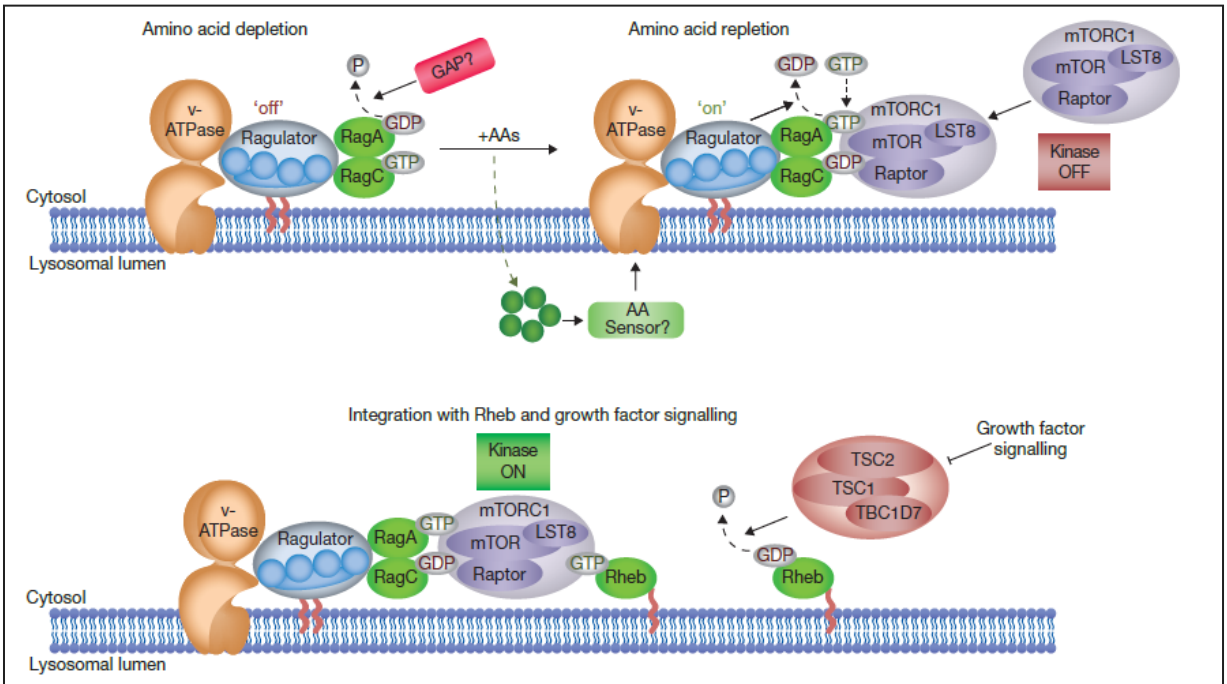

Figure 4: Model for amino acid sensing of mTORC1 at the lysosome (adapted from (Dibble & Manning, 2013)). In the presence of amino acids, the ragulator complex that is anchored at the lysosome and is a GEF becomes active and promotes the generation of RagA/B^{GTP}-RagC/D^{GDP}, which in turn recruits mTORC1 to the lysosome. The availability of amino acids seems to be conveyed to the ragulator complex by the v-ATPase that undergoes an amino acid-induced conformational change. At the lysosome mTORC1 comes in contact with Rheb that integrates signals of growth factors and enables activation of mTORC1.

Two subtypes of Rag proteins exist, RagA/B and RagC/D, that form heterodimers (RagA/B-RagC/D). The interaction of RagA/B-RagC/D with mTORC1 is determined by the nucleotide-binding state of the Rag proteins (Sancak *et al.*, 2008). mTORC1 binds heterodimers consisting of GTP-bound

RagA/B and GDP-bound RagC/D (RagA/B^{GTP}-RagC/D^{GDP}) but not RagA/B^{GDP}-RagC/D^{GTP}. The circumstance that the RagA/B^{GTP}-RagC/D^{GDP} heterodimers are formed only when sufficient amino acids are available, while the RagA/B^{GDP}-RagC/D^{GTP} heterodimer represents starving conditions, allows mTORC1 to sense amino acid availability. The nucleotide switch of Rag heterodimers in response to amino acids is conducted by the ragulator complex that is a guanine nucleotide exchange factor (GEF) and also anchors Rags to lysosomal membranes (Sancak *et al.*, 2010; Bar-Peled *et al.*, 2012) (Fig. 4). It has been suggested that the ragulator complex senses intralysosomal amino acids by interacting with the membrane-spanning vacuolar H^+-ATPase (v-ATPase) that can undergo an amino acid-induced conformational change (Zoncu *et al.*, 2011). However, the relevance of intralysosomal amino acids for the recruitment of mTORC1 to lysosomes is currently unclear.

On the lysosomal surface also the essential upstream activator of mTORC1, Rheb, is present (Sancak *et al.*, 2010). Consequently, an amino acid-dependent recruitment of mTORC1 to the lysosome establishes a contact with Rheb and thereby allows activation of mTORC1. Altogether, this model is in agreement with the observed dominance of amino acid signalling over growth factor signalling to mTORC1. In brief, a lack of amino acids prevents the recruitment of mTORC1 to the lysosomes where it might become activated by Rheb.

Since anabolic processes promoted by mTORC1 consume energy, it is important that mTORC1 is fed with information about the energy level of a cell. mTORC1 is downstream of AMPK, a master regulator of cellular energy metabolism, that becomes activated when the AMP/ATP and ADP/ATP ratios increase as a consequence of reduced ATP levels. Various factors may affect ATP levels of a cell, including glucose deprivation, hypoxia, or inhibition of glycolysis and/or mitochondrial function (Hardie *et al.*, 2012). Activated AMPK reduces mTORC1 activity either in an indirect manner by increasing activity of TSC2 via phosphorylation at Ser1345 (Inoki *et al.*, 2003) or by directly inhibiting mTORC1 via phosphorylation of raptor at Ser792 (Gwinn *et al.*, 2008). In response to hypoxia, mTORC1 activity is not only diminished by AMPK but also via a transcriptional program. Under low oxygen conditions the transcription factor hypoxia inducible factor 1α (HIF1α, that is degraded in the presence of oxygen) is stabilized and promotes expression of REDD1 (regulated in development and DNA damage responses 1). In a yet poorly understood mechanism REDD1 causes inhibition of mTORC1 via the TSC complex (Brugarolas *et al.*, 2004; DeYoung *et al.*, 2008; Vega-Rubin-de-Celis *et al.*, 2010). REDD1-mediated mTORC1 inhibition is also observed under other stress situations, such as accumulation of misfolded proteins and endoplasmatic reticulum stress that may result from impaired protein maturation or aberrantly high protein synthesis. Such conditions result in an unfolded protein response (UPR) that causes an upregulation of REDD1 via the ATF4 transcription factor (Jin *et al.*, 2009; Whitney *et al.*, 2009). Finally, also genotoxic stress and DNA damage act as stress factors on mTORC1 and inhibit its activity. Genotoxic stress stabilizes p53 that is a transcription factor not only for REDD1 (Ellisen *et al.*, 2002; Ben Sahra *et al.*, 2011) but also sestrins that repress mTORC1 via activation of AMPK (Budanov & Karin, 2008).

In order to limit its signal duration and amplitude the mTORC1 signalling pathway possesses negative feedback mechanisms. mTORC1 (Tzatsos, 2009) as well as its downstream target S6K1 (Um *et al.*, 2004; Harrington *et al.*, 2005) both phosphorylate IRS1, thereby inducing its degradation and, hence, reduce PI3K signalling that occurs upstream of mTORC1. In agreement with this negative feedback loop model, inactivation or constitutive activation of mTORC1 has been shown to cause increased or decreased PI3K signalling, respectively (Bentzinger *et al.*, 2008; Romanino *et al.*, 2011; Castets *et al.*, 2013; Cloetta *et al.*, 2013). For example, conditional ablation of mTORC1 in muscle increases Akt activity and the phosphorylation of the glycogen synthase kinase 3 (GSK3), an Akt downstream target (Bentzinger *et al.*, 2008; Romanino *et al.*, 2011). In addition to this well characterized negative feedback mechanism, mTORC1 activity may also diminish its upstream stimulation by directly phosphorylating and stabilizing Grb10. Grb10 is a growth factor receptor-bound adaptor that upon phosphorylation by mTORC1 attenuates PI3K as well as MAPK/Erk signalling (Yu *et al.*, 2011).

3.2. The mTORC2 pathway

In comparison to mTORC1 much less is known about mTORC2. Yet, this does not implicate that mTORC2 is less interesting than mTORC1 as also mTORC2 contributes to disease relevant functions of mTOR as outlined below.

3.2.1. Downstream targets and effects of mTORC2

mTORC2 phosphorylates and activates several members of the AGC kinase family, including Akt, serum- and glucocorticoid-induced protein kinase 1 (SGK1) and protein kinase C (PKC) (Fig. 5). AGC kinases are phosphorylated by mTORC2 in their helix motif (HM) and/or turn motif (TM), which allosterically influences the catalytic activation of these kinases by PDK1 (Cybulski & Hall, 2009; Oh & Jacinto, 2011). For example, Akt is phosphorylated by PDK1 in the activation loop site at residue Thr308 that is essential for the activation of Akt, while mTORC2-mediated phosphorylation of Akt at Ser473 in the HM (Sarbassov *et al.*, 2005) has been suggested to further boost its activity and permit substrate specificity (Alessi *et al.*, 1996; Guertin *et al.*, 2006; Jacinto *et al.*, 2006; Cybulski & Hall, 2009). In line with the suggestion of substrate specificity, disruption of the mTORC2 complex and the concomitant reduced phosphorylation of Akt at Ser473 differently affects phosphorylation of Akt substrates. In mouse embryonic fibroblast cells lacking mTORC2, Akt targets like FoxO1/3a have been reported to be affected by mTORC2 inactivation, while phosphorylation of other Akt targets like GSK3 and TSC2 is normal (Guertin *et al.*, 2006; Jacinto *et al.*, 2006). Given the normal phosphorylation of TSC2 upon mTORC2 inactivation, it is currently believed that mTORC2 function is not needed for mTORC1

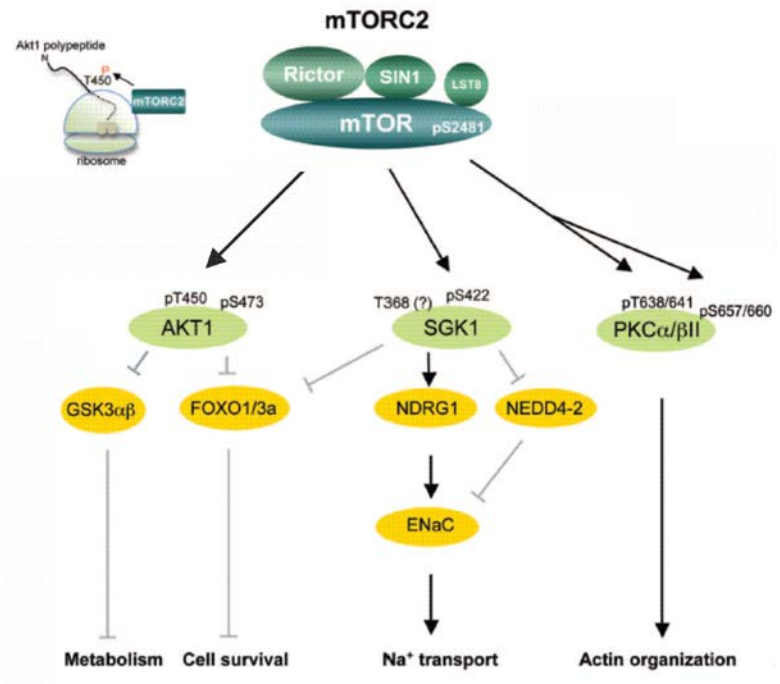

Figure 5: Downstream signalling of mTORC2 (adapted from (Oh & Jacinto, 2011)). mTORC2 phosphorylates members of the AGC kinase family like Akt, PKC and SGK1 and thereby contributes to various cellular processes.

activity (Bentzinger *et al.*, 2008; Thomanetz *et al.*, 2013). Consistently, liver specific ablation of mTORC2 does not change mTORC1 activity, yet, affects GSK3, FoxO and SREBP1c signalling (Hagiwara *et al.*, 2012). Last is known to be a master regulator of lipogenic genes as described above and is also regulated by Akt and, hence, mTORC2 seems to stimultate lipogenesis as well (Yecies *et al.*, 2011).

The mTORC2 downstream target Akt is involved in various cellular processes like metabolism, proliferation, growth and cell death regulation. Due to its role in these processes Akt has been linked to cancer (Fresno Vara *et al.*, 2004; Martini *et al.*, 2014). In a prostate cancer mouse model, induced by deletion of PTEN, which results in increased PI3K signalling and, hence, Akt activation, tumor development is dependent on mTORC2, most likely due to the positive effect of mTORC2 on Akt phosphorylation. This finding ascribes mTORC2 a role in cancer (Guertin *et al.*, 2009; Sparks & Guertin, 2010).

PKCs targeted by mTORC2 are other proteins involved in a multiplicity of cellular functions, such as proliferation, differentiation, survival and motility (Griner & Kazanietz, 2007). PKC is a family of proteins and is subdivided in classical (c)PKC (α, β and γ), novel (n)PKCs (δ, ε, η and θ) and atypical (a)PKCs (protein kinase Mζ, and ι/λ). Phosphorylation of cPKC and nPKC in their HM and TM requires mTORC2 (Sarbassov *et al.*, 2004; Facchinetti *et al.*, 2008; Ikenoue *et al.*, 2008; Lee *et al.*, 2010). mTORC2-mediated phosphorylation of PKCα and β in the TM occurs in a co-translational manner and increases maturation and stability of PKCs (Facchinetti *et al.*, 2008; Ikenoue *et al.*, 2008). Concordantly, mTORC2 ablation has been reported to result in reduced protein levels of classical and novel PKCs (Ikenoue *et al.*, 2008; Thomanetz *et al.*, 2013).

By controlling PKCs, mTORC2 has been suggested to regulate actin cytoskeleton rearrangement (Sarbassov *et al.*, 2004; Larsson, 2006; Thomanetz *et al.*, 2013). Moreover, mTORC2 may affect actin cytoskeleton via other effectors like paxilin and Rac1 (Jacinto *et al.*, 2004). Rac1 has been reported to bind mTOR directly and associates with both mTORC2 as well as mTORC1 upon stimulation with growth factors (Saci *et al.*, 2011). In addition, mTORC2 interacts with Tiam1, a Rac1-specific GEF, giving mTORC2 a tool to regulate Rac1 activity and consequently influence actin cytoskeleton (Huang *et al.*, 2013).

Last but not least, mTORC2 is critical for the activation of SGK1 that is stimulated in response to osmotic stress and growth factors and, in turn, controls ion transport and growth (Garcia-Martinez & Alessi, 2008). Downstream targets of SGK1 include NDRG1 as well as the ubiquitin ligase Nedd4-2 (Lu *et al.*, 2010). Last plays a central role in sodium transport (Debonneville *et al.*, 2001) while the precise function of NDRG1 is elusive (Melotte *et al.*, 2010).

3.2.2. Activation and negative feedback looping of mTORC2

To date, activation of mTORC2 is not well understood. mTORC2 seems to be insensitive to nutrients but well responsive to growth factors, such as insulin (Sarbassov *et al.*, 2004; Sarbassov *et al.*, 2005; Garcia-Martinez & Alessi, 2008; Huang *et al.*, 2008; Laplante & Sabatini, 2012). As summarized below, several publications describe growth factor-mediated effects on the subcellular localization of mTORC2 or its interaction with other proteins. However, the mechanisms that link PI3K signalling to mTORC2 activation remain unclear. mTORC2 associates with the TSC complex, which, in contrary to mTORC1, positively regulates mTORC2 activation that occurs in a manner independent of the GAP function of the TSC complex (Huang *et al.*, 2008). Recent results indicate that growth factor-mediated activation of mTORC2 is dependent on its association with ribosomes (Zinzalla *et al.*, 2011). This association with ribosomes is in line with the finding that mTORC2 regulates PKC phosphorylation and also phosphorylation of Akt at Thr450 in a co-translational manner, which in both cases increases folding and stability of these proteins (Facchinetti *et al.*, 2008; Ikenoue *et al.*, 2008; Oh *et al.*, 2010). Growth factor stimulation has also been shown to stimulate localization of mTORC2 to a subdomain of the endoplasmatic recticulum (ER) called MAM (mitochondria-associated ER membrane) that physically connects to mitochondria. MAM is important for the transfer of lipids and calcium between ER and mitochondria and thereby controls mitochondrial metabolism and apoptosis (Rizzuto *et al.*, 1998; Csordas *et al.*, 1999). mTORC2 ablation and concomitant altered Akt signalling diminishes the integrity of MAM and ultimately affects mitochondrial metabolism and cell survival (Betz *et al.*, 2013). Furthermore, the association of both mTORC1 and mTORC2 with Rac1 is dependent on growth factors. It has been suggested that Rac1 might serve as a point of convergence to co-regulate mTORC1 and mTORC2 upon growth factor stimulation (Saci *et al.*, 2011).

In analogy to mTORC1 signalling, also the mTORC2 pathway is furnished with negative feedback mechanisms. mTORC2 activity leads to the stabilization of the ubiquitin ligase subunit Fbw8 that mediates the degradation of IRS1 and, hence, limits upstream PI3K signalling (Kim *et al.*, 2012). Upon growth factor stimulation mTORC2 may also get negative feedback input from the mTORC1 downstream target S6K1. For example, S6K1 can directly phosphorylate rictor at Thr1135, which reduces mTORC2 signalling (Dibble *et al.*, 2009; Boulbes *et al.*, 2010; Julien *et al.*, 2010; Treins *et al.*, 2010). Additionally, S6K1 has been shown to directly phosphorylate mSin1, a core protein of mTORC2, thereby disrupting mTORC2 function (Liu *et al.*, 2013; Xie & Proud, 2013).

3.3. mTOR signalling in the brain

Development of the brain is a highly complex process that includes growth and proliferation processes that need to be tightly regulated. Because mTOR signalling plays a key role in such processes, this pathway turned out to be crucial for brain development and has also been linked to neurodevelopmental disorders. mTOR is not only crucial in the developing but also in the adult brain that is a highly plastic organ constantly shaping synaptic connectivity, which requires protein synthesis and also other mTOR-dependent processes. Moreover, the mTOR pathway controls cellular mechanisms, for example autophagy, that are essential for a cell to respond to stress situations. Probably due to such features, mTOR signalling is also found to be involved in age-related neurodegenerative diseases. The following chapters summarize the most relevant contributions of mTOR signalling in the developing and adult brain under normal and pathological conditions.

3.3.1. The role of mTOR signalling in brain development

Genetic ablation of mTORC1 specifically in neural progenitor cells clearly impairs embryonic brain development and results in perinatal death of mice. The impaired brain development manifests in a microcephaly that is the consequence of a reduction of the cell size and number. Reduced cell proliferation and increased apoptosis contribute to the diminished cell number (Cloetta *et al.*, 2013). Similar results have recently been published for mice that have mTOR itself conditionally knocked out by the same driver (Ka *et al.*, 2014). Ablation of mTORC1 in the developing brain also affects gliogenesis, which is paralleled by a reduction of the phosphorylation of the transcription factor STAT3 that is important for differentiation of glia cells (Bonni *et al.*, 1997; Yokogami *et al.*, 2000). Not only ablation but also constitutive activation of mTORC1 upon inactivation of the TSC complex has been shown to impair brain development. In contrary to mTORC1 ablation, disruption of the TSC complex causes megalencephaly that is paralleled by an increase in cell size and proliferation as well as impaired neuronal and glial differentiation (Anderl *et al.*, 2011; Magri *et al.*, 2011; Carson *et al.*, 2012; Magri *et al.*, 2013). Also conditional ablation of the TSC complex in neural progenitors results in neonatal death (Anderl *et al.*, 2011). On the other hand, inactivation of mTORC2 in neural progenitors results in a milder phenotype and does not affect mouse viability but causes aberrant brain development and a reduction of the brain size. Last seems to be mainly the consequence of a reduction in cell size since no signs for apoptosis or altered proliferation are detected (Thomanetz *et al.*, 2013). Overlapping results have been reported for mice that have mTORC2 conditionally ablated in dorsal neural progenitor cells. Also this leads to smaller neurons and a reduction of the brain size (Carson *et al.*, 2013). Altogether, the data gained from all these brain-specific knockout mice demonstrate that both mTORC1 and mTORC2 are crucial for proper development of the brain. Below the contributions of mTORC1 and mTORC2 to different aspects of neuronal development are further highlighted.

During brain development neurons start to form synaptic connections with each other, which enables communication between them and finally leads to the generation of neural circuits. Neurons receive synaptic input in their dendritic parts that are elaborately structured in many neurons. The establishment of the dendritic tree is a developmental process that depends on both mTORC1 and mTORC2. Knockdown of either mTORC1 or mTORC2 in cultured hippocampal neurons impairs the development of the dendritic tree and diminishes dendritic arborisation (Urbanska *et al.*, 2012). In neuronal cultures, the brain-derived neurotrophic factor (BDNF), a potent mTORC1 activator, enhances dendritic arborisation. Consistently, this positive effect of BDNF on dendritic arborisation is sensitive to rapamycin treatment (Jaworski *et al.*, 2005). Not only increased activation of mTORC1 upon BDNF treatment but also upon removal of negative regulators of mTORC1, TSC1 or PTEN, increases dendritic length and the number of branch points in hippocampal cultures (Jaworski *et al.*, 2005; Weston *et al.*, 2014). Effects of sustained mTORC1 activation on dendrite morphology are also seen *in vivo*. Conditional TSC1 knockout in dorsal neural progenitor cells for example results in neurons with thickened dendritic arbors (Meikle *et al.*, 2007) as well as abnormal dendrite orientation (Meikle *et al.*, 2008). While *in vivo* effects of mTORC1 deficiency on dendrite morphology have not yet been demonstrated, the dendritic morphology of pyramidal hippocampal neurons and Purkinje cells is altered in mice that have mTORC2 ablated in neural progenitors (Thomanetz *et al.*, 2013).

mTOR signalling is also important for the parts of the dendrite where neurons receive excitatory synaptic input, the spines (Kumar *et al.*, 2005; Tavazoie *et al.*, 2005; Tsai *et al.*, 2012). Spine formation and elimination/pruning is a dynamic process that occurs in the brain throughout life. At early ages in life spine formation exceeds pruning, which results in an excessive production of excitatory synapses that is important for the establishment of neural circuits. In course of development spine pruning takes over, which is important for neural circuit maturation. Most recently, it has been shown that heterozygous loss of TSC2 and the resulting increased mTORC1 activity impairs postnatal, developmental spine elimination/pruning, which results in increased spine density at later time points (Tang *et al.*, 2014). Tang and colleagues suggest that these defects in spine pruning depend on mTORC1-mediated blockade of autophagy (see section 3.1.1). In line with these findings, TSC1 knockout in Purkinje cells causes aberrant autophagic flux (Di Nardo *et al.*, 2014) in these neurons and increases their spine density (Tsai *et al.*, 2012). Not only mTORC1 but also mTORC2 is important for spines since a conditional rictor knockout in CA1 hippocampal neurons has been shown to reduce the spine density of these neurons (Huang *et al.*, 2013). However, the reduced spine density seen in this mouse model is most likely not caused by developmental defects since rictor knockout occurs only several days after birth. Huang and colleagues suggest that mTORC2 may affect spines by regulating actin cytoskeleton as further outlined in section 3.3.2.

Neurons transmit signals to other neurons via axons. Axons start to extend from the somata during neuronal development and are guided to their targets by molecules that act as attractive or repulsive cues. There is evidence that axon guidance depends on mTORC1. For example, semaphorin-3A that

acts as repulsive signal on growth cones of *Xenopus* retinal neurons has been shown to cause phosphorylation of the mTORC1 downstream target 4E-BP1 in growth cones. Consistently, semaphorin-3A induced growth cone collapse was prevented in the presence of the mTORC1 inhibitor rapamycin (Campbell & Holt, 2001). Axonal guidance of retinal ganglion cells is dependent on ephrin-Eph signalling, which has been shown to converge on mTORC1 via the MAPK-TSC2-mTORC1 axis. In line with this finding, aberrant retinogeniculate projections are observed in mice that are haploinsufficient for TSC2, which indicates that axonal guidance in these mice is impaired (Nie *et al.*, 2010).

3.3.2. The role of mTOR signalling in the plasticity of excitatory synapses

It is fundamentally believed that neurons process and store information in the brain by modulating synaptic connections that they form with other neurons in the context of neural circuits. These connections can be structurally modified by regulating the number or size of synapses or in a more functional manner by changing the synaptic strength and efficiency. Synaptic plasticity can be simulated and measured by electrophysiological recordings. The electrophysiological correlates for synaptic strengthening or weakening are long-term potentiation (LTP) or long-term depression (LTD), respectively (Martin *et al.*, 2000). Much knowledge about synaptic plasticity has been gained from studying the excitatory CA3-CA1 synapses formed in the hippocampus. High frequency stimulation (HFS) of these synapses results in high postsynaptic calcium levels and a calcium/calmodulin-dependent protein kinase type II (CamKII)-mediated postsynaptic upregulation of glutamatergic AMPA receptors on the surface, ultimately leading to a potentiation of these synapses (LTP). Low frequency stimulation, in turn, results in moderate postsynaptic calcium influx and a subsequent protein phosphatase 1 (PP1)–mediated endocytosis of AMPA receptors and consequently a weakening of the synaptic strength (LTD) (Xia & Storm, 2005) (Fig. 6). Throughout the brain different forms of LTP and LTD are observed and have been shown to depend on NMDA receptors, metabotropic glutamate receptors (mGluRs), dopaminergic receptors and BDNF, all of which influence mTOR function (Hoeffer & Klann, 2010). For LTP it is also distinguished between early and late forms of LTP, abbreviated as E-LTP and L-LTP, respectively. The stimulation paradigm applied in electrophysiological recording determines the form of LTP at the CA3-CA1 synapses. A single train of HFS triggers an E-LTP while several repetitions thereof cause an L-LTP. While an E-LTP lasts for about 1-2 hours and mostly bases on post translational modifications (Roberson *et al.*, 1996), an L-LTP lasts up to several hours and needs *de novo* protein synthesis and at a certain point also the initiation of transcriptional programs (Reymann & Frey, 2007). Because long durable forms of synaptic plasticity are dependent on protein synthesis, they have been linked to mTORC1 quite a while ago (Tang & Schuman, 2002) (Fig. 6). For example, the maintenance of L-LTP is sensitive to rapamycin treatment (Tang *et al.*, 2002). Moreover, a knockout of the translational repressor and

mTORC1 downstream target 4E-BP2 impairs LTP by rendering E-LTP to an L-LTP, likely by increasing initiation of protein translation (Banko *et al.*, 2005). As the mTORC1 downstream targets 4E-BP and eIF4E are both found at postsynaptic parts (Tang *et al.*, 2002) and since polyribosomes redistribute into activated spines upon L-LTP (Ostroff *et al.*, 2002; Bourne *et al.*, 2007), it is thought that mTORC1 controls protein translation in a local manner in the dendrite without the requirement for transcription in the soma (Costa-Mattioli *et al.*, 2009). In agreement with this notion, NMDA-PI3K-mediated activation of S6K occurs throughout the dendrites but not in the cell bodies of CA1 neurons in hippocampal slices (Cammalleri *et al.*, 2003).

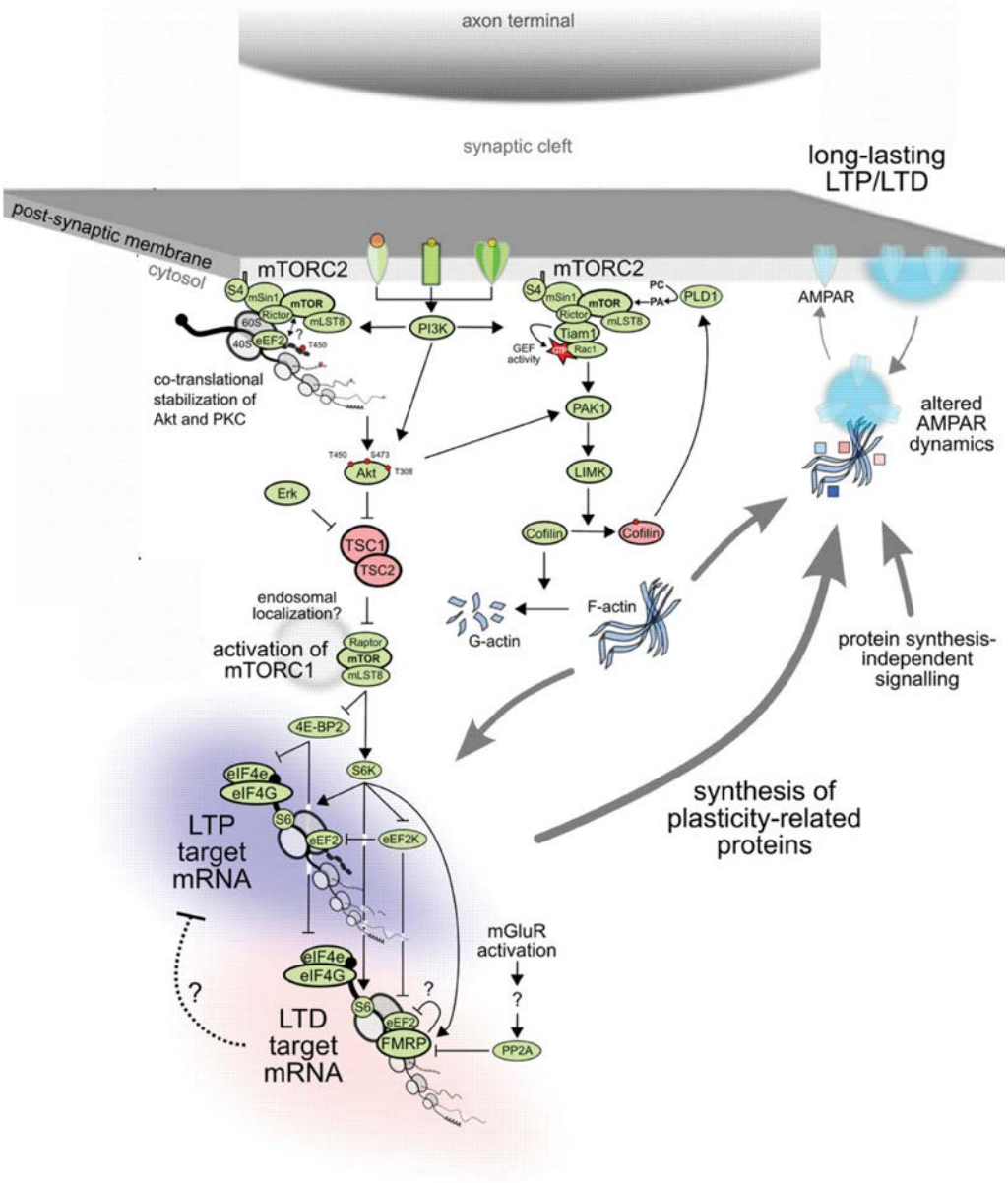

Figure 6: A model of the involvement of mTOR signalling in synaptic plasticity (adapted from (Graber *et al.*, 2013)). Both, mTORC1 and mTORC2 are essential for L-LTP since they regulate local protein synthesis or actin cytoskeletal rearrangement, respectively. mTORC1 may also regulate the translation of mRNAs coding for proteins that are important for LTD.

Not only mTORC1 but also mTORC2 is important for the maintenance of L-LTP as this has recently been shown (Huang *et al.*, 2013). Postnatal genetic inactivation of mTORC2 in the forebrain affects L-LTP of hippocampal CA3-CA1 synapses, which is paralleled by impaired actin polymerisation in CA1 neurons. In the presence of jasplakinolide, a stabilizer of newly formed actin filaments, these L-LTP deficits could be rescued, which demonstrated that the capability of mTORC2 to regulate actin cytoskeleton is crucial for L-LTP maintenance (Fig. 6).

Next to LTP, also LTD depends on mTOR signalling. mGluR-dependent forms of LTD are sensitive to PI3K inhibitors and rapamycin and, hence, rely on the PI3K-Akt-mTORC1 signalling cascade (Hou & Klann, 2004; Collingridge *et al.*, 2010; Luscher & Huber, 2010). Similar to LTP, also mGluR-LTD requires protein synthesis and this in a rapid and most likely local manner (Huber *et al.*, 2000). Proteins synthesized upon mGluR signalling are for example Arc (Park *et al.*, 2008), STEP (Zhang *et al.*, 2008) and MAP1B (Davidkova & Carroll, 2007), all of which are involved in AMPA receptor internalization, a process essential for LTD. mTORC1 may contribute to mGluR-LTD by controlling protein synthesis. This notion is supported by the finding that mGluR-LTD is increased in mice deficient of the mTORC1 downstream target 4E-BP2 that is a negative regulator of protein synthesis (Banko *et al.*, 2006). Congruently, transgenic mice with increased levels of eIF4E also reveal enhanced mGluR-LTD, which is paralleled by elevated levels of protein synthesis (Santini *et al.*, 2013).

3.3.3. A role of mTOR signalling in excitatory/inhibitory synaptic balance?

As described above, there is a plethora of evidence supporting the role of mTOR signalling at excitatory synapses, yet, whether this pathway also plays a role at inhibitory synapses is currently less well understood. More than two decades ago, mTOR was shown to physically interact with gephyrin, an important postsynaptic scaffolding protein at inhibitory synapses (Sabatini *et al.*, 1999; Tyagarajan & Fritschy, 2014). This finding has recently been confirmed by another group in cultured hippocampal neurons (Wuchter *et al.*, 2012). Furthermore, Wuchter and colleagues find that the density of gehyrin clusters in these cultures is sensitive to rapamycin treatment. Another study identified by a phosphoproteomic approach gephyrin residue Ser200 to be rapamycin-sensitive (Demirkan *et al.*, 2011).

Given a possible role of mTOR at inhibitory synapses in addition to its well described function at excitatory synapses, it has been hypothesized that this signalling pathway might be crucial for the balance of excitatory and inhibitory synaptic transmission. This hypothesis has recently been strengthened by the finding that TSC1 knockout in hippocampal CA1 pyramidal neurons indeed causes an excitatory/inhibitory synaptic imbalance by weakening the inhibitory input. As consequence, these mice show hippocampal hyperexcitability and are prone to seizures (Bateup *et al.*, 2013). Additionally, knockout of the mTORC1 downstream target 4E-BP2 also causes an increased

ratio of excitatory to inhibitory synaptic input (Gkogkas *et al.*, 2013). Interestingly, knockout of 4E-BP2 increases the translation of neuroligins that are postsynaptic adhesion molecules important for synapse formation. Several neuroligin isoforms exist that differ in their distribution amongst excitatory and inhibitory synapses (Levinson & El-Husseini, 2005; Krueger *et al.*, 2012). Deficiency of 4E-BP2 enhances translation of neuroligin isoforms that are found at excitatory synapses but also such ones present at inhibitory synapses, supporting the notion that the mTOR signalling pathway may influence both inhibitory and excitatory synaptic transmission, thereby controlling the excitation/inhibition balance (Levinson & El-Husseini, 2005; Gkogkas *et al.*, 2013).

3.3.4. mTOR in brain pathologies

3.3.4.1. Neurodevelopmental disorders

Tuberous sclerosis. Heterozygous loss of *TSC1* or *TSC2* due to genetic mutations causes a multi-organ disorder called Tuberous sclerosis. Due to its genetic basis Tuberous sclerosis affects the development of the brain and results in neurological symptoms, such as intellectual disability, epilepsy and ASD (Curatolo *et al.*, 2008) (Fig. 7). Last are characterized by social deficits, impaired communication as well as stereotyped and repetitive behaviour (Miles, 2011). Tuberous sclerosis mouse models generated by heterozygous deletion or mutation of the *TSC1* or *TSC2* gene recapitulate aspects of these neurological symptoms and reveal learning and memory deficits (Goorden *et al.*, 2007), aberrant social behaviour as well as repetitive behaviour (Young *et al.*, 2010; Chevere-Torres *et al.*, 2012; Tsai *et al.*, 2012; Tang *et al.*, 2014). Several of these behavioural deficits can be rescued by rapamycin treatment of these mice, demonstrating that they are dependent on mTORC1. Heterozygous loss of *TSC1* or *TSC2* in mice increases the spine density (Tsai *et al.*, 2012; Tang *et al.*, 2014), a phenomenon that is also observed with ASD (Hutsler & Zhang, 2010). Recently, it has been suggested that this is due to mTORC1-mediated inhibition of autophagy which impairs spine elimination/pruning (see section 3.3.1). Hence, some of the Tuberous sclerosis symptoms may base on defective spine elimination (Tang *et al.*, 2014). Furthermore, there is evidence that an imbalance of synaptic excitation and inhibition occurs upon loss of the TSC complex, which has been hypothesized to underlie ASD (see also section 3.3.3) (Bourgeron, 2009; Bateup *et al.*, 2013).

Fragile X. Another genetic disease that shares some similarities with Tuberous sclerosis is the Fragile X syndrome that manifests in cognitive deficits and ASD (Martin & Huntsman, 2012). The Fragile X syndrome is associated with the silencing of the *Fmr1* gene that codes for FMRP, an RNA-binding protein that represses the translation of several mRNAs (Brown *et al.*, 2001). Consequently, a lack of FMRP increases the synthesis of specific proteins. FMRP is located in dendrites and spines (Weiler *et al.*, 1997) and regulates for example the translation of mRNAs that are important for synaptic plasticity, such as Arc or CamKII (Zalfa *et al.*, 2003). Deregulated synthesis of plasticity related proteins may serve as an explanation for the increased mGluR-LTD observed in *Fmr1* knockout mice (Bear *et al.*, 2004). *Fmr1* knockout mice phenocopy behavioural aspects seen with Fragile X patients, including learning and memory deficits, behavioural rigidity and susceptibility to seizures (Kooy *et al.*, 1996; D'Hooge *et al.*, 1997; Musumeci *et al.*, 2000).

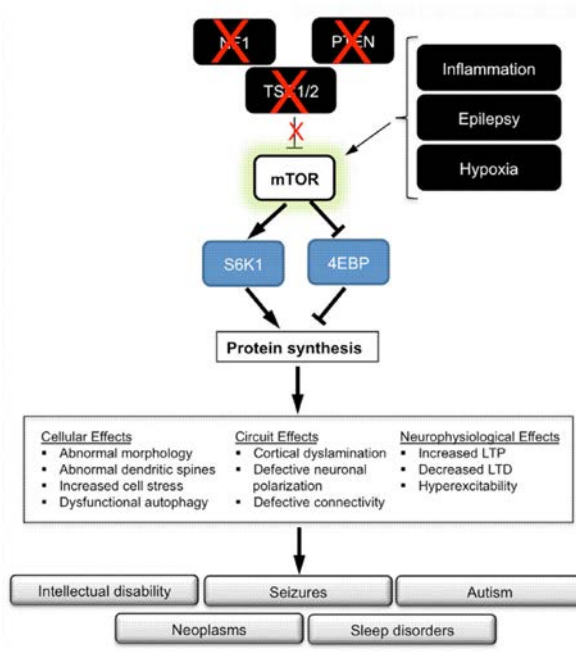

Figure 7: mTORC1 and neurodevelopmental disorders (adapted from (Lipton & Sahin, 2014)). Loss of upstream negative regulators of mTORC1, like TSC1/2 or PTEN, or excessive mTORC1 stimulation by environmental factors increases protein synthesis and affects other cellular processes, which impairs brain development and results in clinical symptoms.

Fragile X syndrome is linked to mTOR signalling because *Fmr1* knockout mice reveal increased mTORC1 signalling possibly due to elevated levels of the PI3K enhancer (PIKE, a predicted FMRP target), which triggers PI3K-Akt signalling that converges on mTORC1 (Sharma *et al.*, 2010). Additionally, the mTORC1 downstream target S6K1 phosphorylates and controls mRNA binding activity of FMRP (Narayanan *et al.*, 2008), which adds more complexity to the role of mTORC1 in the Fragile X syndrome (see also Fig. 6).

3.3.4.2. Psychiatric diseases

Depression. Depression is a mental disorder characterized by sadness, anhedonia, fatigue, insomnia, abnormal appetite and difficulties in concentrating (Krishnan & Nestler, 2008). Treatment of depressive patients with low doses of the NMDA receptor antagonist ketamine is found to alleviate depression (Berman *et al.*, 2000; Zarate *et al.*, 2006). Interestingly, ketamine treatment transiently increases mTORC1 signalling. Moreover, in the presence of rapamycin the antidepressant effect of ketamine gets lost (Li *et al.*, 2010), which ascribes mTORC1 an important role in the treatment of

depressions using ketamine. Given the positive effect of NMDA receptor activation on mTORC1 activity (see section 3.3.2), it is counterintuitive to find that the NMDA receptor antagonist ketamine increases mTORC1 signalling and, hence, it is questionable whether mTORC1 stimulation is a direct downstream effect of the antagonized NMDA receptor.

Schizophrenia. Schizophrenia is a severe mental disorder that manifests in delusions, hallucinations, unclear and confuse thinking and behaviour (Fanous & Kendler, 2008). Genetic forms of schizophrenia have been linked to mutations in the *Akt1* gene and also biochemical analysis of post-mortem brain samples of schizophrenic patients revealed a downregulation of Akt protein levels (Emamian *et al.*, 2004; Zhao *et al.*, 2006). In line with other evidence (Kalkman, 2006), these findings ascribe Akt a crucial role in this neuropsychiatric disorder. Although mTORC1 is downstream of Akt, its involvement in schizophrenia remains uncharacterized. On the other hand, mTORC2 that notably phosphorylates and co-translationally stabilizes Akt (see section 3.2.2) has been reported to be relevant for schizophrenia. Whole brain inactivation of mTORC2 results in mice with sensorimotor gating deficits, a hallmark for schizophrenia (Siuta *et al.*, 2010; van den Buuse, 2010). mTORC2 ablation in the brain decreases phosphorylation of Akt at Ser473, which is paralleled by, and probably causes, an increase in the surface expression of the norepinephrine transporter (NET). Suita and colleagues suggest that the increased NET surface expression may result in enhanced dopamine uptake in noradrenergic neurons where it is converted to norepinephrine, which in turn may explain the cortical hypodopaminergia seen in mTORC2-deficient brains. Aberrant dopamine levels in the cortex are thought to contribute to certain aspects of schizophrenia, for example negative symptoms that include deficits in normal thought processes or emotional responses (Davis *et al.*, 1991; Howes & Kapur, 2009).

3.3.4.3. Neurodegenerative diseases

Alzheimer. Alzheimer is a neurodegenerative disease that results in dementia and is characterized by plaques of amyloid β (Aβ) aggregates and the presence of tau tangles (Benilova *et al.*, 2012). Studies examining Alzheimer-diseased brains have reported enhanced mTORC1 signalling in these brains (An *et al.*, 2003; Li *et al.*, 2004; Griffin *et al.*, 2005; Li *et al.*, 2005). Additional studies positively correlate activity of the mTORC1 downstream target S6K1 with the phosphorylation and expression of Tau (An *et al.*, 2003; Pei & Hugon, 2008). Hence, it has been hypothesized that augmented mTORC1 activity might contribute to Alzheimer's disease by increasing levels of toxic proteins like Tau (Fig. 8). Recently, it has been suggested that regulation of autophagy by mTORC1 is relevant for this disease (see section 3.1.1). In a mouse model of Alzheimer's disease, rapamycin was found to increase autophagy and reduce Aβ and rescue memory impairment (Spilman *et al.*, 2010).

Currently, mTORC1 regulation in Alzheimer's disease is controversially discussed (Swiech *et al.*, 2008). Unlike observed in samples of human diseased brains, mTORC1 signalling has been reported to be decreased in an Alzheimer's disease mouse model (Lafay-Chebassier *et al.*, 2005; Ma *et al.*, 2010). Also, expression of Aβ, the major pathogenic agent of Alzheimer's disease, causes a downregulation of mTORC1 signalling in neuroblastoma cells (Lafay-Chebassier *et al.*, 2005). Given this heterogeneous picture of mTORC1 regulation in different models of this disease, it is difficult to analyse how mTORC1 is involved in Alzheimer's disease.

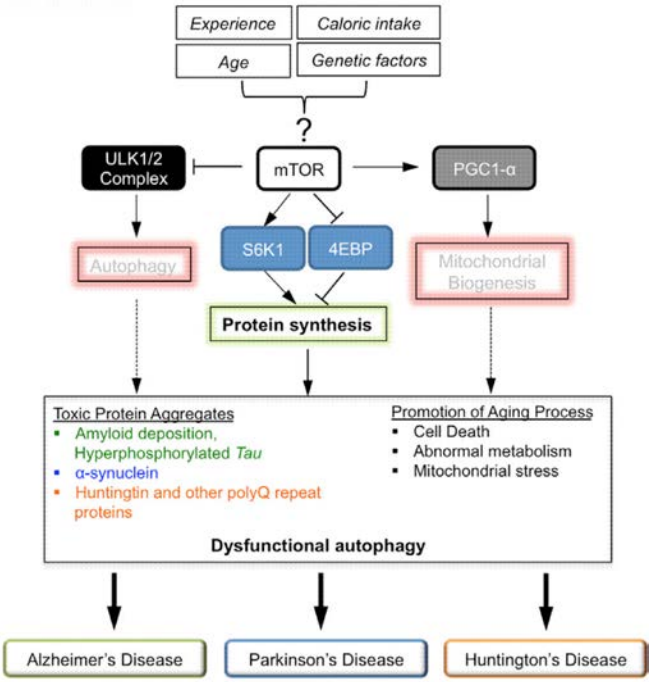

Figure 8: mTORC1 and neurodegenerative diseases (adapted from (Lipton & Sahin, 2014)). mTORC1 signalling is changed in the listed neurodegenerative disorders. The figure provides a model how mTORC1 may be involved in these disorders. Most strikingly, impaired autophagy is associated with many neurodegenerative disorders.

Parkinson. Patients suffering from Parkinson's disease show motor symptoms like tremor, rigidity and bradykinesia, which is the consequence of a progressive loss dopamine producing neurons in the substantia nigra pars compacta (Parkinson, 2002). Postmortem studies of the substantia nigra of Parkinson's disease patients revealed an increased expression of the stress response protein REDD1 that is a negative regulator of mTORC1 (see section 3.1.2). Moreover, it has been demonstrated that REDD1 is upregulated in cellular models upon treatment with Parkinson inducing agents and a knockdown of REDD1 protects against cell death in these cellular Parkinson's disease models (Malagelada *et al.*, 2006; Malagelada *et al.*, 2008). Based on these findings, it has been suggested that REDD1-mediated downregulation of mTORC1 activity accounts for neurodegeneration in Parkinson's disease. Unexpectedly, a subsequent study of the same research group showed that rapamycin treatment has a beneficial effect on the survival of dopaminergic neurons in the substantia nigra of a Parkinson's disease mouse model (Malagelada *et al.*, 2010). The same study also showed that translation of REDD1 depends on mTORC1 as it is sensitive to rapamycin treatment, which may explain the positive effect of rapamycin on the survival of dopaminergic neurons in Parkinson's disease. However, taken together these findings anticipate a complex role of mTORC1 signalling in the pathology of Parkinson's disease.

As described for Alzheimer's, also in Parkinson's disease mTORC1-regulated autophagy seems to be disease relevant. In an *in vitro* model for degenerating dopaminergic neurons, rapamycin treatment

reduced apoptosis. Interestingly, this anti-apoptotic effect of rapamycin was abolished when autophagy was blocked, which indicates that rapamycin might excerpt its positive on survival by inducing autophagy (Pan *et al.*, 2009). Moreover, α-synuclein that is found to be mutated in inherited forms of Parkinson's disease can be degraded by autophagy (Webb *et al.*, 2003). Accumulation and aggregation of α-synuclein is a hallmark of Parkinson's disease (Kahle *et al.*, 2002) and rapamycin has been shown to increase clearance of α-synuclein, offering a possible venue for a therapeutic approach in Parkinson's disease (Webb *et al.*, 2003; Spencer *et al.*, 2009) (Fig. 8).

Huntington. Huntington's disease is a genetic disease caused by an expansion of CAG trinucleotide repeats in the *huntingtin* gene, which results in a huntingtin protein with an abnormally long polyglutamine tract at the N-terminus (MacDonald *et al.*, 1993). Polyglutamine extended huntingtin proteins tend to aggregate, thereby forming intracellular inclusions, and cause neuronal dysfunction and neurodegeneration in a yet poorly understood manner. Dysfunction and degeneration of neurons is paralleled by symptoms like cognitive deficits and involuntary movements (Davies *et al.*, 1997; Walker, 2007). mTOR is sequestered by the intracellular aggregates seen in brain tissue of Huntington's disease patients and mouse models of this disease. This sequestration is paralleled by reduced mTORC1 signalling evidenced by decreased phosphorylation of 4E-BP1 and increased autophagy (Ravikumar *et al.*, 2004). Last is probably a mechanism that helps to protect the cell from toxic effects of the mutant huntingtin. Indeed, the huntingtin protein can be degraded by autophagy (Ravikumar *et al.*, 2002) and an application of rapamycin before disease onset in a Huntington's disease mouse model reduces the number of intracellular inclusions and ameliorates behavioural deficits seen with these mice (Ravikumar *et al.*, 2004). Next to its stimulating effect on autophagy, rapamycin treatment may convey its protective effect also by reducing the protein synthesis, thereby diminishing the production of the pathogenic huntingtin mutant protein (King *et al.*, 2008) (Fig. 8).

3.4. The cerebellum and Purkinje cells

This section provides an introduction to the anatomy, development and functions of the cerebellum with a strong focus on Purkinje cells that are considered as key neurons of the cerebellum. A summary on the current knowledge about the role of mTOR signalling in Purkinje cells is also included in this section and precedes the chapter that finally defines the aim of this thesis.

3.4.1. Anatomy of the cerebellum

The cerebellum is a part of the hindbrain and is positioned dorsal to the pons and the medulla and is connected to the rest of the central nervous system via large fibre bundles called the cerebellar peduncles. Along its mediolateral axis, the cerebellum is divided into four different regions that include the flocculus/paraflocculus that are localized most laterally, followed by the hemisphere, the paravermis and the vermis (Fig. 9). Parasagittal cerebellar sections reveal that the cerebellum is foliated and consists of ten lobes that are numbered from the anterior to the nodular part (Voogd & Glickstein, 1998; Sillitoe & Joyner, 2007). The basic architecture of the lobes is the same throughout the cerebellum and consists of different layers (Fig. 9 and 10). The core of the lobe is composed of white matter (WM) that is flanked by the granule cell layer (GCL). On top of the GCL, a monolayer of Purkinje cell somata is found, called the Purkinje cell layer (PCL), that is followed by the most outward molecular layer (ML). Together, these three layers make up the cerebellar cortex (Welker, 1990). The granule cell layer consists mainly of numerous excitatory granule neurons but it also contains unipolar brush cells (UBCs) and

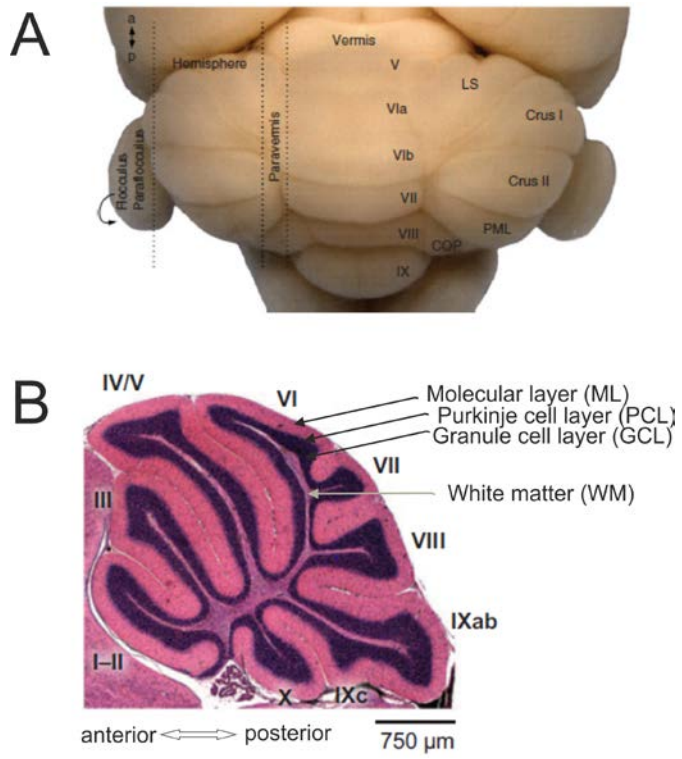

Figure 9: Anatomy of the cerebllum. A, Dorsal view on the cerebellum that is divided along the mediolateral axis into different regions: vermis, paravermis, hemisphere, flocculus/paraflocculus (adapted from (White & Sillitoe, 2013))**. B,** Haematoxylin eosin staining of a parasagittal slice of the cerebellum of a C57/BL6 mouse. The cerebellar cortex is foliated and consists of different lobes that are labelled with roman numbers. Each lobe consists of the indicated layers (adapted from (Sillitoe & Joyner, 2007)).

inhibitory neurons, such as the Golgi and Lugaro cells (Fig. 10) (Mugnaini *et al.*, 1997; White & Sillitoe, 2013). As mentioned above, the Purkinje cell layer primarily consists of aligned Purkinje cell somata, yet, in the same layer also somata of Bergmann glia and candelabrum cells are found (Laine & Axelrad, 1994; Voogd & Glickstein, 1998). The molecular layer is largely made up by dendritic trees of Purkinje cells, axons of granule cells (the so called parallel fibres) and fibres of Bergmann glia. In addition, the molecular layer hosts inhibitory neurons like the basket and stellate cells (Voogd & Glickstein, 1998; White & Sillitoe, 2013).

3.4.2. The major cerebellar circuits

The inhibitory Purkinje cells are considered the principal neurons of the cerebellar cortex since they provide its sole output by projecting to the deep cerebellar nuclei (DCN) and the vestibular nuclei as described further below (Fig. 10). Purkinje cells integrate signals from various inputs. Excitatory input is provided to Purkinje cells via two different sources, the climbing fibres and parallel fibres that convey signals of the inferior olive or the mossy fibre relay system, respectively (Fig. 11) (Sillitoe & Joyner, 2007). The inferior olive neurons are located in the medulla oblongata of the brainstem and project axons, called climbing fibres, to the cerebellum that terminate at the Purkinje cells by wiring their dendritic tree. An axon of the inferior olive provides in average climbing fibres for six to seven Purkinje cells that are located in the same sagittal plane (Sugihara *et al.*, 2001; Sugihara, 2006). An adult Purkinje cell is typically innervated by only one climbing fibre that provides strong excitatory input and causes a profound depolarization when activated (Hashimoto *et al.*, 2009b).

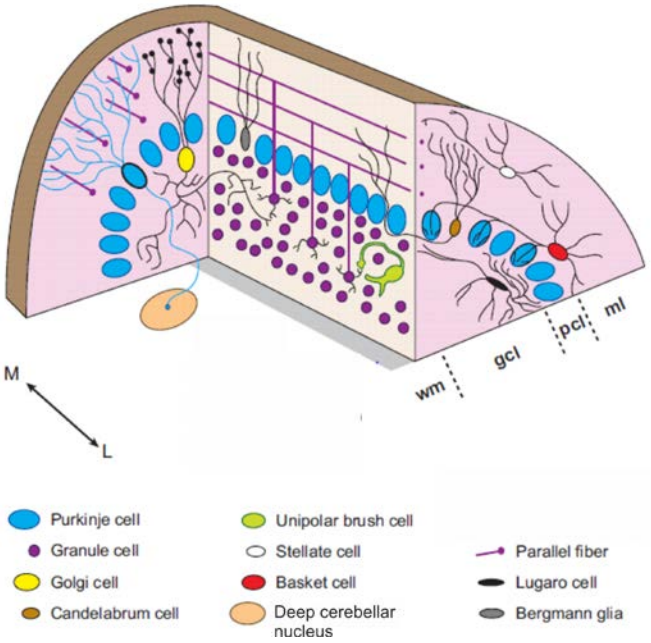

Figure 10: Cellular composition of the cerebellum (adapted from (Sillitoe & Joyner, 2007)). ML: molecular layer; PCL: Purkinje cell layer; GCL: granule cell layer; WM: whiter matter; M: medial; L: lateral.

On the other hand, each Purkinje cell forms synaptic connections with about 100'000 parallel fibres that are axons of excitatory granule cells. Axons of granule cells ascend from the GCL to the ML where they bifurcate and run in a perpendicular manner to the planar and parasagittally oriented dendritic trees of Purkinje cells. Consequently, a single parallel fibre connects to multiple Purkinje cells (Fig. 10 and 11). Granule cells, in turn, receive input from mossy fibres that transmit signals from

many different regions of the brain (vestibular nuclei, external cuneate nucleus, pontine nuclei; last provide input from the cerebral cortex) and spinal cord to the cerebellum (Voogd & Glickstein, 1998; Sillitoe & Joyner, 2007).

Parallel fibres of granule cells also form synaptic connections with inhibitory interneurons, such as Golgi, stellate and basket cells. Stellate and basket cells, that are also summarized as molecular layer interneurons (MLIs), project to the somata or dendritic parts of Purkinje cells, respectively (Fig. 11). Because parallel fibres innervate both Purkinje cells and MLIs, last can limit the excitatory input of parallel fibre synapses onto Purkinje cells by a feed-forward inhibition (Mittmann *et al.*, 2005). Moreover, MLIs excerpt lateral inhibition by projecting to Purkinje cells located in the same sagittal plane (Cohen & Yarom, 2000). Together, these means allow the MLIs to increase the temporal precision of Purkinje cell action potentials and sharpen the Purkinje cell output. On the other hand, the Golgi cells in the granule cell layer can regulate excitatory input of the mossy fibres (D'Angelo *et al.*, 2013) (Fig. 11).

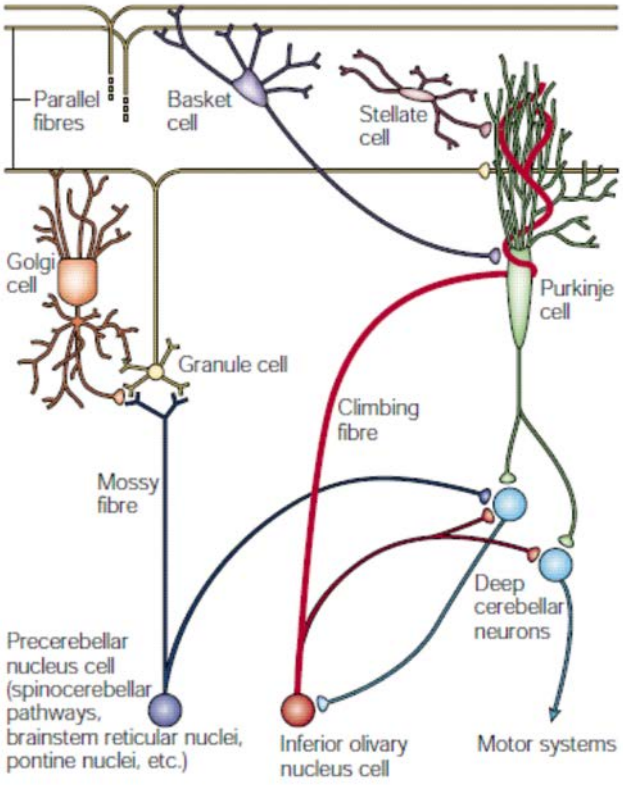

Figure 11: Synaptic connections of the neurons in the cerebellum (adapted from (Wang & Zoghbi, 2001)).

In summary, Purkinje cells integrate input from various sources and subsequently convey the processed information to the DCN and vestibular nuclei. These structures control the final output of the cerebellum and project to the brainstem and via the thalamus to the premotor and motor cortex, thereby allowing the cerebellum to excerpt its well known role in motor control as described in the following section (Voogd & Glickstein, 1998; Purves *et al.*, 2008).

3.4.3. The role of the cerebellum in normal and pathological conditions

Already decades ago, lesion studies in various animal models revealed that in the absence of the cerebellum compound movements, such as walking, can be performed, yet, in an imprecise and unsure manner. Further studies led to the suggestion that the basic program for compound movements may come from the cerebral cortex while the cerebellum is needed to modify and refine it and, hence, the cerebellum is important for movement control (Allen & Tsukahara, 1974; Fetz, 1993; Purves *et al.*,

2008). Prominent signs of cerebellar damage are for example impaired balance and gait alterations (Morton & Bastian, 2004) but also disturbed motor learning (Glickstein & Yeo, 1990; Raymond *et al.*, 1996). Given these crucial functions for motor behaviour, the cerebellum is linked to motor diseases.

Ataxia is a general term for a lack of voluntary coordination of muscle movements and can have various reasons, such as alcoholism, multiple sclerosis, stroke or metabolic diseases. However, the most common form of ataxia is cerebellar ataxia, which includes genetic diseases like spinocerebellar ataxias, Friedrich's ataxia or Fragile X associated ataxia/tremor syndrome (Durr, 2010; Klockgether, 2010). Cerebellar ataxia is typically paralleled by neurodegeneration, in particular by Purkinje cell degeneration (Burright *et al.*, 1995; Hamilton *et al.*, 1996; Serra *et al.*, 2006; Reeber *et al.*, 2013) that causes or at least contributes to the concomitant motor deficits (Liu *et al.*, 2009). Recent studies have demonstrated that Purkinje cell loss in ataxia mouse models is preceded by alterations of electrophysiological properties of Purkinje cells, which is paralleled by ataxic phenotypes as well, yet, moderate ones (Shakkottai *et al.*, 2011; Hansen *et al.*, 2013).

Dystonia is another movement disorder in which the cerebellum is involved. Dystonia is characterized by involuntary, sustained muscle contractions that cause abnormal postures and repetitive movements (Hallett, 2009). Purkinje cells of rodent models for dystonia show aberrant firing patterns in electrophysiological recordings (LeDoux, 2011). Interestingly, a Purkinje cell-specific knockout of the P/Q voltage-dependent calcium channel ($Ca_v2.1$) has been shown to be sufficient to trigger dystonic movements, further underlying the crucial role of these neurons in dystonia (Raike *et al.*, 2013).

Cerebellar lesions in humans are also found to be paralleled by emotional disturbances and/or cognitive deficits, which led to the notion that the cerebellum is relevant for non-motor functions and might be involved in neuropsychiatric and neurodevelopmental disorders (Schmahmann *et al.*, 2007; Stoodley *et al.*, 2012; Reeber *et al.*, 2013). Growing evidence ascribes the cerebellum a role in ASD (Wang *et al.*, 2014). For example, abnormal cerebellar activation is detected in ASD patients in fMRI studies (Allen *et al.*, 2004). Moreover, the number of Purkinje cells is reduced in post-mortem cerebellae of ASD patients (Bauman & Kemper, 2005; Whitney *et al.*, 2008; Fatemi *et al.*, 2012). Autistic individuals also show defects in multisensory learning tasks that require the cerebellum (Wang *et al.*, 2014). A classical sensory-motor learning task that crucially depends on the cerebellum is the eye-blink conditioning (Raymond *et al.*, 1996). An airpuff given to the cornea (unconditioned stimulus) evokes an eye-blink response. If this teaching stimulus is preceded by a neutral (conditional) stimulus, such as a tone, the organism starts to associate these two stimuli and after several repetitions the pure presentation of the conditioned stimulus is sufficient to evoke an eye-blinking. The teaching stimulus is conveyed to the cerebellum via the inferior olive that projects climbing fibres to the cerebellum while the conditioned stimulus reaches the cerebellum via the mossy fibre-parallel fibre axis.

Synaptic plasticity events occurring at the parallel fibre-Purkinje cell synapses are thought to underlie such sensory-motor learning as discussed in section 3.4.5. Abnormal eye-blink conditioning is observed in autistic patients (Sears *et al.*, 1994; Smit *et al.*, 2008; Tobia & Woodruff-Pak, 2009; Oristaglio *et al.*, 2013) as well as mouse models of Fragile X (Koekkoek *et al.*, 2005).

How the cerebellum may contribute to non-motor functions of the cerebellum is currently poorly understood. However, it is assumed that the cerebellar connections to the thalamus and cortex (see section 3.4.2 and Fig. 12) may be crucial for these functions (Strick *et al.*, 2009; Wang *et al.*, 2014).

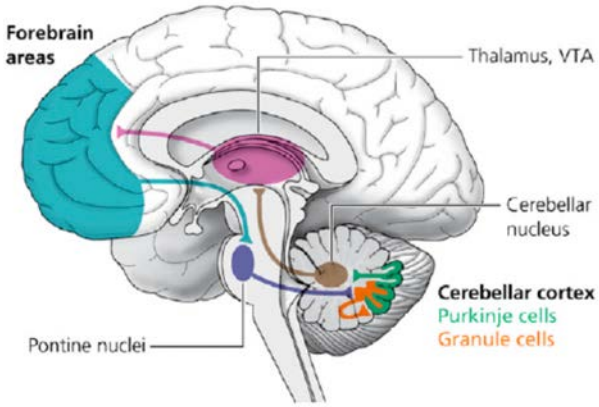

Figure 12: Cerebello-thalamo-cortical loop in the human brain (adapted from (Wang *et al.*, 2014)). Due to its connectivity to the thalamus and cortex the cerebellum may influence also non-motor functions next to its well described role in motor control.

3.4.4. Purkinje cell development

In mice, the cerebellum starts to develop at embryonic day 9 (E9) from the dorsal rhombomere 1 of the developing hindbrain (Sillitoe & Joyner, 2007; Martinez *et al.*, 2013). Cerebellar cells derive from two germinal matrices in the developing cerebellum, the ventricular zone (VZ) and the rhombic lip (RL) that generate basically inhibitory or excitatory neurons, respectively (Wingate & Hatten, 1999; Butts *et al.*, 2011) (Fig. 13). Already between E10-13 the first cerebellar neurons become postmiotic starting with excitatory neurons of the cerebellar nuclei closely followed by inhibitory Purkinje cells (Miale & Sidman, 1961; Pierce, 1975). Postmitotic Purkinje cells that are detected by gene expression at about E14 (Oberdick *et al.*, 1993; Hatten & Heintz, 1995; Morales & Hatten, 2006; Miyata *et al.*, 2010) subsequently undergo migration (Fig. 13). This migration apparently is guided by radial glia cells (Edwards *et al.*, 1990; Morales & Hatten, 2006) and occurs in a radial manner around the already formed DCN. Purkinje cell migration is paralleled by axogenesis as they leave axons behind in their target zone, the DCN (Sillitoe *et al.*, 2009; Miyata *et al.*, 2010). Previous to the formation of the Purkinje cell monolayer that is established at postnatal day 4/5 (P4/5) (Altman, 1972; Kapfhammer, 2004) a multilayer of Purkinje cells is formed below the external granule layer (EGL).

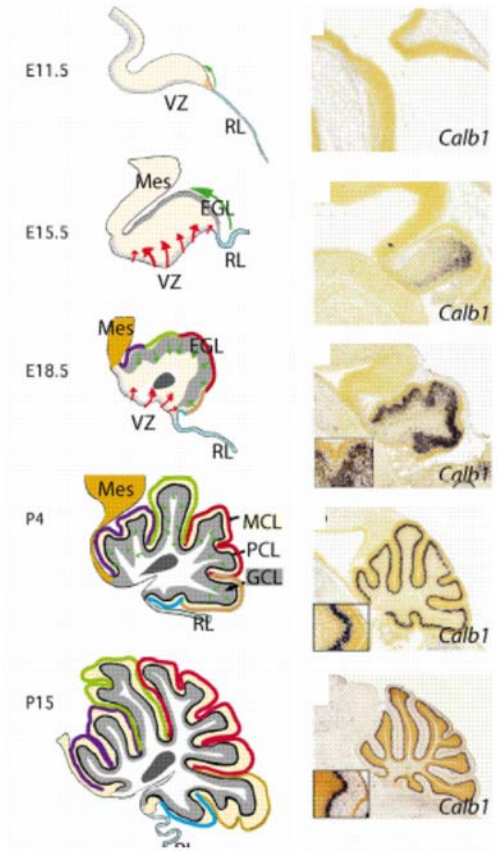

Figure 13: Development of the cerebellum (adapted from (Martinez *et al.*, 2013)). The left column depicts a schematic illustration of the cerebellar development. Each row indicates a different time point during development. The right column shows *in situ* hybridization analysis of the cerebellum at the indicated time points using probes against the Purkinje cell marker calbindin.

The EGL is established by granule cell precursors that derive from the rhombic lip and migrate over the outer surface of the cerebellum (Fig. 13). First postmitotic cells can be identified in the EGL at P0 (Fujita, 1967). The EGL can be subdivided in two distinct zones, an outer proliferative and inner premigratory zone. Cells in the premigratory zone grow processes that finally become parallel fibres. Once the parallel fibre projections have reached an optimal length, the granule cell somata descend vertically beneath the Purkinje cell layer to form the internal granular layer (IGL). First functional parallel fibre-Purkinje cell synapses can be detected at P6 and by P14 most of the granule cell somata are located in the IGL (Scelfo & Strata, 2005).

A big part of the Purkinje cell development occurs postnatally. At birth the Purkinje cells are polarized as they possess an axon and a single, smooth dendrite. This state of Purkinje cell is referred to as "fusiform" (Sotelo, 2004) (Fig. 14). During the first postnatal week the polarization of the fusiform becomes reduced as additional dendritic processes arise from the somata in any direction. These first postnatal days do not include a strong net growth of the dendritic tree but are characterized by an extensive remodelling of these dendritic processes (Kapfhammer, 2004). In contrary to the dendritic tree, the somata of Purkinje cells expand during this first period of postnatal Purkinje cell development. By about P10, the number of primary dendrites is reduced to a single one, which is followed by a rapid dendritic growth and branching that lasts up to P15 (Sotelo & Dusart, 2009). During this phase also the plane orientation of the dendritic tree is achieved. In a third phase, an additional slow growth of the Purkinje cell dendritic tree, as well as a refinement thereof, is observed and at the end of the third postnatal week the Purkinje cell development is largely completed (Hendelman & Aggerwal, 1980; Sotelo & Dusart, 2009).

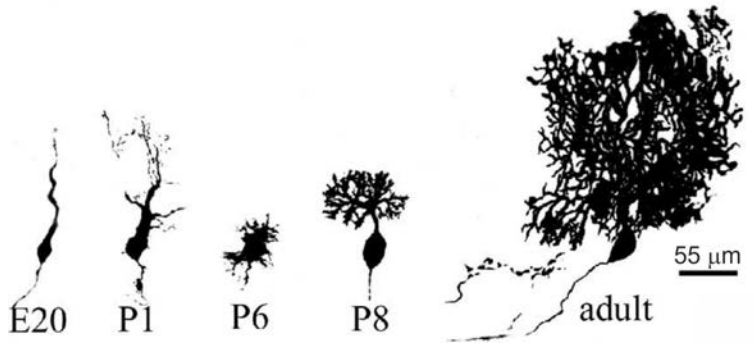

Figure 14: Development of Purkinje cells (adapted from (Sotelo, 2004)). Morphology of rat Purkinje cells at different time points during postnatal development.

In course of postnatal Purkinje cell development not only their morphology but also synaptic input is shaped. Importantly, the mono innervation of Purkinje cells by climbing fibres is established in parallel to dendritogenesis. Axonal projections of the inferior olive form first contacts with Purkinje cells at E19 (Wassef *et al.*, 1992; Morara *et al.*, 2001). At P2 multiple olivo-cerebellar axons, that at this age not yet have the typical climbing fibre morphology, are located at somata of the Purkinje cells. This stage is referred to as the "creeper stage" (Chedotal & Sotelo, 1993) (Fig. 15). Electrophysiological recordings detect functional olivo-cerebellar synapses onto Purkinje cells at around P3 (Crepel, 1971; Woodward *et al.*, 1971) and confirm that they are innervated by multiple climbing fibres (four or even more) of similar synaptic strength (Crepel *et al.*, 1976; Hashimoto & Kano, 2005). In the time period between P3 and P7, a single climbing fibre becomes selectively strengthened, which is assumed to occur upon synaptic competition, but still weaker climbing fibres are present (Hashimoto & Kano, 2003; Hashimoto *et al.*, 2009a). Morphologically, the climbing fibres form a nest-like structure on the lower part of the Purkinje cell somata between P5 and P9 and therefore this stage is referred to as the "pericellular nest stage" (Hashimoto & Kano, 2013) (Fig.15). Although by P6 a main primary dendrite starts to build, which is paralleled by a retraction of surplus perisomatic processes, climbing fibres do not start to translocate to dendritic parts at this point but reside at the Purkinje cell somata until about P9. Somatodendritic translocation of the climbing fibres

only starts at the “capuchon stage” (P8-9) that follows the “pericellular nest stage”. At the beginning of this climbing fibre translocation Purkinje cells are still innervated by surplus climbing fibres. Amongst these multiple climbing fibres only the strongest one translocates to the dendrite. In course of the somatodendritic translocation (Hashimoto *et al.*, 2009a; Carrillo *et al.*, 2013) surplus climbing fibres are eliminated, which occurs in two phases, an early (P8-11) and a late phase (P12-17) (Crepel *et al.*, 1981; Hashimoto *et al.*, 2009b) (Fig. 15). While the early phase of climbing fibre elimination is mechanistically poorly understood, the processes underlying late phase climbing fibre elimination are better characterized (Hashimoto & Kano, 2013). Last has been shown to depend on the parallel fibre input of granule cells. For example, pharmacological interruption of the mossy fibre-mediated stimulation of parallel fibres during P15-P16 impairs proper climbing fibre elimination (Kakizawa *et al.*, 2000). Parallel fibre input can activate mGluR1 (Finch & Augustine, 1998; Takechi *et al.*, 1998). Since a knockout of mGluR1, or any member of its signalling cascade ($G\alpha_q$, PLCβ4 or PKCγ), causes multiple climbing fibre innervation in adult mice, it has been suggested that parallel fibre-mediated mGluR1 activation is essential for proper late phase climbing fibre elimination. Notably, all these knockout mice also show motor coordination deficits, indicating that mono climbing fibre innervation of Purkinje cells is important for normal motor behaviour of adult mice (Chen *et al.*, 1995; Kano *et al.*, 1995; Kano *et al.*, 1997; Offermanns *et al.*, 1997; Kano *et al.*, 1998; Ichise *et al.*, 2000; Kano *et al.*, 2008).

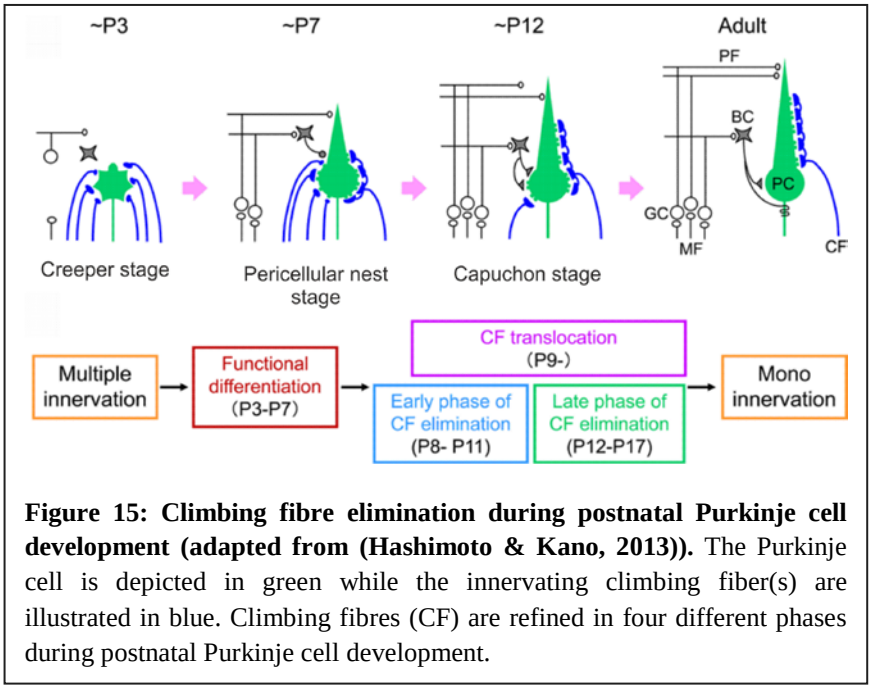

Figure 15: Climbing fibre elimination during postnatal Purkinje cell development (adapted from (Hashimoto & Kano, 2013)). The Purkinje cell is depicted in green while the innervating climbing fiber(s) are illustrated in blue. Climbing fibres (CF) are refined in four different phases during postnatal Purkinje cell development.

3.4.5. Synaptic plasticity of Purkinje cells

As described in section 3.3.2., synaptic connections between neurons are of plastic nature. Hippocampal synapses show bidirectional synaptic plasticity that bases on a kinase/phosphatase switch, which in turn is guided by postsynaptic levels of calcium e.g. a strong postsynaptic calcium influx activates CamKII and promotes LTP while a prolonged modest rise of postsynaptic calcium initiates LTD via PP1 (Yang *et al.*, 1999; Munton *et al.*, 2004). Also for the parallel fibre (PF)-Purkinje cell synapses calcium-dependent bidirectional plasticity is observed although in an "inverse" manner. LTP at the PF-Purkinje cell synapses can be induced by low frequency stimulation of PF synapses, which only moderately increases postsynaptic calcium levels (Lev-Ram *et al.*, 2002; Coesmans *et al.*, 2004). Via calmodulin the transient postsynaptic calcium increase activates protein phosphatase 2B (PP2B) that is essential for this form of LTP (Schonewille *et al.*, 2010). Also the protein phosphatases PP1 and PP2A, but not the kinases CamKII and PKC, are involved in PF-Purkinje cell synapse LTP (Belmeguenai & Hansel, 2005; Kakegawa & Yuzaki, 2005; Hansel *et al.*, 2006; Schonewille *et al.*, 2010).

The bidirectional plasticity of the PF-Purkinje cell synapses has nicely been demonstrated by Coesmans and colleagues who have shown that climbing fibre activity can reverse the PF-Purkinje cell synapse LTP into LTD (Coesmans *et al.*, 2004). Climbing fibre stimulation and the concomitant strong depolarization of Purkinje cells causes calcium influx via voltage-gated calcium channels (VGCCs) in the plasma membrane. This, in conjunction with stimulation of afferent parallel fibres weakens the strength of the PF-Purkinje cell synapses by causing an internalization of the AMPA receptors (Fig. 16) (Ito & Kano, 1982; Matsuda *et al.*, 2000; Wang & Linden, 2000; Linden, 2001). Combined activation of climbing fibre and PF synapses not only opens VGCCs but also stimulates AMPA and mGluR1 receptors, which results in the generation of diacylglycerol (DG) and inositol 1,4,5-trisphosphate (IP3) due to mGluR1-mediated activation of phospholipase C. The generated IP3 additionally increases

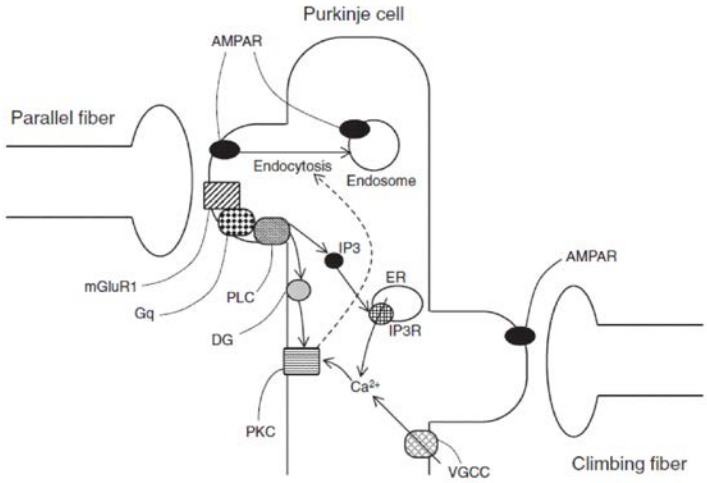

Figure 16: Model for parallel fiber-Purkinje cell synapse LTD (adapted from (Hirano, 2013)). Simultaneous stimulation of parallel fiber and climbing fiber synapses results in a strong calcium influx and internalization of AMPAR at the parallel fiber synapses. AMPAR: AMPA receptor; mGluR1: metabotropic glutamate receptor 1; Gq: Gq protein; PLC: phospholipase C; DG: diacylglycerol; PKC: protein kinase C; IP3: inositol 1,4,5-trisphosphate; IP3R: IP3 receptor; VGCC: voltage-gated calcium channel; ER: endoplasmic reticulum.

cytosolic calcium by releasing it from the endoplasmatic reticulum, which results in large postsynaptic calcium signals (>10 μM (Wang *et al.*, 2000)). Under these conditions (strongly elevated calcium levels and generated DG) PKCα as well as CamKII become activated, both of which have been shown to be essential for PF-Purkinje cell synapse LTD (Leitges *et al.*, 2004; Hansel *et al.*, 2006; Tsuruno & Hirano, 2007; van Woerden *et al.*, 2009). While the role of CamKII in this form of LTD is poorly understood, PKCα seems to be important for AMPA receptor internalization by phosphorylating the GluR2 subunit of AMPA receptors (Chung *et al.*, 2003). Phosphorylation of GluR2 at Ser880 by PKCα regulates the clustering of the AMPA receptors by reducing their binding to glutamate receptor-interacting proteins (GRIP) (Matsuda *et al.*, 1999), thereby facilitating an interaction with the protein-interacting with C kinase 1 (PICK1) that promotes clathrin-mediated endocytosis of AMPA receptor (Wang & Linden, 2000; Xia *et al.*, 2000).

PF-Purkinje cell synapse LTD has been proposed to be the cellular correlate for motor learning (see also section 3.4.3.) (Marr, 1969; Albus, 1971). In line with this theory, motor learning deficits have been shown to positively correlate with defective cerebellar LTD (Aiba *et al.*, 1994; De Zeeuw *et al.*, 1998; Hirano, 2006). However, other studies have challenged the same theory more recently since they report normal motor learning despite impaired LTD (Welsh *et al.*, 2005; Schonewille *et al.*, 2011). Therefore, the relevance of PF-LTD for motor learning is currently controversially discussed. Other evidence indicates that motor learning depends on LTP of PF-Purkinje cell synapses. For example, Purkinje cell-specific knockout of PP2B impairs both LTP and motor learning while it does not affect LTD (Schonewille *et al.*, 2010).

Synaptic plasticity is not only observed for the excitatory parallel fibre synapses but also for inhibitory synapses formed by the molecular layer interneurons (MLIs, see section 3.4.2.) with Purkinje cells. Climbing fibre stimulation of Purkinje cells can cause a calcium-dependent potentiation of the amplitude of spontaneous inhibitory postsynaptic currents (IPSCs). This form of synaptic plasticity is referred to as rebound potentiation (Kano *et al.*, 1992; Kano *et al.*, 1996; Kawaguchi & Hirano, 2002). An upregulation of $GABA_A$ receptor ($GABA_AR$) activity in Purkinje cells is underlying rebound potentiation, which depends on CamKII activity (Kano *et al.*, 1996; Kawaguchi & Hirano, 2007; Kitagawa *et al.*, 2009). CamKII may influence $GABA_AR$ by directly phosphorylating their β and γ2 subunits (Moss & Smart, 1996; Houston *et al.*, 2009) and/or by causing a conformational change of the $GABA_AR$ associated protein (GABARAP) that binds the γ2 subunit of $GABA_AR$ (Wang *et al.*, 1999; Kawaguchi & Hirano, 2007). While the role of CamKII-mediated phosphorylation of β and γ2 subunits in rebound potentiation is elusive, the binding of $GABA_AR$ to GABARAP is needed for induction of rebound potentiation (Kawaguchi & Hirano, 2007). Based on the analysis of inhibitory synapse plasticity of other brain regions, it has been speculated that GABARAP might induce rebound potentiation by supporting the transport of $GABA_AR$ to the cell membrane (Marsden *et al.*, 2007; Hirano & Kawaguchi, 2014). Alternatively, GABARAP might affect the channel conductance or open time of $GABA_AR$ (Everitt *et al.*, 2004; Luu *et al.*, 2006).

Recent evidence demonstrates that transgenic mice with defective rebound potentiation show motor learning deficits, indicating that climbing fibre-dependent plasticity of GABAergic synapses of Purkinje cells is important for cerebellar motor learning (Tanaka *et al.*, 2013; Hirano & Kawaguchi, 2014).

3.4.6. mTOR signalling in Purkinje cells

According to the Allen Brain Atlas, the genes encoding for mTOR, raptor or rictor are all expressed in Purkinje cells (Lein *et al.*, 2007). Properly controlled activation of mTORC1 in Purkinje cells has recently been demonstrated to be essential for their survival since a conditional knockout of TSC1 or TSC2 in Purkinje cells results in an age-dependent loss of these neurons by apoptosis. Previous to their death, knockout Purkinje cells reveal enlarged somata with signs of endoplasmatic reticulum and oxidative stress (Reith *et al.*, 2011; Tsai *et al.*, 2012). The age-dependent loss of Purkinje cells upon knockout of either TSC1 or TSC2 is paralleled by motor coordination deficits (Tsai *et al.*, 2012; Reith *et al.*, 2013). Treatment of Purkinje cell-specific TSC1 or TSC2 knockout mice with rapamycin largely rescues Purkinje cell degeneration and the accompanying motor coordination deficits, demonstrating the mTORC1-dependence of these phenotypes (Reith *et al.*, 2011; Tsai *et al.*, 2012). Interestingly, disruption of the TSC complex in Purkinje cells is sufficient to cause autistic-like phenotypes in mice, including repetitive behaviour and social abnormalities (Tsai *et al.*, 2012; Reith *et al.*, 2013). Also these phenotypes are sensitive to rapamycin treatment. These findings support the role of the cerebellum, in particular the Purkinje cells, in non-motor functions of the brain and ascribe mTORC1 an important role therein (see section 3.4.3.). The fact that a heterozygous loss of TSC1 in Purkinje cells does not result in apoptosis but still causes autistic-like deficits indicates that other reasons than Purkinje cell loss account for this kind of behavioural phenotype (Tsai *et al.*, 2012). Electrophysiological recordings did not reveal significant changes of the synaptic input of TSC1-knockout Purkinje cells although on the morphological level the spine density of these neurons is significantly increased. However, the intrinsic excitability of heterozygous TSC1-knockout Purkinje cells, that notably have a normal soma size, is reduced (Tsai *et al.*, 2012). Tsai and colleagues suggest that this reduced Purkinje cell excitability may underlie the autistic-like behaviour of these conditional knockout mice by changing the Purkinje cell firing rate, which ultimately may affect the cerebellar output. Although this is a possible scenario, mTORC1-dependent mechanisms in Purkinje cells contributing to autistic-like deficits clearly need further investigation.

In addition to mTORC1, also mTORC2 seems to be crucial for Purkinje cells. Ablation of mTORC2 in neural progenitor cells results in a striking cerebellar phenotype, including morphological changes of Purkinje cells and ataxic motor behaviour. Purkinje cells of these knockout mice show a reduction in the soma size and often possess more than a single primary dendrite. Moreover, the excitatory and inhibitory synaptic input of these Purkinje cells is reduced (Thomanetz *et al.*, 2013).

4. Aim of this thesis

The overall goal of this study was to analyse and compare the roles of mTORC1 and mTORC2 in Purkinje cells by conditionally knocking out the genes encoding for raptor or rictor, respectively. For this purpose, mice possessing floxed *Rptor* or *Rictor* genes (Bentzinger *et al.*, 2008) were crossed with mice that express the Cre-recombinase under the *L7/Pcp-2* promoter whose activity is restricted to Purkinje cells and retinal cells (Saito *et al.*, 2005). *L7/Pcp-2*-driven knockout has been reported to start at about E18 and, hence, affects the postnatal development of Purkinje cells (Saito *et al.*, 2005). In a first step, this experimental approach was used to analyse whether the strong Purkinje cell phenotype observed in mice that have rictor conditionally knocked out in neural progenitor cells is cell autonomous in terms of morphology and synaptic input. In further steps, the effect of the Purkinje cell-specific rictor knockout on the mouse behaviour was addressed and mTORC2-dependent mechanisms underlying behavioural phenotypes were explored. In parallel, the same procedure was conducted with Purkinje cell-specific raptor knockout mice. This allowed us to directly compare and dissect roles of mTORC1 and mTORC2 in Purkinje cells. By knocking out raptor exclusively in Purkinje cells, we also aimed for a way to study the importance of mTORC1 in neurons of adult mice, which had been impossible to achieve with mice that have raptor knocked out in neural progenitor cells due to the perinatal death of these mice.

As outlined in section 3.3.3., mTOR signalling may not only be important for excitatory but also inhibitory synapses, however, only limited knowledge is currently available on this topic. Because Purkinje cells receive ubiquitous inhibitory input by stellate and basket neurons, the Purkinje cell-specific mouse lines described above were used to study the impact of mTORC1 and mTORC2 ablation on GABAergic synapses, which was performed in collaboration with the group of Jean-Marc Fritschy.

5. Results

5.1. Publication 1: *Ablation of the mTORC2 component rictor in brain or Purkinje cells affects size and neuron morphology.* Thomanetz, V.*, Angliker, N.*, Cloetta, D., Lustenberger, R.M., Schweighauser, M., Oliveri, F., Suzuki, N. & Ruegg, M.A. (2013) J Cell Biol, 201(2): 293-308.
*Equal contributions

Contributions:
The phenotype of mice that have mTORC2 conditionally ablated in the entire brain using a *nestin-Cre* driver was mainly analysed by Venus Thomanetz. The Purkinje cell-specific rictor knockout mice were used to confirm that the Purkinje cell phenotype seen in the whole brain rictor knockout mice can be recapitulated in terms of morphology and synaptic input. This publication also contains a validation of the *L7/Pcp-2* promoter-driven knockout of rictor in Purkinje cells.

5.2. Publication 2: *mTORC1 and mTORC2 have largely distinct functions in Purkinje cells.* Angliker, N., Burri, M., Zaichuk, M., Fritschy, J.M. and Rüegg, M.A. Manuscript submitted.

Contributions:
This publication describes the phenotype of mice that have rictor or raptor knocked out specifically in Purkinje cells. Michael Burri contributed to the analysis of Purkinje cell survival and degeneration and was involved in footprint analysis of these mice. Mariana Zaichuk performed the immunohistochemical analysis of the GABAergic input of raptor-knockout Purkinje cells.

Published April 8, 2013

Ablation of the mTORC2 component rictor in brain or Purkinje cells affects size and neuron morphology

Venus Thomanetz,[1] Nico Angliker,[1] Dimitri Cloëtta,[1] Regula M. Lustenberger,[1] Manuel Schweighauser,[1] Filippo Oliveri,[1] Noboru Suzuki,[2] and Markus A. Rüegg[1]

[1]Biozentrum, University of Basel, CH-4056 Basel, Switzerland
[2]Department of Animal Genomics, Functional Genomics Institute, Mie University Life Science Research Center, 2-174 Edobashi, Tsu, Mie 514-8507, Japan

The mammalian target of rapamycin (mTOR) assembles into two distinct multi-protein complexes called mTORC1 and mTORC2. Whereas mTORC1 is known to regulate cell and organismal growth, the role of mTORC2 is less understood. We describe two mouse lines that are devoid of the mTORC2 component rictor in the entire central nervous system or in Purkinje cells. In both lines neurons were smaller and their morphology and function were strongly affected. The phenotypes were accompanied by loss of activation of Akt, PKC, and SGK1 without effects on mTORC1 activity. The striking decrease in the activation and expression of several PKC isoforms, the subsequent loss of activation of GAP-43 and MARCKS, and the established role of PKCs in spinocerebellar ataxia and in shaping the actin cytoskeleton strongly suggest that the morphological deficits observed in rictor-deficient neurons are mediated by PKCs. Together our experiments show that mTORC2 has a particularly important role in the brain and that it affects size, morphology, and function of neurons.

Introduction

Mammalian target of rapamycin (mTOR) is a highly conserved serine/threonine protein kinase that controls cell and organismal growth induced by growth factors and nutrients (Wullschleger et al., 2006; Laplante and Sabatini, 2012). mTOR assembles into two distinct, multi-protein complexes, called mTOR complex 1 (mTORC1) and mTORC2, which can be distinguished by their associated proteins and their sensitivity to inhibition by the immunosuppressive drug rapamycin. Whereas rapamycin inhibits mTORC1 acutely, mTORC2 is not inhibited. However, more recent data indicate that prolonged treatment with rapamycin also inhibits mTORC2 (Sarbassov et al., 2006). Thus, some of the effects observed by the application of rapamycin might be mediated by mTORC2. Indeed, insulin resistance in patients that undergo long-term treatment with rapamycin (Cole et al., 2008) has recently been shown to be likely due to inhibition of mTORC2 and not of mTORC1 (Lamming et al., 2012). Thus, the only possibility to clearly distinguish between the function of mTORC1 and mTORC2 in vivo is the generation of mice that selectively lack components that are essential for the function of either mTORC1 or mTORC2.

One of the essential and unique components of mTORC1 is the protein raptor (regulatory associated protein of mTOR; Kim et al., 2002), whereas the protein rictor (rapamycin-insensitive companion of mTOR) is essential and unique for mTORC2 (Jacinto et al., 2004; Sarbassov et al., 2004). Several lines of evidence indicate that mTORC1 is mainly responsible for cell growth and proliferation in response to growth factors, nutrients, or stress, and the two main downstream targets of mTORC1, p70S6 kinase (S6K) and elongation factor 4E binding protein (4E-BP), are key regulators of cap-dependent protein translation (Wullschleger et al., 2006; Laplante and Sabatini, 2012). In contrast, the function of mTORC2 is much less well defined, but experiments in yeast and in cultured mammalian cells have indicated a role of mTORC2 in the regulation of the actin cytoskeleton (Loewith et al., 2002; Jacinto et al., 2004; Sarbassov et al., 2004). mTORC2 also controls phosphorylation of the hydrophobic motif of Akt/protein kinase B (Akt/PKB), protein

V. Thomanetz and N. Angliker contributed equally to this paper.

Correspondence to Markus A. Rüegg: markus-a.ruegg@unibas.ch

Abbreviations used in this paper: CNS, central nervous system; DIV, day in vitro; GAP43, growth-associated protein 43; GSK3, glycogen synthase kinase 3; MARCKS, myristoylated alanine-rich protein kinase C substrate; mEPSC, miniature excitatory postsynaptic current; mIPSC, miniature inhibitory postsynaptic current; mTOR, mammalian target of rapamycin; mTORC, mTOR complex; PKB, protein kinase B; RibKO, rictor brain knockout; rictor, rapamycin-insensitive companion of TOR; RiPuKO, rictor Purkinje cell knockout; SGK, serum- and glucocorticoid-induced kinase; vGLUT, vesicular glutamate transporter.

Supplemental Material can be found at:
http://jcb.rupress.org/content/suppl/2013/04/05/jcb.201205030.DC1.html

The Rockefeller University Press $30.00
J. Cell Biol. Vol. 201 No. 2 293–308
www.jcb.org/cgi/doi/10.1083/jcb.201205030

Published April 8, 2013

kinase C (PKC), and the serum- and glucocorticoid-induced kinase 1 (SGK1), which are all members of the AGC kinase family (Sarbassov et al., 2005; Facchinetti et al., 2008; García-Martínez and Alessi, 2008; Ikenoue et al., 2008).

Germline deletion of *rictor* in mice causes embryonic death (Guertin et al., 2006; Shiota et al., 2006), whereas tissue-specific deletion of *rictor* often results in only minor phenotypes. This is the case in skeletal muscle (Bentzinger et al., 2008; Kumar et al., 2008), adipose tissue (Cybulski et al., 2009), or kidney (Gödel et al., 2011). Importantly, in none of those conditional knockout mice have changes in the actin organization been observed. The rather weak phenotypes caused by *rictor* deletion are in stark contrast to the severe phenotypes observed upon deletion of *rptor* (gene encoding raptor) in the same tissues (Bentzinger et al., 2008; Polak et al., 2008; Gödel et al., 2011). Interestingly, double knockout of both *rptor* and *rictor* aggravate the phenotypes in kidney (Gödel et al., 2011) but not in skeletal muscle (Bentzinger et al., 2008). Moreover, skeletal muscle–specific deletion of *mTOR* largely resembles the phenotype of mice lacking raptor (Risson et al., 2009). These results therefore indicate that most of the known functions of mTOR in several tissues are carried by mTORC1 and that there are significant differences in the importance of mTORC1 and mTORC2 between tissues.

In the nervous system, mTOR has mainly been implicated in protein synthesis–dependent control of synaptic plasticity in learning and memory (Richter and Klann, 2009). More recently, mTOR has been suggested to be deregulated in developmental brain disorders and in neurodegenerative diseases (Crino, 2011). Interestingly, tuberous sclerosis (TSC) patients who suffer from a benign brain tumor caused by mutations in *TSC1* or *TSC2*, which encode proteins that form the main upstream inhibitor complex of mTORC1, frequently also show autism spectrum disorder-like symptoms (Ehninger and Silva, 2011). Thus, the evidence is strong that mTOR signaling is also important in the nervous system. The finding that deletion of the two mTORC1 downstream targets *S6K* or *4E-BP*, and that treatment of mice or rats with rapamycin also affects learning and memory, has resulted in the concept that mTOR in the brain mainly acts via mTORC1 and not mTORC2. Only very recent work has suggested roles of mTORC2 in the regulation of dopaminergic neurons in the adult brain (Siuta et al., 2010; Mazei-Robison et al., 2011). Both of those reports base their findings on the known role of Akt in schizophrenia and morphine-induced addiction, respectively. As mTORC2 has been shown to induce phosphorylation of Akt at Ser473 (Sarbassov et al., 2005), loss of mTORC2 may thus affect the Akt pathway in dopaminergic neurons. Although these conclusions are reasonable, deletion of *rictor* in other species and in other tissues has not revealed strong phenotypes that are based on diminished Akt signaling (Hietakangas and Cohen, 2007; Bentzinger et al., 2008; Cybulski et al., 2009; Gödel et al., 2011). In addition, phosphorylation of Akt at Ser473 is still high in mice deficient for mTOR in skeletal muscle (Risson et al., 2009), indicating that mTORC2 is not essential for the phosphorylation of Akt at Ser473.

We now report on the phenotype of two distinct mouse models where *rictor* was conditionally deleted either in the entire developing central nervous system (CNS) or selectively in cerebellar Purkinje cells, the cell type with highest rictor expression in the brain (Shiota et al., 2006). We show that deletion of *rictor* in the entire CNS causes a strong phenotype that includes severe microcephaly starting at birth and impairment of motor function. Rictor-deficient neurons are smaller and have altered neurite organization. Both the changes in neuron size and neurite morphology are also observed in mice lacking rictor solely in Purkinje cells. Importantly, the morphological changes correlate with the substantial loss of several PKC isoforms and the decrease in phosphorylation of PKC-downstream targets growth-associated protein-43 (GAP-43) and myristoylated alanine-rich protein kinase C substrate (MARCKS), and they are in agreement with the established role of PKCγ in the morphology of Purkinje cell neurons. In addition, mutations in PKCγ cause spinocerebellar ataxia (Chen et al., 2003; Seki et al., 2011), which resembles the motor phenotype of our knockout mice. Thus, our work shows that mTORC2 plays an important role in the brain and that its function in Purkinje cells is cell autonomous.

Results

Germline deletion of *rictor* in mice causes growth arrest and subsequent death between embryonic day 10.5 and 11.5 (Guertin et al., 2006; Shiota et al., 2006). Rictor mRNA is expressed ubiquitously with highest expression in neurons of the adult hippocampus and cerebellum (Shiota et al., 2006; Lein et al., 2007). To circumvent embryonic lethality and to study the role of rictor in the brain, we set out to conditionally delete *rictor* using the Cre/loxP system (Fig.1 A). To do this, we crossed mice homozygous for the *rictor* alleles, in which exons 4 and 5 are flanked by loxP sites (Bentzinger et al., 2008), with mice expressing Cre under the control of the CNS-specific nestin promoter and enhancer (Tronche et al., 1999). This Cre mouse has been shown to induce recombination in all neural tube–derived cells around embryonic day 10.5 (Graus-Porta et al., 2001). After several crosses, we eventually obtained mice that were homozygous for the floxed *rictor* alleles and expressed nestin-Cre (abbreviated herein RibKO [for rictor brain knockout] mice). As controls, littermates were used that either did not express nestin-Cre (and carried the floxed *rictor* alleles) or that were Cre-positive but carried only one targeted *rictor* allele. Successful recombination of the floxed alleles was tested by PCR using primers P1 and P2 (Fig. 1 A) and a nestin-Cre–specific primer set. In genomic DNA isolated from brain, successful recombination was detected in RibKO mice and in mice heterozygous for the floxed *rictor* allele and positive for nestin-Cre (Fig. 1 A). In contrast, no recombination was seen in control littermates that did not express Cre. These data show that our strategy indeed led to the deletion of exon 4 and 5 in the *rictor* gene. This deletion introduces a frameshift and causes a premature stop of translation.

RibKO mice were born in a Mendelian ratio and could not be distinguished from their littermate controls at birth (unpublished data). After a few weeks, RibKO mice developed a rather strong motor phenotype that included a waddling gait (unpublished data), hindlimb clasping upon tail suspension (Fig. 1 B), and a decreased latency to fall off an accelerating rotarod (Fig. 1 C). The brains of RibKO mice were smaller (Fig. 1 D) and weighed

Published April 8, 2013

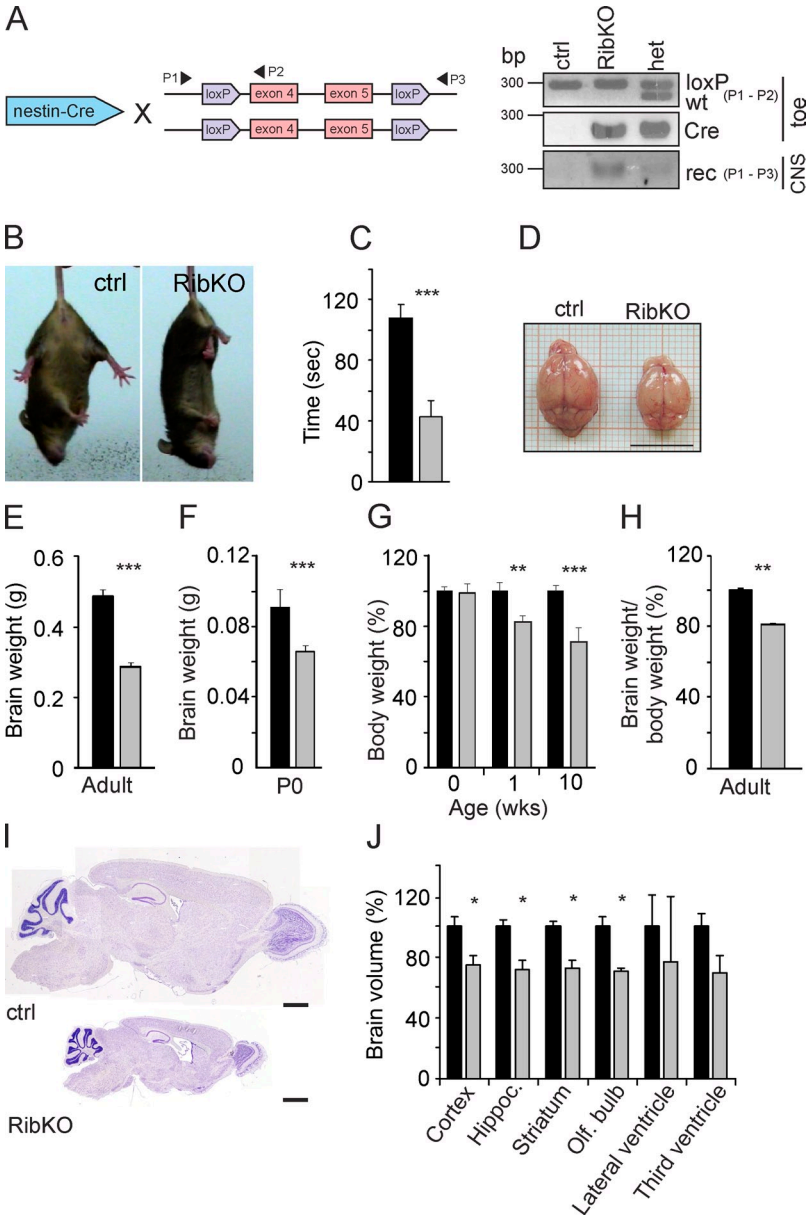

Figure 1. **Rictor knockout in brain causes microcephaly.** (A) Schematic representation of the alleles in the *rictor* gene targeted for nestin-Cre–mediated recombination. PCR primers P1 to P3 are indicated. Right: PCR using genomic DNA from toe lysate of control (ctrl), RibKO, and heterozygous (het) mice to detect the wild-type (wt), the floxed allele (loxP), and Cre. PCR using brain tissue (CNS) and primers P1 and P3 shows successful recombination. (B) Representative images of a control and a RibKO mouse during tail suspension in the clasping test. (C) Average time until control (black bar) or RibKO mice (gray) fell off the rotarod that accelerated from 5 to 30 rpm during 2 min. (D) Photograph of brains from adult control and RibKO mice. (E and F) Quantification of the relative brain weight of adult and newborn (P0) mice. Data represent mean ± SEM with $n = 7$ (adult, control); $n = 6$ (adult, RibKO); $n = 26$ (P0, control); and $n = 7$ (P0, RibKO). (G) Body weight of control and RibKO mice at different postnatal ages. Data represent mean ± SEM with $n = 13$ (P0, control); $n = 8$ (P0, RibKO); $n = 8$ (P7, control); $n = 5$ (P7, RibKO); $n = 10$ (10 wk, control); and $n = 13$ (10 wk, RibKO). (H) Brain weight relative to body weight in the adult. Data represent mean ± SEM with $n = 7$ (control) and $n = 6$ (RibKO). (I) Cresyl violet staining of mid-sagittal sections of brains from adult RibKO and control mice. (J) Quantification of the volumes of several brain regions from 1-yr-old mice. Data represent mean ± SEM with $n = 3$ mice for each genotype. Black bars denote controls, light gray bars denote RibKO mice. Statistical analysis used Student's *t* test: ***, $P < 0.001$; **, $P < 0.01$; *, $P < 0.05$. n.s., nonsignificant; $P \geq 0.05$. Bars: (D) 1 cm; (I) 1 mm.

~40% less than those from littermate controls (Fig. 1 E). Although less striking than in the adult, the brains of newborn RibKO mice were already significantly lighter (Fig. 1 F). In contrast to brain, the total body weight of newborn RibKO mice was still the same as in controls, but RibKO mice did not gain weight like controls so that they became significantly lighter after one week and remained lighter throughout adulthood (Fig. 1 G). Nevertheless, the brains of the RibKO remained significantly and disproportionally lighter (Fig. 1 H). Mid-saggital sections of cresyl violet–stained brains showed that the effect on brain size was rather uniform and affected all brain regions (Fig. 1 I). This uniformity in the size difference was further confirmed by measuring the relative volume of different brain regions using cresyl violet–stained coronal paraffin sections (Fig. 1 J). In contrast to the brain proper, the ventricles were not smaller in RibKO mice (Fig. 1 J). These data thus show that deletion of *rictor* results in a smaller brain, which already manifests at birth. Moreover, the weight difference between RibKO and control brains is larger than the difference in body weight in the adult. These results suggest a direct role of mTORC2 in the control of brain size. RibKO mice also show a strong motor phenotype, indicating that neuronal connectivity in some brain regions might be impaired.

Cells are smaller in rictor-deficient brains

To determine the reasons for the difference in brain size of RibKO mice, we first investigated the proliferation capacity of stem/progenitor cells. To this end, primary neurospheres isolated from newborn pups were cultured for 4 d, followed by trypsinization and resuspension into single cells. The secondary neurospheres were then cultured for another 6 d. The size of the secondary neurospheres from RibKO mice was the same as those isolated from controls (Fig. 2 A) and the number of BrdU-positive cells, when labeled for 24 h before analysis, was indistinguishable (Fig. 2 B). These results indicate that proliferation of stem/progenitor cells

Published April 8, 2013

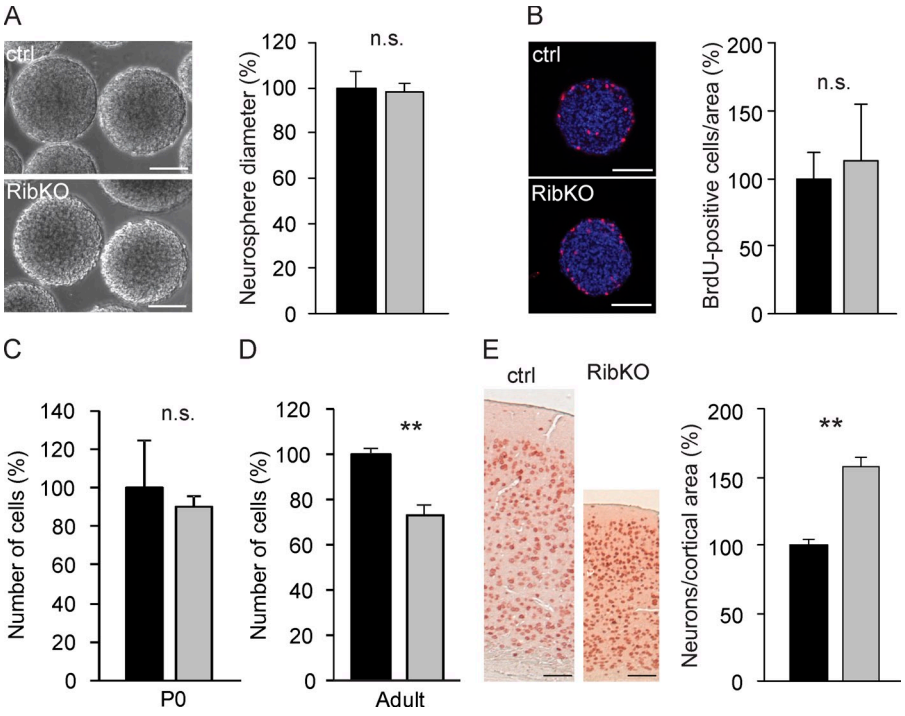

Figure 2. **Changes in cell density in rictor-deficient brains.** (A) Brightfield images of secondary neurospheres isolated from P0 mice, split into single cells after 4–5 d in culture and grown for another 6 d (left), and quantification of the neurosphere diameter (right). Data represent mean ± SEM from n = 613 spheres (control) and n = 583 spheres (RibKO); n = 5 mice for each genotype. (B) Cross sections at the mid-region of neurospheres, stained with antibodies to BrdU (red) and with Hoechst (blue). Neurospheres were labeled with BrdU for 24 h. Quantification of the number of BrdU-labeled cells (right). Data represent mean ± SEM from n = 3 mice per genotype. (C and D) Quantification of the total number of cells in the brains of P0 and adult mice using isotropic fractionation. Data represent mean ± SEM from n = 3 mice per genotype. (E) Picture of cortex sections of adult control and RibKO mice stained with antibodies to NeuN (left) and quantification of neuron density (right). Data represent mean ± SEM from n = 36 areas (control) and n = 3 mice (control), and n = 58 areas and n = 4 RibKO mice. Black bars denote controls, light gray bars denote RibKO mice. Statistical analysis used Student's t test: **, $P < 0.01$. n.s., nonsignificant; $P \geq 0.05$. Bars (A, B, and E) 100 µm.

in RibKO mice is not affected. Likewise, despite the reduced brain weight, the number of cells in brains isolated from newborn RibKO mice was not significantly different from controls (Fig. 2 C). In contrast, the number of cells was lower in adult RibKO mice (Fig. 2 D). The difference in cell number at the adult stage seemed not to be due to increased apoptosis, as the number of cleaved caspase3-positive cells did not differ between the cortex of RibKO and control mice (Fig. S1 A). The number of caspase3-positive cells was, however, rather low and the data varied substantially between animals, which does not allow to exclude the possibility that RibKO mice might be more affected by apoptosis.

To assess whether cell size might cause the difference in brain size, we next stained sagittal sections with antibodies directed against the neuron-specific antigen NeuN. These antibodies strongly stain the nuclei and more weakly the cytoplasm of neurons. As shown in Fig. 2 E, the density of neurons in the retrosplenial and visual cortex of 9-wk-old RibKO mice was more than 1.5 times higher than in controls. This difference in neuron density was already clearly detected in postnatal day (P7) RibKO mice (Fig. S1 B). These data therefore show that loss of rictor in the brain affects neuron density but not proliferation of cells.

To get a more detailed view on the effect on neuron size in RibKO mice, we next reconstructed the shape of single hippocampal neurons using Golgi staining. Examination of pyramidal neurons in the CA1 region (Fig. 3 A) and quantification of their size by the tracing of single neurons using a Neurolucida camera revealed that the mean total dendritic length of both the apical and basal dendrites was reduced by ~15% (Fig. 3 B). This effect could be reproduced in cultured hippocampal neurons that were isolated from P0 brains, transfected with GFP-expression constructs at day in vitro (DIV) 7 (to visualize individual neurons), and examined at DIV 14 (Fig. 3 C). Quantification revealed

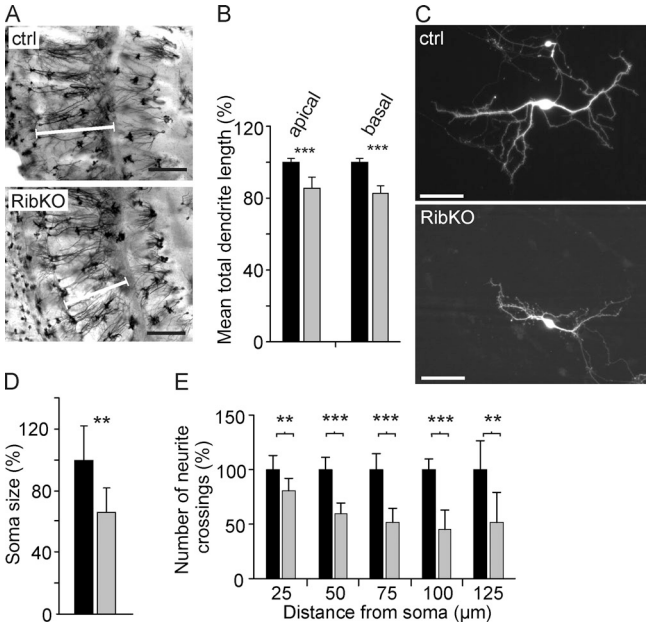

Figure 3. **Rictor regulates neuron size.** (A) Cross sections of hippocampus after Golgi impregnation. The white bar indicates the length of CA1 pyramidal dendrites. (B) Quantification of the mean length of Neurolucida-reconstructed apical and basal dendrites. Data represent mean ± SEM from n = 38 control neurons, n = 32 RibKO neurons derived from 4 different mice of each genotype. (C) Dissociated hippocampal neurons derived from P0 mice, transfected with GFP after 7 d, and grown for 14 d. (D) Mean soma size of hippocampal neurons from dissociated cultures at DIV 14. Data represent mean ± SD from n = 6 mice per genotype. (E) Sholl analysis of hippocampal neurons at DIV 14. Data represent mean ± SD from n = 6 mice per genotype. Black bars denote control, light gray bars denote RibKO mice. Statistical analysis used Student's t test: ***, $P < 0.001$; **, $P < 0.01$. Bars: (A) 200 µm; (C) 50 µm.

Published April 8, 2013

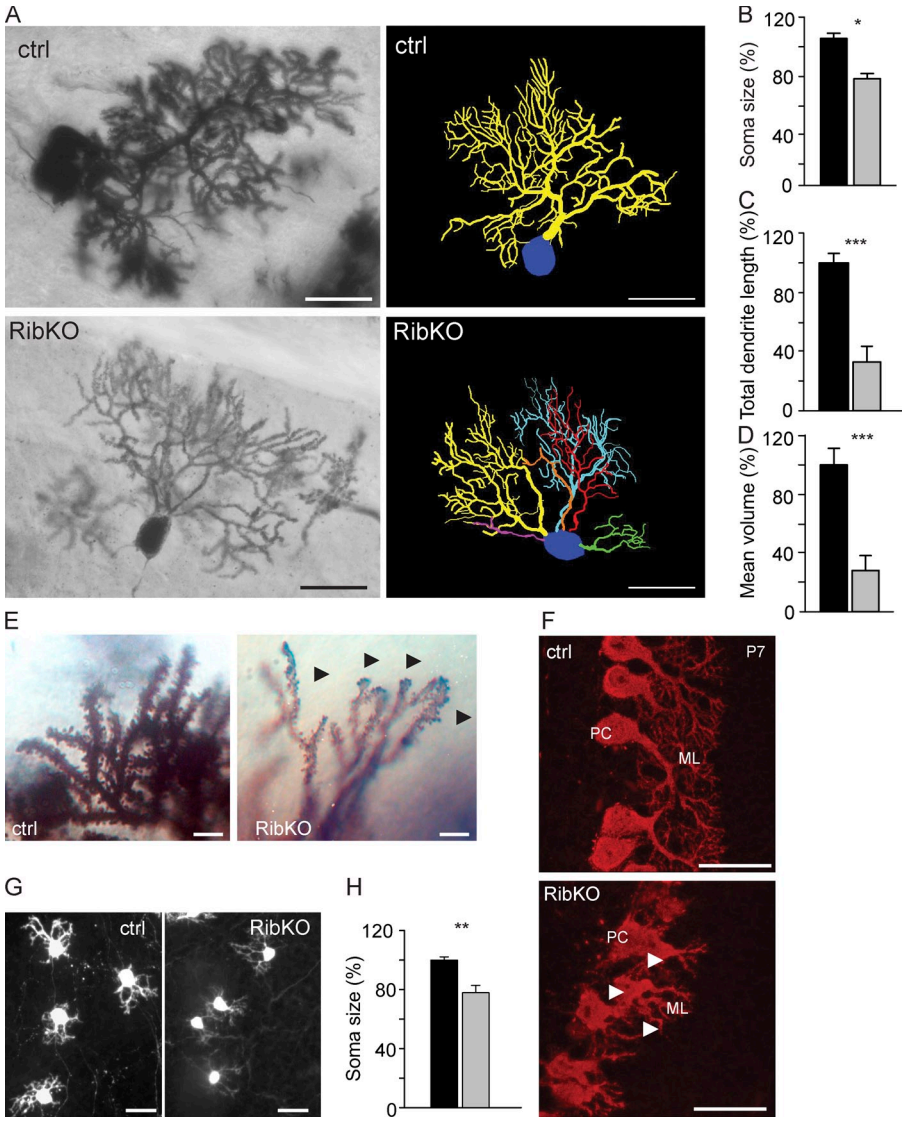

Figure 4. **Rictor is involved in the regulation of Purkinje cell size and shape.** (A) Golgi-stained Purkinje cells from adult control and RibKO mice (left) and reconstruction of a Purkinje cell using Neurolucida. Primary dendrites are indicated by different colors. Examples of a dendritic tree with little or no higher order branches are depicted in purple and orange. (B) Quantification of Purkinje cell soma size. The cell soma perimeter was measured in sections stained with antibodies to calbindin. Data represent mean ± SEM from $n = 4$ mice per genotype. (C) Quantification of the mean Purkinje cell dendrite length and (D) the mean dendrite volume in Neurolucida-reconstructed cells. Data represent mean ± SEM from $n = 4$ mice per genotype. (E) High magnification picture of Purkinje cell terminals of Golgi-stained preparations. Purkinje cell dendrites are often deformed (black arrows) and appear to have fewer spine-like structures. (F) Neurons of P7 stained with antibodies to calbindin. White arrows mark misshaped dendritic trees in RibKO mice. (G) Purkinje cells in organotypic cerebellar slice cultures derived from P0 mice and cultured for 14 d, stained with antibodies to calbindin. (H) Quantification of the soma size of Purkinje cells in organotypic cultures. Data represent mean ± SEM from $n = 4$ (control) and $n = 3$ RibKO mice. Black bars denote control, light gray bars denote RibKO mice. Statistical analysis used Student's *t* test: ***, $P < 0.001$; **, $P < 0.01$; *, $P < 0.05$. PC, Purkinje cell; ML, molecular layer. Bars: (A and G) 50 µm; (F) 20 µm; (E) 10 µm.

that the soma size of RibKO neurons was only ∼ 70% of control neurons (Fig. 3 D) and Sholl analysis at DIV 14 showed a highly significant decrease in the complexity of the neurites (Fig. 3 E). These experiments thus indicate that changes in neuron size in RibKO mice are rather a consequence of cell-intrinsic changes than of alterations in the surroundings (e.g., changes in glial cells).

Cerebellar phenotype of RibKO mice

Rictor expression is highest in Purkinje cells of the cerebellum (Shiota et al., 2006) and RibKO mice show an ataxia-like phenotype (Fig. 1, B and C). To see whether loss of rictor would affect Purkinje cells, we next analyzed single cells from Golgi-stained preparations (Fig. 4 A). Reconstruction of cells by tracing them using a Neurolucida camera revealed several distinct structural alterations. One of the most striking differences between Purkinje cells from RibKO and control mice was an increase in the number of primary dendrites. Whereas control neurons always had one primary dendrite, Purkinje cells from RibKO mice often contained two to six primary dendrites (see Neurolucida drawing in Fig. 4 A). Quantification of the size of the Purkinje cells showed a significant decrease in soma size (Fig. 4 B) and a decrease in the length and the volume covered by single dendrites (Fig. 4, C and D). Examination of the Purkinje cell dendrites at high magnification revealed that the thickness of the dendrites was often irregular, fluctuating from very thin to rather thick (swollen) regions (Fig. 4 E, arrows). Thus, deletion of *rictor* causes multiple changes in Purkinje cells that affect the size of the somata and of the dendrites and increases the number of primary dendrites.

To examine whether any of the structural changes could already be observed at early stages of development, we examined the cerebella at P7. In the first postnatal week, Purkinje cells migrate into the periphery and start to align in a monolayer. At that stage, most cells have formed one primary dendrite, which spreads out perpendicularly to the pial surface into the molecular layer where it forms numerous side branches (Kapfhammer, 2004). This alignment and spreading of the primary dendrites was well visible in control mice (Fig. 4 F), whereas the dendrites of Purkinje cells in RibKO mice appeared swollen (arrows) and several

Published April 8, 2013

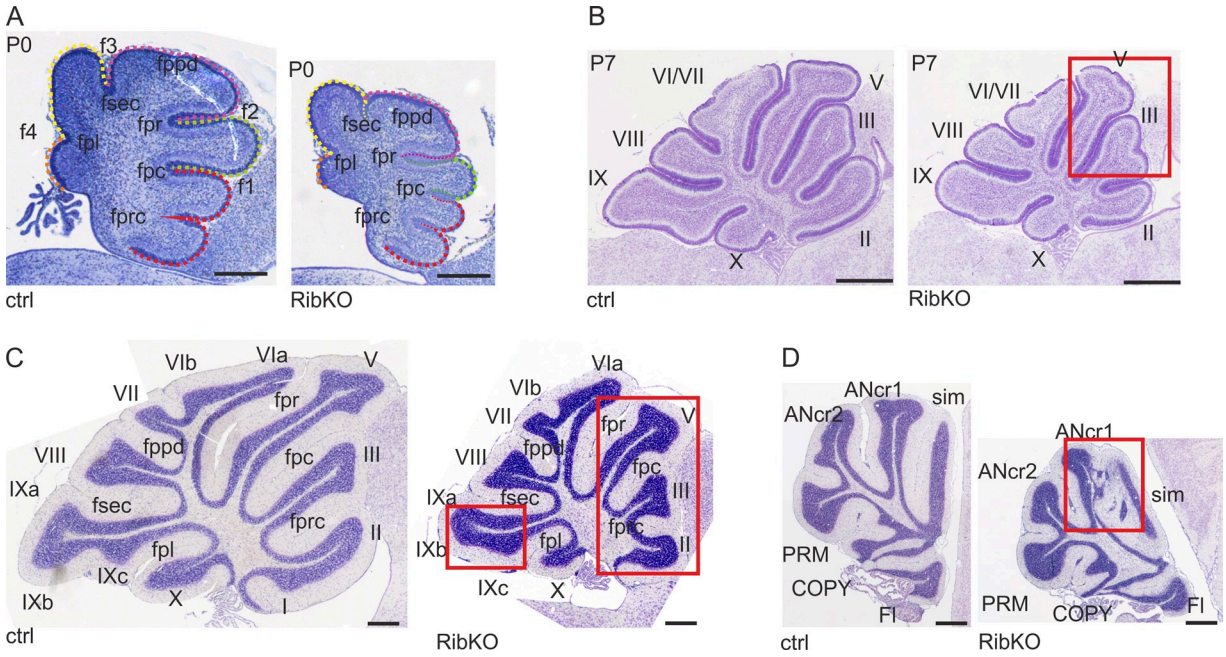

Figure 5. **Rictor deficiency leads to foliation defects in the cerebellum.** (A) Cresyl violet staining of cerebella from P0 control and RibKO mice. (B) Cresyl violet–stained, mid-sagittal sections of P7 cerebella from control and RibKO mice. (C) Sagittal sections of cerebellar vermis from adult control and RibKO mice stained with cresyl violet. (D) Sagittal sections of the lateral cerebellar lobules of adult control and RibKO mice. Foliation defects are marked by red inserts. Fpl, posterolateral fissure; fsec, secondary fissure; fppd, prepyramidal fissure; fpr, primary fissure; fprc, precentral fissure. Vermal lobules are numbered from I to X. Lateral lobules: Ancr, Ansiform cruciform lobule; COPY, Copula pyramidis; Fl, Flocculus; PRM, paramedian lobule; Sim, simple lobule. Bars: (A and B) 250 µm; (C and D) 1 mm.

primary dendrites emerged from the cell bodies (Fig. 4 F). The aberrant Purkinje cell morphology was also reproduced in slice cultures derived from newborn mice and cultured for 14 d. There, the somata of RibKO Purkinje cells were significantly smaller (Fig. 4, G and H). As Purkinje cells in culture retain several primary dendrites because of the lack of climbing fiber innervation (Kapfhammer, 2004), the difference in the number of primary dendrites between RibKO and control mice could not be seen. In summary, these results show that RibKO mice display pronounced structural changes in their Purkinje cells, the most prominent ones being changes in dendritogenesis and overall cell size.

The changes in Purkinje cell size and shape in RibKO mice observed at early postnatal stages suggested to us that mTORC2 might also be involved in cerebellar development and maturation. It is known that mice with defects in Purkinje cells may develop simplified lobule patterns (Sidman et al., 1962; Wetts and Herrup, 1982). Moreover, the structure of the cerebellar lobes is highly conserved and aberrations in their morphology often correlate with defects in motor behavior (Sillitoe and Joyner, 2007). To test whether this would also be the case in RibKO mice, we analyzed the overall structure of the cerebellum. At birth (P0), the cerebellum only consists of the 5 cardinal lobes, which will then develop into 10 mature lobules within the following 21 d (Larsell, 1952). In cerebella of newborn RibKO mice, lobule formation was unchanged (Fig. 5 A). At P7, cerebellar defects became clearly visible as the cerebella were smaller and the structure of lobules III to VII of the cerebellar vermis in RibKO mice already deviated from that of control mice (Fig. 5 B). In 8–10-wk-old RibKO mice, the size of the cerebellum was strongly decreased (Fig. 5 C) and most lobules appeared shortened and the cells seemed more densely packed than in control mice. Moreover, in some regions, changes in the structure of the lobules could be detected. The cerebellar hemisphere was even more affected than the cerebellar vermis. There, both the simple lobule (Sim) and the Ansiform cruciform lobule 1 (ANcr1) were not properly formed and appeared to be fused so that they could not be distinguished as separate lobules (Fig. 5 D). Thus, deletion of *rictor* caused structural changes in the cerebellar morphology. As RibKO mice also show changes in motor behavior, the morphological alterations of the cerebellum might underlie these defects.

Synaptic defects in RibKO mice

The structural changes in the Purkinje cells of RibKO mice suggested that synaptic connectivity might also be affected. To test this, we visualized the Purkinje cells with antibodies to calbindin and the presynaptic terminals of the climbing fibers, which synapse onto Purkinje cells, with antibodies to the vesicular glutamate transporter protein 2 (vGLUT2; Fremeau et al., 2001; Hisano et al., 2002). The density of vGLUT2-positive puncta in the molecular layer was decreased in RibKO mice (Fig. 6 A). The number of synaptic inputs from parallel fibers onto Purkinje cells was estimated by Western blot analysis using antibodies against the vesicular glutamate transporter vGLUT1, which is enriched in parallel fiber synapses (Fremeau et al., 2001; Hisano et al., 2002). Compared with control lysates, vGLUT1-like immunoreactivity was reduced to less than 80% in RibKO mice (Fig. 6 B). These results therefore indicate that both excitatory inputs onto Purkinje cells are altered in RibKO mice.

To test for functional differences, we next measured miniature excitatory postsynaptic currents (mEPSCs) and miniature

Published April 8, 2013

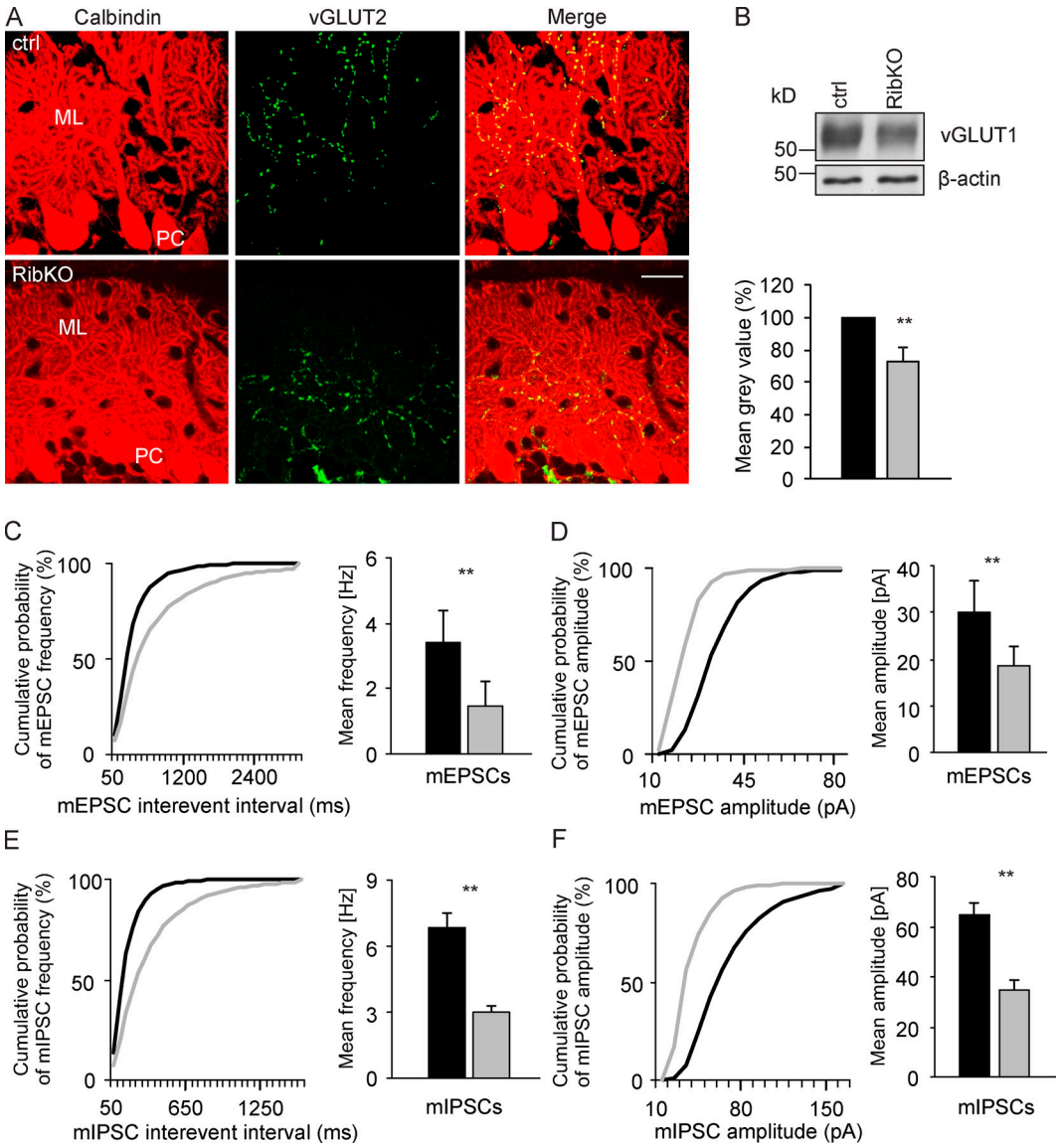

Figure 6. **Synaptic functions are altered in Purkinje cells of RibKO mice.** (A) Confocal image of cerebellar vermal lobule III of adult control and RibKO mice stained with antibodies to calbindin to visualize Purkinje cells (PC, red) and antibodies to vGLUT2 for climbing fiber terminals (green). ML, molecular layer. (B) Western blot analysis of vGLUT1 in cerebellar lysates of control and RibKO mice and corresponding quantification of the mean gray values. β-Actin was used as loading control. Data represent mean ± SEM from $n = 6$ control and $n = 7$ RibKO mice. (C and D) Miniature excitatory postsynaptic currents (mEPSCs) and (E and F) miniature inhibitory postsynaptic currents (mIPSCs) recorded from Purkinje cells in acute sagittal slices of 25-d-old control and RibKO mice. Data represent mean ± SEM from $n = 4$ control and $n = 3$ RibKO mice. Black bars/lines are from control; gray bars/lines are from RibKO mice. Statistical analysis used Student's *t* test: **, $P < 0.01$. Bar, 20 µm.

inhibitory postsynaptic currents (mIPSCs) in single Purkinje cells using the patch-clamp technique. As expected from the histological assessment, the inter-event interval of the mEPSCs was strongly increased in Purkinje cells from RibKO mice, which resulted in the lowering of the mEPSC frequency by about half (Fig. 6 C). In addition, the amplitude of the mEPSCs was reduced in RibKO mice as seen by the leftward shift in the cumulative probability curve and the decrease of the mean mEPSC amplitude (Fig. 6 D). Recordings of the inhibitory synaptic input revealed that both the frequency and the amplitude of mIPSCs were reduced in RibKO mice to an extent that was quite similar to that observed for the mEPSCs (Fig. 6, E and F). In summary, these results show that synaptic connectivity of Purkinje cells in the cerebellum of RibKO mice is strongly affected, suggesting that these synaptic changes might be the basis for the ataxia-like phenotype of RibKO mice.

Biochemical analysis of RibKO mice

Our findings that deletion of *rictor* results in a microcephalic phenotype and a decrease in the size of neurons is rather unexpected, as such an effect has not been documented in other tissue upon *rictor* deletion. In stark contrast, deletion of mTORC1 has strong effects on organ and cell size (Russell et al., 2011). To investigate whether mTORC1 signaling was also affected in the RibKO mice and to unravel the molecular mechanisms that underlie the different aspects of the phenotype in RibKO mice,

Published April 8, 2013

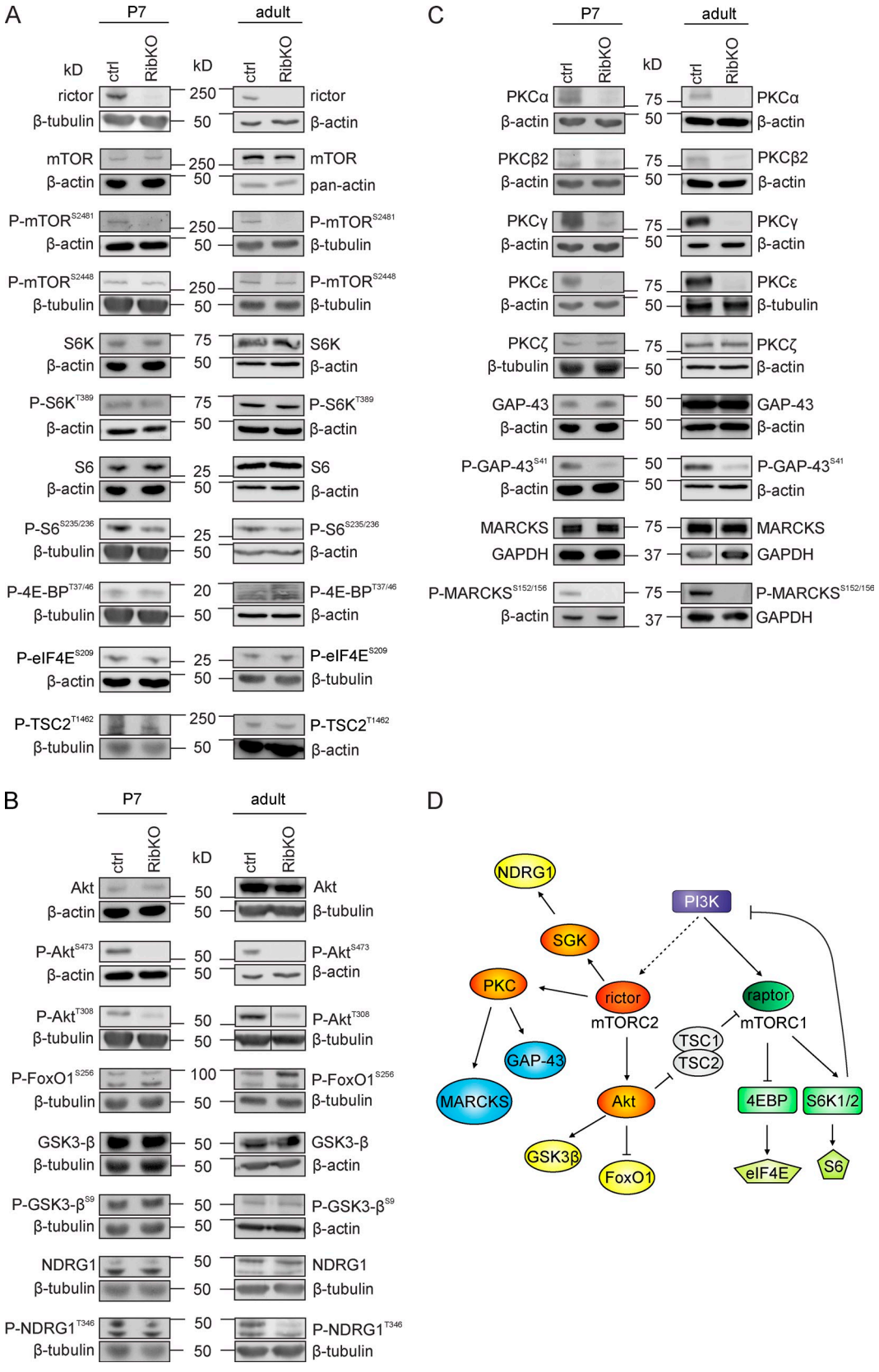

Figure 7. **Biochemical analysis of RibKO mice indicates altered activation of AGC kinases but not of mTORC1.** (A–C) Western blot analysis of brain lysates from P7 and adult control and RibKO mice. β-Tubulin, GAPDH, β-actin, or pan-actin were used as loading controls. Some loading controls are intentionally shown more than once because experimental data were derived from the same SDS gel. (A) Detection of the phosphorylation levels of proteins involved in mTORC1 and mTORC2 signaling. Please note that phosphorylation levels of mTOR at Ser2481 and Ser2448 in adult mice showed a substantial variation. The P-mTOR(S2481) and P-mTOR(S2448) bands shown are representative for the averaged band intensities of all tested mice (see Table 1). (B) Phosphorylation

Published April 8, 2013

we analyzed brain lysates of P7 and adult mice using Western blot analysis. As expected from nestin-Cre–mediated recombination that affects all precursor cells of the CNS (Tronche et al., 1999; Graus-Porta et al., 2001), rictor protein could not be detected in brain lysates from adult RibKO mice and was significantly reduced in P7 RibKO brain lysates (Fig. 7 A; see Table 1 for quantification). The loss of rictor did not affect the levels of mTOR but abrogated phosphorylation of mTOR at the mTORC2-specific residue Ser2481 (Fig. 7 A; Table 1). Importantly, all the phosphorylation sites indicative of mTORC1 signaling were not altered in RibKO mice. These included phosphorylation of mTOR at Ser2448, of S6K and its substrate S6, and of 4E-BP and its substrate elongation initiation factor 4E (eIF4E). In addition, phosphorylation of tuberous sclerosis complex 2 (TSC2), a downstream target of Akt and upstream inhibitor of mTORC1, was also not altered (Fig. 7 A; Table 1). These results indicate that inactivation of mTORC2 in the developing and adult brain does not affect mTORC1 activity and thus suggests that an mTORC1-independent mechanism is responsible for the microcephaly in RibKO mice.

Previous work has shown that mTORC2 affects phosphorylation of AGC kinases including Akt (Sarbassov et al., 2005), SGK1 (García-Martínez and Alessi, 2008), and PKC (Facchinetti et al., 2008; Ikenoue et al., 2008). Although the protein levels of Akt were not changed in comparison to control mice, phosphorylation at Ser473 was strongly diminished in RibKO mice (Fig. 7 B; Table 1). Phosphorylation of Akt at Thr308 was reduced in RibKO mice but reached significance only in the adult brain. However, activation of the Akt downstream targets FoxO1 and GSK3-β was unchanged (Fig. 7 B; Table 1). These results indicate that Akt activation toward the mTORC1, the GSK3-β, and the FoxO1 branch was not altered in RibKO mice despite the lower levels of phosphorylation at Ser473. Activation of SGK1, as indicated by the phosphorylation of its downstream substrate, N-myc downstream regulated gene 1 (NDRG1), was decreased in the adult but not in the brains of P7 RibKO mice (Fig. 7 B; Table 1).

As mTORC2 was also shown to regulate phosphorylation and thereby protein levels of certain isoforms of PKC (Facchinetti et al., 2008; Ikenoue et al., 2008), we also tested brain lysates of RibKO mice for changes in PKC. There are at least nine different isoforms that are grouped into three classes based on their structural and enzymatic properties. These include the conventional isoforms (PKCα, -β, and -γ), the novel isoforms (PKCε, -δ, and -η), and the atypical isoforms (PKCζ, -λ, -ι, and -μ). The conventional PKC isoforms are activated by phosphorylation and second messengers (elevated Ca^{2+} concentrations and diacylglycerol [DAG]), whereas the novel isoforms are regulated only by DAG and phosphorylation (Ohno and Nishizuka, 2002). In P7 and adult RibKO mice, phosphorylation and protein levels of all three conventional PKCs and the novel PKCε was strongly decreased (Fig. 7 C; Fig. S2; Table 1). In contrast, the atypical isoform PKCζ was not affected (Fig. 7 C; Table 1). The strong decrease in PKCs had functional consequences, as phosphorylation levels of the well-known downstream substrates GAP-43 and MARCKS were much lower in RibKO mice than in controls (Fig. 7 C; Table 1). In conclusion, this biochemical analysis indicates that the growth defect in RibKO mice is a consequence of changes in downstream substrates of mTORC2 and not by affecting mTORC1 signaling. In addition, loss of rictor leads to the profound loss of several PKC isoforms in the brain, which has not been reported for other tissues.

Purkinje cell–specific deletion of *rictor*

As RibKO mice lack rictor in all cells of the CNS, this animal model cannot answer if the observed phenotypes were the consequence of cell-autonomous function of mTORC2 or a consequence of altered cell–cell communication. To address this question, we crossed floxed *rictor* mice with mice in which the Cre recombinase was knocked-in into the *L7/Pcp-2* locus (Fig. 8 A; Saito et al., 2005). *L7/Pcp-2-Cre* mice start to express the Cre recombinase during late embryogenesis and its expression is restricted to Purkinje cells in a mosaic pattern (Saito et al., 2005). Offspring that was heterozygous for *L7/Pcp-2-Cre* and homozygous for the floxed *rictor* allele (called RiPuKO$^{Cre/+}$ for *rictor* Purkinje cell knockout) were born in a Mendelian ratio and mice could not be distinguished from their control littermates. Successful recombination of the floxed alleles in Purkinje cells was indicated by the significant loss of rictor and of PKCγ from cerebellar lysates of adult RiPuKO$^{Cre/+}$ mice (Fig. 8 B). Staining of sagittal cerebellar sections of adult RiPuKO$^{Cre/+}$ mice with antibodies to calbindin and PKCγ revealed that ∼1/3 of the cells were negative for PKCγ (Fig. 8 C; Fig. S3 A). The proportion of PKCγ-negative Purkinje cells increased to ∼3/4 when mice were made homozygous for the *L7/Pcp-2-Cre* allele (Fig. S3 A). In contrast, Purkinje cells from mice lacking *L7/Pcp-2-Cre* were all PKCγ positive (Fig. 8 C; Fig. S3 A). These results indicate that Cre expression in Purkinje cells is indeed mosaic and that an increase in gene dosage for the Cre recombinase results in a higher rate of excision of the floxed alleles.

To assure that PKCγ-negative Purkinje cells were indeed deficient for rictor, single Purkinje cells were labeled with biocytin during whole-cell patch clamping and the mRNA was analyzed by single-cell RT-PCR (Sucher et al., 2000). The biocytin-labeled Purkinje cells were then stained with antibodies to PKCγ and staining results were compared with those from single-cell RT-PCR. As shown in Fig. S3 B, out of the nine cells analyzed all the PKCγ-negative cells also expressed *rictor* transcripts lacking exons 4 and 5 (Fig. S3 B). There was one cell that was still positive for PKCγ even though only mRNA for the recombined *rictor* locus was amplified (Fig. S3 B; cell #7). These experiments show that all the PKCγ-negative Purkinje cells are deficient for rictor, whereas the majority of the PKCγ-positive cells are rictor positive.

Morphological analysis of Purkinje cells from RiPuKO$^{Cre/+}$ and RiPuKO$^{Cre/Cre}$ mice showed that the somata of the PKCγ-negative

of mTORC2 targets Akt and SGK1 and downstream targets. (C) Western blot analysis of several PKC isoforms and the PKC targets GAP-43 and MARCKS. Levels of MARCKS showed considerable variations in adult mice. The shown bands are representative for the averaged band intensities of all tested mice (see Table 1). (D) Schematic view of the signaling mechanisms up- and downstream of mTORC1 and mTORC2.

Published April 8, 2013

Table 1. **Quantification of Western blot analyses**

Antibody target	P7 brain		Adult brain	
	Control	RibKO	Control	RibKO
rictor	100 ± 8.1	13.7 ± 2.4***	100 ± 24	n.d.
mTOR	100 ± 10.5	108.5 ± 7.9	100 ± 31	64.9 ± 7.5
P-mTOR (Ser2481)	100 ± 2.8	21.2 ± 5***	100 ± 25.2	2.7 ± 2.2**
P-mTOR (Ser2448)	100 ± 7	96.5 ± 12.3	100 ± 20.7	79 ± 21
S6K	100 ± 12.2	93.6 ± 8.2	100 ± 8.8	91.4 ± 5.8
PS6K (Thr389)	100 ± 8.3	116.5 ± 5.9	100 ± 5.2	85.6± 9.2
S6	100 ± 9.1	107.2 ± 13.8	100 ± 6.1	169.3 ± 29.4
P-S6 (Ser235/236)	100 ± 6.2	83.2 ± 3.3	100 ± 10	105.2 ± 17.5
P-4E-BP (Thr37/46)	100 ± 8.3	94 ± 7.6	100 ± 11	179.7 ± 37.2
P-eIF4E (Ser209)	100 ± 13	84.6 ± 3.1	100 ± 10	107.0 ± 13.8
P-TSC2 (Thr1462)	100 ± 9.8	177.5 ± 45.6	100 ± 22	80.2 ± 22.4
Akt	100 ± 10.5	127.6 ± 17.3	100 ± 4.7	99.4 ± 6.1
P-Akt (Ser473)	100 ± 10	3.9 ± 0.9***	100 ± 12	18.3 ± 4.8***
P-Akt (Thr308)	100 ± 7	52 ± 17	100 ± 15	36.9 ± 8.1**
P-FoxO1 (Ser256)	100 ± 15.7	141.1 ± 13.3	100 ± 9.3	164.6 ± 26.7
GSK3-β	100 ± 5.0	101.5 ± 5.5	100 ± 5.1	97.1 ± 4.7
P-GSK3-β (Ser9)	100 ± 11.7	115.8 ± 12.4	100 ± 17	103.7 ± 5.1
NDRG1	100 ± 19.8	115.3 ± 6.5	100 ± 5.4	94.2 ± 7.9
P-NDRG1 (T346)	100 ± 13.7	92 ± 15.9	100 ± 3.8	52.4 ± 7.3***
PKCα	100 ± 6.8	55.8 ± 3.4***	100 ± 23.8	2.6 ± 1.7***
PKCβ2	100 ± 7.0	78.6 ± 3.7*	100 ± 11.4	3.7 ± 0.4***
PKCγ	100 ± 6.2	58.5 ± 2.1***	100 ± 6.6	7.4 ± 1.8***
PKCε	100 ± 12	17.7 ± 2.8***	100 ± 22.9	15.5 ± 5*
PKCζ	100 ± 17.1	106 ± 11.9	100 ± 14.6	60.0 ± 7.8
GAP-43	100 ± 1.2	105 ± 5.8	100 ± 5	99.9 ± 6.6
P-GAP-43 (Ser41)	100 ± 13.1	22.4 ± 3.9**	100 ± 27	19.5 ± 4.7**
MARCKS	100 ± 2.3	94.2 ± 3.4	100 ± 22	109.7 ± 3
P-MARCKS	100 ± 8.8	n.d.	100 ± 25	n.d.

Quantification of protein and phosphorylation levels of proteins shown in Fig. 7. Percentage given represents the relative intensity of the protein bands as detected by Western blot analysis from control and RibKO mice. Equal amount of protein was loaded and immunodetection of β-tubulin, GAPDH, β-actin, or pan-actin served as loading control. Amount of each protein listed was normalized to loading control. All values obtained in controls were set to 100%. Data represent mean ± SEM from $n \geq 3$–15 mice for each genotype. n.d., not detected. Student's *t* test: ***, $P < 0.001$; **, $P < 0.01$; *, $P < 0.05$.

cells were significantly smaller than those of Purkinje cells in control mice (Fig. 8, D and E). Importantly, PKCγ-positive Purkinje cells were also significantly bigger than the PKCγ-negative cells in the RiPuKO$^{Cre/+}$ mice (Fig. 8 E). In addition, the average diameter of the primary dendrites of PKCγ-negative Purkinje cells in the RiPuKO$^{Cre/+}$ mice was significantly smaller than in cells from control mice (Fig. 8 F), and PKCγ-negative Purkinje cells in RiPuKO$^{Cre/Cre}$ mice formed in more than 30% of the cases two or more primary dendrites (Fig. 8, D and G). Rictor-deficient (i.e., PKCγ-negative) Purkinje cells that were isolated from RiPuKO$^{Cre/Cre}$ mice and were cultured for 14 d in organotypic slices also displayed aberrations in axon structure compared with PKCγ-positive neurons (Fig. 8 H). In particular, the diameter of the axons was significantly diminished in the PKCγ-negative but not the PKCγ-positive Purkinje cells (Fig. 8 I). Thus, selective elimination of rictor in Purkinje cells causes multiple morphological changes that affect cell size and neurite morphology.

To test whether these morphological changes of the PKCγ-negative Purkinje cells from RiPuKO$^{Cre/Cre}$ mice also affected synaptic properties, we measured mEPSCs and mIPSCs in acute cerebellar slices from 6-wk-old mice. The single-cell recordings revealed a strong decrease in the mEPSC frequency (Fig. 9, A and B) and no change in the amplitude (Fig. 9 C). In contrast, the mIPSC frequency in control Purkinje cells was the same as in PKCγ-negative and PKCγ-positive Purkinje cells in RiPuKO$^{Cre/Cre}$ mice. However, PKCγ-negative cells from RiPuKO$^{Cre/Cre}$ mice showed a reduction in the mIPSC amplitude compared with PKCγ-positive cells from RiPuKO$^{Cre/Cre}$ or from control mice (Fig. 9, E and F). The reduction in mEPSC frequency indicates that RiPuKO$^{Cre/Cre}$ mice have fewer functional excitatory synapses, whereas the reduction in mIPSC amplitude points to a reduction in the number or the functionality of inhibitory receptors at the Purkinje cell membrane. Thus, in contrast to RibKO mice where all parameters of the mEPSCs and mIPSCs are diminished, RiPuKO$^{Cre/Cre}$ mice show changes only in mEPSC frequency and in the mIPSC amplitude. These results therefore suggest that presynaptic input onto Purkinje cells might in addition be affected in RibKO mice because of the broad expression of *nestin-Cre*. In conclusion, specific elimination of mTORC2-associated protein rictor in Purkinje cells using *L7/Pcp-2-Cre* results in the reiteration of several phenotypic distortions observed in RibKO mice, including the reduction of cell size, the change in cell morphology, and in synaptic function. Thus, those common phenotypes are based on a cell-autonomous function of mTORC2.

Published April 8, 2013

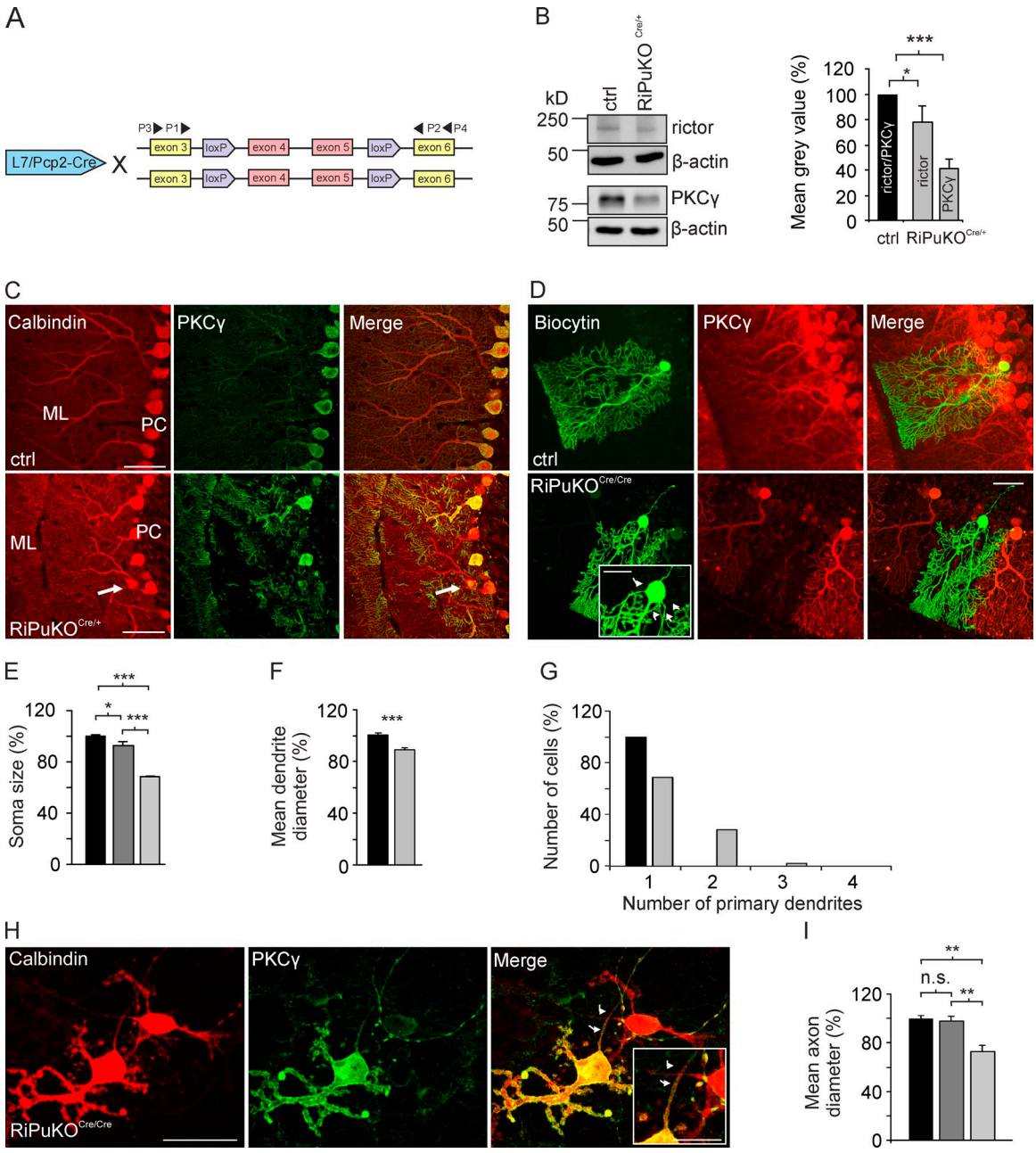

Figure 8. **The role of rictor on cell size and cell morphology is cell-autonomous.** (A) Schematic representation of the genetic organization of mice homozygous for the targeted *rictor* alleles and mice expressing Cre-recombinase from the *L7/Pcp-2* locus. Please note the localization of the primers used to detect *rictor* recombination in single-cell PCR (see Fig. S3). (B) Western blot analysis of cerebellar lysates from adult control and RiPuKO$^{Cre/+}$ mice for rictor and PKCγ (left) and quantification of their mean gray value (normalized to β-actin; right). Values for rictor and PKCγ in controls (ctrl) were set to 100% (black bar). Gray bars represent values for rictor and PKCγ in RiPuKO$^{Cre/+}$ mice. Data represent mean ± SEM from $n = 5$ mice per genotype. (C) Cross section of cerebella stained with antibodies to calbindin (red) and PKCγ (green). PKCγ staining is lost in some, but not all Purkinje cells in RiPuKO$^{Cre/+}$ mice because of the mosaic recombination of the *rictor* allele (see Fig. S3). Some of the PKCγ-negative cells have several primary dendrites, are misaligned, and diverge from the perpendicular plain (white arrow). (D) Immunostaining for PKCγ (red) of biocytin-filled (green) Purkinje cells from control or RiPuKO$^{Cre/Cre}$ mice. Purkinje cells that are negative for PKCγ often have more than one primary dendrite (white arrows). (E) Quantification of the Purkinje cell soma size in control mice (black bar), in PKCγ-positive cells (dark gray), and in PKCγ-negative cells (light gray) from RiPuKO$^{Cre/+}$ mice. Data represent mean ± SEM from $n = 3$ mice for each genotype. (F) Quantification of the Purkinje dendrite diameter in control (black) and PKCγ-negative cells in RiPuKO$^{Cre/+}$ mice (gray). Data represent mean ± SEM from $n = 3$ mice. (G) Quantification of the number of primary dendrites in biocytin-filled Purkinje cells of control (black) and of PKCγ-negative cells from RiPuKO$^{Cre/Cre}$ mice (gray). Numbers derive from $n = 38$ cells of a total of 5 control mice, and from $n = 42$ cells of a total of 7 RiPuKO$^{Cre/Cre}$ mice. (H) Cerebellar slice cultures isolated from RiPuKO$^{Cre/Cre}$ mice and stained for calbindin and PKCγ. The white arrows indicate axons. The inset shows a high magnification picture of those axons. (I) Quantification of the Purkinje axon diameter in cerebellar slice cultures isolated from control mice (black), and PKCγ-positive (dark gray), and PKCγ-negative cells (gray) isolated from RiPuKO$^{Cre/Cre}$ mice. Data represent mean ± SEM from $n = 5$ mice for each genotype. Statistical analysis used Student's *t* test (B and F) or one-way Anova followed by Tukey's test (E and I): ***, $P < 0.001$; **, $P < 0.01$; *, $P < 0.05$. n.s., nonsignificant; $P \geq 0.05$. Bars: (H, inset) 10 µm; (C, H, and inset in D) 25 µm; (D) 50 µm.

Published April 8, 2013

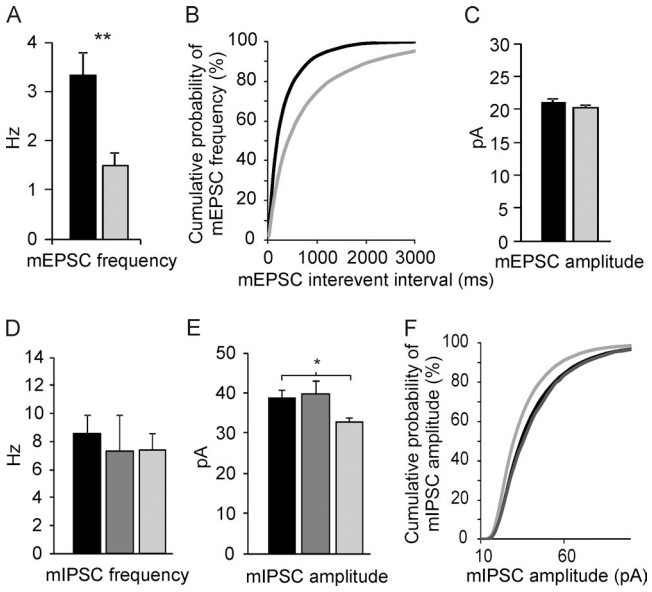

Figure 9. **Altered synaptic properties in Purkinje cells of RiPuKO$^{Cre/Cre}$ mice.** (A and B) Electrophysiological recording of the mean mEPSC frequency in control (black) and PKCγ-negative Purkinje cells of RiPuKO$^{Cre/Cre}$ mice (gray) and (C) the mean mEPSC amplitude in those mice. Data represent mean ± SEM from n = 19 neurons from 5 different control mice and n = 19 cells from 8 different RiPuKO$^{Cre/Cre}$ mice. (D–F) Measurement of the mean frequency (D) and the mean amplitude (E and F) of mIPSCs in Purkinje cells from control mice (black), PKCγ-positive (dark gray), and PKCγ-negative (light gray) cells from RiPuKO$^{Cre/Cre}$ mice. Data represent mean ± SEM from n = 21 cells from 4 different control mice; n = 25 PKCγ-positive cells from 5 RiPuKO$^{Cre/Cre}$ mice; and n = 7 PKCγ-negative cells from a total of 3 RiPuKO$^{Cre/Cre}$ mice. Statistical analysis used Student's t test (A and C) or one-way Anova followed by Tukey's test (D and E): **, $P < 0.01$; *, $P < 0.05$.

Discussion

Germline deletion of *rictor* in mice causes their death around embryonic day 10.5 to 11.5 (Guertin et al., 2006; Shiota et al., 2006). Here we show that deletion of *rictor* in brain precursor cells does not cause early death, indicating that the embryonic lethality in whole-body *rictor* knockout mice is not due to brain abnormalities. We find that RibKO mice have a smaller brain and that this is mainly caused by a reduction in cell size. Moreover, we find a strong phenotype in Purkinje cells that affects the morphology and connectivity of those neurons, both features that might contribute to the motor deficits. Interestingly, a recent publication where exon 3 of *rictor* was deleted using the same nestin-Cre mice linked the phenotype to schizophrenia by demonstrating that the knockout mice were impaired in prepulse inhibition without changes in gross motor function (Siuta et al., 2010). Although this paper reports an interesting aspect of mTORC2 function, the use of the same *nestin* promoter to drive expression of Cre resulted in our hands in a severe phenotype that affected motor behavior and all basic synaptic functions (mEPSCs and mIPSCs) and that did not allow us to test the mice in more elaborated behavioral tasks. We cannot explain the difference between the phenotypes of the two mouse models; one possibility might be that the targeting of exon 3 (Siuta et al., 2010), instead of both exons 4 and 5 (this paper) results in only a partial loss of rictor.

mTORC2 affects cell size

Rictor has been removed in several other organs including skeletal muscle (Bentzinger et al., 2008; Kumar et al., 2008), adipose tissue (Cybulski et al., 2009), and kidney (Gödel et al., 2011). In all those tissues, the phenotype is rather weak and does not affect organ size. Our work now provides strong evidence that deletion of mTORC2 in the entire CNS resulted in a phenotype that was already evident at birth and that affected brain size. This size difference was also seen upon deletion of *rictor* in Purkinje cells, indicating that this function is cell-autonomous. Recent evidence indicates that the morphine-induced decrease in the size of dopaminergic neurons in the ventral tegmental area also involves mTORC2 and that this cell-autonomous effect is rapamycin insensitive (i.e., mTORC1 independent; Mazei-Robison et al., 2011).

Similar size effects in the brain have been reported in mice lacking Akt3/PKBγ, which is the main Akt isoform expressed in the brain (Easton et al., 2005; Tschopp et al., 2005). Although RibKO mice show a strong reduction in the phosphorylation of Akt at Ser473 and some reduction in phosphorylation at Thr308, our biochemical analysis of the mTOR pathway indicates that the growth defect is not based on changes in mTORC1 signaling, as its two downstream targets 4E-BP and S6K and phosphorylation of mTOR at its mTORC1 site Ser2448 were not affected. Although *rictor* deletion does not affect growth in most tissues, such an effect has been described in *Drosophila* (Hietakangas and Cohen, 2007) and in tumors induced by inactivation of the tumor suppressor PTEN (Guertin et al., 2009). Like in our work, signaling to mTORC1 was not affected and under normal conditions, and thus low PI3K signaling, the effect of rictor inactivation on cell growth was rather small or not detectable (Hietakangas and Cohen, 2007; Guertin et al., 2009). The observed microcephaly in the RibKO mice and the reduced cell size in RiPuKO mice might thus be the result of a highly active PI3K pathway in cells of the brain. However, we cannot exclude that the additional downstream targets of mTORC2, such as SGK1 and PKC isoforms, also contribute to the size difference. Such alternative explanations are particularly important as our biochemical analysis did not reveal changes in the activation of the two Akt targets FoxO1 and GSK3-β.

mTORC2 affects neuron morphology

Besides the effect of *rictor* deletion on cell size, we also observed a striking difference in neurite morphology. The most obvious difference to control mice, which was observed in both RibKO and RiPuKO mice, was an increase in the number of primary dendrites in Purkinje cells. Although both SGK1 and Akt have also been implicated in neurite growth (Read and Gorman, 2009), there is no direct evidence for their involvement in the shaping of neurites in Purkinje cells. We therefore hypothesize that those morphological changes are rather due to the loss of PKC isoforms in RibKO and RiPuKO mice. As shown previously, mTORC2 is required for the phosphorylation of some PKC isoforms at the turn motif site (Facchinetti et al., 2008; Ikenoue et al., 2008). This phosphorylation is important for the stability of the protein as nonphosphorylated forms are rapidly degraded by the proteasome pathway (Facchinetti et al., 2008; Ikenoue et al., 2008).

Published April 8, 2013

Our findings that several PKC isoforms are almost undetectable in brain lysates of adult RibKO mice are strong in vivo support for the importance of mTORC2 in stabilizing PKCs. Mutations in PKCγ cause spinocerebellar ataxia (SCA) type 14 (Chen et al., 2003) and as of today, more than 20 causative mutations have been described (Seki et al., 2011). Interestingly, some of the phenotypes described for Purkinje cells expressing those PKC mutants are similar to those observed in RibKO and RiPuKO mice. Most of the PKCγ mutations act in an autosomal-dominant way and it is not clear whether the ataxia is due to a dominant effect or the consequence of a loss of function of those mutants.

We also found that the two PKC substrates GAP-43 and MARCKS were not phosphorylated in RibKO mice. Whereas GAP-43 is well known to affect axon growth and terminal sprouting (Benowitz and Routtenberg, 1997), MARCKS affects dendritic branching (Li et al., 2008) and the morphology and density of postsynaptic spines (Calabrese and Halpain, 2005). Interestingly, the function of MARCKS is modulated by PKC-dependent phosphorylation. Thus, the resemblance of the phenotypes from PKCγ, GAP-43, and MARCKS mutants with those in RibKO or RiPuKO mice indicates that mTORC2 affects neuron morphology via the PKC pathway. The fact that only some aspects of the rictor-deficient phenotype are also observed in PKCγ- or PKCα-deficient Purkinje cells (Metzger, 2010) suggests that a knockout of individual PKC isoforms might be compensated by other isoforms.

Synaptic function

Another interesting result of our work is that synaptic function is also influenced by the deletion of *rictor* from the mouse brain. Because of the very severe morphological changes in the cerebellum of the RibKO mice, it is not that surprising to detect changes in the function of both excitatory and inhibitory synapses. The reduction in the frequency and the amplitude of the mEPSCs also correlated well with the observed changes in synaptic markers. More importantly, we also observed significant changes of synaptic function in the RiPuKO mice and those changes were restricted to Purkinje cells that were negative for PKCγ (i.e., deficient for rictor). While the amplitude of the mEPSCs was not changed in RiPuKO mice, mEPSC frequency was only ∼50% of that in control cells. In contrast, the frequency of the mIPSCs was like in controls but the amplitude was significantly smaller. The finding that a Purkinje cell–specific elimination of rictor differentially affected both excitatory and inhibitory synapses suggests a role of mTORC2 in synaptic homeostasis. Interestingly, homeostatic adaptation of synapses is discussed as a mechanism that contributes to the overall changes upon sustained exposure to morphine, and mTORC2 has been implicated in this process (Mazei-Robison et al., 2011).

In summary, our data show that mTORC2 has an important function in neurons and thus the removal of rictor from brain results in a considerably more severe phenotype than its inactivation in other tissues. Although our results on nestin-Cre–mediated *rictor* deletion suggest that mTORC2 might have similar functions in different neurons, it will be important in the future to analyze other neuron-specific *rictor* knockout models for the contribution of mTORC2 to specific psychiatric and neurological diseases.

Materials and methods

Generation of mice

Mice, homozygous for an allele containing LoxP sites flanking exon 4 and 5 of the *rictor* gene were crossed with nestin-Cre transgenic mice (B6.Cg-Tg(Nes-cre)1Kln/J; The Jackson Laboratory). These mice were then crossed with homozygously floxed *rictor* mice ($rictor^{fl/fl}$) to obtain RibKO mice ($rictor^{fl/fl}$; Tg(Nes-cre). Littermates that either lacked Cre ($rictor^{fl/fl}$) or were heterozygous for the floxed allele ($rictor^{fl/+}$; Tg(Nes-cre)) were used as controls. Purkinje cell–specific knockouts (RiPuKO mice) were obtained by crossing mice where *Cre* was knocked into the *L7/Pcp-2* locus (Saito et al., 2005) with $rictor^{fl/fl}$ mice. Further crossing yielded mice that carried two floxed *rictor* alleles and were heterozygous or homozygous for *L7/Pcp-2*-Cre and are referred to as $RiPuKO^{Cre/+}$ or $RiPuKO^{Cre/Cre}$, respectively. Control mice for $RiPuKO^{Cre/+}$ mice were ($rictor^{fl/fl}$; $L7/Pcp\text{-}2^{+/+}$). Controls for $RiPuKO^{Cre/Cre}$ mice were ($rictor^{fl/+}$; $L7/Pcp\text{-}2^{Cre/Cre}$). Genotyping was performed by PCR on DNA isolated from toe using specific primers for the floxed region, the Cre transgenes, or the recombined alleles as described elsewhere (Bentzinger et al., 2008).

Tissue homogenization and Western blot analysis

Brains were dissected, transferred to protein lysate buffer (50 mM Tris-HCl, pH 7.5, 150 mM NaCl, 1 mM EDTA, 1% Triton X-100 supplemented with EDTA-free protease inhibitor cocktail tablets [Roche], and phosphatase inhibitor tablets PhosSTOP [Roche]), and homogenized with a glass/Teflon homogenizer using 10 strokes at 800 rpm. The homogenate was centrifuged at 13,600 *g* for 15 min at 4°C. Cleared lysates were then used to determine total protein amount (BCA Protein Assay; Thermo Fisher Scientific). After dilution with 4× SDS sample buffer, equal protein amounts were loaded onto SDS gels.

Antibodies

Rabbit polyclonal antibodies were as follows: P-PKCα (Ser657), PKCγ, and P-GAP-43 (Ser41) from Santa Cruz Biotechnology, Inc.; P-FoxO1 (Ser256), P-mTOR (Ser2448), P-mTOR (Ser2481), Akt, P-Akt (Thr308), P-GSK-3β (Ser9), mTOR, PKCα, S6 ribosomal protein, P-S6 ribosomal protein (Ser235/236), P-S6 kinase(Thr389), S6K, NDRG1, P-NDRG1 (Thr346), P-4E-BP (Thr37/46), P-eIF4E (Ser209), cleaved caspase3, P-MARCKS (Ser152/156), and PKCζ from Cell Signaling Technology; and P-PKCβ2 (Thr641) and P-PKCε (Ser729) from Abcam. Rabbit monoclonal antibodies were as follows: PKCε, β-actin, P-Akt (Ser473), GSK-3β, P-Tuberin (Thr1462), and Rictor from Cell Signaling Technology; and PKCβ2 from Abcam. Mouse monoclonal antibodies were as follows: β-tubulin from BD, Calbindin D-28K from Swant, GAP-43 from Invitrogen, NeuN from EMD Millipore, and MARCKS from Abcam. Guinea pig polyclonal antibodies were as follows: vGLUT1 and vGLUT2 from Synaptic Systems. Rat monoclonal antibodies were as follows: anti-BrdU from AbD Serotec.

Histology and immunohistochemistry

Mice were anesthetized with a lethal dose of Pentobarbital (300 mg/kg) and transcardially perfused with 4% PFA. Brains were removed and tissue processed with a Shandon Pathcenter and embedded in paraffin (Merck). Paraffin blocks were cut with a microtome into 3–5-µm-thick sagittal or coronal sections. Antigen retrieval was performed before immunostaining by boiling the sections in sodium citrate buffer (10 mM sodium citrate and 0.05% Tween 20, pH 6) for 20 min. Sections were rinsed twice in PBS, blocked with blocking buffer (5% BSA in PBS, and 0.2% Triton X-100) for 30 min, and incubated with primary antibody overnight at 4°C. Samples were washed three times with PBS and then stained with appropriate fluorescently labeled, secondary antibodies for 1 h at room temperature. Samples were mounted with Kaiser's glycerol gelatin (Merck). General histology on sections was performed using cresyl violet. Immunohistochemically stained sections were examined with a fluorescence microscope (model DM5000B; Leica) and a 10× objective (HC PL Apo, NA 0.4; Leica), a 20× objective (PL Fluotar, NA 0.5; Leica), a 40× objective (HCX Plan APO, NA 0.75; Leica), or a 63× objective (HCX PL APO, NA 1.32; Leica). Pictures were captured with a digital camera (F-View; Soft Imaging System) and analySIS software (Soft Imaging System). In some experiments, sections were imaged with the SPE confocal laser scanning microscope (model DMI4000B; Leica) using an ACS APO 40× objective (NA 1.15) or an ACS APO 63× objective (NA 1.3) at a resolution of 1024 × 1024 pixels. Pictures were captured using the built-in digital camera and software. Image analysis was performed using Imaris (Bitplane AG) or Adobe Photoshop CS5.

Golgi staining was performed by incubating freshly perfused mouse brains in Golgi solution (5% potassium dichromate, 5% potassium chromate,

Published April 8, 2013

and 5% mercuric chloride dissolved in H_2O) for 6 wk. The solution was changed every 2–3 days. Brains were subsequently dehydrated in 50, 70, 90, and 100% ethanol, each step for several days and then transferred to 2, 4, and 8% Celloidin solution. For embedding, 8% Celloidin was evaporated to 16%, hardened to a block, and cut with a vibratome into 200-µm sagittal sections. The sections were transferred onto gelatinized slides and stained first in ammonium hydroxide (14%) for 30 min followed by Kodak fix solution for 30 min. The sections were then dehydrated in 50, 70, 90, and 100% ethanol followed by 15 min in CXA solution (1:1:1 chloroform/xylol/ethanol) and embedded with Merckoglas (Merck). Microscopy was performed with a light microscope (model DM RB, Leica) using bright-field optics and 10, 20, or 40× objectives (PL Fluotar, NA 0.3–0.7; Leica). Pictures were captured with a digital camera (model DFC 420; Leica) and the appropriate software.

Quantification

Quantification of cell numbers used the method of isotropic fractionation as described elsewhere (Herculano-Houzel and Lent, 2005). In brief, brains were fixed for 3–30 d in 4% PFA and then mechanically dissociated with a glass/Teflon homogenizer in 40 mM sodium citrate and 1% Triton X-100. The homogenate was centrifuged for 10 min at 4,000 *g* and the supernatant was carefully removed. The pellet containing the nuclei was resuspended in 10 ml PBS containing 1% Hoechst dye. After sufficient agitation to achieve isotropy, 5-µl aliquots were removed and the number of nuclei was counted in a hemocytometer using a fluorescence microscope. Quantification of Golgi-stained neurons was performed by Neurolucida reconstruction and analysis with Neurolucida software. Volumetric quantification of brain areas was performed on cresyl violet–stained, 25-µm coronal paraffin sections. The arbitrary area of microscopic pictures taken at 2.5× was analyzed with Analysis software. Analysis of cell density was performed on sagittal, NeuN-stained, 5-µm-thick paraffin sections in the retrosplenial and visual cortex. Sholl analysis of dissociated hippocampal neurons was performed with Analysis software by counting the number of neurite crossings starting from the soma in a defined distance of 25 µm up to 125 µm. Quantification of Western blot protein band intensity was performed with the ImageJ program (National Institutes of Health). Quantification of the mean dendrite diameter of Purkinje cells was performed in sagittal, calbindin-stained cerebellar sections by measuring the dendrite diameter within the primary dendrite from the soma up to the first node. Apoptotic cells were quantified by staining P7 cortical sections with antibodies to cleaved caspase3. Cells were distinguished from blood vessels by counterstaining with Hoechst and the number of caspase3-positive cells per 1,000 cells (identified by Hoechst staining) was determined.

Statistical analysis

Statistical significance was assessed with the Student's *t* test or one-way Anova. Differences were considered to be statistically significant if the P value was less than 0.05. Quantitative data are presented as means ± SEM as indicated in the figure legends.

Electrophysiology

Mice were deeply sedated with isoflurane. After decapitation, the brain was rapidly removed and immediately transferred into ice-cold, oxygenated (95% O_2, 5% CO_2), low calcium artificial cerebrospinal fluid (ACSF) containing 119 mM NaCl, 1 mM NaH_2PO_4, 2.5 mM KCl, 0.125 mM $CaCl_2$, 3.3 mM $MgCl_2$, 11 mM D-glucose, and 26.2 mM $NaHCO_3$. Cerebella were cut with a vibratome into 250-µm sagittal sections in low calcium ACSF. Slices were transferred to oxygenated ACSF containing 119 mM NaCl, 1 mM NaH_2PO_4, 2.5 mM KCl, 2.5 mM $CaCl_2$, 1.3 mM $MgCl_2$, 11 mM D-glucose, and 26.2 mM $NaHCO_3$, incubated for 30 min at 34°C, and subsequently retained for at least 30 min at room temperature in oxygenated ACSF before recording. Miniature events were recorded using an Axopatch Multiclamp 700B amplifier (Molecular Devices) and borosilicate glass pipettes (4–6 mΩ) filled with intracellular solution (135 mM $CsMeSO_4$, 8 mM NaCl, 10 mM Hepes, 0.5 mM EGTA, 4 mM Mg-ATP, 0.3 mM Na-GTP, and 5 mM lidocaine-*N*-ethylbromide). For mEPSC recording, the holding potential was set to −70 mV. For mIPSC recording, the holding potential was set to 0 mV. In both conditions, the postsynaptic current was recorded for 10 min in the presence of 0.5 µM tetrodotoxin (TTX). Traces were further analyzed with the Mini Analysis Program v6 (Synaptosoft).

Biocytin labeling of single Purkinje cells

Biocytin was dissolved in the intracellular solution at a concentration of 3 mg/ml by sonication at 4°C. The orientation of the acute slice was noted for the whole-cell recordings. Staining procedure was adapted from Wierenga et al. (2008). In brief, after the recording, slices were fixed overnight at 4°C in 4% PFA dissolved in PBS. After extensive washing in PBS, slices were permeabilized and blocked for 24 h at 4°C in blocking solution (10% FBS in PBS, containing 0.4% Triton X-100) on a shaker. Anti-PKC-γ antibody was applied overnight at 4°C in blocking solution (5% FBS in PBS, containing 0.4% Triton X-100) on a shaker. After extensive washing with PBS, appropriate secondary antibodies were applied. Acute slices were mounted in Kaiser's glycerol gelatin with the patched side facing up. Stained slices were analyzed by confocal microscopy as described above using the 40× objective.

Single-cell RT-PCR

Purkinje cells were cell patch-clamped for 10–20 min using silanized patch pipettes filled with 7 µl of intracellular solution that contained biocytin as described above. After whole-cell recording, cytosol was harvested by aspiration and expelled into a PCR tube containing rRNasin (Promega), random hexamer primers, and dNTP (final concentrations are indicated below). The mixture was incubated for 5 min at 65°C and then chilled on ice before adding further components. mRNA was reverse transcribed in a 20-µl reaction volume containing 100 ng random hexamer primers, 0.5 mM dNTPs, 40 U rRNasin, 5 mM dithiothreitol, and 10 U SuperScript III reverse transcription (Invitrogen) in 1× "first strand buffer" (5× buffer: 0.25 M Tris-HCl, pH 8.3 at 25°C, 375 mM KCl, and 15 mM $MgCl_2$). The reaction mixture was incubated for 45 min at 50°C, followed by inactivation at 70°C for 15 min. 2 µl of the stopped reaction mixture were used as input cDNA for the subsequent nested two-step PCR, which was performed with the primer pairs P3–P4 for the first and P1–P2 for the second PCR, respectively. 35 cycles were performed for each PCR. The primer sequences are P1: 5′-GCCAAATTGCAAGGAGTATCA-3′; P2: 5′-TGAGTTGGCCACAGAACTAGG-3′; P3: 5′-CTGACCCGAGAACCTTCTGA-3′; P4: 5′-TTCCTGAAGCCCATCATTTC-3′. The primer pair P1–P2 results in an amplicon of 365 bp or 172 bp in case of the wild-type or the recombined allele, respectively.

Tissue cultures

Neurospheres were isolated from newborn (P0) mice. Pups were decapitated, and brains were removed and transferred into ice-cold Hank's buffered salt solution (HBSS; Invitrogen). Meninges were carefully removed under the dissection microscope and one brain half was transferred into freshly prepared neurosphere medium (NM) consisting of DMEM-F12 (1:1), supplemented with 1% penicillin/streptomycin, 0.2 mg/ml glutamine, 2% B27, 2 µg/ml heparin, 20 ng/ml EGF, and 10 ng/ml FGF2. The brain was carefully homogenized and plated on a 6-cm dish containing 4 ml NM and maintained in an incubator (36.5°C, 5% CO_2). After 4–5 d the neurospheres were trypinized, dissociated into single cell suspension, and the resulting secondary neurospheres were cultured for 6 d. 24 h before fixation, 10 µM BrdU was added to the medium. Neurospheres were fixed with 4% PFA and imaged at low magnification to determine the diameter of the neurospheres. To assess the number of the BrdU-positive cells, neurospheres were embedded in cryoprotective material, cut into 12-µm-thick sections, and immunostained with antibodies to BrdU. The number of BrdU-positive cells per sphere was counted and normalized to the sphere diameter.

Organotypic cerebellar slices were cultured as described elsewhere (Boukhtouche et al., 2006). In brief, P0 brains were dissected and transferred into ice-cold Gey's balanced salt solution. Meninges were carefully removed and cerebella dissected. With a tissue chopper (McIlwain), 350-µm-thick sagittal slices were cut and transferred into fresh Gey's solution. Slices were cultured on 0.4-µm membranes in 1 ml culture medium (50% basal medium with Earl's salts, 25% HBSS, 25% horse serum, 1 mM glutamine, and 5 mg/ml glucose) for 14 d. Culture medium was changed every 2–3 d.

Cultures of dissociated hippocampal neurons were prepared as follows: brains of P0 mice were dissected and transferred into ice-cold HBSS. Hippocampi were removed, trypsinized for 15 min, and dissociated. Cells were plated onto poly-L-lysine–coated coverslips at a density of 90,000 cells per well in a 24-well plate. Neurons were grown for 14 d. After 7 d, neurons were transfected with constructs encoding GFP under the synapsin promoter using Lipofectamine. After 14 d, cultures were fixed with 4% PFA in PBS containing 120 mM sucrose, washed in PBS, and embedded with Kaiser's glycerol gelatin.

Mouse behavior

For hindlimb clasping assessment, 1-yr-old mice were lifted by the tail and held over the cage for up to 2 min. Clasping was scored when mice crossed hindlimbs for more than 3 s. The rotarod test was performed by placing 10-wk-old mice on a rod that accelerated from 5 rpm to 30 rpm in 2 min. Latency to fall off the rod was measured.

Published April 8, 2013

Online supplemental material

Fig. S1 shows that the number of apoptotic cells as visualized by caspase3 staining is not increased and that cell density of NeuN-positive neurons is increased in RibKO mice. Fig. S2 shows that phosphorylation of PKCα, PKCβ2, and PKCε is greatly reduced in RibKO mice. Fig. S3 shows that PKCγ-negative Purkinje cells in RiPuKO mice are deficient for rictor. Online supplemental material is available at http://www.jcb.org/cgi/content/full/jcb.201205030/DC1.

We thank M. Gassmann and J. Kapfhammer for reading the manuscript; S. Frank for his help in the initial analysis of the histology; members of the laboratory of M. Hall for reagents and discussions; F. Boukhtouche for the help in setting up cerebellar slice cultures; and P. Scheiffele for providing us with the *L7/Pcp-2-Cre* mice.

This work was supported by the Swiss National Science Foundation, the Cantons of Basel-Stadt and Basel-Landschaft, and Swiss Life.

Submitted: 4 May 2012
Accepted: 12 March 2013

References

Benowitz, L.I., and A. Routtenberg. 1997. GAP-43: an intrinsic determinant of neuronal development and plasticity. *Trends Neurosci.* 20:84–91. http://dx.doi.org/10.1016/S0166-2236(96)10072-2

Bentzinger, C.F., K. Romanino, D. Cloëtta, S. Lin, J.B. Mascarenhas, F. Oliveri, J. Xia, E. Casanova, C.F. Costa, M. Brink, et al. 2008. Skeletal muscle-specific ablation of raptor, but not of rictor, causes metabolic changes and results in muscle dystrophy. *Cell Metab.* 8:411–424. http://dx.doi.org/10.1016/j.cmet.2008.10.002

Boukhtouche, F., S. Janmaat, G. Vodjdani, V. Gautheron, J. Mallet, I. Dusart, and J. Mariani. 2006. Retinoid-related orphan receptor alpha controls the early steps of Purkinje cell dendritic differentiation. *J. Neurosci.* 26:1531–1538. http://dx.doi.org/10.1523/JNEUROSCI.4636-05.2006

Calabrese, B., and S. Halpain. 2005. Essential role for the PKC target MARCKS in maintaining dendritic spine morphology. *Neuron*. 48:77–90. http://dx.doi.org/10.1016/j.neuron.2005.08.027

Chen, D.H., Z. Brkanac, C.L. Verlinde, X.J. Tan, L. Bylenok, D. Nochlin, M. Matsushita, H. Lipe, J. Wolff, M. Fernandez, et al. 2003. Missense mutations in the regulatory domain of PKC gamma: a new mechanism for dominant nonepisodic cerebellar ataxia. *Am. J. Hum. Genet.* 72:839–849. http://dx.doi.org/10.1086/373883

Cole, E.H., O. Johnston, C.L. Rose, and J.S. Gill. 2008. Impact of acute rejection and new-onset diabetes on long-term transplant graft and patient survival. *Clin. J. Am. Soc. Nephrol.* 3:814–821. http://dx.doi.org/10.2215/CJN.04681107

Crino, P.B. 2011. mTOR: A pathogenic signaling pathway in developmental brain malformations. *Trends Mol. Med.* 17:734–742. http://dx.doi.org/10.1016/j.molmed.2011.07.008

Cybulski, N., P. Polak, J. Auwerx, M.A. Rüegg, and M.N. Hall. 2009. mTOR complex 2 in adipose tissue negatively controls whole-body growth. *Proc. Natl. Acad. Sci. USA*. 106:9902–9907. http://dx.doi.org/10.1073/pnas.0811321106

Easton, R.M., H. Cho, K. Roovers, D.W. Shineman, M. Mizrahi, M.S. Forman, V.M. Lee, M. Szabolcs, R. de Jong, T. Oltersdorf, et al. 2005. Role for Akt3/protein kinase Bgamma in attainment of normal brain size. *Mol. Cell. Biol.* 25:1869–1878. http://dx.doi.org/10.1128/MCB.25.5.1869-1878.2005

Ehninger, D., and A.J. Silva. 2011. Rapamycin for treating Tuberous sclerosis and Autism spectrum disorders. *Trends Mol. Med.* 17:78–87. http://dx.doi.org/10.1016/j.molmed.2010.10.002

Facchinetti, V., W. Ouyang, H. Wei, N. Soto, A. Lazorchak, C. Gould, C. Lowry, A.C. Newton, Y. Mao, R.Q. Miao, et al. 2008. The mammalian target of rapamycin complex 2 controls folding and stability of Akt and protein kinase C. *EMBO J.* 27:1932–1943. http://dx.doi.org/10.1038/emboj.2008.120

Fremeau, R.T. Jr., M.D. Troyer, I. Pahner, G.O. Nygaard, C.H. Tran, R.J. Reimer, E.E. Bellocchio, D. Fortin, J. Storm-Mathisen, and R.H. Edwards. 2001. The expression of vesicular glutamate transporters defines two classes of excitatory synapse. *Neuron*. 31:247–260. http://dx.doi.org/10.1016/S0896-6273(01)00344-0

García-Martínez, J.M., and D.R. Alessi. 2008. mTOR complex 2 (mTORC2) controls hydrophobic motif phosphorylation and activation of serum- and glucocorticoid-induced protein kinase 1 (SGK1). *Biochem. J.* 416:375–385. http://dx.doi.org/10.1042/BJ20081668

Gödel, M., B. Hartleben, N. Herbach, S. Liu, S. Zschiedrich, S. Lu, A. Debreczeni-Mór, M.T. Lindenmeyer, M.P. Rastaldi, G. Hartleben, et al. 2011. Role of mTOR in podocyte function and diabetic nephropathy in humans and mice. *J. Clin. Invest.* 121:2197–2209. http://dx.doi.org/10.1172/JCI44774

Graus-Porta, D., S. Blaess, M. Senften, A. Littlewood-Evans, C. Damsky, Z. Huang, P. Orban, R. Klein, J.C. Schittny, and U. Müller. 2001. Beta1-class integrins regulate the development of laminae and folia in the cerebral and cerebellar cortex. *Neuron*. 31:367–379. http://dx.doi.org/10.1016/S0896-6273(01)00374-9

Guertin, D.A., D.M. Stevens, C.C. Thoreen, A.A. Burds, N.Y. Kalaany, J. Moffat, M. Brown, K.J. Fitzgerald, and D.M. Sabatini. 2006. Ablation in mice of the mTORC components raptor, rictor, or mLST8 reveals that mTORC2 is required for signaling to Akt-FOXO and PKCalpha, but not S6K1. *Dev. Cell*. 11:859–871. http://dx.doi.org/10.1016/j.devcel.2006.10.007

Guertin, D.A., D.M. Stevens, M. Saitoh, S. Kinkel, K. Crosby, J.H. Sheen, D.J. Mullholland, M.A. Magnuson, H. Wu, and D.M. Sabatini. 2009. mTOR complex 2 is required for the development of prostate cancer induced by Pten loss in mice. *Cancer Cell*. 15:148–159. http://dx.doi.org/10.1016/j.ccr.2008.12.017

Herculano-Houzel, S., and R. Lent. 2005. Isotropic fractionator: a simple, rapid method for the quantification of total cell and neuron numbers in the brain. *J. Neurosci.* 25:2518–2521. http://dx.doi.org/10.1523/JNEUROSCI.4526-04.2005

Hietakangas, V., and S.M. Cohen. 2007. Re-evaluating AKT regulation: role of TOR complex 2 in tissue growth. *Genes Dev.* 21:632–637. http://dx.doi.org/10.1101/gad.416307

Hisano, S., K. Sawada, M. Kawano, M. Kanemoto, G. Xiong, K. Mogi, H. Sakata-Haga, J. Takeda, Y. Fukui, and H. Nogami. 2002. Expression of inorganic phosphate/vesicular glutamate transporters (BNPI/VGLUT1 and DNPI/VGLUT2) in the cerebellum and precerebellar nuclei of the rat. *Brain Res. Mol. Brain Res.* 107:23–31. http://dx.doi.org/10.1016/S0169-328X(02)00442-4

Ikenoue, T., K. Inoki, Q. Yang, X. Zhou, and K.L. Guan. 2008. Essential function of TORC2 in PKC and Akt turn motif phosphorylation, maturation and signalling. *EMBO J.* 27:1919–1931. http://dx.doi.org/10.1038/emboj.2008.119

Jacinto, E., R. Loewith, A. Schmidt, S. Lin, M.A. Rüegg, A. Hall, and M.N. Hall. 2004. Mammalian TOR complex 2 controls the actin cytoskeleton and is rapamycin insensitive. *Nat. Cell Biol.* 6:1122–1128. http://dx.doi.org/10.1038/ncb1183

Kapfhammer, J.P. 2004. Cellular and molecular control of dendritic growth and development of cerebellar Purkinje cells. *Prog. Histochem. Cytochem.* 39:131–182. http://dx.doi.org/10.1016/j.proghi.2004.07.002

Kim, D.H., D.D. Sarbassov, S.M. Ali, J.E. King, R.R. Latek, H. Erdjument-Bromage, P. Tempst, and D.M. Sabatini. 2002. mTOR interacts with raptor to form a nutrient-sensitive complex that signals to the cell growth machinery. *Cell*. 110:163–175. http://dx.doi.org/10.1016/S0092-8674(02)00808-5

Kumar, A., T.E. Harris, S.R. Keller, K.M. Choi, M.A. Magnuson, and J.C. Lawrence Jr. 2008. Muscle-specific deletion of rictor impairs insulin-stimulated glucose transport and enhances Basal glycogen synthase activity. *Mol. Cell. Biol.* 28:61–70. http://dx.doi.org/10.1128/MCB.01405-07

Lamming, D.W., L. Ye, P. Katajisto, M.D. Goncalves, M. Saitoh, D.M. Stevens, J.G. Davis, A.B. Salmon, A. Richardson, R.S. Ahima, et al. 2012. Rapamycin-induced insulin resistance is mediated by mTORC2 loss and uncoupled from longevity. *Science*. 335:1638–1643. http://dx.doi.org/10.1126/science.1215135

Laplante, M., and D.M. Sabatini. 2012. mTOR signaling in growth control and disease. *Cell*. 149:274–293. http://dx.doi.org/10.1016/j.cell.2012.03.017

Larsell, O. 1952. The morphogenesis and adult pattern of the lobules and fissures of the cerebellum of the white rat. *J. Comp. Neurol.* 97:281–356. http://dx.doi.org/10.1002/cne.900970204

Lein, E.S., M.J. Hawrylycz, N. Ao, M. Ayres, A. Bensinger, A. Bernard, A.F. Boe, M.S. Boguski, K.S. Brockway, E.J. Byrnes, et al. 2007. Genome-wide atlas of gene expression in the adult mouse brain. *Nature*. 445:168–176. http://dx.doi.org/10.1038/nature05453

Li, H., G. Chen, B. Zhou, and S. Duan. 2008. Actin filament assembly by myristoylated alanine-rich C kinase substrate-phosphatidylinositol-4, 5-diphosphate signaling is critical for dendrite branching. *Mol. Biol. Cell*. 19:4804–4813. http://dx.doi.org/10.1091/mbc.E08-03-0294

Loewith, R., E. Jacinto, S. Wullschleger, A. Lorberg, J.L. Crespo, D. Bonenfant, W. Oppliger, P. Jenoe, and M.N. Hall. 2002. Two TOR complexes, only one of which is rapamycin sensitive, have distinct roles in cell growth control. *Mol. Cell*. 10:457–468. http://dx.doi.org/10.1016/S1097-2765(02)00636-6

Published April 8, 2013

Mazei-Robison, M.S., J.W. Koo, A.K. Friedman, C.S. Lansink, A.J. Robison, M. Vinish, V. Krishnan, S. Kim, M.A. Siuta, A. Galli, et al. 2011. Role for mTOR signaling and neuronal activity in morphine-induced adaptations in ventral tegmental area dopamine neurons. *Neuron*. 72:977–990. http://dx.doi.org/10.1016/j.neuron.2011.10.012

Metzger, F. 2010. Molecular and cellular control of dendrite maturation during brain development. *Curr Mol Pharmacol*. 3:1–11.

Ohno, S., and Y. Nishizuka. 2002. Protein kinase C isotypes and their specific functions: prologue. *J. Biochem.* 132:509–511. http://dx.doi.org/10.1093/oxfordjournals.jbchem.a003249

Polak, P., N. Cybulski, J.N. Feige, J. Auwerx, M.A. Rüegg, and M.N. Hall. 2008. Adipose-specific knockout of raptor results in lean mice with enhanced mitochondrial respiration. *Cell Metab.* 8:399–410. http://dx.doi.org/10.1016/j.cmet.2008.09.003

Read, D.E., and A.M. Gorman. 2009. Involvement of Akt in neurite outgrowth. *Cell. Mol. Life Sci.* 66:2975–2984. http://dx.doi.org/10.1007/s00018-009-0057-8

Richter, J.D., and E. Klann. 2009. Making synaptic plasticity and memory last: mechanisms of translational regulation. *Genes Dev*. 23:1–11. http://dx.doi.org/10.1101/gad.1735809

Risson, V., L. Mazelin, M. Roceri, H. Sanchez, V. Moncollin, C. Corneloup, H. Richard-Bulteau, A. Vignaud, D. Baas, A. Defour, et al. 2009. Muscle inactivation of mTOR causes metabolic and dystrophin defects leading to severe myopathy. *J. Cell Biol.* 187:859–874. http://dx.doi.org/10.1083/jcb.200903131

Russell, R.C., C. Fang, and K.L. Guan. 2011. An emerging role for TOR signaling in mammalian tissue and stem cell physiology. *Development*. 138:3343–3356. http://dx.doi.org/10.1242/dev.058230

Saito, H., H. Tsumura, S. Otake, A. Nishida, T. Furukawa, and N. Suzuki. 2005. L7/Pcp-2-specific expression of Cre recombinase using knock-in approach. *Biochem. Biophys. Res. Commun.* 331:1216–1221. http://dx.doi.org/10.1016/j.bbrc.2005.04.043

Sarbassov, D.D., S.M. Ali, D.H. Kim, D.A. Guertin, R.R. Latek, H. Erdjument-Bromage, P. Tempst, and D.M. Sabatini. 2004. Rictor, a novel binding partner of mTOR, defines a rapamycin-insensitive and raptor-independent pathway that regulates the cytoskeleton. *Curr. Biol.* 14:1296–1302. http://dx.doi.org/10.1016/j.cub.2004.06.054

Sarbassov, D.D., D.A. Guertin, S.M. Ali, and D.M. Sabatini. 2005. Phosphorylation and regulation of Akt/PKB by the rictor-mTOR complex. *Science*. 307:1098–1101. http://dx.doi.org/10.1126/science.1106148

Sarbassov, D.D., S.M. Ali, S. Sengupta, J.H. Sheen, P.P. Hsu, A.F. Bagley, A.L. Markhard, and D.M. Sabatini. 2006. Prolonged rapamycin treatment inhibits mTORC2 assembly and Akt/PKB. *Mol. Cell*. 22:159–168. http://dx.doi.org/10.1016/j.molcel.2006.03.029

Seki, T., N. Adachi, N. Abe-Seki, T. Shimahara, H. Takahashi, K. Yamamoto, N. Saito, and N. Sakai. 2011. Elucidation of the molecular mechanism and exploration of novel therapeutics for spinocerebellar ataxia caused by mutant protein kinase Cγ. *J. Pharmacol. Sci.* 116:239–247. http://dx.doi.org/10.1254/jphs.11R04CP

Shiota, C., J.T. Woo, J. Lindner, K.D. Shelton, and M.A. Magnuson. 2006. Multiallelic disruption of the rictor gene in mice reveals that mTOR complex 2 is essential for fetal growth and viability. *Dev. Cell*. 11:583–589. http://dx.doi.org/10.1016/j.devcel.2006.08.013

Sidman, R.L., P.W. Lane, and M.M. Dickie. 1962. Staggerer, a new mutation in the mouse affecting the cerebellum. *Science*. 137:610–612. http://dx.doi.org/10.1126/science.137.3530.610

Sillitoe, R.V., and A.L. Joyner. 2007. Morphology, molecular codes, and circuitry produce the three-dimensional complexity of the cerebellum. *Annu. Rev. Cell Dev. Biol.* 23:549–577. http://dx.doi.org/10.1146/annurev.cellbio.23.090506.123237

Siuta, M.A., S.D. Robertson, H. Kocalis, C. Saunders, P.J. Gresch, V. Khatri, C. Shiota, J.P. Kennedy, C.W. Lindsley, L.C. Daws, et al. 2010. Dysregulation of the norepinephrine transporter sustains cortical hypodopaminergia and schizophrenia-like behaviors in neuronal rictor null mice. *PLoS Biol.* 8:e1000393. http://dx.doi.org/10.1371/journal.pbio.1000393

Sucher, N.J., D.L. Deitcher, D.J. Baro, R.M. Warrick, and E. Guenther. 2000. Genes and channels: patch/voltage-clamp analysis and single-cell RT-PCR. *Cell Tissue Res.* 302:295–307. http://dx.doi.org/10.1007/s004410000289

Tronche, F., C. Kellendonk, O. Kretz, P. Gass, K. Anlag, P.C. Orban, R. Bock, R. Klein, and G. Schütz. 1999. Disruption of the glucocorticoid receptor gene in the nervous system results in reduced anxiety. *Nat. Genet.* 23:99–103. http://dx.doi.org/10.1038/12703

Tschopp, O., Z.Z. Yang, D. Brodbeck, B.A. Dummler, M. Hemmings-Mieszczak, T. Watanabe, T. Michaelis, J. Frahm, and B.A. Hemmings. 2005. Essential role of protein kinase B gamma (PKB gamma/Akt3) in postnatal brain development but not in glucose homeostasis. *Development*. 132:2943–2954. http://dx.doi.org/10.1242/dev.01864

Wetts, R., and K. Herrup. 1982. Interaction of granule, Purkinje and inferior olivary neurons in lurcher chimeric mice. II. Granule cell death. *Brain Res.* 250:358–362. http://dx.doi.org/10.1016/0006-8993(82)90431-0

Wierenga, C.J., N. Becker, and T. Bonhoeffer. 2008. GABAergic synapses are formed without the involvement of dendritic protrusions. *Nat. Neurosci.* 11:1044–1052. http://dx.doi.org/10.1038/nn.2180

Wullschleger, S., R. Loewith, and M.N. Hall. 2006. TOR signaling in growth and metabolism. *Cell*. 124:471–484. http://dx.doi.org/10.1016/j.cell.2006.01.016

Published April 8, 2013

Thomanetz et al., http://www.jcb.org/cgi/content/full/jcb.201205030/DC1

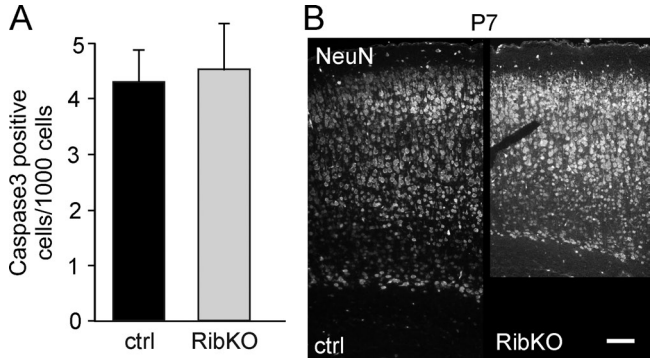

Figure S1. **Rictor deficiency does not increase apoptosis and affects the size of neurons.** (A) Quantification of the number of caspase3-positive cells in the cortex of P7 control and RibKO mice. The mean number of caspase-positive cells per 1,000 cells did not differ between control and RibKO mice. Data represent mean ± SEM; $n = 3$ mice and 13 sections (ctrl); $n = 4$ mice and 15 sections (RibKO). (B) Representative pictures of cortical sections of P7 control and RibKO mice stained with antibodies against NeuN. Note that the cortex is smaller and the cell density is increased in RibKO mice. Bar, 100 µm.

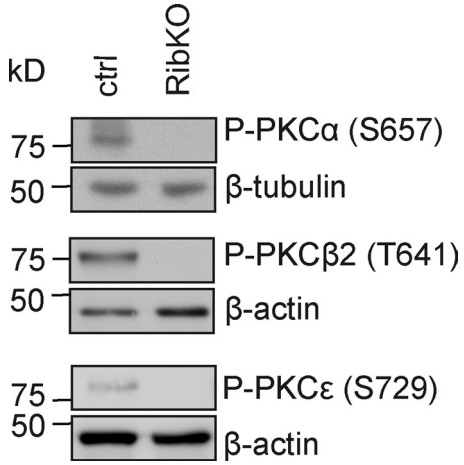

Figure S2. **Phosphorylation of several PKC isoforms is diminished in RibKO mice.** Western blot analysis of adult brain lysate from control and RibKO mice for phosphorylated PKCα, PKCβ2, and PKCε.

Published April 8, 2013

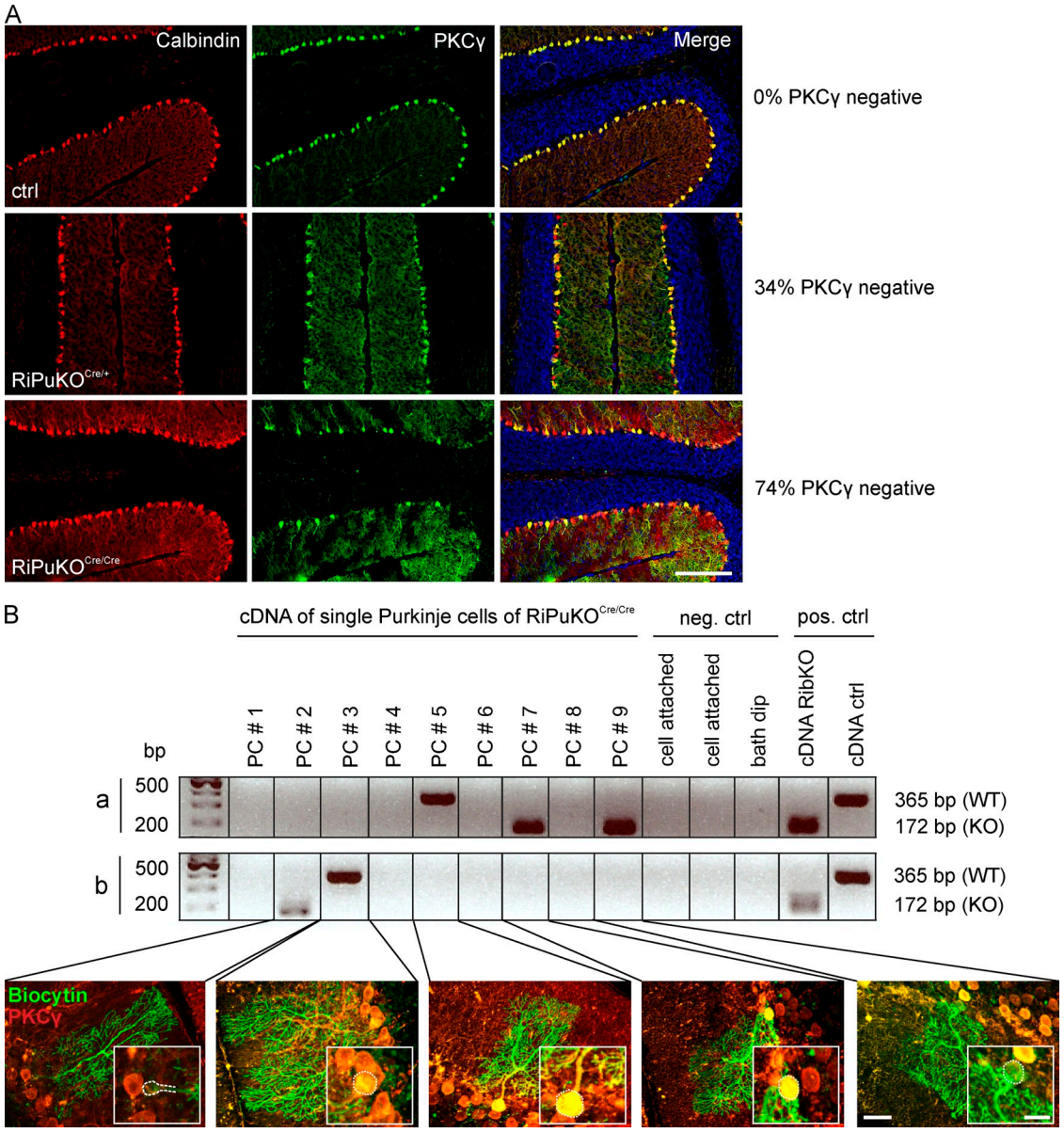

Figure S3. **PKCγ immunoreactivity is indicative of the *rictor* deletion in Purkinje cells.** (A) Immunostaining of sagittal cerebellar sections from control, RiPuKO$^{Cre/+}$, and RiPuKO$^{Cre/Cre}$ mice for calbindin and PKCγ. Note that the number of PKCγ-negative cells increases with higher Cre expression from 34% in RiPuKO$^{Cre/+}$ cerebella to 74% in RiPuKO$^{Cre/Cre}$ mice. (B) PCR of reverse-transcribed cDNA from RNA isolated from single Purkinje cells of RiPuKO$^{Cre/Cre}$ mice and immunostaining of the corresponding biocytin-filled cells with antibodies to PKCγ. Single-cell PCR was performed in duplicates (a and b). Bars: (A) 200 µm; (B) 50 µm (25 µm in insets).

mTORC1 and mTORC2 have largely distinct functions in Purkinje cells

Nico Angliker[1], Michael Burri[1], Mariana Zaichuk[2], Jean-Marc Fritschy[2] and Markus A. Rüegg[1]

[1]Biozentrum, University of Basel, CH-4056 Basel, Switzerland

[2]Institute of Pharmacology and Toxicology, University of Zürich, CH-8057 Zurich, Switzerland

Abbreviated title: mTORC1 and mTORC2 inactivation in Purkinje cells

Key words: raptor, rictor, cerebellum, motor coordination, neurodegeneration, climbing fibre innervation, dendritic self-avoidance

Number of pages: 36

Number of figures: 7

Number of tables: 0

Abstract: 249; Introduction: 496; Discussion: 1245 words

Acknowledgements

We thank Dr. J. S. Tchorz and Prof. B. Bettler for providing a *Rosa26* reporter line, Prof. P. Scheiffele for the *L7/Pcp-2 Cre* line and Dr. E. Pérez-Garci and Dr. J. R. Reinhard for comments on the manuscript. The monoclonal antibody GAD-6, developed by Dr. D.I. Gottlieb, was obtained from the Developmental Studies Hybridoma Bank, created by the NICHD of the NIH and maintained at the University of Iowa, Department of Biology, Iowa City, IA 52242. The Car8 antibody was obtained from Dr. Masahiko Watanabe, Hokkaido University Graduate School of Medicine, Sapporo, Japan. This work was supported by the Cantons of Basel-Stadt and Baselland (MAR) and a Sinergia grant of the Swiss National Science Foundation to MAR and JMF. The authors declare no competing financial interests.

Send correspondence to:

Markus A. Rüegg, Ph.D.

Biozentrum, University of Basel

Klingelbergstrasse 70

CH-4056 Basel, Switzerland

Phone: +41 61 267 22 23

Fax: +41 61 267 22 08

email: markus-a.ruegg@unibas.ch

ABSTRACT

The mammalian target of rapamycin (mTOR) is a key regulator of cellular growth and associates with other proteins to two different multi-protein complexes, called mTORC1 and mTORC2. Dysregulation of mTORC1 signalling in brain is implicated in neuropathological conditions, such as autism spectrum or neurodegenerative disorders. Accordingly, allosteric mTOR inhibitors are currently in clinical trials for the treatment of such disorders. Here, we ablated either mTORC1 or mTORC2 conditionally in Purkinje cells of the cerebellum to dissect their role in the development, function and survival of these neurons. We find that the two mouse models are largely different from each other by phenotype and cellular responses. Inactivation of mTORC2 but not mTORC1 led to motor coordination deficits at an early age. This phenotype correlated with developmental deficits in climbing fibre elimination and impaired dendritic self-avoidance in mTORC2-deficient Purkinje cells. In contrast, inactivation of mTORC1 but not mTORC2 affected social interest of the mice and caused a progressive loss of Purkinje cells due to apoptosis. This loss was paralleled by age-dependent motor deficits. Comparison of mTORC1-deficient Purkinje cells with those deficient for the mTORC1 inhibitor TSC1 revealed a striking overlap in Purkinje cell degeneration and death, which included neurofilamentopathy and reactive gliosis. Altogether, our study reveals distinct roles of mTORC1 and mTORC2 in Purkinje cells for the behaviour of mice and the survival of targeted neurons. Our study also highlights a convergence between the phenotypes of Purkinje cells lacking mTORC1 activity and those expressing constitutively active mTORC1 due to TSC1 deficiency.

INTRODUCTION

In mammalian cells, the serine/threonine protein kinase mTOR assembles into two multi-protein complexes, called mTORC1 and mTORC2. The composition of these two complexes overlaps for some proteins but differs for others such as raptor or rictor, which are essential for the function of mTORC1 and mTORC2, respectively (Laplante and Sabatini, 2012). mTORC1 integrates various signals from growth factors, energy status or amino acid availability and as output promotes protein synthesis, contributes to lipogenesis and inhibits autophagy (Shimobayashi and Hall, 2014). In line with these functions, mTORC1 was found to be essential for cell growth and proliferation. Activation of mTORC2 is less well understood, but it is well established that this complex phosphorylates and activates members of the AGC kinase family, including Akt, SGK1 and PKCs, which ascribes this complex a role in cell survival/metabolism and actin cytoskeletal organization (Oh and Jacinto, 2011). As previously described, whole brain raptor knockout mice die perinatally (Cloetta et al., 2013) while the corresponding rictor knockout mice are viable but ataxic and show a pronounced Purkinje cell phenotype (Thomanetz et al., 2013). To prevent perinatal lethality of raptor depletion in the brain and to further analyse the importance of mTOR signalling in Purkinje cells, we generated conditional knockout mice in which *Rptor* or *Rictor* was knocked out exclusively in this subpopulation of neurons. This allowed us to analyse and dissect the roles of mTORC1 and mTORC2 in developing and adult Purkinje cells and to investigate the resulting effect on mouse behaviour. Purkinje cells provide the only output of the cerebellar cortex and growing evidence indicates that the cerebellum is not only essential for motor control but may also be involved in other behavioural aspects, such as social behaviour, and therefore has been linked to neurodevelopmental disorders (Schmahmann et al., 2007; Wang et al., 2014). This notion has recently been supported by the finding that Purkinje cell-specific loss of TSC1, which results in mTORC1 activation, induced autistic-like behaviour in mice (Tsai et al., 2012).

We find that ablation of either mTORC1 or mTORC2 in Purkinje cells is sufficient to impair motor control but the motor phenotypes differ in the time of onset and have distinct origins. Motor deficits in the rictor knockout mice correlate with developmental deficits in climbing fibre elimination and impaired dendritic self-avoidance whereas the age-dependent motor phenotype of raptor knockout

mice is paralleled by neurodegeneration in form of a neurofilamentopathy and a progressive loss of Purkinje cells due to apoptosis. Neurofilamentopathy and Purkinje cell apoptosis is also seen in mice in which TSC1 was deleted in Purkinje cells. Hence, the cellular response to inactivation and activation of mTORC1 in Purkinje cells surprisingly converges. This is further corroborated by the finding that ablation of mTORC1, but not mTORC2, in Purkinje cells impairs social behaviour of mice, as this is also seen with TSC1 Purkinje cell knockout mice (Tsai et al., 2012). In summary, our findings highlight that mTORC1 and mTORC2 signalling pathways play fundamental and distinct roles in Purkinje cells.

MATERIALS AND METHODS

Mouse strains. All animal procedures complied with Swiss animal experimental regulations. Mice expressing the Cre recombinase under the endogenous *L7/Pcp-2* promoter *(L7/Pcp-2$^{Cre/+}$)* (Saito et al., 2005) were crossed with mice carrying floxed alleles coding for raptor *(Rptor$^{loxp/loxp}$)*, rictor *(Rictor$^{loxp/loxp}$)* (Bentzinger et al., 2008) or TSC1 *(Tsc1$^{loxp/loxp}$)* (Kwiatkowski et al., 2002) to obtain the following mouse lines: *L7/Pcp-2$^{Cre/Cre}$; Rptor$^{loxp/loxp}$*, *L7/Pcp-2$^{Cre/Cre}$*; *Rictor$^{loxp/loxp}$* and *L7/Pcp-2$^{Cre/Cre}$*; *Tsc1$^{loxp/loxp}$* that were called RAPuKO, RIPuKO or TSCPuKO, respectively. As control mice, littermates of the following genotype *L7/Pcp-2$^{Cre/Cre}$; Rptor$^{loxp/+}$*, *L7/Pcp-2$^{Cre/Cre}$; Rictor$^{loxp/+}$* and *L7/Pcp-2$^{Cre/Cre}$; Tsc1$^{loxp/+}$* were used for RAPuKO, RIPuKO or TSCPuKO, respectively. To label cells undergoing Cre-mediated recombination, a *Rosa26* locus-targeted EGFP reporter carrying a loxp stop cassette between the promoter and the coding sequence (*R26-EGFP$^{T/+}$* (Tchorz et al., 2012)) was crossed into the RIPuKO background. The resulting knockout mice of the following genotype *L7/Pcp-2$^{Cre/Cre}$; Rictor$^{loxp/loxp}$; R26-EGFP$^{T/+}$* are referred to as RIPuKO GFP and littermates of the *L7/Pcp-2$^{Cre/Cre}$; Rictor$^{loxp/+}$; R26-EGFP$^{T/+}$* genotype were used as controls. For the conditional knockout of *Rptor* in neural progenitors (RAbKO), mice previously described were used (Cloetta et al., 2013). Genotyping of the mice used toe tissue and was done as described elsewhere (Kwiatkowski et al., 2002; Cloetta et al., 2013; Thomanetz et al., 2013). The *L7/Pcp-2$^{Cre/?}$* locus was detected using primers Fw 5' TGTGGCTGATGATCCGAATA and Bw 5' GCTTGCATGATCTCCGGTAT resulting in an amplicon of 249 bp. *L7/Pcp-2$^{Cre/Cre}$* mice were identified using primers Fw 5' GAAGGCTTCTTCAACCTGCT and Bw 5' ATATCCATGAGATTGTCCAT, resulting in the absence of a 292 bp. To detect EGFP knocked-in at the *Rosa26* locus a nested PCR was performed using primers Fw 5' TGATATTGCTGAAGAGCTTGGCGGC and Bw 5' TGTGTGTATTCCTGGCTATCC for the first PCR (35 cycles) and Fw 5' AGCGCATCGCCTTCTATCGCC and Bw 5' TGATGTGTAGACCAGGCTGG for the second PCR (25 cycles) resulting in an amplicon of 253 bp.

Antibodies. β-Tubulin (Mouse, BD Pharmingen, #556321, 1:500), CAR8 (Goat, Watanabe lab (Patrizi et al., 2008), 1:5000), calbindin D28k (Guinea pig, Synaptic Systems, #214 004, 1:500), calbindin D-28k (Mouse, Swant, #300, 1:2500), cleaved caspase-3 (Asp175) (Rabbit, Cell Signaling,

#9661, 1:300), cytochrome c clone 6H2.B4 (Mouse, BD Pharmingen, #556432, 1:100), glial fibrillary acidic protein (GFAP) clone CA5 (Mouse, Millipore, #MAB360, 1:100), $GABA_A$ α1 subunit (Guinea pig, (Fritschy et al., 2006), 1:5000), GAD65 (Monoclonal GAD-6, DSHB, Iowa, 1:1000), GSK3α (Rabbit, Cell Signaling, #9338, 1:1000), GSK3β (Rabbit, Cell Signaling, #9315, 1:1000), phospho-GSK3α/β (Ser21/9) (Rabbit, Cell Signaling, #9331, 1:1000), neurofilament H (Rabbit, Millipore, #AB1989, 1:200), phosphorylated neurofilaments (Mouse, Covance, #SMI-31P, 1:1000), phospho-S6 ribosomal protein (Ser235/236) (Rabbit, Cell Signaling, #2211, 1:100), PKCγ (Rabbit, Santa Cruz, #sc-211; 1:100), synaptophysin (Rabbit, GeneTex, #GTX100865, 1:100), fluorescein (DTAF) Streptavidin (Jackson ImmunoResearch, #016-010-084, 1:300), Cy3-Streptavidin (Jackson ImmunoResearch, #016-160-084, 1:1000)

Tissue homogenization and Western blot analysis. Brains were dissected, transferred to protein lysate buffer (50 mM Tris-HCl, pH 7.5, 150 mM NaCl, 1 mM EDTA, 1% Triton X-100 supplemented with EDTA-free protease inhibitor cocktail tablets (Roche), and phosphatase inhibitor tablets PhosSTOP (Roche)), and homogenized with a glass/Teflon homogenizer using 10 strokes at 800 rpm. The homogenate was centrifuged at 13,600 g for 15 min at 4°C. Cleared lysates were used to determine total protein amount (BCA Protein Assay; Thermo Fisher Scientific). After dilution with 5x SDS sample buffer, equal protein amounts were loaded onto SDS gels.

Immunohistochemistry. Mice were deeply sedated with isoflurane. After decapitation, the brain was rapidly removed and immediately transferred into ice-cold, oxygenated (95% O_2, 5% CO_2), standard artificial cerebrospinal fluid (ACSF) containing (in mM) 119 NaCl, 1 NaH_2PO_4, 2.5 KCl, 2.5 $CaCl_2$, 1.3 $MgCl_2$, 11 D-glucose and 26.2 $NaHCO_3$. 250-µm-thick sagittal sections of cerebella were cut with a Leica VT1200S vibratome and transferred to oxygenated standard ACSF at room temperature and allowed to recover for about 30 min. Sections were fixed in 2-3 ml 4% paraformaldehyde (PFA) in PBS for at least 20 minutes and subsequently 3 times rinsed for 20 min with PBS. Slices were then stored overnight or longer at 4°C in 30% (w/v) sucrose in 0.1 M sodium phosphate buffer pH 7.4. The cryoprotected slices were then re-sliced as previously described (Schneider Gasser et al., 2006). In brief, the slices were shortly rinsed in ice-cold PBS and then mounted on a pre-cut frozen block of O.C.T. (optimal cutting temperature compound) and stored for

30 min at -20°C. 15-µm-thick cryosections were made with a Leica CM1950 cryostat with a cryochamber and object head temperature of -20°C and -12°C, respectively, and subsequently stored at -20°C. Cryosections were thawed for about 2 min at 37°C and then incubated with blocking buffer (10% fetal bovine serum (FBS) and 0.2% Triton X-100 in PBS) for 1 h at room temperature. The primary antibodies were applied in blocking buffer overnight at 4°C and after washing in PBS (3 x 10 min), the corresponding secondary antibodies were added for 1 h at room temperature in blocking buffer. After washing in PBS (3 x 10 min), the slides were drained and coverslipped using Kaiser's glycerol gelatine (Merck, #1.09242.0100).

For $GABA_A$ α1 stainings, mice were deeply anesthetized with pentobarbital (Nembutal, 50 mg/kg, i.p.) followed by transcardiac perfusion with ice-cold standard ACSF at a flow rate of 10–15 ml/min (Notter et al., 2014). The brains were extracted immediately after the perfusion and postfixed in ice-cold 4% PFA in 0.15 M sodium phosphate buffer, pH 7.4 for 90 min. Tissue was then cryoprotected with 30% sucrose in PBS (w/v). Coronal sections (thickness 40 µm) were cut from frozen blocks with a sliding microtome (Microm Heidelberg, HM 400). Sections were collected in PBS and stored at -20°C in anti-freeze solution (15% glucose and 30% ethylene glycol in 50 mM sodium phosphate buffer, pH 7.4) prior use. Free-floating sections were incubated overnight at 4°C with primary antibodies and for 30 minutes at room temperature with secondary antibodies in Tris-HCl buffer, pH 7.4, containing 2% normal goat (or donkey) serum and 0.2% Triton X-100.

Fluoro-Jade B staining. Cryosections were thawed and dried at room temperature. The sections were first incubated for 5 min with 1% sodium hydroxide in 80% ethanol and then for 2 min with 70% ethanol for rehydration. The slides were transferred to 0.06% potassium permanganate for 10 min. Subsequently, they were rinsed for 2 min with ddH_2O and incubated with the staining solution for 20 min in the dark. The staining solution contained 2 µg/ml Fluoro-Jade B (FJB; Merck Millipore, #AG310) and 2 µg/ml Hoechst 33342 in 0.1% acetic acid. The slides were then washed three times 1 min in ddH_2O, drained and dried at 50°C. The dried slides were cleared in xylene for at least 1 min, drained and coverslipped using D.P.X. mounting medium (Sigma, #3176116).

Staining of biocytin-labelled Purkinje cells in acute slices. Purkinje cells were labelled with biocytin by the cell patch clamp method using intracellular solutions containing 3 mg/ml biocytin. The

orientation of the acute slice was noted for the whole cell recordings. The staining procedure was adapted from (Wierenga et al., 2008). In brief, after the recording, slices were fixed overnight at 4°C in 4% PFA dissolved in PBS. Slices were extensively rinsed with PBS and subsequently incubated for 24 h at 4°C in blocking solution (10% FBS in PBS, containing 0.4% Triton X-100) on a shaker. The primary antibody was applied overnight at 4°C in blocking solution (5% FBS in PBS; 0.4% Triton X-100) on a shaker. After extensive washing with PBS, appropriate secondary antibodies were applied overnight at 4°C in blocking solution. Acute slices were mounted in Kaiser's glycerol gelatine with the patched side facing up. Stained slices were analysed by confocal microscopy.

Image acquisition. Fluorescence pictures were taken using a Leica 5000B microscope with a 10x (NA 0.4) or 20x (NA 0.5) objective in combination with the software AnalySIS (Soft Imaging System). Confocal pictures were taken using the Leica TCS SPE confocal system with a 20x (NA 0.7), 40x (NA 1.15), 63x (NA 1.3) or 100x (NA 1.47) oil immersion objective or with a Zeiss LSM 710 microscope with a 63x lens (NA 1.4). For GFAP stainings whole automated multiple image acquisitions were made with the Olympus IX81 using a 10x objective (NA 0.3).

Quantification. For image analysis and processing, ImageJ was used. All analyses were done on sagittal sections of the cerebellar vermis. To analyse Purkinje cell density and soma size, fluorescence pictures of calbindin stainings taken from the cerebellar lobes 4&5 using a 10x objective were used. Purkinje cell density was determined by dividing the number of Purkinje cells by the length of the analysed Purkinje cell layer segment and is indicated in cells per mm. Data of RIPuKO, RIPuKO GFP and corresponding control mice were pooled. For Purkinje cell soma size analysis, only somata were included where the primary dendrite was clearly visible. For each mouse, the mean Purkinje cell density and soma size of $n \geq 3$ cerebellar slices was determined.

Quantification of apoptotic cells, axonal swellings or FJB patches was done by counting their appearance in the entire cerebellar slice ($n \geq 3$ slices per mouse). For each mouse, the cerebellar slices were binned according to the number of observed events on the entire slice and finally the fraction of slices assigned to each bin was calculated. Apoptotic cells were positive for cleaved caspase-3 and showed a pyknotic nucleus. Calbindin staining was used to quantify axonal swellings of Purkinje cells in the granule cell layer.

The area covered by the dendritic tree of Purkinje cells was determined by merging *z*-stacks of confocal images (taken with 20x or 40x objectives) from biocytin-labeled Purkinje cells that were detected by Fluorescein (DTAF) Streptavidin in acute slices. The entire dendritic tree was encircled by connecting the most apical points of the dendritic branches and the covered area was determined. Purkinje cell dendrite self-crossings were quantified on confocal pictures taken with a 63x objective from re-sliced (15 µm thick), biocytin-labelled Purkinje cells of RIPuKO GFP or corresponding control mice that were stained with Cy3-Streptavidin. Merged *z*-stacks of confocal pictures taken from randomly chosen regions of spiny distal branches of biocytin-labelled cells were analysed for self-crossings. The number of dendritic self-crossings was normalized to the analysed area and the normalized values of RIPuKO GFP mice were then set in relation to the ones of control mice. The experimenter was blinded to the mouse genotype. $GABA_A$ α1 subunit clusters and GAD65-positive terminals were quantified based on threshold segmentation using self-written macros for ImageJ and Excel. Statistical analysis (one-way ANOVA) was performed in Prism Graphpad software and with a Kolmogorov-Smirnov test.

Electrophysiology. Sagittal cerebellar slices were prepared as described above in low calcium ACSF containing (in mM) 119 NaCl, 1 NaH_2PO_4, 2.5 KCl, 0.125 $CaCl_2$, 3.3 $MgCl_2$, 11 D-glucose and 26.2 $NaHCO_3$. Slices were then transferred for 30 min to 34°C-warm, oxygenated standard ACSF and subsequently stored in oxygenated standard ACSF at room temperature until they were used. Whole cell recordings were taken at room temperature using an Axon MultiClamp 700A or 700B amplifier (Molecular Devices) and borosilicate glass pipettes (2-4 MΩ). The following internal solutions (all containing 3 mg/ml biocytin) were used for the different recordings: for mEPSCs and mIPSC (in mM) 135 Cs-methanesulfonate, 8 NaCl, 10 HEPES, 0.5 EGTA, 4 Mg-ATP, 0.3 Na-GTP, 5 Lidocaine-N-ethyl bromide, pH 7.25; for climbing fibre stimulation (in mM) 150 CsCl, 1.5 mM $MgCl_2$, 10 HEPES, 0.1 EGTA, 2 Mg-ATP, 0.4 Na-GTP, 5 Lidocaine-N-ethyl bromide, pH 7.3; for LTD recordings (in mM) 65 Cs-methanesulfonate, 65 K-gluconate, 10 KCl, 1 $MgCl_2$, 20 HEPES, 0.4 EGTA, 4 Na_2-ATP, 1 mM Na_2-GTP, 5 sucrose, pH 7.3. mEPSCs and mIPSCs were recorded at a holding potential of -70 mV or 0 mV, respectively, in the presence of 0.5 µM TTX for 10 minutes using the pClamp system (Molecular Devices, version 10.2). Traces were further analysed with the Mini Analysis Program v6

(Synaptosoft). Climbing fibre innervation was analysed by placing a patch pipette (2 MΩ), filled with standard ACSF, in the granule cell layer in the vicinity of the patched Purkinje cell. Two current pulses (0.1 ms, paired-pulse interval: 62.5 or 100 ms) generated by a stable IS4 stimulator (SC-Devices) were applied every 20 s. The stimulation pipette was moved in the granule cell layer until the climbing fibre response (CF-EPSC) could be elicited with minimal stimulation intensity. The holding potential was set at -10 mV to inactivate voltage-gated conductances and to reduce the driving force. The stimulation intensity was reduced until all synaptic responses disappeared and was progressively increased again. The climbing fibre response as a function of the stimulation intensity was analysed and only events showing paired-pulse depression as well as a clear threshold were included for analysis. The number of innervating climbing fibres was estimated from the number of discrete CF-EPSC steps. Climbing fibre recordings were made and analysed using the pClamp system. For climbing fibre analysis, 4-week-old RIPuKO and 12-week-old RIPuKO GFP mice and corresponding littermate control mice were used.

For LTD recordings, acute cerebellar slices were perfused with standard ACSF containing 100 μM picrotoxin (Sigma #P1675) and a patch pipette (2 MΩ) filled with perfusion solution was placed in the molecular layer in the vicinity of the voltage-clamped Purkinje cell. Parallel fibre (PF) responses were elicited by applying two current pulses using a stable IS4 stimulator (0.2 ms, paired-pulse interval: 100 ms) every 10 s while the cell was held at -60 mV. The stimulation intensity was chosen to obtain a PF-EPSC response of approximately 200 pA. A baseline was recorded for at least 10 min and when judged stable, LTD was induced by increasing the holding potential from -60 to +20 mV for 500 ms in conjunction with a single PF stimulus, which was repeated 30 times at a frequency of 1 Hz. Access resistance was measured every 10 s and recordings were discarded if it changed by more than 20% from the initial value. LTD was recorded and analysed using IGOR Pro software (WaveMetrics). For all types of electrophysiological recordings, biocytin-labelled Purkinje cells were subsequently analysed by immunohistochemistry as described above to confirm recombination of the targeted alleles in the recorded cell.

Behavioural assays. Mice were housed in a standard colony room with a 12:12 light:dark cycle and food and water was provided *ad libitum*. For behavioural tests, mice were transferred to a separate

room at least 1 h prior to the experiment for adaptation. Tests were performed at the same time of day and the experimenter was blinded to the mouse genotype.

Balance beam test. For the balance beam test, a 70-cm-long, wooden beam, which was covered with masking tape, was horizontally connected to a dark box. The entire system was elevated to preventing mice to jump off. The starting area was brightly illuminated to motivate the mice to move towards the dark target box. The number of slips of the hind legs was counted. Mice were given 2 training sessions prior to the test session, each session consisted of 3 runs. During the training sessions, the diameter of the beam was gradually decreased. 4 to 8-week-old, female RIPuKO and 9 to 11-week-old, male RAPuKO mice and corresponding littermate controls were tested on a 1.1-cm-thick beam. For 14 to 20-week-old, female RIPuKO and 29 to 41-week-old, male RAPuKO mice and the corresponding littermate controls, the diameter of the beam was 1.3 cm. For each mouse, the mean number of slips from three runs was calculated.

Footprint analysis. Paws of the mice were painted with nontoxic paint (forepaws in red, hindpaws in black). Mice were placed into an acrylic glass corridor of 1 m length and 8 cm width. The corridor was lined with white paper. The starting point was brightly illuminated to motivate the mouse to walk towards the dark box placed at the end of the corridor. For analysis, ten steps during which the mouse walked continuously and did not touch the wall were selected. The paper stripes were scanned, the coordinates of the footprints were evaluated using ImageJ and the mean gait width of the ten steps was calculated for each mouse. Female RIPuKO and male RAPuKO mice and corresponding littermate control mice of the indicated age were used for the footprint analysis.

Olfactory habituation/dishabituation. Olfactory habituation/dishabituation tests were performed as previously described (Yang and Crawley, 2009; Silverman et al., 2010). 9 to 11-week-old male RAPuKO mice and 13 to 26-week-old RIPuKO and RIPuKO GFP mice and corresponding littermate control mice were used. In brief, mice were accommodated to a fresh cage with a clean and dry cotton tipped swab (cotton tip 2 cm over the cage ground) suspended from the cage lid for 30 min. After this acclimation period, odours were presented for 2 min in intervals of 1 min and the time of interest of the mouse in the cotton swab was measured. Interest was scored if the nose of the mouse was within 2 cm of the cotton tip. Odours were presented twice or three times to analyse olfactory habituation. The

order of presented odours was water, water, banana, banana, social odour 1, social odour 1, social odour 1, social odour 2, social odour 2, social odour 2. For the water and banana odours, 100 µl of ddH_2O or isoamyl acetate (Sigma #W205532) diluted 1:1500 in ddH_2O were dripped onto the cotton tip. Social odours were obtained by wiping the cotton tipped swab in a zig-zag pattern across the bottom surface of a cage that had been used by 3-4 age-matched, unfamiliar male mice of the same strain (C57BL/6) for 7 days. Results of RIPuKO and RIPuKO GFP mice and the corresponding control mice were pooled. Raw data were cleaned from statistical outliers by GraphPad prism software (ROUT method; Q = 0.1%) prior to statistical analysis.

Statistics. All data are presented as mean ± SEM. An unpaired Student's t-test or a one- or two-way ANOVA followed by a Tukey's or a Bonferroni's post hoc test was used to analyse data for statistical significance. A probability of 0.05 was taken as the level of statistical significance.

RESULTS

Motor deficits and social behaviour of RAPuKO and RIPuKO mice

Purkinje cell-specific ablation of mTORC1 or mTORC2 was achieved by crossing *L7/Pcp-2-Cre* mice (Saito et al., 2005) with *Rptor*$^{loxp/loxp}$ or *Rictor*$^{loxp/loxp}$ mice (Bentzinger et al., 2008) as previously described (Thomanetz et al., 2013). The resulting mouse lines are called RAPuKO or RIPuKO (for raptor- or rictor Purkinje cell knockout). *L7/Pcp-2*-driven Cre expression starts at embryonic day 17.5 (E17.5) (Saito et al., 2005) and thus targeted alleles will be deleted during the development, including the establishment of the dendritic tree and of synapses, and the maintenance of Purkinje cells (Watanabe and Kano, 2011).

As Purkinje cells provide the sole output of the cerebellar cortex and are known to be essential for motor control, we first analysed how raptor and rictor depletion in these neurons would affect motor coordination. For this reason, RAPuKO and RIPuKO mice were tested on a balance beam and the number of hind leg slips was quantified. In RIPuKO mice, the number of slips was significantly increased compared to control littermates independent of the age of the mice (Fig. 1A). In contrast, young RAPuKO mice did not show any motor coordination deficits, whereas a significant deficit was noted at the age of 29-41 weeks (Fig. 1B). In addition to the early-onset coordination deficits, RIPuKO mice showed an increase in the gait width of their hind legs (Fig. 1C), whereas RAPuKO mice did not show any change in gait (Fig. 1D). Thus, mTORC2 deficiency in Purkinje cells results in early deficits in motor coordination whereas inactivation of mTORC1 seemed to affect this behaviour only at a rather high age.

Recent reports have indicated that Purkinje cell-specific depletion of TSC1, which results in sustained activation of mTORC1, causes autism spectrum disorder-like changes in mice that manifested by altered social behaviour (Tsai et al., 2012). To evaluate whether a similar phenotype could also be noted in mice deficient for mTORC1, we tested RAPuKO mice in an olfactory habituation/dishabituation test. To rule out that motor deficits interfere with this test, we used young mice. While RAPuKO mice spent the same time sniffing non-social odours as control mice, the interest in social odours was significantly reduced (Fig. 1F). As depletion of TSC1 also affects

mTORC2 signalling (Goto et al., 2011; Carson et al., 2012), we also tested RIPuKO mice in the same behavioural paradigm. However, no significant difference in the interest in either non-social or social odours was observed (Fig. 1E). These data indicate that mTORC1 and mTORC2 have different functions in Purkinje cells as the phenotypes in motor coordination and social interest are distinct.

Morphology and synaptic alterations in Purkinje cells of RAPuKO mice

Expression of Cre under the control of the *L7/Pcp-2* promoter has been shown to be mosaic in Purkinje cells (Saito et al., 2005). Similarly, we have previously shown that rictor was depleted in only 75% of the Purkinje cells in RIPuKO mice and that lack of expression of PKCγ is a reliable marker for successful removal of rictor (Thomanetz et al., 2013). To test whether a similar mosaic pattern was observed in RAPuKO mice, we stained sagittal sections of the cerebellum for the phosphorylated form of S6 (pS6), which is activated by mTORC1 (Wullschleger et al., 2006). Thus, lack of pS6 can be seen as an indicator of successful depletion of raptor. In young, 3 to 11-week-old RAPuKO mice, 49 ± 5% (mean ± SEM; n = 19 mice) of the Purkinje cells were negative for pS6 (pS6(-)) while all Purkinje cells of control mice were pS6-positive (pS6(+)) (Fig. 2A). Consistent with the important role of mTORC1 in controlling cell size, pS6(-) Purkinje cells were by 40-50% smaller in RAPuKO mice compared to Purkinje cells of age-matched control mice (Fig. 2B). In addition, a small but significant increase in the soma size of the non-recombined, pS6(+) Purkinje cells in older RAPuKO mice could be observed (Fig. 2B). Besides the difference in soma size, ~40% of raptor-depleted Purkinje cells of 4-6-week-old RAPuKO mice contained multiple primary dendrites (Fig. 2C and D) while ~90% of Purkinje cells in control mice contained only one primary dendrite. Multiple primary dendrites with a similar frequency like in RAPuKO mice have also been observed in RIPuKO mice (Thomanetz et al., 2013). Moreover, the area covered by the dendritic tree of raptor-knockout Purkinje cells was significantly decreased by 42 ± 3% (mean ± SEM; Student's t-test; $p < 0.001$; $n \geq 36$ cells of n = 7 mice). Thus, raptor depletion in Purkinje cells results in rather severe, morphological changes in Purkinje cells, similar, but even more severe, to what we reported in RIPuKO mice (Thomanetz et al., 2013).

To test whether those morphological alterations also affected synapse function, we next examined miniature excitatory and inhibitory postsynaptic currents (mEPSC and mIPSC, respectively). We pre-identified the raptor-deficient Purkinje cells in the electrophysiological set-up by their reduced soma size and confirmed their identity by filling the recorded cells with biocytin via the recording pipette for a postfixation analysis. While there was no difference in the mEPSCs of raptor-deficient Purkinje cells at the age of 6 weeks compared to cells in control mice (Fig. 3A - C), a pronounced reduction in the frequency of mIPSCs (Fig. 3D and E), but not the amplitude (Fig. 3D and F), was observed. By quantitative immunohistochemistry using antibodies against the α1 subunit of $GABA_A$ receptors, we also found that the mean number of $GABA_A$ α1 clusters on the soma of pS6(-) Purkinje cells was reduced by 43% (Fig. 3G and I) while the density of the $GABA_A$ α1 clusters in the molecular layer was not changed (Fig. 3H and J). Together, these data indicate a lowering of the number of inhibitory synapses formed by raptor-deficient Purkinje cells.

Raptor deficiency also affected the size of GABAergic synapses but this effect differed between the soma and the molecular layer. While the size of $GABA_A$ α1 clusters on the somata of raptor-deficient Purkinje cells was increased (Fig. 3K), the size of GAD65/$GABA_A$ α1-positive clusters in the molecular layer was smaller (Fig. 3L). The fact that the size differences are opposite between the soma and the dendrites of the raptor-deficient neurons may explain why we could not detect any alteration in the amplitude of the mIPSCs. In summary, these data combined indicate a misbalance between the inhibitory and the excitatory input in Purkinje neurons that are deficient of raptor. Such a misbalance, in turn, might contribute to the behavioural deficit in social interest of RAPuKO mice. Noteworthy, rictor knockout in Purkinje cells affects both excitatory and inhibitory synaptic properties as previously described (Thomanetz et al., 2013).

Multiple climbing fibre innervation accounts for ataxia of RIPuKO mice

Rictor knockout in Purkinje cells is paralleled by a striking down regulation of PKCγ (Thomanetz et al., 2013), the major PKC isoform expressed by these neurons (Barmack et al., 2000). Mice with a conventional knockout of PKCγ show impaired motor coordination (Chen et al., 1995). This motor coordination deficit is paralleled by multiple innervation of Purkinje cells by climbing fibres (CF)

(Kano et al., 1995). As RIPuKO mice have a motor coordination phenotype, we analysed CF innervation in RIPuKO mice. In a first set of experiments, we analysed 4-week-old mice, as this is one week after finalization of developmental elimination of surplus CFs in wild-type mice (Hashimoto and Kano, 2013). CF innervation was tested by whole-cell recordings of EPSCs in Purkinje cells in response to electrical stimulation of CFs. Stimulation of CFs in cerebellar slices obtained from control mice evoked EPSCs whose amplitude developed in an "all or nothing" manner thus reflecting single CF innervation of Purkinje cells (Fig. 4A and D). Similar stimulation parameters applied to rictor-deficient Purkinje cells resulted in multiple discrete steps in ~40% of the analysed neurons indicating innervation by multiple CFs (Fig. 4B and D). To rule out that the multiple CF innervation was simply due to a delay in CF elimination, we also measured CF-EPSC responses in 12-week-old RIPuKO mice. The percentage of knockout cells showing multiple discrete steps in CF-EPSC responses was very similar to those in the younger mice (Fig. 4C and D), indicating that multiple CF innervation of rictor-knockout Purkinje cells persists throughout adulthood. Hence, multiple CF innervation, like in PKCγ knockout mice, might be responsible for the motor deficits observed in RIPuKO mice. In contrast, 4-week-old RAPuKO mice did not show multiple CF innervation (Fig. 4E – G).

Another cellular correlate that has been implicated in altered motor behaviour is a failure to undergo cerebellar long-term depression (LTD) (Kano et al., 2008; Hirano, 2013). Cerebellar LTD is induced by a simultaneous stimulation of the parallel fibre (PF) and CF synapses, which leads to a profound depolarization of the Purkinje cell and a weakening of the PF synapse. Because rictor-deficient Purkinje cells are frequently innervated by multiple CFs, LTD was induced by directly depolarizing the voltage-clamped Purkinje cell via the recording electrode and simultaneously stimulating the PFs as depicted (Fig. 4H) (Kakegawa et al., 2011). Application of this protocol led to a ~20% reduction of the PF-EPSC in both control and rictor-deficient Purkinje cells after 30 minutes (Fig. 4I - K), showing that cerebellar LTD is normal in RIPuKO mice.

Another phenomenon that has been correlated with impairment of gait and motor coordination is an increased number of dendritic self-crossings of Purkinje cells, which has been suggested to result from defective dendritic self-avoidance (Gibson et al., 2014). Purkinje cells deficient of γ-protocadherins, a class of molecules that acts via the mTORC2 target PKC (Garrett et al., 2012), show

impaired dendritic self-avoidance (Lefebvre et al., 2012). Thus, we also analysed dendritic self-avoidance in 12-week-old RIPuKO mice by re-slicing biocytin-labelled Purkinje cells and staining them for Cy3-streptavidin and PKCγ. Confocal microscopy analysis of randomly selected regions of spiny distal branches of the dendritic tree (Fig. 4L and M) revealed a significant increase in the number of dendritic self-crossings in rictor-knockout Purkinje cells (Fig. 4N). Hence, loss of mTORC2 in Purkinje cells also decreases dendritic self-avoidance. Thus, in summary, a failure in CF synapse elimination and hampered self-avoidance of dendrites might be the basis of the motor coordination phenotype of RIPuKO mice. Interestingly, both of those cellular phenomena have previously been linked to dysregulation of the mTORC2 target PKC.

Age-dependent loss of Purkinje cells in RAPuKO but not RIPuKO mice due to apoptosis

As described above, the motor coordination phenotype of RIPuKO mice was observed at an early age whereas the motor coordination deficits of RAPuKO mice were only observed at a higher age. This together with the previous finding that ablation of mTORC1 causes increased apoptosis of neurons (Cloetta et al., 2013), led us to hypothesize that death of Purkinje cells might underlie the age-dependent motor deficits of RAPuKO mice. To test this, we counted the number of Purkinje cells in RAPuKO and RIPuKO mice in the course of mouse ageing. While the density of the Purkinje cells remained the same in RIPuKO mice (Fig. 5A and B), it significantly decreased in RAPuKO mice after the age of 11 weeks (Fig. 5C and D). To investigate whether cell loss was due to apoptosis, cells were stained for cleaved caspase-3 (CC3), a well know apoptosis marker (Gown and Willingham, 2002). No CC3-positive Purkinje cells were found in 6-week-old RAPuKO mice (data not shown) but many positive cells could be detected at the age of 11 weeks (Fig. 5E and F). Those cells also showed signs of a condensed and fragmented nucleus in the Hoechst staining (Fig. 5E), which is an additional characteristic of apoptosis (Robertson et al., 2000). The apoptotic events were also accompanied by the appearance of GFAP-positive fibres in the molecular layer (Fig. 5G and H). The localization of the GFAP-positive fibres and their palisade-like arrangement (Fig. 5H) suggested that these were Bergmann glia cells that are known to be closely associated with Purkinje cells (Yamada and Watanabe, 2002). An increase of GFAP-positive fibres is a hallmark of reactive astrogliosis that can

be a consequence of neurodegeneration (Pekny and Nilsson, 2005). Thus, at a higher age, Purkinje cells in RAPuKO mice are lost because of apoptosis. Most probably, the age-dependent loss of Purkinje cells underlies the motor coordination deficits that are visible in old RAPuKO mice.

Neurofilamentopathy upon ablation or sustained activation of mTORC1 in Purkinje cells

To further investigate the cause of cell death in RAPuKO mice, we next stained for degenerating neurons using Fluoro-Jade B (FJB), as this compound specifically stains degenerating neurons (Schmued and Hopkins, 2000). FJB-positive puncta were visible in the molecular and Purkinje cell layer of 6 and 11-week-old RAPuKO but not control mice (Fig. 6A and B), indicating that neurodegeneration precedes the apoptosis in raptor-knockout Purkinje cells. Also signs of dendritic atrophy and beading could be detected in biocytin-labelled, raptor-deficient Purkinje cells of 6-week-old mice (Fig. 6C). Additionally, we often detected swellings of axons proximal to raptor-deficient Purkinje cell somata whereas such swellings were only very rarely observed in control mice (Fig. 6D - H). Such swellings are thought to be an early sign of axonal degeneration and have been reported to frequently contain organelles or cargo proteins, such as mitochondria, synaptic vesicles and neurofilaments (Ching et al., 1999; Louis et al., 2009; Watanabe et al., 2010; Yang et al., 2013). In accordance, 84.8 ± 0.7% (mean ± SEM; n = 390 swellings of n = 4 mice) of the axonal swellings in RAPuKO mice were strongly positive for neurofilament heavy (neurofilament H) and 81.2 ± 5% (mean ± SEM; n = 196 swellings of n = 4 mice) were positive for the phospho-neurofilament epitope (SMI31) (Fig. 6E). In contrast, the swellings did not show any accumulation of mitochondria (Fig. 6F) or synaptic vesicles (Fig. 6G). Neurofilaments are known to undergo axonal transport and there is evidence that this is regulated by phosphorylation in the C-terminal KSP repeats (reviewed in (Shea et al., 2009; Holmgren et al., 2012)) and glycogen synthase kinase 3 (GSK3) has been shown to phosphorylate neurofilament H at the KSP repeats (Bajaj and Miller, 1997). Because phosphorylation of GSK3α/β at residue Ser21/9 is downstream of Akt (Cross et al., 1995) and because changes in mTORC1 activity also affect activation of Akt (Bentzinger et al., 2008), we examined phosphorylation of GSK3 in mice that lack raptor in all brain cells (Cloetta et al., 2013). In those mice, phosphorylation of GSK3 was strongly increased (Fig. 6I and J), indicating that aberrant GSK3 signalling might be the

cause of the axonal accumulation of neurofilaments in raptor-knockout Purkinje cells. Similar proximal axonal swellings have also been reported in mice deficient for TSC1 in Purkinje cells (Tsai et al., 2012). Because TSC1 knockout in brain tissue is known to affect GSK3 signalling (Meikle et al., 2008), we hypothesized that the swollen axons of TSC1 knockout in Purkinje cells might also contain neurofilaments. Indeed, axonal swellings in 11-week-old TSC1 Purkinje cell knockout (TSCPuKO) mice were in 78.5 ± 3% (mean ± SEM; n = 266 swellings of n = 4 mice) and 79.6 ± 2% (mean ± SEM; n = 276 swellings of n = 4 mice) of the cases clearly positive for neurofilament H (Fig. 7A) and phosphorylated neurofilament, respectively (Fig. 7B). TSC1-knockout Purkinje cells not only show signs of axonal degradation but finally also undergo apoptosis as previously reported (Tsai et al., 2012). Consistently, we identified apoptotic Purkinje cells and a lowered Purkinje cell density in 11-week-old TSCPuKO mice (data not shown). Like in RAPuKO mice, Purkinje cell degeneration/apoptosis in TSCPuKO mice was paralleled by reactive Bergmann glia that manifested in palisade-like, GFAP-positive structures in the molecular layer (Fig. 7C). Altogether, both ablation and sustained activation of mTORC1 in Purkinje cells results in a neurofilamentopathy, accompanied by the accumulation of neurofilaments in the axonal swellings proximal to the soma of Purkinje cells, and causes Purkinje cell death by apoptosis.

DISCUSSION

Here we describe the phenotypes of mice that lack mTORC1 or mTORC2 in developing and adult Purkinje cells. While some of the phenotypes, such as the changes in cell morphology, are shared between RAPuKO and RIPuKO mice, most of them differ between the two mouse models. Phenotypes that are exclusive for the RAPuKO mice are (*i*) the reduced social interest and (*ii*) the progressive loss of Purkinje cells that starts at the age of 11 weeks. Phenotypes exclusive to RIPuKO mice are (*i*) the early changes in motor coordination and the gait alterations and (*ii*) the impairment of CF synapse elimination. Thus, our work provides strong evidence that mTORC1 and mTORC2 have only a few common but many very distinct functions in Purkinje neurons although they share many of the molecular components including mTOR.

A role of mTORC1 for the morphology of Purkinje cells

Given the important role of mTORC1 for cell growth (Wullschleger et al., 2006), our observation that raptor-deficient Purkinje cells have smaller cell somata and a smaller dendritic tree is not surprising. The size difference was seen already at a rather early age of 3 weeks and persisted throughout adulthood. Thus, raptor-deficient Purkinje cells seem to never reach the size of wild-type neurons. The observed change of the dendritic tree in raptor-deficient Purkinje cells and in particular the presence of several primary dendrites was, however, not expected. The development of the Purkinje cell dendrites occurs mainly in the first three postnatal weeks. Purkinje cells transiently express multiple primary dendrites around birth and all but one are subsequently eliminated within the first two weeks. Later, the final size of the dendritic tree is established by a rapid and a slow growth phase (Sotelo and Dusart, 2009). While the detailed molecular mechanisms involved in this developmental reshaping of the dendrites are not well established, several pathways have been shown to affect similar processes. For example, the PI3K-Akt-GSK3 pathway is well known to affect neuronal polarity (Arimura and Kaibuchi, 2007) and inhibition of GSK3 by phosphorylation increases the number of primary dendrites in cultured neurons (Naska et al., 2006). Finally, brain-selective deletion of the PI3K-Akt inhibitor PTEN results in the formation of ectopic dendrites in neurons, which correlates with increased phosphorylation of Akt and GSK3 (Kwon et al., 2006). Inactivation of mTORC1 by raptor

depletion increases Akt signalling (Cloetta et al., 2013) because the inhibitory feedback loop via S6K is dampened (Um et al., 2004). Thus, increased GSK3 inhibition because of Akt-mediated phosphorylation in raptor-deficient Purkinje neurons may cause the multiple primary dendrites.

Interestingly, Purkinje cells deficient for rictor have also several primary dendrites (Thomanetz et al., 2013). Despite the similar phenotype to the RAPuKO mice, the underlying mechanism in RIPuKO mice is more likely based on abnormal PKC signalling including the dysregulation of its downstream targets MARCKS and GAP-43, as previously commented (Angliker and Ruegg, 2013). Consistent with this PKC-mediated mechanism, rictor-deficient Purkinje cells also exhibit extensive self-crossings of spiny distal dendritic branches. A very similar phenotype was also observed in mice deficient for γ-protocadherins, which also affect PKC signalling and its downstream target MARCKS (Garrett et al., 2012; Lefebvre et al., 2012).

Effect of mTORC1 and mTORC2 on synaptic connectivity

Purkinje cells from RIPuKO mice are innervated by multiple climbing fibres throughout adulthood and there is no change in LTD. Multiple CF innervation in the absence of disturbed LTD is also evident in PKCγ knockout mice (Chen et al., 1995). PKCγ has been suggested to be crucial for the late phase of climbing fibre elimination that lasts from P12-17 (Hashimoto and Kano, 2013). During this late phase, climbing fibre elimination is driven by parallel fibre synaptic input (Kakizawa et al., 2000) and the underlying postsynaptic mGluR1 signalling via $G\alpha_q$, PLCβ4 and PKCγ (Chen et al., 1995; Kano et al., 1995; Offermanns et al., 1997; Kano et al., 1998; Ichise et al., 2000). Concordantly, Purkinje cells in mice deficient for members of this signalling cascade are innervated by multiple climbing fibres and all these knockout mice also show motor deficits. Thus, the motor coordination deficit in the RIPuKO mice correlates with the pronounced loss of PKCγ (Thomanetz et al., 2013), suggesting that perturbed PKC signalling is the molecular basis of this phenotype.

While CF innervation and mEPSC recordings were normal in RAPuKO mice, analysis of the mIPSCs indicated a reduction in the number of functional inhibitory synapses. Consistent with the electrophysiological recordings, the number of perisomatic $GABA_A$ α1 clusters was also reduced in raptor-deficient Purkinje cells when measured by immunohistochemistry. Raptor knockout also

affected the size of $GABA_A$ α1 clusters but the effect depended on the subcellular localization. While $GABA_A$ α1 cluster size was increased on the somata of Purkinje cells, it was decreased in the dendrites (i.e. the molecular layer). In rats, the size of $GABA_A$ α1 clusters on the soma of Purkinje cells has been shown to become reduced during the first three postnatal weeks while the size of $GABA_A$ α1 clusters in the molecular layer is increased (Viltono et al., 2008). As $GABA_A$ α1 cluster size is increased on the soma of knockout cells but decreased in the molecular layer in 6-week-old RAPuKO mice, it is possible that these changes are a consequence of impaired postnatal development of GABAergic synapses.

Convergent phenotypes of sustained activation or inactivation of mTORC1 in Purkinje cells

Another interesting aspect of our work is the rather similar phenotypes of RAPuKO and TSCPuKO mice although the immediate downstream signalling is the opposite. For example, both mouse models show a strong accumulation of neurofilaments in axonal swellings and a progressive loss of Purkinje cells due to apoptosis, which is paralleled by reactive gliosis. We also provide evidence that aberrant GSK3 signalling may underlie this convergence in the neurofilamentopathy as phosphorylation of GSK3 is strongly increased in RAbKO mice and GSK3 signalling is also altered in mice deficient for TSC1 in the brain (Meikle et al., 2008). GSK3 phosphorylates neurofilaments at the E-segment (Sasaki et al., 2002; Sasaki et al., 2009) and KSP repeats (Bajaj and Miller, 1997). While phosphorylation of KSP repeats is crucial for various functions including axonal transport (Shea et al., 2009; Holmgren et al., 2012), the E-segment has been suggested to affect the conformation of the C-terminal KSP repeats (Sasaki et al., 2009). Thus, differential modification of the neurofilaments in the RAPuKO and TSCPuKO mice by GSK3 may result in a similar functional effect.

Besides the similarity in the neurodegenerative phenotype, RAPuKO and TSCPuKO mice also share behavioural similarities. Like in TSCPuKO mice (Tsai et al., 2012), the social interest of RAPuKO mice was reduced at young age, when the Purkinje cell density was unaffected. Alterations in inhibitory synaptic input and in dendritic morphology in the RAPuKO mice discussed above might underlie this abnormal social behaviour. A similar convergence of the phenotypes has been observed in mice deficient for raptor or TSC1 in skeletal muscle. In both cases the genetic manipulations result

in myopathies that are characterized by vacuoles (Bentzinger et al., 2008; Castets et al., 2013). In skeletal muscle, changes in autophagy flux, although at different steps of the process, might underlie this convergence. In summary, our findings demonstrate that both, sustained activation and inhibition of mTORC1 in Purkinje cells, affect non-motor related functions of the cerebellum and, at later time points, the survival of these neurons. Consequently, our data advice caution in treating brain disorders with rapamycin or other mTORC1 inhibitors, as has recently been suggested (Santini and Klann, 2011; Costa-Mattioli and Monteggia, 2013).

References

Angliker N, Ruegg MA (2013) In vivo evidence for mTORC2-mediated actin cytoskeleton rearrangement in neurons. Bioarchitecture 3:113-118.

Arimura N, Kaibuchi K (2007) Neuronal polarity: from extracellular signals to intracellular mechanisms. Nat Rev Neurosci 8:194-205.

Bajaj NP, Miller CC (1997) Phosphorylation of neurofilament heavy-chain side-arm fragments by cyclin-dependent kinase-5 and glycogen synthase kinase-3alpha in transfected cells. J Neurochem 69:737-743.

Barmack NH, Qian Z, Yoshimura J (2000) Regional and cellular distribution of protein kinase C in rat cerebellar Purkinje cells. J Comp Neurol 427:235-254.

Bentzinger CF, Romanino K, Cloetta D, Lin S, Mascarenhas JB, Oliveri F, Xia J, Casanova E, Costa CF, Brink M, Zorzato F, Hall MN, Ruegg MA (2008) Skeletal muscle-specific ablation of raptor, but not of rictor, causes metabolic changes and results in muscle dystrophy. Cell Metab 8:411-424.

Carson RP, Van Nielen DL, Winzenburger PA, Ess KC (2012) Neuronal and glia abnormalities in Tsc1-deficient forebrain and partial rescue by rapamycin. Neurobiol Dis 45:369-380.

Castets P, Lin S, Rion N, Di Fulvio S, Romanino K, Guridi M, Frank S, Tintignac LA, Sinnreich M, Ruegg MA (2013) Sustained activation of mTORC1 in skeletal muscle inhibits constitutive and starvation-induced autophagy and causes a severe, late-onset myopathy. Cell Metab 17:731-744.

Chen C, Kano M, Abeliovich A, Chen L, Bao S, Kim JJ, Hashimoto K, Thompson RF, Tonegawa S (1995) Impaired motor coordination correlates with persistent multiple climbing fiber innervation in PKC gamma mutant mice. Cell 83:1233-1242.

Ching GY, Chien CL, Flores R, Liem RK (1999) Overexpression of alpha-internexin causes abnormal neurofilamentous accumulations and motor coordination deficits in transgenic mice. J Neurosci 19:2974-2986.

Cloetta D, Thomanetz V, Baranek C, Lustenberger RM, Lin S, Oliveri F, Atanasoski S, Ruegg MA (2013) Inactivation of mTORC1 in the developing brain causes microcephaly and affects gliogenesis. J Neurosci 33:7799-7810.

Costa-Mattioli M, Monteggia LM (2013) mTOR complexes in neurodevelopmental and neuropsychiatric disorders. Nat Neurosci 16:1537-1543.

Cross DA, Alessi DR, Cohen P, Andjelkovich M, Hemmings BA (1995) Inhibition of glycogen synthase kinase-3 by insulin mediated by protein kinase B. Nature 378:785-789.

Fritschy JM, Panzanelli P, Kralic JE, Vogt KE, Sassoe-Pognetto M (2006) Differential dependence of axo-dendritic and axo-somatic GABAergic synapses on GABAA receptors containing the alpha1 subunit in Purkinje cells. J Neurosci 26:3245-3255.

Garrett AM, Schreiner D, Lobas MA, Weiner JA (2012) gamma-protocadherins control cortical dendrite arborization by regulating the activity of a FAK/PKC/MARCKS signaling pathway. Neuron 74:269-276.

Gibson DA, Tymanskyj S, Yuan RC, Leung HC, Lefebvre JL, Sanes JR, Chedotal A, Ma L (2014) Dendrite self-avoidance requires cell-autonomous slit/robo signaling in cerebellar purkinje cells. Neuron 81:1040-1056.

Goto J, Talos DM, Klein P, Qin W, Chekaluk YI, Anderl S, Malinowska IA, Di Nardo A, Bronson RT, Chan JA, Vinters HV, Kernie SG, Jensen FE, Sahin M, Kwiatkowski DJ (2011) Regulable neural progenitor-specific Tsc1 loss yields giant cells with organellar dysfunction in a model of tuberous sclerosis complex. Proc Natl Acad Sci U S A 108:E1070-1079.

Gown AM, Willingham MC (2002) Improved detection of apoptotic cells in archival paraffin sections: immunohistochemistry using antibodies to cleaved caspase 3. J Histochem Cytochem 50:449-454.

Hashimoto K, Kano M (2013) Synapse elimination in the developing cerebellum. Cell Mol Life Sci 70:4667-4680.

Hirano T (2013) Long-term depression and other synaptic plasticity in the cerebellum. Proc Jpn Acad Ser B Phys Biol Sci 89:183-195.

Holmgren A, Bouhy D, Timmerman V (2012) Neurofilament phosphorylation and their proline-directed kinases in health and disease. J Peripher Nerv Syst 17:365-376.

Ichise T, Kano M, Hashimoto K, Yanagihara D, Nakao K, Shigemoto R, Katsuki M, Aiba A (2000) mGluR1 in cerebellar Purkinje cells essential for long-term depression, synapse elimination, and motor coordination. Science 288:1832-1835.

Kakegawa W, Miyoshi Y, Hamase K, Matsuda S, Matsuda K, Kohda K, Emi K, Motohashi J, Konno R, Zaitsu K, Yuzaki M (2011) D-serine regulates cerebellar LTD and motor coordination through the delta2 glutamate receptor. Nat Neurosci 14:603-611.

Kakizawa S, Yamasaki M, Watanabe M, Kano M (2000) Critical period for activity-dependent synapse elimination in developing cerebellum. J Neurosci 20:4954-4961.

Kano M, Hashimoto K, Tabata T (2008) Type-1 metabotropic glutamate receptor in cerebellar Purkinje cells: a key molecule responsible for long-term depression, endocannabinoid signalling and synapse elimination. Philos Trans R Soc Lond B Biol Sci 363:2173-2186.

Kano M, Hashimoto K, Chen C, Abeliovich A, Aiba A, Kurihara H, Watanabe M, Inoue Y, Tonegawa S (1995) Impaired synapse elimination during cerebellar development in PKC gamma mutant mice. Cell 83:1223-1231.

Kano M, Hashimoto K, Watanabe M, Kurihara H, Offermanns S, Jiang H, Wu Y, Jun K, Shin HS, Inoue Y, Simon MI, Wu D (1998) Phospholipase cbeta4 is specifically involved in climbing fiber synapse elimination in the developing cerebellum. Proc Natl Acad Sci U S A 95:15724-15729.

Kwiatkowski DJ, Zhang H, Bandura JL, Heiberger KM, Glogauer M, el-Hashemite N, Onda H (2002) A mouse model of TSC1 reveals sex-dependent lethality from liver hemangiomas, and up-regulation of p70S6 kinase activity in Tsc1 null cells. Hum Mol Genet 11:525-534.

Kwon CH, Luikart BW, Powell CM, Zhou J, Matheny SA, Zhang W, Li Y, Baker SJ, Parada LF (2006) Pten regulates neuronal arborization and social interaction in mice. Neuron 50:377-388.

Laplante M, Sabatini DM (2012) mTOR Signaling. Cold Spring Harb Perspect Biol 4.

Lefebvre JL, Kostadinov D, Chen WV, Maniatis T, Sanes JR (2012) Protocadherins mediate dendritic self-avoidance in the mammalian nervous system. Nature 488:517-521.

Louis ED, Yi H, Erickson-Davis C, Vonsattel JP, Faust PL (2009) Structural study of Purkinje cell axonal torpedoes in essential tremor. Neurosci Lett 450:287-291.

Meikle L, Pollizzi K, Egnor A, Kramvis I, Lane H, Sahin M, Kwiatkowski DJ (2008) Response of a neuronal model of tuberous sclerosis to mammalian target of rapamycin (mTOR) inhibitors: effects on mTORC1 and Akt signaling lead to improved survival and function. J Neurosci 28:5422-5432.

Naska S, Park KJ, Hannigan GE, Dedhar S, Miller FD, Kaplan DR (2006) An essential role for the integrin-linked kinase-glycogen synthase kinase-3 beta pathway during dendrite initiation and growth. J Neurosci 26:13344-13356.

Notter T, Panzanelli P, Pfister S, Mircsof D, Fritschy JM (2014) A protocol for concurrent high-quality immunohistochemical and biochemical analyses in adult mouse central nervous system. Eur J Neurosci 39:165-175.

Offermanns S, Hashimoto K, Watanabe M, Sun W, Kurihara H, Thompson RF, Inoue Y, Kano M, Simon MI (1997) Impaired motor coordination and persistent multiple climbing fiber innervation of cerebellar Purkinje cells in mice lacking Galphaq. Proc Natl Acad Sci U S A 94:14089-14094.

Oh WJ, Jacinto E (2011) mTOR complex 2 signaling and functions. Cell Cycle 10:2305-2316.

Patrizi A, Scelfo B, Viltono L, Briatore F, Fukaya M, Watanabe M, Strata P, Varoqueaux F, Brose N, Fritschy JM, Sassoe-Pognetto M (2008) Synapse formation and clustering of neuroligin-2 in the absence of GABAA receptors. Proc Natl Acad Sci U S A 105:13151-13156.

Pekny M, Nilsson M (2005) Astrocyte activation and reactive gliosis. Glia 50:427-434.

Robertson JD, Orrenius S, Zhivotovsky B (2000) Review: nuclear events in apoptosis. J Struct Biol 129:346-358.

Saito H, Tsumura H, Otake S, Nishida A, Furukawa T, Suzuki N (2005) L7/Pcp-2-specific expression of Cre recombinase using knock-in approach. Biochem Biophys Res Commun 331:1216-1221.

Santini E, Klann E (2011) Dysregulated mTORC1-Dependent Translational Control: From Brain Disorders to Psychoactive Drugs. Front Behav Neurosci 5:76.

Sasaki T, Ishiguro K, Hisanaga S (2009) Novel axonal distribution of neurofilament-H phosphorylated at the glycogen synthase kinase 3beta-phosphorylation site in its E-segment. J Neurosci Res 87:3088-3097.

Sasaki T, Taoka M, Ishiguro K, Uchida A, Saito T, Isobe T, Hisanaga S (2002) In vivo and in vitro phosphorylation at Ser-493 in the glutamate (E)-segment of neurofilament-H subunit by glycogen synthase kinase 3beta. J Biol Chem 277:36032-36039.

Schmahmann JD, Weilburg JB, Sherman JC (2007) The neuropsychiatry of the cerebellum - insights from the clinic. Cerebellum 6:254-267.

Schmued LC, Hopkins KJ (2000) Fluoro-Jade B: a high affinity fluorescent marker for the localization of neuronal degeneration. Brain Res 874:123-130.

Schneider Gasser EM, Straub CJ, Panzanelli P, Weinmann O, Sassoe-Pognetto M, Fritschy JM (2006) Immunofluorescence in brain sections: simultaneous detection of presynaptic and postsynaptic proteins in identified neurons. Nat Protoc 1:1887-1897.

Shea TB, Chan WK, Kushkuley J, Lee S (2009) Organizational dynamics, functions, and pathobiological dysfunctions of neurofilaments. Results Probl Cell Differ 48:29-45.

Shimobayashi M, Hall MN (2014) Making new contacts: the mTOR network in metabolism and signalling crosstalk. Nat Rev Mol Cell Biol 15:155-162.

Silverman JL, Yang M, Lord C, Crawley JN (2010) Behavioural phenotyping assays for mouse models of autism. Nat Rev Neurosci 11:490-502.

Sotelo C, Dusart I (2009) Intrinsic versus extrinsic determinants during the development of Purkinje cell dendrites. Neuroscience 162:589-600.

Tchorz JS, Suply T, Ksiazek I, Giachino C, Cloetta D, Danzer CP, Doll T, Isken A, Lemaistre M, Taylor V, Bettler B, Kinzel B, Mueller M (2012) A modified RMCE-compatible Rosa26 locus for the expression of transgenes from exogenous promoters. PLoS One 7:e30011.

Thomanetz V, Angliker N, Cloetta D, Lustenberger RM, Schweighauser M, Oliveri F, Suzuki N, Ruegg MA (2013) Ablation of the mTORC2 component rictor in brain or Purkinje cells affects size and neuron morphology. J Cell Biol 201:293-308.

Tsai PT, Hull C, Chu Y, Greene-Colozzi E, Sadowski AR, Leech JM, Steinberg J, Crawley JN, Regehr WG, Sahin M (2012) Autistic-like behaviour and cerebellar dysfunction in Purkinje cell Tsc1 mutant mice. Nature 488:647-651.

Um SH, Frigerio F, Watanabe M, Picard F, Joaquin M, Sticker M, Fumagalli S, Allegrini PR, Kozma SC, Auwerx J, Thomas G (2004) Absence of S6K1 protects against age- and diet-induced obesity while enhancing insulin sensitivity. Nature 431:200-205.

Viltono L, Patrizi A, Fritschy JM, Sassoe-Pognetto M (2008) Synaptogenesis in the cerebellar cortex: differential regulation of gephyrin and GABAA receptors at somatic and dendritic synapses of Purkinje cells. J Comp Neurol 508:579-591.

Wang SS, Kloth AD, Badura A (2014) The Cerebellum, Sensitive Periods, and Autism. Neuron 83:518-532.

Watanabe M, Kano M (2011) Climbing fiber synapse elimination in cerebellar Purkinje cells. Eur J Neurosci 34:1697-1710.

Watanabe S, Endo S, Oshima E, Hoshi T, Higashi H, Yamada K, Tohyama K, Yamashita T, Hirabayashi Y (2010) Glycosphingolipid synthesis in cerebellar Purkinje neurons: roles in myelin formation and axonal homeostasis. Glia 58:1197-1207.

Wierenga CJ, Becker N, Bonhoeffer T (2008) GABAergic synapses are formed without the involvement of dendritic protrusions. Nat Neurosci 11:1044-1052.

Wullschleger S, Loewith R, Hall MN (2006) TOR signaling in growth and metabolism. Cell 124:471-484.

Yamada K, Watanabe M (2002) Cytodifferentiation of Bergmann glia and its relationship with Purkinje cells. Anat Sci Int 77:94-108.

Yang M, Crawley JN (2009) Simple behavioral assessment of mouse olfaction. Curr Protoc Neurosci Chapter 8:Unit 8 24.

Yang Y, Coleman M, Zhang L, Zheng X, Yue Z (2013) Autophagy in axonal and dendritic degeneration. Trends Neurosci 36:418-428.

Figures

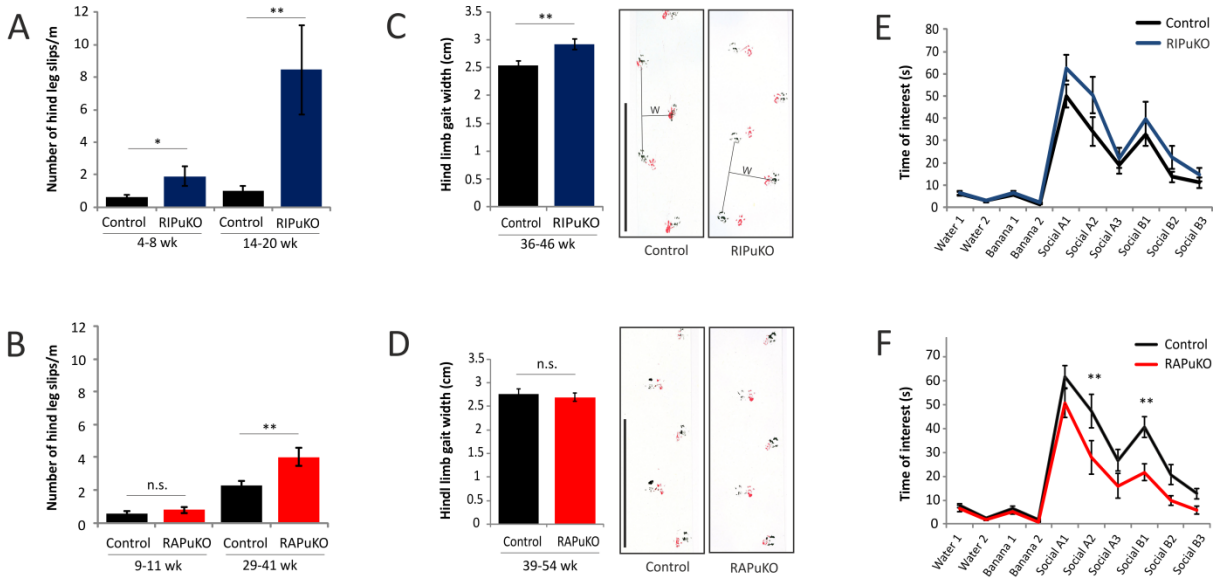

Figure 1: Behavioural assessment of RIPuKO and RAPuKO mice. ***A*** and ***B***, Balance beam tests of RIPuKO (*A*) and RAPuKO (*B*) mice and their respective control littermates at different ages. The number of hind leg slips per meter was measured as a readout of ataxia. For each group n ≥ 8 mice were tested. ***C*** and ***D***, Footprint pattern analysis of RIPuKO (*C*) and RAPuKO (*D*) mice and their control mice (n ≥ 7 mice for each group) of the indicated age. The steps of the hind and front paws are indicated in black and red, respectively. Hind limb gait width (W) was measured as indicated in (*C*). ***E*** and ***F***, Olfactory habituation/dishabituation test with n ≥ 12 male RIPuKO or RAPuKO mice and corresponding control mice. Non-social and social odours were presented to the mice on a cotton swab in 2 and 3 repetitions as indicated. Bars represent mean ± SEM. Data of (*A* – *D*) were analysed by a Student's t-test and for (*E* – *F*) a two-way ANOVA, Bonferroni's post hoc analysis was used. p-values: ** $p < 0.01$; * $p < 0.05$; ns $p \geq 0.05$. Scale bar: 10 cm.

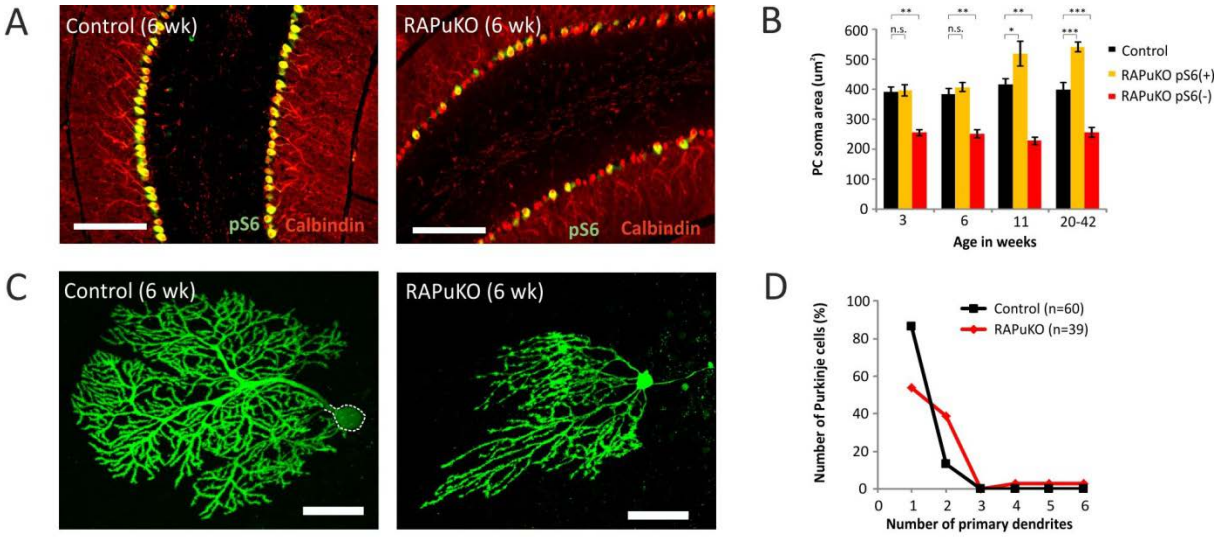

Figure 2. Morphology of Purkinje cells is altered in RAPuKO mice. ***A***, Sagittal cerebellar slices of 6-week-old RAPuKO mice and corresponding control mice were co-stained for calbindin (red) and pS6 (green). All the calbindin-positive neurons are also pS6-positive (yellow) in control mice (left) whereas most Purkinje cells are pS6-negative in RAPuKO mice (right). ***B***, Average soma area of Purkinje cells of control mice (black bars) and pS6-positive (yellow) or pS6-negative (red) Purkinje cells in RAPuKO mice of different age. Data represent Purkinje cell somata of lobes IV&V of $n \geq 3$ mice for each time point and genotype. ***C***, Purkinje cells of 4-6-week-old RAPuKO or control mice ($n \geq 8$) were labelled with biocytin by the whole-cell patch clamp technique and detected by FITC-streptavidin after a fixation of the entire acute slice. Pictures in (*C*) represent merged *z*-stacks of confocal microscopy pictures. ***D***, Quantification of the number of primary dendrites originating from a Purkinje cell soma. Bars in (*B*) represent mean ± SEM. Statistical analysis in (*B*) used one-way ANOVA with Tukey's post hoc analysis. p-values: *** $p < 0.001$; ** $p < 0.01$; * $p < 0.05$; ns $p \geq 0.05$. Scale bars: 200 μm (*A*), 50 μm (*C*).

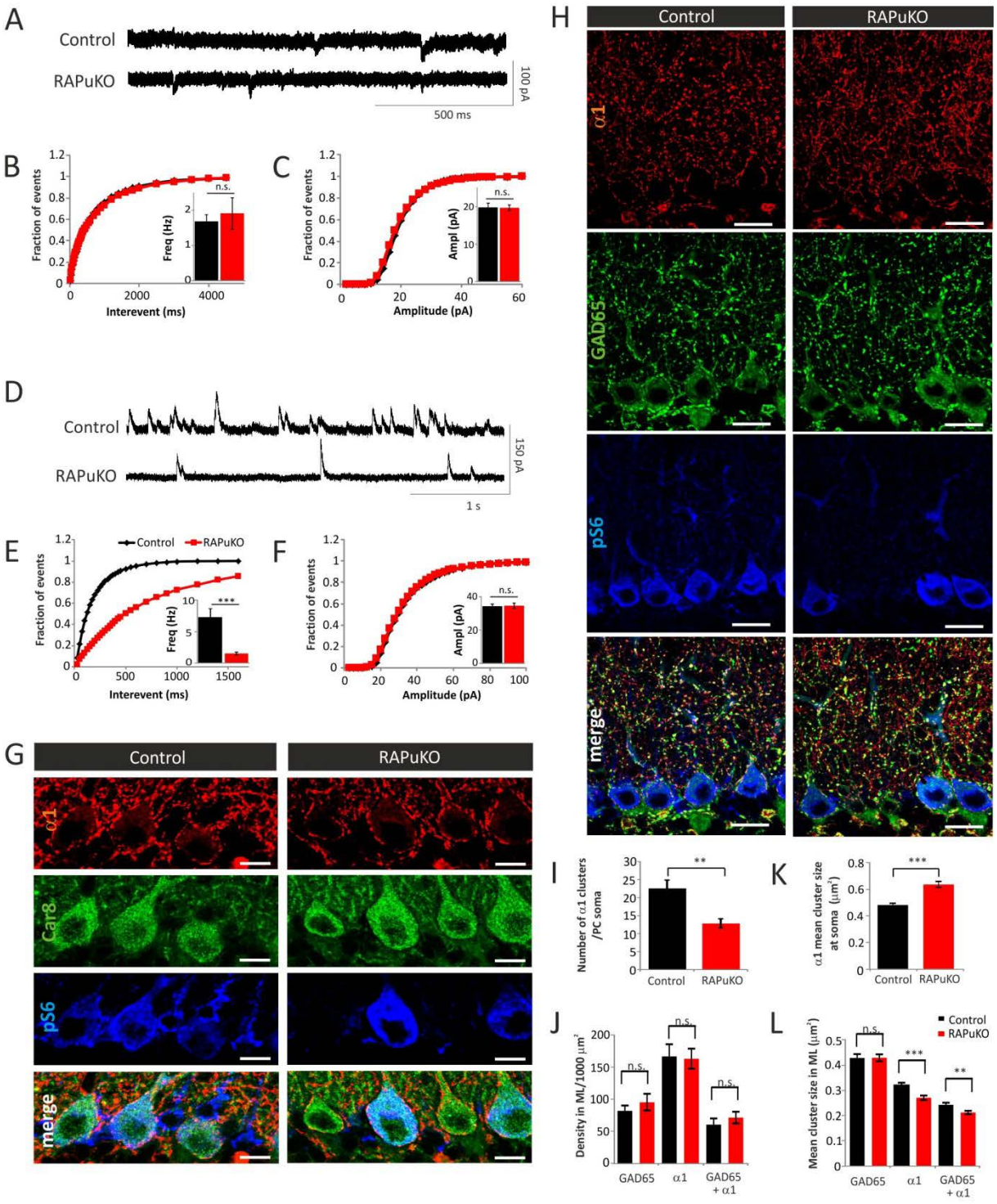

Figure 3. Inhibitory synaptic input is altered in raptor-knockout Purkinje cells. ***A***, Sample traces of mEPSC recordings taken from Purkinje cells of 6-week-old control or RAPuKO mice. ***B*** *and* ***C***, Quantification of mEPSC frequency (*B*) and amplitude (*C*) recorded from 5 RAPuKO (red) and 4

control (black) mice. Mean values and cumulative distributions of recordings from 12 raptor-deficient (red) and 14 control (black) Purkinje cells are shown. ***D***, mIPSC sample traces of Purkinje cells of 6-week-old control or RAPuKO mice. ***E*** and ***F***, Quantification of mIPSC frequency (*E*) and amplitude (*F*) recorded from 3 RAPuKO (red) and 3 control (black) mice. Mean values and cumulative distributions of recordings from 14 raptor-deficient (red) and 16 control (black) Purkinje cells are shown. ***G***, Sagittal cerebellar sections of 6-week-old RAPuKO or control mice stained with antibodies to the α1 subunit of $GABA_A$ receptors (red). Co-staining against Car8 (green) and pS6 (blue) was used to identify Purkinje cell somata and to confirm raptor deficiency, respectively. Merged *z*-stacks of confocal microscopy pictures are shown. ***H***, Staining of the molecular layer of the same mice used in (*G*) for $GABA_A$ α1 (red), GAD65 (green; stains GABAergic presynaptic terminals) and for pS6 (blue). ***I*** and ***K***, Analysis of the perisomatic $GABA_A$ α1 subunit clusters shown in (*G*). (*I*) shows the average number of $GABA_A$ α1 subunit clusters at the soma of pS6-negative Purkinje cells ($n \geq 5$ per mouse) of RAPuKO mice ($n = 6$) or Purkinje cells ($n \geq 10$ per mouse) of control mice ($n = 6$). (*K*) shows the quantification of the $GABA_A$ α1 subunit cluster size at these somata. ***J*** and ***L***, Quantification of the mean density (*J*) or size (*L*) of the clusters positive for GAD65, for the $GABA_A$ α1 subunit (α1) and for both (GAD65 + α1), detected in the molecular layer of control (black) or RAPuKO (red) mice ($n \geq 4$ per genotype). Bars represent mean ± SEM. Data in *B, C, E, F* and *I* - *L* were analysed by a Student's t-test. p-values: *** $p < 0.001$; ** $p < 0.01$; ns $p \geq 0.05$. Scale bars: 10 μm (*G*) and 20 μm (*H*).

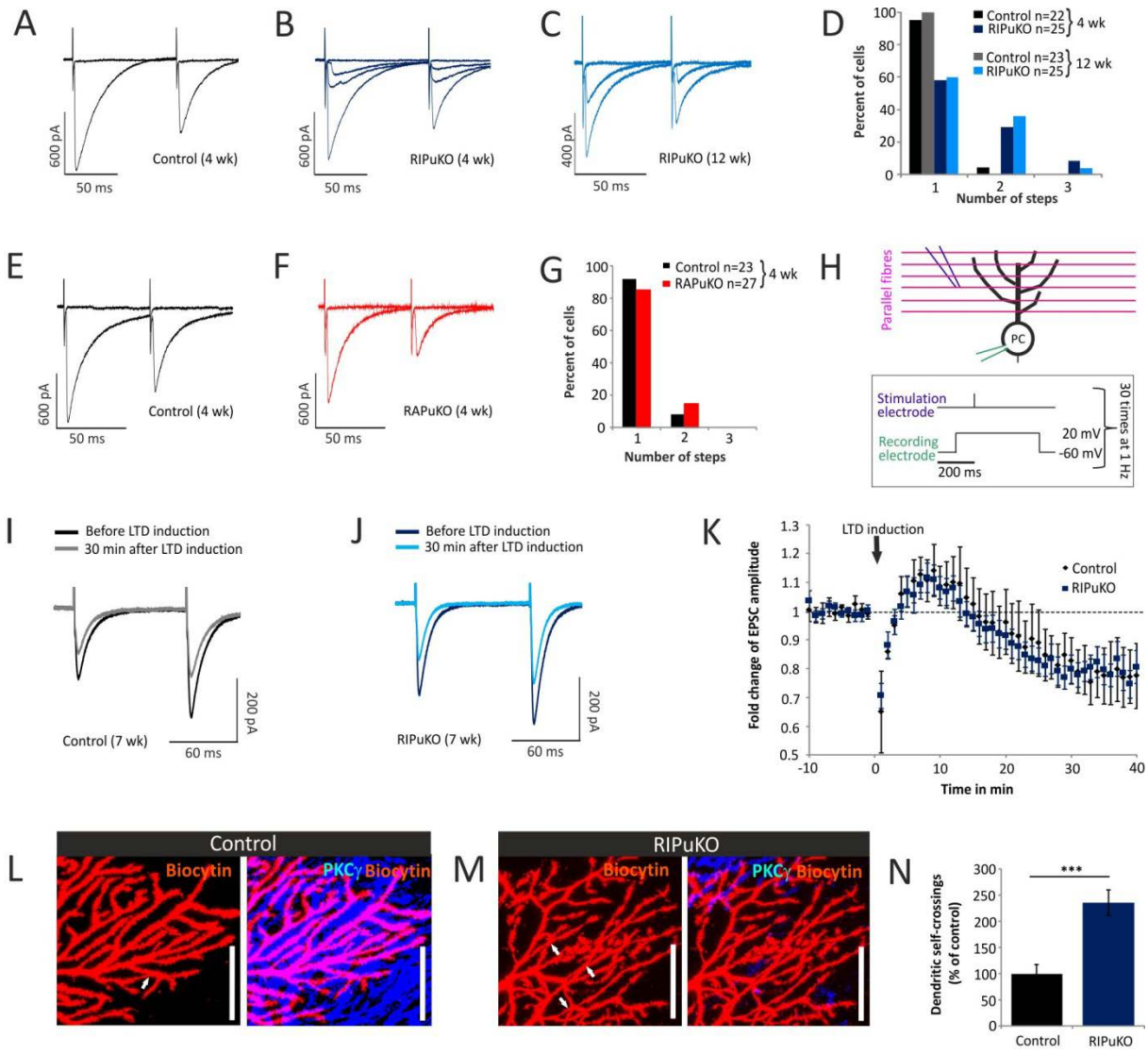

Figure 4. Rictor-knockout Purkinje cells are innervated by multiple CFs, show impairment in dendritic self-avoidance but show normal LTD. ***A*** **-** ***C***, Paired current pulses in the granule cell layer were used to elicit CF-EPSC responses in Purkinje cells. Stimulation intensity was continuously increased and the size of the postsynaptic response was recorded. In control mice (*A*), the CF-EPSC response occurred in an "all or nothing" manner and did not change by further increasing the stimulation intensity, indicating mono CF innervation of the Purkinje cell. In 4-week-old RIPuKO (*B*) or 12-week-old RIPuKO mice (*C*), CF-EPSC responses revealed 2 or 3 discrete steps in response to increasing stimulation intensity, indicating multiple innervation by CFs. ***D***, Percentage of the Purkinje cells showing the indicated number of discrete CF-EPSC steps of 4 or 12-week-old RIPuKO or corresponding control mice. The indicated numbers of Purkinje cells were analysed from n ≥ 4 mice for each genotype and age. ***E*** **-** ***G***, Analysis of climbing fibre innervation of Purkinje cells of 4-week-

old RAPuKO or control mice (n ≥ 4) using the same experimental approach as described in (*A* - *D*). ***H***, Stimulation paradigm to elicit cerebellar LTD by repetitive stimulation of afferent parallel fibres and simultaneous depolarization of the voltage-clamped Purkinje cell to 20 mV for 500 ms. ***I*** and ***J***, Sample traces of PF-EPSCs recorded in Purkinje cells of a 7-week-old control (*I*) or RIPuKO mouse (*J*) before and 30 minutes after LTD induction. ***K***, Fold change of the PF-EPSC amplitude monitored in 6 control and 11 rictor-deficient Purkinje cells over 40 minutes after LTD induction (n ≥ 3 individual mice of each genotype). There is no difference between control- and rictor-deficient neurons. ***L*** and ***M***, Confocal microscopy pictures (merged *z*-stacks) of spiny distal dendritic branches of biocytin-labelled Purkinje cells of 12-week-old control or RIPuKO mice. Acute slices containing the labelled cells were re-sliced and stained with Cy3-streptdavidin (red) and an anti-PKCγ antibody (blue) to detect the labelled cells and to confirm the mTORC2 ablation, respectively, as previously described (Thomanetz et al., 2013). The number of dendritic self-crossings (white arrows) was counted. ***N***, Relative number of dendritic self-crossings detected in RIPuKO mice expressed as percentage of dendritic self-crossings detected in control mice. n ≥ 30 Purkinje cells of RIPuKO or corresponding control mice (n = 4 for each genotype) were analysed. Data in (*K* and *N*) represent mean ± SEM. Data of (*N*) were analysed by a Student's t-test. p-values: *** $p < 0.001$. Scale bars: 25 μm (*L and M*).

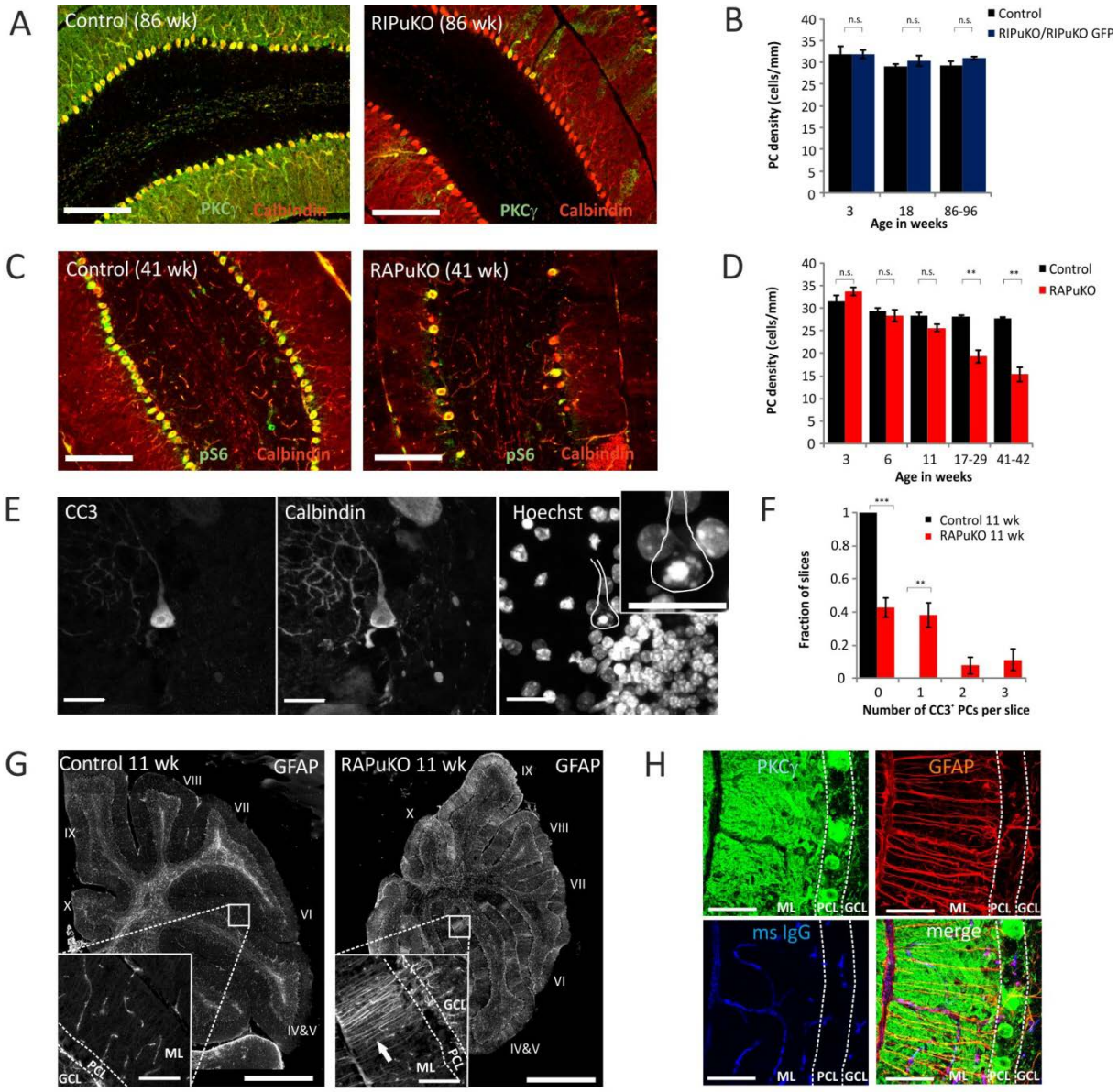

Figure 5. Depletion of raptor, but not rictor causes age-dependent loss of Purkinje cells due to apoptosis. ***A***, Sagittal cerebellar slices of 86-week-old RIPuKO mice and corresponding control mice were co-stained for calbindin (red) and PKCγ (green) to confirm mTORC2 ablation in Purkinje cells. Calbindin staining was used to determine Purkinje cell density in the cerebellar lobes IV&V of RIPuKO and control mice. ***B***, Purkinje cell density determined for RIPuKO and corresponding control mice in course of ageing. For each indicated age and genotype n ≥ 3 mice were analysed with n ≥ 3 cerebellar slices per mouse. ***C*** and ***D***, Staining for calbindin (red) and pS6 (green) to analyse Purkinje cell density and mTORC1 ablation in 41-week-old RAPuKO and control mice. Purkinje cell density in course of mouse ageing was monitored as described in (*A* and *B*). ***E***, Confocal pictures (merged *z*-

stacks) of an apoptotic Purkinje cell detected by a co-staining of a cerebellar slice of an 11-week-old RAPuKO mouse using Hoechst and antibodies against calbindin and CC3. ***F***, The fraction of cerebellar slices containing the indicated numbers of CC3-positive Purkinje cells were determined for RAPuKO or control mice (n = 4 mice per genotype). ***G***, GFAP staining of a sagittal cerebellar slice of an 11-week-old RAPuKO or control mouse. Similar findings were made with additional RAPuKO and control mice of the same age (n = 3 mice per genotype). The inset highlights increased GFAP expression in form of palisade-like structures in RAPuKO mice (white arrow). IV - X indicate the numbers of the cerebellar lobes. ***H***, Cerebellar section of an 11-week-old RAPuKO mouse co-stained against GFAP, PKCγ and mouse-IgG followed by confocal microscopy analysis (merged *z*-stacks). PKCγ labels Purkinje cells while mouse-IgG stains blood vessels which helps to differentiate between GFAP staining and blood vessels that are also seen in the insets of (*G*). Bars represent mean ± SEM. Data of (*B, D* and *F*) were analysed by a Student's t-test. p-values: *** $p < 0.001$; ** $p < 0.01$; ns $p \geq 0.05$. Scale bars: 200 μm (*A* and *C*), 20 μm (*E*), 1 mm (*G*), 100 μm (inset of *G*), 50 μm (*H*). PCL: Purkinje cell layer; ML: molecular layer; GCL: granule cell layer.

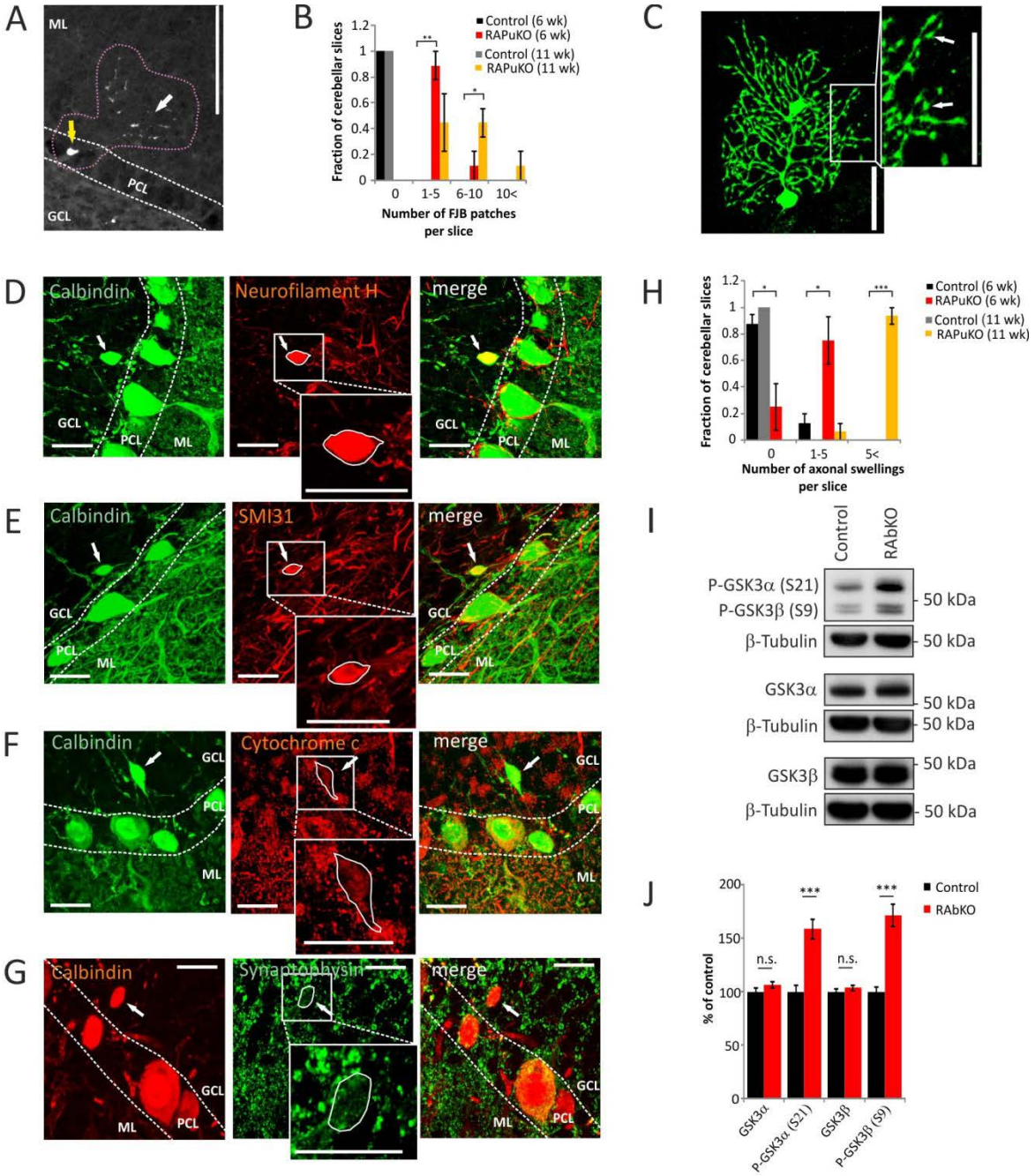

Figure 6. Raptor-deficient Purkinje cells show dendritic degeneration and axonal swellings that accumulate neurofilaments. ***A***, Example of Fluoro-Jade B (FJB) puncta seen in the molecular layer (white arrow) and in the Purkinje cell layer (yellow arrow) of RAPuKO mice. For quantification shown in (*B*), accumulation of FJB-positive puncta were counted as one FJB patch (encircled with the dashed, pink line). ***B***, Fraction of cerebellar slices of 6 and 11-week-old RAPuKO or control mice (n = 3 for each age and genotype) that contain 0; 1-5; 6-10 or > 10 FJB patches. ***C***, Confocal picture (merged *z*-stacks) of a biocytin-labelled Purkinje cell of a 6-week-old RAPuKO mouse that shows

signs of atrophy and beadings (white arrows), indicative of dendritic degeneration. ***D – G***, Confocal pictures of sagittal cerebellar slices of 11-week-old RAPuKO mice stained for calbindin and for neurofilament H (*D*), phosphorylated neurofilaments (SMI31) (*E*), cytochrome c (*F*), or synaptophysin (*G*). Axonal swelling (white arrows) contained neurofilament H and phosphorylated forms of neurofilaments (SMI31-positive) but were devoid of cytochrome c and synaptophysin. ***H***, Relative proportion of cerebellar sections of 6 and 11-week-old RAPuKO or control mice (n = 3 mice per age and genotype) that reveal 0; 1-5 or > 5 axonal swellings proximal to the Purkinje cell somata as shown in (*D* - *G*). ***I***, Western blot analysis of total brain lysates derived from embryonic day 19.5 mice depleted of raptor as previously described (Cloetta et al., 2013). Lysates were probed with a phospho-specific antibody recognizing P-Ser21 on GSK3α and P-Ser9 in GSK3β (top) and antibodies recognizing the total protein. Antibodies to β-Tubulin were used as loading control. ***J***, Quantification of Western blot signals shown in (*I*) relative to the intensities in control mice (n = 5 per genotype). Bars represent mean ± SEM. Data in (*B*, *H* and *J*) were analysed by a Student's t-test. p-values: *** $p < 0.001$; ** $p < 0.01$; * $p < 0.05$. Scale bars: 100 μm (*A*), 50 μm (*C*) and 25 μm (*D* – *G*). PCL: Purkinje cell layer; ML: molecular layer; GCL: granule cell layer.

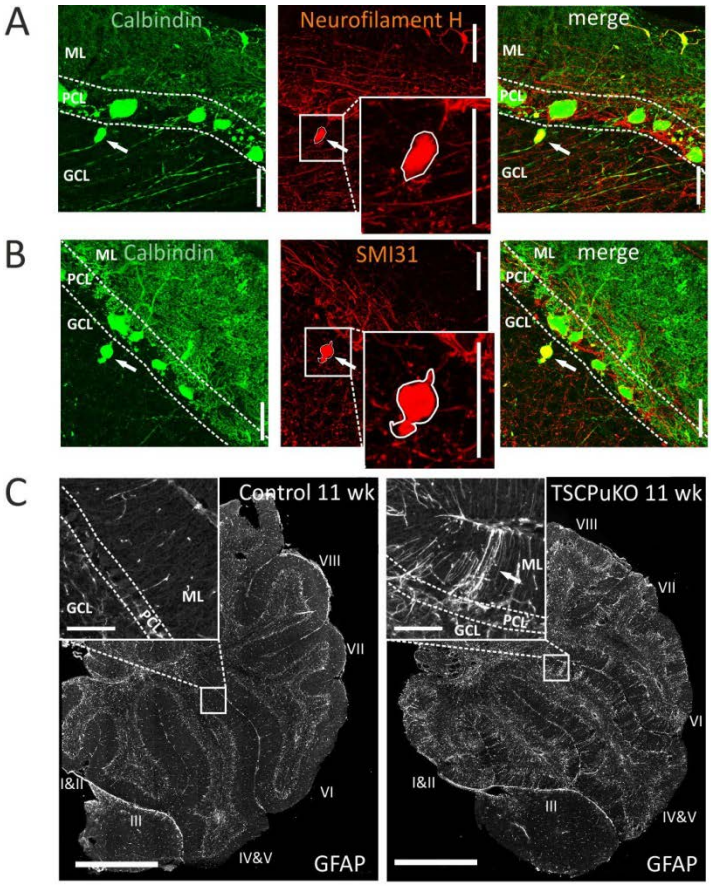

Figure 7. Depletion of TSC1 in Purkinje cells results in the accumulation of neurofilaments in axons and in reactive gliosis. ***A*** and ***B***, Sagittal cerebellar slices of 11-week-old TSCPuKO mice were stained with anti-calbindin and anti-neurofilament H (*A*) or SMI31 antibodies (*B*). Like in RAPuKO mice, axonal swellings (white arrows) that are positive for neurofilament H and phosphorylated neurofilaments (SMI31-positive) are detected in TSC1-deficient Purkinje cells. ***C***, Sagittal cerebellar slices of 11-week-old TSCPuKO or control mice stained for GFAP. The white arrow indicates reactive gliosis that manifests as palisade-like, GFAP-positive structures in the molecular layer of TSCPuKO but not control mice (n = 3 mice per genotype). Scale bars: 50 μm (*A* and *B*), 1 mm (*C*), 100 μm (inset of *C*). PCL: Purkinje cell layer; ML: molecular layer; GCL: granule cell layer. I to VIII designate numbers of the cerebellar lobes.

6. General discussion and outlook

The findings presented in this study demonstrate that both mTORC1 and mTORC2 are crucial for Purkinje cells, yet, in mostly distinct manners since an inactivation of either of them in Purkinje cells results in phenotypes that mainly diverge. Below, the phenotypes seen with RAPuKO and RIPuKO mice are briefly summarized and further discussed on a behavioural, cellular and molecular level.

Behaviour. On the behavioural level, both RAPuKO and RIPuKO mice showed motor coordination deficits but these deficits had different temporal onsets. The motor coordination deficits of RIPuKO mice could be detected at any tested age and correlated with multiple climbing fibre innervation and increased dendritic self-crossings of knockout Purkinje cells. Both phenomena have been linked to motor deficits (Chen *et al.*, 1995; Kano *et al.*, 1995; Offermanns *et al.*, 1997; Kano *et al.*, 1998; Ichise *et al.*, 2000; Gibson *et al.*, 2014) and most likely have a developmental origin, which explains the fact that RIPuKO mice showed motor deficits already at a young age. On the other hand, motor coordination deficits of RAPuKO mice coincided with an age-dependent loss of Purkinje cells and, hence, were detected only with old, but not young mice. At the age when motor coordination deficits were detected for RAPuKO mice, their Purkinje cell density is supposed to be reduced by about 40% based on an extrapolation from immunohistochemistry data gained from knockout mice of a similar age. This rather substantial loss of Purkinje cells seems to cause only mild motor coordination deficits since RAPuKO mice performed only mildly worse on the balance beam than control mice and did not show alterations of the footprint pattern. Apparently, motor control excerpted by the cerebellum is rather robust to a loss of Purkinje cells, which is in line with the observations of another research group (Ko *et al.*, 2005).

Distinct behavioural phenotypes were also detected for RAPuKO and RIPuKO mice regarding the social interest measured in the olfactory habituation/dishabituation test. While RIPuKO mice showed normal interest in social odours, the interest of RAPuKO mice therein was reduced. Last was detected at an age when Purkinje cell density was unchanged in RAPuKO mice. Similar to mice that have TSC1 heterozygously knocked out in Purkinje cells (see section 3.4.6.) there are most likely other reasons than a Purkinje cell loss for this aberrant social behaviour (Tsai *et al.*, 2012). We hypothesize that the strong impact of raptor knockout on the inhibitory synaptic input of Purkinje cells, evidenced by electrophysiological recordings and immunohistochemical analysis, might contribute to this behavioural deficit. Because the mEPSCs recorded from raptor-knockout Purkinje cells did not reveal alterations, we think that the ratio of excitatory/inhibitory synaptic input of these neurons might be increased. An analysis of the ratio of evoked EPSCs and IPSCs might provide further insight if this is indeed the case. EPSCs and IPSCs can be evoked by stimulating parallel fibres that generate not only an excitatory stimulation of Purkinje cells via the parallel fibre synapses but also an inhibitory stimulation via the MLIs that are connected to parallel fibres as well (see section 3.4.2.).

Using this approach, only a trend for a reduction of the excitatory/inhibitory ratio was observed with TSC1-knockout Purkinje cells (Tsai *et al.*, 2012). Solid evidence for an involvement of mTORC1 in the maintenance of the excitatory/inhibitory balance has recently been reported from mice that have TSC1 knocked out in the hippocampus (see section 3.3.3) (Bateup *et al.*, 2013).

Although a direct comparison is not possible, a knockout of TSC1 in Purkinje cells seems to reduce the interest of mice in social odours in a more pronounced manner than the one of raptor (Tsai *et al.*, 2012). While Tsai and colleagues do not indicate the precise percentage of Purkinje cells affected by the *L7/Pcp-2*-driven knockout (but seems to affect the majority of the Purkinje cells based on the shown pictures), we found that in average 50% of the Purkinje cells of RAPuKO mice had mTORC1 ablated. Using the same Cre driver, a higher knockout frequency (75%) was achieved in RIPuKO mice, which indicates that the knockout frequency may depend on the targeted locus, however, the reason for this discrepancy is unsolved. The severity of behavioural phenotypes most likely correlates with the percentage of knockout Purkinje cells and, hence, the reduction of the social interest of RAPuKO mice might become even more pronounced if the knockout frequency were higher. In addition to social abnormalities, TSC1 Purkinje cell knockout mice also revealed repetitive behaviour, which led to the conclusion that these mice display an autistic-like phenotype (Tsai *et al.*, 2012). Whether RAPuKO mice are also bound to repetitive behaviour needs to be further investigated. Using a marble burying test as a readout for repetitive behaviour, no signs for such a phenotype could be detected for RAPuKO mice in preliminary testings (data not shown).

Altogether, the behavioural data presented in this study show that ablation of either mTORC1 or mTORC2 specifically in Purkinje cells results in measurable behavioural deficits, which underlines the importance of both complexes for cerebellar functions. The importance of mTOR signalling for cerebellar functions is also supported by the notion that most of the brain disorders that are linked to mTOR (see section 3.3.4.) also reveal a cerebellar component. Tuberous sclerosis patients show cerebellar abnormalities that positively correlate with the severity of the comorbid ASD (Weber *et al.*, 2000; Asano *et al.*, 2001; Eluvathingal *et al.*, 2006; Ertan *et al.*, 2010) and, as described above, Purkinje cell-specific TSC1 knockout in mice is sufficient to recapitulate hallmarks of ASD. Patients suffering from the Fragile X syndrome show cerebellar learning deficits that manifest in abnormal eye-blink conditioning (Smit *et al.*, 2008; Tobia & Woodruff-Pak, 2009), which notably is also seen with mice that have *Fmr1* conditionally knocked out specifically in Purkinje cells (Koekkoek *et al.*, 2005). Fragile X is caused by expansion of CGG trinucleotide repeats in the *Fmr1* gene, which ultimately silences this gene. Fragile X syndrome occurs beyond a threshold of 200 repeats. Motor deficits are not only seen with Fragile X patients but also with humans that carry *Fmr1* "premutations". Carriers of *Fmr1* "premutations" in the range between 55-200 CGG repeats are prone to develop age-dependent motor deficits that are summarized as Fragile X associated ataxia/tremor syndrome (Jacquemont *et al.*, 2007; Hall & O'Keefe J, 2012). Cerebellar abnormalities and motor symptoms are also documented for schizophrenia (Andreasen & Pierson, 2008; Walther & Strik, 2012;

Parker *et al.*, 2014), which includes for example a reduction in the volume of the anterior cerebellar vermis (Weinberger *et al.*, 1980; Nopoulos *et al.*, 1999) and a decrease of the size and number of Purkinje cells (Reyes & Gordon, 1981; Tran *et al.*, 1998; Maloku *et al.*, 2010). Furthermore, also the neurodegenerative Parkinson's and Huntington's diseases reveal alterations in the cerebellum. Although the hallmark of Parkinson's disease is a loss of dopaminergic neurons in the substantia nigra, a recent review outlines that the cerebellum may also substantially contribute to symptoms of this disease (Wu & Hallett, 2013). Functional and structural changes are detected in the cerebellum in Parkinson's disease and a treatment of mice with the Parkinson inducing agent MPTP causes a loss of Purkinje cells (Takada *et al.*, 1993). However, the role of the cerebellum in Parkinson's disease is unknown and it is not clear whether it excerpts a pathological or rather a compensating effect in this disease as discussed by Wu and Hallett (Wu & Hallett, 2013). In Huntington's disease patients, as well as in mouse models of this disease, a reduction of the Purkinje cell density is seen (Rodda, 1981; Jeste *et al.*, 1984; Turmaine *et al.*, 2000; Dougherty *et al.*, 2013). Single cell RT-PCR indicates transcriptional changes in Purkinje cells of Huntington's disease mouse models (Euler *et al.*, 2012) and also the firing rate of Purkinje cells is altered (Dougherty *et al.*, 2013).

Cellular. Purkinje cells deficient of either mTORC1 or mTORC2 showed morphological alterations that resembled each other and included multiple primary dendrites and a reduction of the overall neuron size. Last was more pronounced for mTORC1-deficient cells. Additionally, we found that mTORC2 ablation in Purkinje cells increased the number of self-crossings of dendritic branches. We think that most, if not even all, of these morphological changes originate from developmental deficits as this is further described in the commentary attached in the appendix and in the discussion of publication 2.

Self-crossings of dendritic branches can be prevented by a process called dendritic self-avoidance, which helps a neuron to minimize redundant input (Grueber & Sagasti, 2010). Additionally, this process allows to reduce the gaps between the dendritic branches and therefore enables a neuron to maximize the receptive field coverage. An impairment of dendritic self-avoidance, as this is seen with rictor-deficient Purkinje cells, will result in an imperfect definition of the receptive field of these neurons, which in turn may affect motor circuit function and thereby cause motor deficits as this has recently been suggested (Gibson *et al.*, 2014).

Developmental deficits in climbing fibre elimination observed with rictor-knockout Purkinje cells have been linked to motor coordination deficits as well (see above). But how may the resulting multiple climbing fibre innervation of Purkinje cells impair motor coordination? To understand how this cellular phenomenon may alter the motor behaviour, first the modular setup of the cerebellum has to be explained. Along the mediolateral axis, the cerebellar cortex is divided in several longitudinal zones that become visible upon expression analysis of several genes, for example *zebrin II* (Brochu *et al.*, 1990). The longitudinal zones are also defined by a mediolateral organization of Purkinje cell

projections in the DCN (Apps & Hawkes, 2009). Furthermore, the olivocerebellar climbing fibre projections are topographically arranged in a mediolateral manner. Consequently, these longitudinal zones are thought to reflect "modules" of Purkinje cell efferents and olivocerebellar climbing fibre afferents that together form discrete complexes (Apps & Hawkes, 2009). Longitudinal zones of different cerebellar regions seem to be important for distinct cerebellar functions. Modules in the paravermis are for example important for limb movements and spinal reflexes (Pijpers *et al.*, 2008) while modules in the flocculus control compensatory eye movements (Schonewille *et al.*, 2006). Longitudinal zones can be further subdivided in "microzones". Climbing fibres that convey signals from a similar receptive field of a certain part of the body innervate Purkinje cell groups that are located in a narrow stripe (100-300 um), termed microzone, within a broader longitudinal zone (1 mm). On the other hand, Purkinje cells of a microzone project to a small group of neurons in the DCN. These microzones seem to be the basic operational unit of the cerebellar cortex (Garwicz *et al.*, 1998; Apps & Hawkes, 2009). Mono climbing fibre innervation most likely is essential for proper establishment of such microzones as it assures that a Purkinje cell receives error signals by only one subgroup of olivary neurons. In case of multiple climbing fibre innervation, the setup of microzones may become impaired as certain Purkinje cells respond to not only one but several subgroups of olivary neurons. An impairment of these microzones diminishes the coherence of neural activity in the cerebellum, which ultimately may affect the motor control excerpted by this part of the brain.

Developmental climbing fibre elimination in raptor-knockout Purkinje cells was not defective, yet, we hypothesize that their altered inhibitory synaptic input is due to impaired postnatal GABAergic synaptogenesis. During postnatal Purkinje cell development the number of $GABA_A$ α1 clusters at the soma increases, which is paralleled by a reduction of the cluster size (Viltono *et al.*, 2008). The finding that the absolute number of $GABA_A$ α1 clusters at the soma of raptor-knockout Purkinje cells was reduced in 6-week-old mice, while their size was increased, indicated that the GABAergic synaptogenesis might be impaired. However, to further support this hypothesis, $GABA_A$ α1 clusters in younger mice have to be analysed to more closely monitor the development of GABAergic synapses of raptor-knockout Purkinje cells.

In contrary to mTORC1-deficient Purkinje cells, no alterations of $GABA_A$ α1 clusters could be detected for rictor-knockout Purkinje cells (personal communication with the Fritschy laboratory). Yet, a staining against the synapse adhesion molecule neuroligin 2 that is specific for GABAergic synapses and important for their formation (Varoqueaux *et al.*, 2004; Poulopoulos *et al.*, 2009) indicated that the size, but not number, of the neuroligin 2 clusters in the molecular layer of rictor Purkinje cell knockout mice was reduced (personal communication with the Fritschy laboratory). In line with these immunohistochemistry data, we observed a reduction of the strength, but not number, of functional inhibitory synapses of rictor-knockout Purkinje cells. Notably, reduced inhibitory synaptic transmission has also been reported for mice that have the postsynaptic neuroligin 2 protein

knocked out, underlining the importance of this protein for functional inhibitory synapses (Poulopoulos *et al.*, 2009). How mTORC2 connects to neurolign 2 needs to be further investigated.

The reduced strength of inhibitory synapses of rictor-knockout Purkinje cells detected by electrophysiological recordings might also be the consequence of impaired GABAergic synaptic plasticity. As described in section 3.4.5., the strength of inhibitory synapses can be augmented in Purkinje cells by a process called rebound potentiation. In mice that have the β2 subunit of $GABA_AR$ ablated rebound potentiation was absent (personal communication with the laboratory of Trevor Smart). Interestingly, this subunit is known to be phosphorylated by the mTORC2 downstream targets Akt (Wang *et al.*, 2003) and PKC (McDonald & Moss, 1997) and, hence, it is possible that ablation of mTORC2 in Purkinje cells impairs rebound potentiation and consequently reduces the strength of inhibitory synapses in these neurons. For example, phosphorylation of the β2 subunit by Akt is known to increase the number of $GABA_AR$ in the plasma membrane (Wang *et al.*, 2003). Therefore, it might be worth to analyse rebound potentiation in rictor-knockout Purkinje cells. Also in terms of cerebellar functions this might be interesting to investigate, since rebound potentiation has been shown to be relevant for motor behaviour (Tanaka *et al.*, 2013) that notably is altered in RIPuKO mice.

In summary, our electrophysiological and immunohistochemistry data point out that both mTORC1 and mTORC2 are important for inhibitory synapses, yet, in a different manner since different phenotypes were observed in these readouts for the RAPuKO and RIPuKO mice. Further experiments are needed to study more precisely how mTORC1 and mTORC2 contribute to different aspects, such as development and plasticity of inhibitory synapses in Purkinje cells. Because altered GABAergic functions are seen in different neurodevelopmental and psychiatric diseases like depression, schizophrenia, epilepsy and ASD (Fritschy & Panzanelli, 2014) that all share a link to mTOR signalling (see section 3.3.4), a better understanding of this pathway at GABAergic synapses may be very helpful and open new venues for a treatment of such disorders.

Probably the most striking difference between raptor and rictor-knockout Purkinje cells was that a knockout of first affected the survival while second did not. Raptor-knockout Purkinje cells survived at least up to a mouse age of 6 weeks but subsequently became apoptotic, which resulted in a progressive Purkinje cell loss. What may cause the death of raptor-knockout Purkinje cells? Apoptosis of raptor-knockout Purkinje cells was preceded by signs of neurodegeneration, such as swollen axons or dendritic beading (Yang *et al.*, 2013). The swollen axons accumulated neurofilaments, a phenomenon that is also observed with neurodegenerative diseases for example amyotrophic lateral sclerosis (ALS) (Al-Chalabi & Miller, 2003). In ALS it has been hypothesized that such neurofilament accumulations may play a pathological role by impairing the axonal transport, thereby causing a "strangulation" of the motorneurons (Julien, 2001). However, it is rather unlikely that impaired axonal transport causes apoptosis in Purkinje cells since these neurons survive up to a year upon axotomy (Dusart & Sotelo, 1994; Morel *et al.*, 2002).

It has recently been shown that Purkinje cells are vulnerable to impaired autophagy since a conditional knockout of the autophagy-related protein ATG7 in these neurons affects their survival (Komatsu *et al.*, 2007). Indications of aberrant autophagic flux in form of accumulated autophagic organelles are observed in Purkinje cells that have TSC1 knocked out (Di Nardo *et al.*, 2014). As mentioned above, TSC1-knockout Purkinje cells undergo apoptosis (Tsai *et al.*, 2012) and it is possible that impaired autophagy contributes to, or even causes, the death of these neurons. In line with the inhibitory effect of mTORC1 on the initiation of autophagy (see section 3.1.1.), autophagic flux is impaired in mice that have TSC1 conditionally knocked out in muscle tissue. Interestingly, a raptor knockout in the same tissue impairs autophagy as well (Castets *et al.*, 2013). Ablation of mTORC1 has been suggested to impair autophagy by disrupting the negative feedback loop on IRS1, which results in an increased activation of Akt. Increased Akt activity, in turn, seems to suppress expression of different genes involved in autophagy by augmenting inhibition on the transcription factors FoxO. Consequently, mTORC1 ablation in muscle impairs autophagic flux by downregulating genes important for autophagy, such as cathepsin L or beclin1 (Castets *et al.*, 2013). It is under current investigation how mTORC1 ablation affects autophagy in the brain, and in particular in Purkinje cells. If autophagic flux was impaired in raptor-knockout Purkinje cells, this might be a possible cause for their death.

Molecular. The distinct behavioural and cellular phenotypes of RAPuKO and RIPuKO mice fit with the model that mTORC1 and mTORC2 largely feed separate signalling pathways. Although the data presented in this study are of descriptive nature and do not allow causal links of cellular and/or behavioural phenotypes with molecular mechanisms, some phenotypes observed for raptor or rictor-knockout Purkinje cells may be associated with certain mTORC1 or mTORC2 downstream targets, respectively.

For example, the multiple climbing fibre innervation of rictor-knockout Purkinje cells most likely is the consequence of the concomitant strong PKCγ downregulation in these cells since a conventional knockout of PKCγ has been reported to result in similar climbing fibre elimination deficits of Purkinje cells (Kano *et al.*, 1995). Also the impaired dendritic self-avoidance of mTORC2-deficient Purkinje cells may depend on disturbed PKC signalling in these neurons since a Purkinje cell-specific knockout of γ-protocadherins, a class of proteins that act via PKC as well, results in a similar phenotype (Garrett *et al.*, 2012; Lefebvre *et al.*, 2012). In contrast, PF-Purkinje cell synapse LTD a phenomenon that also depends on PKC, in particular PKCα (De Zeeuw *et al.*, 1998; Saito & Shirai, 2002; Leitges *et al.*, 2004), was not affected by the rictor knockout. Given the striking effect of whole brain mTORC2 ablation on the protein levels of all classical PKCs, this was an unexpected finding. However, currently we do not know how mTORC2 ablation in Purkinje cells affects other PKC isoforms than PKCγ, such as PKCα. Moreover, it is possible that PKC isoforms compensate for the loss of each other regarding certain functions. Purkinje cells express mainly the PKC isoforms γ

and δ (Barmack *et al.*, 2000). The protein level of last has recently been found to be only mildly reduced (21%) in mTORC2-deficient brains (data not shown). Hence, PKCδ might be a candidate to compensate for a possible loss of other isoforms in Purkinje cells and consequently enable a normal LTD in rictor-knockout Purkinje cells.

Whole brain rictor knockout also affected the mTORC2 downstream target Akt by decreasing its phosphorylation at Ser473 and Thr308 strongly or moderately, respectively. Yet, the consequences for the Akt downstream signalling did not seem to be very strong since no changes in phosphorylation of GSK3β and FoxO1 could be detected in these mice. On the other hand, the effect of mTORC2 ablation in brain on the PKC branch seemed to be more pronounced as the phosphorylation of the PKC downstream targets GAP-43 and MARCKS were significantly reduced.

In agreement with the notion of distinct signalling of mTORC1 and mTORC2, raptor-knockout Purkinje cells did not show obvious alterations of PKCγ levels (Fig. 5H of publication 2). Moreover, raptor knockout in neural progenitors resulted in an increased phosphorylation of Akt due to disruption of the negative feedback loop on IRS1 (Cloetta *et al.*, 2013), while Akt phosphorylation was decreased in the corresponding rictor-knockout mice as described above. In raptor, but not rictor-knockout brains, alterations in Akt downstream signalling were observed in form of an increased phosphorylation of GSK3α/β at Ser21/9 and FoxO3a at Thr32 (data for last is not shown). Phosphorylation of GSK3 at these residues inhibits GSK3 activity (Cross *et al.*, 1995). Although the phosphorylation state of GSK3 has not yet been analysed in raptor-knockout Purkinje cells, we speculate that some of the observed phenotypes seen with these knockout Purkinje cells may depend on increased inhibition of GSK3. Aberrant GSK3 signalling may contribute to the neurofilament accumulation in axonal swellings that were found proximal to raptor-knockout Purkinje cell somata, possibly by deregulating the axonal transport of neurofilaments (Bajaj & Miller, 1997; Holmgren *et al.*, 2012). Also the multiple primary dendrites of raptor-knockout Purkinje cells may depend on increased inhibition of GSK3, given the role of this kinase in neuronal polarization (Hur & Zhou, 2010). Moreover, it is possible that aberrant GSK3 signalling may contribute to the increased $GABA_A$ α1 cluster size at the somata of raptor-knockout Purkinje cells. As described above, the cluster size of $GABA_A$ α1 at the Purkinje cell soma is reduced in course of the postnatal development of these neurons. This process coincides with the loss of gephyrin from the soma (Viltono *et al.*, 2008). Gephyrin is a scaffolding protein at inhibitory synapses where it anchors and thereby clusters glycine receptors (GlyR) and $GABA_AR$ (Essrich *et al.*, 1998; Feng *et al.*, 1998; Fritschy *et al.*, 2008; Tyagarajan & Fritschy, 2014). Postsynaptic clustering of gephyrin, in turn, is mainly regulated via phosphorylation of this protein (Tyagarajan & Fritschy, 2014). Gephyrin is phosphorylated by GSK3β at residue Ser270 and a mutation at this site from serine to alanine, which prevents phosphorylation, causes supernumary gephyrin clusters. Similarly, increased gephyrin clustering is seen *in vitro* and *in vivo* upon exposure to lithium chloride that is an inhibitor of GSK3β (Tyagarajan *et al.*, 2011). Because raptor knockout in brain resulted in an increased GSK3 inhibition, we hypothesized that in

raptor-knockout neurons gephyrin clustering might be increased as well. Indeed, preliminary data of the laboratory of Jean-Marc Fritschy indicated that gephyrin clusters were still present at the soma of post developmental raptor-knockout Purkinje cells while they were mostly absent at the soma of control Purkinje cells (personal communication with the Fritschy laboratory). On the one hand, this preliminary finding supports the notion of a developmental deficit of GABAergic synaptogenesis upon raptor ablation in Purkinje cells. On the other hand, it offers a hint how raptor knockout might impair GABAergic synaptogenesis of these neurons. The current hypothesis is that the increased inhibition of GSK3 upon mTORC1 ablation prevents the developmental loss of gephyrin clusters from the Purkinje cell soma by promoting gephyrin clustering. The defective elimination of gephyrin clusters from the soma, in turn, may affect the clustering of $GABA_AR$ and cause the increased $GABA_A$ $\alpha 1$ cluster size that is seen at the soma of raptor-knockout Purkinje cells.

7. References

Aiba, A., Kano, M., Chen, C., Stanton, M.E., Fox, G.D., Herrup, K., Zwingman, T.A. & Tonegawa, S. (1994) Deficient cerebellar long-term depression and impaired motor learning in mGluR1 mutant mice. *Cell*, **79**, 377-388.

Al-Chalabi, A. & Miller, C.C. (2003) Neurofilaments and neurological disease. *Bioessays*, **25**, 346-355.

Albus, J.S. (1971) A theory of cerebellar function *Math. Biosci.*, **10**, 25–61.

Alessi, D.R., Andjelkovic, M., Caudwell, B., Cron, P., Morrice, N., Cohen, P. & Hemmings, B.A. (1996) Mechanism of activation of protein kinase B by insulin and IGF-1. *Embo J*, **15**, 6541-6551.

Alessi, D.R., James, S.R., Downes, C.P., Holmes, A.B., Gaffney, P.R., Reese, C.B. & Cohen, P. (1997) Characterization of a 3-phosphoinositide-dependent protein kinase which phosphorylates and activates protein kinase Balpha. *Curr Biol*, **7**, 261-269.

Allen, G., Muller, R.A. & Courchesne, E. (2004) Cerebellar function in autism: functional magnetic resonance image activation during a simple motor task. *Biol Psychiatry*, **56**, 269-278.

Allen, G.I. & Tsukahara, N. (1974) Cerebrocerebellar communication systems. *Physiol Rev*, **54**, 957-1006.

Altman, J. (1972) Postnatal development of the cerebellar cortex in the rat. II. Phases in the maturation of Purkinje cells and of the molecular layer. *J Comp Neurol*, **145**, 399-463.

An, W.L., Cowburn, R.F., Li, L., Braak, H., Alafuzoff, I., Iqbal, K., Iqbal, I.G., Winblad, B. & Pei, J.J. (2003) Up-regulation of phosphorylated/activated p70 S6 kinase and its relationship to neurofibrillary pathology in Alzheimer's disease. *Am J Pathol*, **163**, 591-607.

Anderl, S., Freeland, M., Kwiatkowski, D.J. & Goto, J. (2011) Therapeutic value of prenatal rapamycin treatment in a mouse brain model of tuberous sclerosis complex. *Hum Mol Genet*, **20**, 4597-4604.

Andreasen, N.C. & Pierson, R. (2008) The role of the cerebellum in schizophrenia. *Biol Psychiatry*, **64**, 81-88.

Apps, R. & Hawkes, R. (2009) Cerebellar cortical organization: a one-map hypothesis. *Nat Rev Neurosci*, **10**, 670-681.

Asano, E., Chugani, D.C., Muzik, O., Behen, M., Janisse, J., Rothermel, R., Mangner, T.J., Chakraborty, P.K. & Chugani, H.T. (2001) Autism in tuberous sclerosis complex is related to both cortical and subcortical dysfunction. *Neurology*, **57**, 1269-1277.

Bajaj, N.P. & Miller, C.C. (1997) Phosphorylation of neurofilament heavy-chain side-arm fragments by cyclin-dependent kinase-5 and glycogen synthase kinase-3alpha in transfected cells. *J Neurochem*, **69**, 737-743.

Banko, J.L., Hou, L., Poulin, F., Sonenberg, N. & Klann, E. (2006) Regulation of eukaryotic initiation factor 4E by converging signaling pathways during metabotropic glutamate receptor-dependent long-term depression. *J Neurosci*, **26**, 2167-2173.

Banko, J.L., Poulin, F., Hou, L.F., DeMaria, C.T., Sonenberg, N. & Klann, E. (2005) The translation repressor 4E-BP2 is critical for eIF4F complex formation, synaptic plasticity, and memory in the hippocampus. *Journal of Neuroscience*, **25**, 9581-9590.

Bar-Peled, L., Schweitzer, L.D., Zoncu, R. & Sabatini, D.M. (2012) Ragulator is a GEF for the rag GTPases that signal amino acid levels to mTORC1. *Cell*, **150**, 1196-1208.

Barmack, N.H., Qian, Z. & Yoshimura, J. (2000) Regional and cellular distribution of protein kinase C in rat cerebellar Purkinje cells. *J Comp Neurol*, **427**, 235-254.

Bateup, H.S., Johnson, C.A., Denefrio, C.L., Saulnier, J.L., Kornacker, K. & Sabatini, B.L. (2013) Excitatory/inhibitory synaptic imbalance leads to hippocampal hyperexcitability in mouse models of tuberous sclerosis. *Neuron*, **78**, 510-522.

Bauman, M.L. & Kemper, T.L. (2005) Neuroanatomic observations of the brain in autism: a review and future directions. *Int J Dev Neurosci*, **23**, 183-187.

Bear, M.F., Huber, K.M. & Warren, S.T. (2004) The mGluR theory of fragile X mental retardation. *Trends Neurosci*, **27**, 370-377.

Belmeguenai, A. & Hansel, C. (2005) A role for protein phosphatases 1, 2A, and 2B in cerebellar long-term potentiation. *J Neurosci*, **25**, 10768-10772.

Ben Sahra, I., Regazzetti, C., Robert, G., Laurent, K., Le Marchand-Brustel, Y., Auberger, P., Tanti, J.F., Giorgetti-Peraldi, S. & Bost, F. (2011) Metformin, independent of AMPK, induces mTOR inhibition and cell-cycle arrest through REDD1. *Cancer Res*, **71**, 4366-4372.

Benilova, I., Karran, E. & De Strooper, B. (2012) The toxic Abeta oligomer and Alzheimer's disease: an emperor in need of clothes. *Nat Neurosci*, **15**, 349-357.

Bentzinger, C.F., Romanino, K., Cloetta, D., Lin, S., Mascarenhas, J.B., Oliveri, F., Xia, J., Casanova, E., Costa, C.F., Brink, M., Zorzato, F., Hall, M.N. & Ruegg, M.A. (2008) Skeletal muscle-specific ablation of raptor, but not of rictor, causes metabolic changes and results in muscle dystrophy. *Cell Metab*, **8**, 411-424.

Berman, R.M., Cappiello, A., Anand, A., Oren, D.A., Heninger, G.R., Charney, D.S. & Krystal, J.H. (2000) Antidepressant effects of ketamine in depressed patients. *Biol Psychiatry*, **47**, 351-354.

Betz, C., Stracka, D., Prescianotto-Baschong, C., Frieden, M., Demaurex, N. & Hall, M.N. (2013) Feature Article: mTOR complex 2-Akt signaling at mitochondria-associated endoplasmic reticulum membranes (MAM) regulates mitochondrial physiology. *Proc Natl Acad Sci U S A*, **110**, 12526-12534.

Bonni, A., Sun, Y., Nadal-Vicens, M., Bhatt, A., Frank, D.A., Rozovsky, I., Stahl, N., Yancopoulos, G.D. & Greenberg, M.E. (1997) Regulation of gliogenesis in the central nervous system by the JAK-STAT signaling pathway. *Science*, **278**, 477-483.

Boulbes, D., Chen, C.H., Shaikenov, T., Agarwal, N.K., Peterson, T.R., Addona, T.A., Keshishian, H., Carr, S.A., Magnuson, M.A., Sabatini, D.M. & Sarbassov dos, D. (2010) Rictor phosphorylation on the Thr-1135 site does not require mammalian target of rapamycin complex 2. *Mol Cancer Res*, **8**, 896-906.

Bourgeron, T. (2009) A synaptic trek to autism. *Curr Opin Neurobiol*, **19**, 231-234.

Bourne, J.N., Sorra, K.E., Hurlburt, J. & Harris, K.M. (2007) Polyribosomes are increased in spines of CA1 dendrites 2 h after the induction of LTP in mature rat hippocampal slices. *Hippocampus*, **17**, 1-4.

Brochu, G., Maler, L. & Hawkes, R. (1990) Zebrin II: a polypeptide antigen expressed selectively by Purkinje cells reveals compartments in rat and fish cerebellum. *J Comp Neurol*, **291**, 538-552.

Brown, E.J., Albers, M.W., Shin, T.B., Ichikawa, K., Keith, C.T., Lane, W.S. & Schreiber, S.L. (1994) A mammalian protein targeted by G1-arresting rapamycin-receptor complex. *Nature*, **369**, 756-758.

Brown, V., Jin, P., Ceman, S., Darnell, J.C., O'Donnell, W.T., Tenenbaum, S.A., Jin, X., Feng, Y., Wilkinson, K.D., Keene, J.D., Darnell, R.B. & Warren, S.T. (2001) Microarray identification of FMRP-associated brain mRNAs and altered mRNA translational profiles in fragile X syndrome. *Cell*, **107**, 477-487.

Brugarolas, J., Lei, K., Hurley, R.L., Manning, B.D., Reiling, J.H., Hafen, E., Witters, L.A., Ellisen, L.W. & Kaelin, W.G., Jr. (2004) Regulation of mTOR function in response to hypoxia by REDD1 and the TSC1/TSC2 tumor suppressor complex. *Genes Dev*, **18**, 2893-2904.

Budanov, A.V. & Karin, M. (2008) p53 target genes sestrin1 and sestrin2 connect genotoxic stress and mTOR signaling. *Cell*, **134**, 451-460.

Burright, E.N., Clark, H.B., Servadio, A., Matilla, T., Feddersen, R.M., Yunis, W.S., Duvick, L.A., Zoghbi, H.Y. & Orr, H.T. (1995) SCA1 transgenic mice: a model for neurodegeneration caused by an expanded CAG trinucleotide repeat. *Cell*, **82**, 937-948.

Butts, T., Chaplin, N. & Wingate, R.J. (2011) Can clues from evolution unlock the molecular development of the cerebellum? *Mol Neurobiol*, **43**, 67-76.

Cammalleri, M., Lutjens, R., Berton, F., King, A.R., Simpson, C., Francesconi, W. & Sanna, P.P. (2003) Time-restricted role for dendritic activation of the mTOR-p70S6K pathway in the induction of late-phase long-term potentiation in the CA1. *Proc Natl Acad Sci U S A*, **100**, 14368-14373.

Campbell, D.S. & Holt, C.E. (2001) Chemotropic responses of retinal growth cones mediated by rapid local protein synthesis and degradation. *Neuron*, **32**, 1013-1026.

Carriere, A., Cargnello, M., Julien, L.A., Gao, H., Bonneil, E., Thibault, P. & Roux, P.P. (2008) Oncogenic MAPK signaling stimulates mTORC1 activity by promoting RSK-mediated raptor phosphorylation. *Curr Biol*, **18**, 1269-1277.

Carriere, A., Romeo, Y., Acosta-Jaquez, H.A., Moreau, J., Bonneil, E., Thibault, P., Fingar, D.C. & Roux, P.P. (2011) ERK1/2 phosphorylate Raptor to promote Ras-dependent activation of mTOR complex 1 (mTORC1). *J Biol Chem*, **286**, 567-577.

Carrillo, J., Nishiyama, N. & Nishiyama, H. (2013) Dendritic translocation establishes the winner in cerebellar climbing fiber synapse elimination. *J Neurosci*, **33**, 7641-7653.

Carson, R.P., Fu, C., Winzenburger, P. & Ess, K.C. (2013) Deletion of Rictor in neural progenitor cells reveals contributions of mTORC2 signaling to tuberous sclerosis complex. *Hum Mol Genet*, **22**, 140-152.

Carson, R.P., Van Nielen, D.L., Winzenburger, P.A. & Ess, K.C. (2012) Neuronal and glia abnormalities in Tsc1-deficient forebrain and partial rescue by rapamycin. *Neurobiol Dis*, **45**, 369-380.

Castets, P., Lin, S., Rion, N., Di Fulvio, S., Romanino, K., Guridi, M., Frank, S., Tintignac, L.A., Sinnreich, M. & Ruegg, M.A. (2013) Sustained activation of mTORC1 in skeletal muscle inhibits constitutive and starvation-induced autophagy and causes a severe, late-onset myopathy. *Cell Metab*, **17**, 731-744.

Chauvin, C., Koka, V., Nouschi, A., Mieulet, V., Hoareau-Aveilla, C., Dreazen, A., Cagnard, N., Carpentier, W., Kiss, T., Meyuhas, O. & Pende, M. (2014) Ribosomal protein S6 kinase activity controls the ribosome biogenesis transcriptional program. *Oncogene*, **33**, 474-483.

Chedotal, A. & Sotelo, C. (1993) The 'creeper stage' in cerebellar climbing fiber synaptogenesis precedes the 'pericellular nest'--ultrastructural evidence with parvalbumin immunocytochemistry. *Brain Res Dev Brain Res*, **76**, 207-220.

Chen, C., Kano, M., Abeliovich, A., Chen, L., Bao, S., Kim, J.J., Hashimoto, K., Thompson, R.F. & Tonegawa, S. (1995) Impaired motor coordination correlates with persistent multiple climbing fiber innervation in PKC gamma mutant mice. *Cell*, **83**, 1233-1242.

Chevere-Torres, I., Maki, J.M., Santini, E. & Klann, E. (2012) Impaired social interactions and motor learning skills in tuberous sclerosis complex model mice expressing a dominant/negative form of tuberin. *Neurobiol Dis*, **45**, 156-164.

Chiu, M.I., Katz, H. & Berlin, V. (1994) RAPT1, a mammalian homolog of yeast Tor, interacts with the FKBP12/rapamycin complex. *Proc Natl Acad Sci U S A*, **91**, 12574-12578.

Chung, H.J., Steinberg, J.P., Huganir, R.L. & Linden, D.J. (2003) Requirement of AMPA receptor GluR2 phosphorylation for cerebellar long-term depression. *Science*, **300**, 1751-1755.

Cloetta, D., Thomanetz, V., Baranek, C., Lustenberger, R.M., Lin, S., Oliveri, F., Atanasoski, S. & Ruegg, M.A. (2013) Inactivation of mTORC1 in the developing brain causes microcephaly and affects gliogenesis. *J Neurosci*, **33**, 7799-7810.

Coesmans, M., Weber, J.T., De Zeeuw, C.I. & Hansel, C. (2004) Bidirectional parallel fiber plasticity in the cerebellum under climbing fiber control. *Neuron*, **44**, 691-700.

Cohen, D. & Yarom, Y. (2000) Cerebellar on-beam and lateral inhibition: two functionally distinct circuits. *J Neurophysiol*, **83**, 1932-1940.

Collingridge, G.L., Peineau, S., Howland, J.G. & Wang, Y.T. (2010) Long-term depression in the CNS. *Nat Rev Neurosci*, **11**, 459-473.

Costa-Mattioli, M., Sossin, W.S., Klann, E. & Sonenberg, N. (2009) Translational control of long-lasting synaptic plasticity and memory. *Neuron*, **61**, 10-26.

Crepel, F. (1971) Maturation of climbing fiber responses in the rat. *Brain Res*, **35**, 272-276.

Crepel, F., Delhaye-Bouchaud, N. & Dupont, J.L. (1981) Fate of the multiple innervation of cerebellar Purkinje cells by climbing fibers in immature control, x-irradiated and hypothyroid rats. *Brain Res*, **227**, 59-71.

Crepel, F., Mariani, J. & Delhaye-Bouchaud, N. (1976) Evidence for a multiple innervation of Purkinje cells by climbing fibers in the immature rat cerebellum. *J Neurobiol*, **7**, 567-578.

Cross, D.A., Alessi, D.R., Cohen, P., Andjelkovich, M. & Hemmings, B.A. (1995) Inhibition of glycogen synthase kinase-3 by insulin mediated by protein kinase B. *Nature*, **378**, 785-789.

Csordas, G., Thomas, A.P. & Hajnoczky, G. (1999) Quasi-synaptic calcium signal transmission between endoplasmic reticulum and mitochondria. *Embo J*, **18**, 96-108.

Cunningham, J.T., Rodgers, J.T., Arlow, D.H., Vazquez, F., Mootha, V.K. & Puigserver, P. (2007) mTOR controls mitochondrial oxidative function through a YY1-PGC-1alpha transcriptional complex. *Nature*, **450**, 736-740.

Curatolo, P., Bombardieri, R. & Jozwiak, S. (2008) Tuberous sclerosis. *Lancet*, **372**, 657-668.

Cybulski, N. & Hall, M.N. (2009) TOR complex 2: a signaling pathway of its own. *Trends Biochem Sci*, **34**, 620-627.

Cybulski, N., Polak, P., Auwerx, J., Ruegg, M.A. & Hall, M.N. (2009) mTOR complex 2 in adipose tissue negatively controls whole-body growth. *Proc Natl Acad Sci U S A*, **106**, 9902-9907.

D'Angelo, E., Solinas, S., Mapelli, J., Gandolfi, D., Mapelli, L. & Prestori, F. (2013) The cerebellar Golgi cell and spatiotemporal organization of granular layer activity. *Front Neural Circuits*, **7**, 93.

D'Hooge, R., Nagels, G., Franck, F., Bakker, C.E., Reyniers, E., Storm, K., Kooy, R.F., Oostra, B.A., Willems, P.J. & De Deyn, P.P. (1997) Mildly impaired water maze performance in male Fmr1 knockout mice. *Neuroscience*, **76**, 367-376.

Dangelmaier, C., Manne, B.K., Liverani, E., Jin, J., Bray, P. & Kunapuli, S.P. (2014) PDK1 selectively phosphorylates Thr(308) on Akt and contributes to human platelet functional responses. *Thromb Haemost*, **111**, 508-517.

Davidkova, G. & Carroll, R.C. (2007) Characterization of the role of microtubule-associated protein 1B in metabotropic glutamate receptor-mediated endocytosis of AMPA receptors in hippocampus. *J Neurosci*, **27**, 13273-13278.

Davies, S.W., Turmaine, M., Cozens, B.A., DiFiglia, M., Sharp, A.H., Ross, C.A., Scherzinger, E., Wanker, E.E., Mangiarini, L. & Bates, G.P. (1997) Formation of neuronal intranuclear inclusions underlies the neurological dysfunction in mice transgenic for the HD mutation. *Cell*, **90**, 537-548.

Davis, K.L., Kahn, R.S., Ko, G. & Davidson, M. (1991) Dopamine in schizophrenia: a review and reconceptualization. *Am J Psychiatry*, **148**, 1474-1486.

Dazert, E. & Hall, M.N. (2011) mTOR signaling in disease. *Curr Opin Cell Biol*, **23**, 744-755.

De Zeeuw, C.I., Hansel, C., Bian, F., Koekkoek, S.K., van Alphen, A.M., Linden, D.J. & Oberdick, J. (1998) Expression of a protein kinase C inhibitor in Purkinje cells blocks cerebellar LTD and adaptation of the vestibulo-ocular reflex. *Neuron*, **20**, 495-508.

Debonneville, C., Flores, S.Y., Kamynina, E., Plant, P.J., Tauxe, C., Thomas, M.A., Munster, C., Chraibi, A., Pratt, J.H., Horisberger, J.D., Pearce, D., Loffing, J. & Staub, O. (2001) Phosphorylation of Nedd4-2 by Sgk1 regulates epithelial Na(+) channel cell surface expression. *Embo J*, **20**, 7052-7059.

Demirkan, G., Yu, K., Boylan, J.M., Salomon, A.R. & Gruppuso, P.A. (2011) Phosphoproteomic profiling of in vivo signaling in liver by the mammalian target of rapamycin complex 1 (mTORC1). *PLoS One*, **6**, e21729.

DeYoung, M.P., Horak, P., Sofer, A., Sgroi, D. & Ellisen, L.W. (2008) Hypoxia regulates TSC1/2-mTOR signaling and tumor suppression through REDD1-mediated 14-3-3 shuttling. *Genes Dev*, **22**, 239-251.

Di Nardo, A., Wertz, M.H., Kwiatkowski, E., Tsai, P.T., Leech, J.D., Greene-Colozzi, E., Goto, J., Dilsiz, P., Talos, D.M., Clish, C.B., Kwiatkowski, D.J. & Sahin, M. (2014) Neuronal Tsc1/2 complex controls autophagy through AMPK-dependent regulation of ULK1. *Hum Mol Genet*, **23**, 3865-3874.

Dibble, C.C., Asara, J.M. & Manning, B.D. (2009) Characterization of Rictor phosphorylation sites reveals direct regulation of mTOR complex 2 by S6K1. *Mol Cell Biol*, **29**, 5657-5670.

Dibble, C.C., Elis, W., Menon, S., Qin, W., Klekota, J., Asara, J.M., Finan, P.M., Kwiatkowski, D.J., Murphy, L.O. & Manning, B.D. (2012) TBC1D7 is a third subunit of the TSC1-TSC2 complex upstream of mTORC1. *Mol Cell*, **47**, 535-546.

Dibble, C.C. & Manning, B.D. (2013) Signal integration by mTORC1 coordinates nutrient input with biosynthetic output. *Nat Cell Biol*, **15**, 555-564.

Dougherty, S.E., Reeves, J.L., Lesort, M., Detloff, P.J. & Cowell, R.M. (2013) Purkinje cell dysfunction and loss in a knock-in mouse model of Huntington disease. *Exp Neurol*, **240**, 96-102.

Dunlop, E.A. & Tee, A.R. (2014) mTOR and autophagy: A dynamic relationship governed by nutrients and energy. *Semin Cell Dev Biol*.

Durr, A. (2010) Autosomal dominant cerebellar ataxias: polyglutamine expansions and beyond. *Lancet Neurol*, **9**, 885-894.

Dusart, I. & Sotelo, C. (1994) Lack of Purkinje cell loss in adult rat cerebellum following protracted axotomy: degenerative changes and regenerative attempts of the severed axons. *J Comp Neurol*, **347**, 211-232.

Duvel, K., Yecies, J.L., Menon, S., Raman, P., Lipovsky, A.I., Souza, A.L., Triantafellow, E., Ma, Q., Gorski, R., Cleaver, S., Vander Heiden, M.G., MacKeigan, J.P., Finan, P.M., Clish, C.B., Murphy, L.O. & Manning, B.D. (2010) Activation of a metabolic gene regulatory network downstream of mTOR complex 1. *Mol Cell*, **39**, 171-183.

Edwards, M.A., Yamamoto, M. & Caviness, V.S., Jr. (1990) Organization of radial glia and related cells in the developing murine CNS. An analysis based upon a new monoclonal antibody marker. *Neuroscience*, **36**, 121-144.

Ellisen, L.W., Ramsayer, K.D., Johannessen, C.M., Yang, A., Beppu, H., Minda, K., Oliner, J.D., McKeon, F. & Haber, D.A. (2002) REDD1, a developmentally regulated transcriptional target of p63 and p53, links p63 to regulation of reactive oxygen species. *Mol Cell*, **10**, 995-1005.

Eluvathingal, T.J., Behen, M.E., Chugani, H.T., Janisse, J., Bernardi, B., Chakraborty, P., Juhasz, C., Muzik, O. & Chugani, D.C. (2006) Cerebellar lesions in tuberous sclerosis complex: neurobehavioral and neuroimaging correlates. *J Child Neurol*, **21**, 846-851.

Emamian, E.S., Hall, D., Birnbaum, M.J., Karayiorgou, M. & Gogos, J.A. (2004) Convergent evidence for impaired AKT1-GSK3beta signaling in schizophrenia. *Nat Genet*, **36**, 131-137.

Ertan, G., Arulrajah, S., Tekes, A., Jordan, L. & Huisman, T.A. (2010) Cerebellar abnormality in children and young adults with tuberous sclerosis complex: MR and diffusion weighted imaging findings. *J Neuroradiol*, **37**, 231-238.

Essrich, C., Lorez, M., Benson, J.A., Fritschy, J.M. & Luscher, B. (1998) Postsynaptic clustering of major GABAA receptor subtypes requires the gamma 2 subunit and gephyrin. *Nat Neurosci*, **1**, 563-571.

Euler, P., Friedrich, B., Ziegler, R., Kuhn, A., Lindenberg, K.S., Weiller, C. & Zucker, B. (2012) Gene expression analysis on a single cell level in Purkinje cells of Huntington's disease transgenic mice. *Neurosci Lett*, **517**, 7-12.

Everitt, A.B., Luu, T., Cromer, B., Tierney, M.L., Birnir, B., Olsen, R.W. & Gage, P.W. (2004) Conductance of recombinant GABA (A) channels is increased in cells co-expressing GABA(A) receptor-associated protein. *J Biol Chem*, **279**, 21701-21706.

Facchinetti, V., Ouyang, W., Wei, H., Soto, N., Lazorchak, A., Gould, C., Lowry, C., Newton, A.C., Mao, Y., Miao, R.Q., Sessa, W.C., Qin, J., Zhang, P., Su, B. & Jacinto, E. (2008) The mammalian target of rapamycin complex 2 controls folding and stability of Akt and protein kinase C. *Embo J*, **27**, 1932-1943.

Fang, Y., Vilella-Bach, M., Bachmann, R., Flanigan, A. & Chen, J. (2001) Phosphatidic acid-mediated mitogenic activation of mTOR signaling. *Science*, **294**, 1942-1945.

Fanous, A.H. & Kendler, K.S. (2008) Genetics of clinical features and subtypes of schizophrenia: a review of the recent literature. *Curr Psychiatry Rep*, **10**, 164-170.

Fatemi, S.H., Aldinger, K.A., Ashwood, P., Bauman, M.L., Blaha, C.D., Blatt, G.J., Chauhan, A., Chauhan, V., Dager, S.R., Dickson, P.E., Estes, A.M., Goldowitz, D., Heck, D.H., Kemper, T.L., King, B.H., Martin, L.A., Millen, K.J., Mittleman, G., Mosconi, M.W., Persico, A.M., Sweeney, J.A., Webb, S.J. & Welsh, J.P. (2012) Consensus paper: pathological role of the cerebellum in autism. *Cerebellum*, **11**, 777-807.

Feng, G., Tintrup, H., Kirsch, J., Nichol, M.C., Kuhse, J., Betz, H. & Sanes, J.R. (1998) Dual requirement for gephyrin in glycine receptor clustering and molybdoenzyme activity. *Science*, **282**, 1321-1324.

Fetz, E.E. (1993) Cortical mechanisms controlling limb movement. *Curr Opin Neurobiol*, **3**, 932-939.

Finch, E.A. & Augustine, G.J. (1998) Local calcium signalling by inositol-1,4,5-trisphosphate in Purkinje cell dendrites. *Nature*, **396**, 753-756.

Fresno Vara, J.A., Casado, E., de Castro, J., Cejas, P., Belda-Iniesta, C. & Gonzalez-Baron, M. (2004) PI3K/Akt signalling pathway and cancer. *Cancer Treat Rev*, **30**, 193-204.

Fritschy, J.M., Harvey, R.J. & Schwarz, G. (2008) Gephyrin: where do we stand, where do we go? *Trends Neurosci*, **31**, 257-264.

Fritschy, J.M. & Panzanelli, P. (2014) GABAA receptors and plasticity of inhibitory neurotransmission in the central nervous system. *Eur J Neurosci*, **39**, 1845-1865.

Fujita, S. (1967) Quantitative analysis of cell proliferation and differentiation in the cortex of the postnatal mouse cerebellum. *J Cell Biol*, **32**, 277-287.

Garcia-Martinez, J.M. & Alessi, D.R. (2008) mTOR complex 2 (mTORC2) controls hydrophobic motif phosphorylation and activation of serum- and glucocorticoid-induced protein kinase 1 (SGK1). *Biochem J*, **416**, 375-385.

Garrett, A.M., Schreiner, D., Lobas, M.A. & Weiner, J.A. (2012) gamma-protocadherins control cortical dendrite arborization by regulating the activity of a FAK/PKC/MARCKS signaling pathway. *Neuron*, **74**, 269-276.

Garwicz, M., Ekerot, C.F. & Jorntell, H. (1998) Organizational Principles of Cerebellar Neuronal Circuitry. *News Physiol Sci*, **13**, 26-32.

Gibson, D.A., Tymanskyj, S., Yuan, R.C., Leung, H.C., Lefebvre, J.L., Sanes, J.R., Chedotal, A. & Ma, L. (2014) Dendrite self-avoidance requires cell-autonomous slit/robo signaling in cerebellar purkinje cells. *Neuron*, **81**, 1040-1056.

Gkogkas, C.G., Khoutorsky, A., Ran, I., Rampakakis, E., Nevarko, T., Weatherill, D.B., Vasuta, C., Yee, S., Truitt, M., Dallaire, P., Major, F., Lasko, P., Ruggero, D., Nader, K., Lacaille, J.C. & Sonenberg, N. (2013) Autism-related deficits via dysregulated eIF4E-dependent translational control. *Nature*, **493**, 371-377.

Glickstein, M. & Yeo, C. (1990) The cerebellum and motor learning. *J Cogn Neurosci*, **2**, 69-80.

Godel, M., Hartleben, B., Herbach, N., Liu, S., Zschiedrich, S., Lu, S., Debreczeni-Mor, A., Lindenmeyer, M.T., Rastaldi, M.P., Hartleben, G., Wiech, T., Fornoni, A., Nelson, R.G., Kretzler, M., Wanke, R., Pavenstadt, H., Kerjaschki, D., Cohen, C.D., Hall, M.N., Ruegg, M.A., Inoki, K., Walz, G. & Huber, T.B. (2011) Role of mTOR in podocyte function and diabetic nephropathy in humans and mice. *J Clin Invest*, **121**, 2197-2209.

Goorden, S.M., van Woerden, G.M., van der Weerd, L., Cheadle, J.P. & Elgersma, Y. (2007) Cognitive deficits in Tsc1+/- mice in the absence of cerebral lesions and seizures. *Ann Neurol*, **62**, 648-655.

Graber, T.E., McCamphill, P.K. & Sossin, W.S. (2013) A recollection of mTOR signaling in learning and memory. *Learn Mem*, **20**, 518-530.

Green, D.R. & Levine, B. (2014) To be or not to be? How selective autophagy and cell death govern cell fate. *Cell*, **157**, 65-75.

Griffin, R.J., Moloney, A., Kelliher, M., Johnston, J.A., Ravid, R., Dockery, P., O'Connor, R. & O'Neill, C. (2005) Activation of Akt/PKB, increased phosphorylation of Akt substrates and loss and altered distribution of Akt and PTEN are features of Alzheimer's disease pathology. *J Neurochem*, **93**, 105-117.

Griner, E.M. & Kazanietz, M.G. (2007) Protein kinase C and other diacylglycerol effectors in cancer. *Nat Rev Cancer*, **7**, 281-294.

Grueber, W.B. & Sagasti, A. (2010) Self-avoidance and tiling: Mechanisms of dendrite and axon spacing. *Cold Spring Harb Perspect Biol*, **2**, a001750.

Guertin, D.A., Stevens, D.M., Saitoh, M., Kinkel, S., Crosby, K., Sheen, J.H., Mullholland, D.J., Magnuson, M.A., Wu, H. & Sabatini, D.M. (2009) mTOR complex 2 is required for the development of prostate cancer induced by Pten loss in mice. *Cancer Cell*, **15**, 148-159.

Guertin, D.A., Stevens, D.M., Thoreen, C.C., Burds, A.A., Kalaany, N.Y., Moffat, J., Brown, M., Fitzgerald, K.J. & Sabatini, D.M. (2006) Ablation in mice of the mTORC components raptor, rictor, or mLST8 reveals that mTORC2 is required for signaling to Akt-FOXO and PKCalpha, but not S6K1. *Dev Cell*, **11**, 859-871.

Gwinn, D.M., Shackelford, D.B., Egan, D.F., Mihaylova, M.M., Mery, A., Vasquez, D.S., Turk, B.E. & Shaw, R.J. (2008) AMPK phosphorylation of raptor mediates a metabolic checkpoint. *Mol Cell*, **30**, 214-226.

Hagiwara, A., Cornu, M., Cybulski, N., Polak, P., Betz, C., Trapani, F., Terracciano, L., Heim, M.H., Ruegg, M.A. & Hall, M.N. (2012) Hepatic mTORC2 activates glycolysis and lipogenesis through Akt, glucokinase, and SREBP1c. *Cell Metab*, **15**, 725-738.

Hall, D.A. & O'Keefe J, A. (2012) Fragile x-associated tremor ataxia syndrome: the expanding clinical picture, pathophysiology, epidemiology, and update on treatment. *Tremor Other Hyperkinet Mov (N Y)*, **2**.

Hallett, M. (2009) Dystonia: a sensory and motor disorder of short latency inhibition. *Ann Neurol*, **66**, 125-127.

Hamilton, B.A., Frankel, W.N., Kerrebrock, A.W., Hawkins, T.L., FitzHugh, W., Kusumi, K., Russell, L.B., Mueller, K.L., van Berkel, V., Birren, B.W., Kruglyak, L. & Lander, E.S. (1996) Disruption of the nuclear hormone receptor RORalpha in staggerer mice. *Nature*, **379**, 736-739.

Hansel, C., de Jeu, M., Belmeguenai, A., Houtman, S.H., Buitendijk, G.H., Andreev, D., De Zeeuw, C.I. & Elgersma, Y. (2006) alphaCaMKII Is essential for cerebellar LTD and motor learning. *Neuron*, **51**, 835-843.

Hansen, S.T., Meera, P., Otis, T.S. & Pulst, S.M. (2013) Changes in Purkinje cell firing and gene expression precede behavioral pathology in a mouse model of SCA2. *Hum Mol Genet*, **22**, 271-283.

Hara, K., Yonezawa, K., Weng, Q.P., Kozlowski, M.T., Belham, C. & Avruch, J. (1998) Amino acid sufficiency and mTOR regulate p70 S6 kinase and eIF-4E BP1 through a common effector mechanism. *J Biol Chem*, **273**, 14484-14494.

Hardie, D.G., Ross, F.A. & Hawley, S.A. (2012) AMPK: a nutrient and energy sensor that maintains energy homeostasis. *Nat Rev Mol Cell Biol*, **13**, 251-262.

Harrington, L.S., Findlay, G.M. & Lamb, R.F. (2005) Restraining PI3K: mTOR signalling goes back to the membrane. *Trends Biochem Sci*, **30**, 35-42.

Hashimoto, K., Ichikawa, R., Kitamura, K., Watanabe, M. & Kano, M. (2009a) Translocation of a "winner" climbing fiber to the Purkinje cell dendrite and subsequent elimination of "losers" from the soma in developing cerebellum. *Neuron*, **63**, 106-118.

Hashimoto, K. & Kano, M. (2003) Functional differentiation of multiple climbing fiber inputs during synapse elimination in the developing cerebellum. *Neuron*, **38**, 785-796.

Hashimoto, K. & Kano, M. (2005) Postnatal development and synapse elimination of climbing fiber to Purkinje cell projection in the cerebellum. *Neurosci Res*, **53**, 221-228.

Hashimoto, K. & Kano, M. (2013) Synapse elimination in the developing cerebellum. *Cell Mol Life Sci*, **70**, 4667-4680.

Hashimoto, K., Yoshida, T., Sakimura, K., Mishina, M., Watanabe, M. & Kano, M. (2009b) Influence of parallel fiber-Purkinje cell synapse formation on postnatal development of climbing fiber-Purkinje cell synapses in the cerebellum. *Neuroscience*, **162**, 601-611.

Hatten, M.E. & Heintz, N. (1995) Mechanisms of neural patterning and specification in the developing cerebellum. *Annu Rev Neurosci*, **18**, 385-408.

Heitman, J., Movva, N.R. & Hall, M.N. (1991) Targets for cell cycle arrest by the immunosuppressant rapamycin in yeast. *Science*, **253**, 905-909.

Hendelman, W.J. & Aggerwal, A.S. (1980) The Purkinje neuron: I. A Golgi study of its development in the mouse and in culture. *J Comp Neurol*, **193**, 1063-1079.

Hirano, T. (2006) Cerebellar regulation mechanisms learned from studies on GluRdelta2. *Mol Neurobiol*, **33**, 1-16.

Hirano, T. (2013) Long-term depression and other synaptic plasticity in the cerebellum. *Proc Jpn Acad Ser B Phys Biol Sci*, **89**, 183-195.

Hirano, T. & Kawaguchi, S.Y. (2014) Regulation and functional roles of rebound potentiation at cerebellar stellate cell-Purkinje cell synapses. *Front Cell Neurosci*, **8**, 42.

Hoeffer, C.A. & Klann, E. (2010) mTOR signaling: at the crossroads of plasticity, memory and disease. *Trends Neurosci*, **33**, 67-75.

Holmgren, A., Bouhy, D. & Timmerman, V. (2012) Neurofilament phosphorylation and their proline-directed kinases in health and disease. *J Peripher Nerv Syst*, **17**, 365-376.

Hou, L. & Klann, E. (2004) Activation of the phosphoinositide 3-kinase-Akt-mammalian target of rapamycin signaling pathway is required for metabotropic glutamate receptor-dependent long-term depression. *J Neurosci*, **24**, 6352-6361.

Houston, C.M., He, Q. & Smart, T.G. (2009) CaMKII phosphorylation of the GABA(A) receptor: receptor subtype- and synapse-specific modulation. *J Physiol*, **587**, 2115-2125.

Howes, O.D. & Kapur, S. (2009) The dopamine hypothesis of schizophrenia: version III--the final common pathway. *Schizophr Bull*, **35**, 549-562.

Hsieh, A.C., Liu, Y., Edlind, M.P., Ingolia, N.T., Janes, M.R., Sher, A., Shi, E.Y., Stumpf, C.R., Christensen, C., Bonham, M.J., Wang, S., Ren, P., Martin, M., Jessen, K., Feldman, M.E., Weissman, J.S., Shokat, K.M., Rommel, C. & Ruggero, D. (2012) The translational landscape of mTOR signalling steers cancer initiation and metastasis. *Nature*, **485**, 55-61.

Hsu, P.P., Kang, S.A., Rameseder, J., Zhang, Y., Ottina, K.A., Lim, D., Peterson, T.R., Choi, Y., Gray, N.S., Yaffe, M.B., Marto, J.A. & Sabatini, D.M. (2011) The mTOR-regulated phosphoproteome reveals a mechanism of mTORC1-mediated inhibition of growth factor signaling. *Science*, **332**, 1317-1322.

Huang, J., Dibble, C.C., Matsuzaki, M. & Manning, B.D. (2008) The TSC1-TSC2 complex is required for proper activation of mTOR complex 2. *Mol Cell Biol*, **28**, 4104-4115.

Huang, K. & Fingar, D.C. (2014) Growing knowledge of the mTOR signaling network. *Semin Cell Dev Biol*.

Huang, W., Zhu, P.J., Zhang, S., Zhou, H., Stoica, L., Galiano, M., Krnjevic, K., Roman, G. & Costa-Mattioli, M. (2013) mTORC2 controls actin polymerization required for consolidation of long-term memory. *Nat Neurosci*, **16**, 441-448.

Huber, K.M., Kayser, M.S. & Bear, M.F. (2000) Role for rapid dendritic protein synthesis in hippocampal mGluR-dependent long-term depression. *Science*, **288**, 1254-1257.

Hur, E.M. & Zhou, F.Q. (2010) GSK3 signalling in neural development. *Nat Rev Neurosci*, **11**, 539-551.

Hutsler, J.J. & Zhang, H. (2010) Increased dendritic spine densities on cortical projection neurons in autism spectrum disorders. *Brain Res*, **1309**, 83-94.

Ichise, T., Kano, M., Hashimoto, K., Yanagihara, D., Nakao, K., Shigemoto, R., Katsuki, M. & Aiba, A. (2000) mGluR1 in cerebellar Purkinje cells essential for long-term depression, synapse elimination, and motor coordination. *Science*, **288**, 1832-1835.

Ikenoue, T., Inoki, K., Yang, Q., Zhou, X. & Guan, K.L. (2008) Essential function of TORC2 in PKC and Akt turn motif phosphorylation, maturation and signalling. *Embo J*, **27**, 1919-1931.

Inoki, K., Li, Y., Zhu, T., Wu, J. & Guan, K.L. (2002) TSC2 is phosphorylated and inhibited by Akt and suppresses mTOR signalling. *Nat Cell Biol*, **4**, 648-657.

Inoki, K., Zhu, T. & Guan, K.L. (2003) TSC2 mediates cellular energy response to control cell growth and survival. *Cell*, **115**, 577-590.

Ito, M. & Kano, M. (1982) Long-lasting depression of parallel fiber-Purkinje cell transmission induced by conjunctive stimulation of parallel fibers and climbing fibers in the cerebellar cortex. *Neurosci Lett*, **33**, 253-258.

Jacinto, E., Facchinetti, V., Liu, D., Soto, N., Wei, S., Jung, S.Y., Huang, Q., Qin, J. & Su, B. (2006) SIN1/MIP1 maintains rictor-mTOR complex integrity and regulates Akt phosphorylation and substrate specificity. *Cell*, **127**, 125-137.

Jacinto, E., Loewith, R., Schmidt, A., Lin, S., Ruegg, M.A., Hall, A. & Hall, M.N. (2004) Mammalian TOR complex 2 controls the actin cytoskeleton and is rapamycin insensitive. *Nat Cell Biol*, **6**, 1122-1128.

Jacquemont, S., Hagerman, R.J., Hagerman, P.J. & Leehey, M.A. (2007) Fragile-X syndrome and fragile X-associated tremor/ataxia syndrome: two faces of FMR1. *Lancet Neurol*, **6**, 45-55.

Jaworski, J., Spangler, S., Seeburg, D.P., Hoogenraad, C.C. & Sheng, M. (2005) Control of dendritic arborization by the phosphoinositide-3'-kinase-Akt-mammalian target of rapamycin pathway. *J Neurosci*, **25**, 11300-11312.

Jeste, D.V., Barban, L. & Parisi, J. (1984) Reduced Purkinje cell density in Huntington's disease. *Exp Neurol*, **85**, 78-86.

Jin, H.O., Seo, S.K., Woo, S.H., Kim, E.S., Lee, H.C., Yoo, D.H., An, S., Choe, T.B., Lee, S.J., Hong, S.I., Rhee, C.H., Kim, J.I. & Park, I.C. (2009) Activating transcription factor 4 and CCAAT/enhancer-binding protein-beta negatively regulate the mammalian target of rapamycin via Redd1 expression in response to oxidative and endoplasmic reticulum stress. *Free Radic Biol Med*, **46**, 1158-1167.

Julien, J.P. (2001) Amyotrophic lateral sclerosis. unfolding the toxicity of the misfolded. *Cell*, **104**, 581-591.

Julien, L.A., Carriere, A., Moreau, J. & Roux, P.P. (2010) mTORC1-activated S6K1 phosphorylates Rictor on threonine 1135 and regulates mTORC2 signaling. *Mol Cell Biol*, **30**, 908-921.

Ka, M., Condorelli, G., Woodgett, J.R. & Kim, W.Y. (2014) mTOR regulates brain morphogenesis by mediating GSK3 signaling. *Development*, **141**, 4076-4086.

Kahle, P.J., Haass, C., Kretzschmar, H.A. & Neumann, M. (2002) Structure/function of alpha-synuclein in health and disease: rational development of animal models for Parkinson's and related diseases. *J Neurochem*, **82**, 449-457.

Kakegawa, W. & Yuzaki, M. (2005) A mechanism underlying AMPA receptor trafficking during cerebellar long-term potentiation. *Proc Natl Acad Sci U S A*, **102**, 17846-17851.

Kakizawa, S., Yamasaki, M., Watanabe, M. & Kano, M. (2000) Critical period for activity-dependent synapse elimination in developing cerebellum. *J Neurosci*, **20**, 4954-4961.

Kalkman, H.O. (2006) The role of the phosphatidylinositide 3-kinase-protein kinase B pathway in schizophrenia. *Pharmacol Ther*, **110**, 117-134.

Kano, M., Fukunaga, K. & Konnerth, A. (1996) Ca(2+)-induced rebound potentiation of gamma-aminobutyric acid-mediated currents requires activation of Ca2+/calmodulin-dependent kinase II. *Proc Natl Acad Sci U S A*, **93**, 13351-13356.

Kano, M., Hashimoto, K., Chen, C., Abeliovich, A., Aiba, A., Kurihara, H., Watanabe, M., Inoue, Y. & Tonegawa, S. (1995) Impaired synapse elimination during cerebellar development in PKC gamma mutant mice. *Cell*, **83**, 1223-1231.

Kano, M., Hashimoto, K., Kurihara, H., Watanabe, M., Inoue, Y., Aiba, A. & Tonegawa, S. (1997) Persistent multiple climbing fiber innervation of cerebellar Purkinje cells in mice lacking mGluR1. *Neuron*, **18**, 71-79.

Kano, M., Hashimoto, K. & Tabata, T. (2008) Type-1 metabotropic glutamate receptor in cerebellar Purkinje cells: a key molecule responsible for long-term depression, endocannabinoid signalling and synapse elimination. *Philos Trans R Soc Lond B Biol Sci*, **363**, 2173-2186.

Kano, M., Hashimoto, K., Watanabe, M., Kurihara, H., Offermanns, S., Jiang, H., Wu, Y., Jun, K., Shin, H.S., Inoue, Y., Simon, M.I. & Wu, D. (1998) Phospholipase cbeta4 is specifically involved in climbing fiber synapse elimination in the developing cerebellum. *Proc Natl Acad Sci U S A*, **95**, 15724-15729.

Kano, M., Rexhausen, U., Dreessen, J. & Konnerth, A. (1992) Synaptic excitation produces a long-lasting rebound potentiation of inhibitory synaptic signals in cerebellar Purkinje cells. *Nature*, **356**, 601-604.

Kapfhammer, J.P. (2004) Cellular and molecular control of dendritic growth and development of cerebellar Purkinje cells. *Prog Histochem Cytochem*, **39**, 131-182.

Kawaguchi, S.Y. & Hirano, T. (2002) Signaling cascade regulating long-term potentiation of GABA(A) receptor responsiveness in cerebellar Purkinje neurons. *J Neurosci*, **22**, 3969-3976.

Kawaguchi, S.Y. & Hirano, T. (2007) Sustained structural change of GABA(A) receptor-associated protein underlies long-term potentiation at inhibitory synapses on a cerebellar Purkinje neuron. *J Neurosci*, **27**, 6788-6799.

Keith, C.T. & Schreiber, S.L. (1995) PIK-related kinases: DNA repair, recombination, and cell cycle checkpoints. *Science*, **270**, 50-51.

Kim, J., Kundu, M., Viollet, B. & Guan, K.L. (2011) AMPK and mTOR regulate autophagy through direct phosphorylation of Ulk1. *Nat Cell Biol*, **13**, 132-141.

Kim, S.J., DeStefano, M.A., Oh, W.J., Wu, C.C., Vega-Cotto, N.M., Finlan, M., Liu, D., Su, B. & Jacinto, E. (2012) mTOR complex 2 regulates proper turnover of insulin receptor substrate-1 via the ubiquitin ligase subunit Fbw8. *Mol Cell*, **48**, 875-887.

King, M.A., Hands, S., Hafiz, F., Mizushima, N., Tolkovsky, A.M. & Wyttenbach, A. (2008) Rapamycin inhibits polyglutamine aggregation independently of autophagy by reducing protein synthesis. *Mol Pharmacol*, **73**, 1052-1063.

Kitagawa, Y., Hirano, T. & Kawaguchi, S.Y. (2009) Prediction and validation of a mechanism to control the threshold for inhibitory synaptic plasticity. *Mol Syst Biol*, **5**, 280.

Klockgether, T. (2010) Sporadic ataxia with adult onset: classification and diagnostic criteria. *Lancet Neurol*, **9**, 94-104.

Ko, D.C., Milenkovic, L., Beier, S.M., Manuel, H., Buchanan, J. & Scott, M.P. (2005) Cell-autonomous death of cerebellar purkinje neurons with autophagy in Niemann-Pick type C disease. *PLoS Genet*, **1**, 81-95.

Koekkoek, S.K., Yamaguchi, K., Milojkovic, B.A., Dortland, B.R., Ruigrok, T.J., Maex, R., De Graaf, W., Smit, A.E., VanderWerf, F., Bakker, C.E., Willemsen, R., Ikeda, T., Kakizawa, S.,

Onodera, K., Nelson, D.L., Mientjes, E., Joosten, M., De Schutter, E., Oostra, B.A., Ito, M. & De Zeeuw, C.I. (2005) Deletion of FMR1 in Purkinje cells enhances parallel fiber LTD, enlarges spines, and attenuates cerebellar eyelid conditioning in Fragile X syndrome. *Neuron*, **47**, 339-352.

Komatsu, M., Wang, Q.J., Holstein, G.R., Friedrich, V.L., Jr., Iwata, J., Kominami, E., Chait, B.T., Tanaka, K. & Yue, Z. (2007) Essential role for autophagy protein Atg7 in the maintenance of axonal homeostasis and the prevention of axonal degeneration. *Proc Natl Acad Sci U S A*, **104**, 14489-14494.

Kooy, R.F., D'Hooge, R., Reyniers, E., Bakker, C.E., Nagels, G., De Boulle, K., Storm, K., Clincke, G., De Deyn, P.P., Oostra, B.A. & Willems, P.J. (1996) Transgenic mouse model for the fragile X syndrome. *Am J Med Genet*, **64**, 241-245.

Koren, I., Reem, E. & Kimchi, A. (2010) DAP1, a novel substrate of mTOR, negatively regulates autophagy. *Curr Biol*, **20**, 1093-1098.

Krishnan, V. & Nestler, E.J. (2008) The molecular neurobiology of depression. *Nature*, **455**, 894-902.

Krueger, D.D., Tuffy, L.P., Papadopoulos, T. & Brose, N. (2012) The role of neurexins and neuroligins in the formation, maturation, and function of vertebrate synapses. *Curr Opin Neurobiol*, **22**, 412-422.

Kumar, A., Harris, T.E., Keller, S.R., Choi, K.M., Magnuson, M.A. & Lawrence, J.C., Jr. (2008) Muscle-specific deletion of rictor impairs insulin-stimulated glucose transport and enhances Basal glycogen synthase activity. *Mol Cell Biol*, **28**, 61-70.

Kumar, V., Zhang, M.X., Swank, M.W., Kunz, J. & Wu, G.Y. (2005) Regulation of dendritic morphogenesis by Ras-PI3K-Akt-mTOR and Ras-MAPK signaling pathways. *J Neurosci*, **25**, 11288-11299.

Lafay-Chebassier, C., Paccalin, M., Page, G., Barc-Pain, S., Perault-Pochat, M.C., Gil, R., Pradier, L. & Hugon, J. (2005) mTOR/p70S6k signalling alteration by Abeta exposure as well as in APP-PS1 transgenic models and in patients with Alzheimer's disease. *J Neurochem*, **94**, 215-225.

Laine, J. & Axelrad, H. (1994) The candelabrum cell: a new interneuron in the cerebellar cortex. *J Comp Neurol*, **339**, 159-173.

Laplante, M. & Sabatini, D.M. (2012) mTOR Signaling. *Cold Spring Harb Perspect Biol*, **4**.

Larsson, C. (2006) Protein kinase C and the regulation of the actin cytoskeleton. *Cell Signal*, **18**, 276-284.

LeDoux, M.S. (2011) Animal models of dystonia: Lessons from a mutant rat. *Neurobiol Dis*, **42**, 152-161.

Lee, K., Gudapati, P., Dragovic, S., Spencer, C., Joyce, S., Killeen, N., Magnuson, M.A. & Boothby, M. (2010) Mammalian target of rapamycin protein complex 2 regulates differentiation of Th1 and Th2 cell subsets via distinct signaling pathways. *Immunity*, **32**, 743-753.

Lefebvre, J.L., Kostadinov, D., Chen, W.V., Maniatis, T. & Sanes, J.R. (2012) Protocadherins mediate dendritic self-avoidance in the mammalian nervous system. *Nature*, **488**, 517-521.

Lein, E.S. & Hawrylycz, M.J. & Ao, N. & Ayres, M. & Bensinger, A. & Bernard, A. & Boe, A.F. & Boguski, M.S. & Brockway, K.S. & Byrnes, E.J. & Chen, L. & Chen, T.M. & Chin, M.C. & Chong, J. & Crook, B.E. & Czaplinska, A. & Dang, C.N. & Datta, S. & Dee, N.R. & Desaki, A.L. & Desta, T. & Diep, E. & Dolbeare, T.A. & Donelan, M.J. & Dong, H.W. & Dougherty, J.G. & Duncan, B.J. & Ebbert, A.J. & Eichele, G. & Estin, L.K. & Faber, C. & Facer, B.A. & Fields, R. & Fischer, S.R. & Fliss, T.P. & Frensley, C. & Gates, S.N. & Glattfelder, K.J. & Halverson, K.R. & Hart, M.R. & Hohmann, J.G. & Howell, M.P. & Jeung, D.P. & Johnson, R.A. & Karr, P.T. & Kawal, R. & Kidney, J.M. & Knapik, R.H. & Kuan, C.L. & Lake, J.H. & Laramee, A.R. & Larsen, K.D. & Lau, C. & Lemon, T.A. & Liang, A.J. & Liu, Y. & Luong, L.T. & Michaels, J. & Morgan, J.J. & Morgan, R.J. & Mortrud, M.T. & Mosqueda, N.F. & Ng, L.L. & Ng, R. & Orta, G.J. & Overly, C.C. & Pak, T.H. & Parry, S.E. & Pathak, S.D. & Pearson, O.C. & Puchalski, R.B. & Riley, Z.L. & Rockett, H.R. & Rowland, S.A. & Royall, J.J. & Ruiz, M.J. & Sarno, N.R. & Schaffnit, K. & Shapovalova, N.V. & Sivisay, T. & Slaughterbeck, C.R. & Smith, S.C. & Smith, K.A. & Smith, B.I. & Sodt, A.J. & Stewart, N.N. & Stumpf, K.R. & Sunkin, S.M. & Sutram, M. & Tam, A. & Teemer, C.D. & Thaller, C. & Thompson, C.L. & Varnam, L.R. & Visel, A. & Whitlock, R.M. & Wohnoutka, P.E. & Wolkey, C.K. & Wong, V.Y. & Wood, M. & Yaylaoglu, M.B. & Young, R.C. & Youngstrom, B.L. & Yuan, X.F. & Zhang, B. & Zwingman, T.A. & Jones, A.R. (2007) Genome-wide atlas of gene expression in the adult mouse brain. *Nature*, **445**, 168-176.

Leitges, M., Kovac, J., Plomann, M. & Linden, D.J. (2004) A unique PDZ ligand in PKCalpha confers induction of cerebellar long-term synaptic depression. *Neuron*, **44**, 585-594.

Lev-Ram, V., Wong, S.T., Storm, D.R. & Tsien, R.Y. (2002) A new form of cerebellar long-term potentiation is postsynaptic and depends on nitric oxide but not cAMP. *Proc Natl Acad Sci U S A*, **99**, 8389-8393.

Levinson, J.N. & El-Husseini, A. (2005) Building excitatory and inhibitory synapses: balancing neuroligin partnerships. *Neuron*, **48**, 171-174.

Li, N., Lee, B., Liu, R.J., Banasr, M., Dwyer, J.M., Iwata, M., Li, X.Y., Aghajanian, G. & Duman, R.S. (2010) mTOR-dependent synapse formation underlies the rapid antidepressant effects of NMDA antagonists. *Science*, **329**, 959-964.

Li, X., Alafuzoff, I., Soininen, H., Winblad, B. & Pei, J.J. (2005) Levels of mTOR and its downstream targets 4E-BP1, eEF2, and eEF2 kinase in relationships with tau in Alzheimer's disease brain. *Febs J*, **272**, 4211-4220.

Li, X., An, W.L., Alafuzoff, I., Soininen, H., Winblad, B. & Pei, J.J. (2004) Phosphorylated eukaryotic translation factor 4E is elevated in Alzheimer brain. *Neuroreport*, **15**, 2237-2240.

Linden, D.J. (2001) The expression of cerebellar LTD in culture is not associated with changes in AMPA-receptor kinetics, agonist affinity, or unitary conductance. *Proc Natl Acad Sci U S A*, **98**, 14066-14071.

Lipton, J.O. & Sahin, M. (2014) The Neurology of mTOR. *Neuron*, **84**, 275-291.

Liu, J., Tang, T.S., Tu, H., Nelson, O., Herndon, E., Huynh, D.P., Pulst, S.M. & Bezprozvanny, I. (2009) Deranged calcium signaling and neurodegeneration in spinocerebellar ataxia type 2. *J Neurosci*, **29**, 9148-9162.

Liu, P., Gan, W., Inuzuka, H., Lazorchak, A.S., Gao, D., Arojo, O., Liu, D., Wan, L., Zhai, B., Yu, Y., Yuan, M., Kim, B.M., Shaik, S., Menon, S., Gygi, S.P., Lee, T.H., Asara, J.M., Manning, B.D., Blenis, J., Su, B. & Wei, W. (2013) Sin1 phosphorylation impairs mTORC2 complex integrity and inhibits downstream Akt signalling to suppress tumorigenesis. *Nat Cell Biol*, **15**, 1340-1350.

Long, X., Lin, Y., Ortiz-Vega, S., Yonezawa, K. & Avruch, J. (2005) Rheb binds and regulates the mTOR kinase. *Curr Biol*, **15**, 702-713.

Lu, M., Wang, J., Jones, K.T., Ives, H.E., Feldman, M.E., Yao, L.J., Shokat, K.M., Ashrafi, K. & Pearce, D. (2010) mTOR complex-2 activates ENaC by phosphorylating SGK1. *J Am Soc Nephrol*, **21**, 811-818.

Luscher, C. & Huber, K.M. (2010) Group 1 mGluR-dependent synaptic long-term depression: mechanisms and implications for circuitry and disease. *Neuron*, **65**, 445-459.

Luu, T., Gage, P.W. & Tierney, M.L. (2006) GABA increases both the conductance and mean open time of recombinant GABAA channels co-expressed with GABARAP. *J Biol Chem*, **281**, 35699-35708.

Ma, L., Chen, Z., Erdjument-Bromage, H., Tempst, P. & Pandolfi, P.P. (2005) Phosphorylation and functional inactivation of TSC2 by Erk implications for tuberous sclerosis and cancer pathogenesis. *Cell*, **121**, 179-193.

Ma, T., Hoeffer, C.A., Capetillo-Zarate, E., Yu, F., Wong, H., Lin, M.T., Tampellini, D., Klann, E., Blitzer, R.D. & Gouras, G.K. (2010) Dysregulation of the mTOR pathway mediates impairment of synaptic plasticity in a mouse model of Alzheimer's disease. *PLoS One*, **5**.

Ma, X.M. & Blenis, J. (2009) Molecular mechanisms of mTOR-mediated translational control. *Nat Rev Mol Cell Biol*, **10**, 307-318.

MacDonald, M.E., Barnes, G., Srinidhi, J., Duyao, M.P., Ambrose, C.M., Myers, R.H., Gray, J., Conneally, P.M., Young, A., Penney, J. & et al. (1993) Gametic but not somatic instability of CAG repeat length in Huntington's disease. *J Med Genet*, **30**, 982-986.

Magri, L., Cambiaghi, M., Cominelli, M., Alfaro-Cervello, C., Cursi, M., Pala, M., Bulfone, A., Garcia-Verdugo, J.M., Leocani, L., Minicucci, F., Poliani, P.L. & Galli, R. (2011) Sustained activation of mTOR pathway in embryonic neural stem cells leads to development of tuberous sclerosis complex-associated lesions. *Cell Stem Cell*, **9**, 447-462.

Magri, L., Cominelli, M., Cambiaghi, M., Cursi, M., Leocani, L., Minicucci, F., Poliani, P.L. & Galli, R. (2013) Timing of mTOR activation affects tuberous sclerosis complex neuropathology in mouse models. *Dis Model Mech*, **6**, 1185-1197.

Malagelada, C., Jin, Z.H. & Greene, L.A. (2008) RTP801 is induced in Parkinson's disease and mediates neuron death by inhibiting Akt phosphorylation/activation. *J Neurosci*, **28**, 14363-14371.

Malagelada, C., Jin, Z.H., Jackson-Lewis, V., Przedborski, S. & Greene, L.A. (2010) Rapamycin protects against neuron death in in vitro and in vivo models of Parkinson's disease. *J Neurosci*, **30**, 1166-1175.

Malagelada, C., Ryu, E.J., Biswas, S.C., Jackson-Lewis, V. & Greene, L.A. (2006) RTP801 is elevated in Parkinson brain substantia nigral neurons and mediates death in cellular models of Parkinson's disease by a mechanism involving mammalian target of rapamycin inactivation. *J Neurosci*, **26**, 9996-10005.

Maloku, E., Covelo, I.R., Hanbauer, I., Guidotti, A., Kadriu, B., Hu, Q., Davis, J.M. & Costa, E. (2010) Lower number of cerebellar Purkinje neurons in psychosis is associated with reduced reelin expression. *Proc Natl Acad Sci U S A*, **107**, 4407-4411.

Manning, B.D., Tee, A.R., Logsdon, M.N., Blenis, J. & Cantley, L.C. (2002) Identification of the tuberous sclerosis complex-2 tumor suppressor gene product tuberin as a target of the phosphoinositide 3-kinase/akt pathway. *Mol Cell*, **10**, 151-162.

Marr, D. (1969) A theory of cerebellar cortex. *J Physiol*, **202**, 437-470.

Marsden, K.C., Beattie, J.B., Friedenthal, J. & Carroll, R.C. (2007) NMDA receptor activation potentiates inhibitory transmission through GABA receptor-associated protein-dependent exocytosis of GABA(A) receptors. *J Neurosci*, **27**, 14326-14337.

Martin, B.S. & Huntsman, M.M. (2012) Pathological plasticity in fragile X syndrome. *Neural Plast*, **2012**, 275630.

Martin, S.J., Grimwood, P.D. & Morris, R.G. (2000) Synaptic plasticity and memory: an evaluation of the hypothesis. *Annu Rev Neurosci*, **23**, 649-711.

Martina, J.A., Chen, Y., Gucek, M. & Puertollano, R. (2012) MTORC1 functions as a transcriptional regulator of autophagy by preventing nuclear transport of TFEB. *Autophagy*, **8**, 903-914.

Martinez, S., Andreu, A., Mecklenburg, N. & Echevarria, D. (2013) Cellular and molecular basis of cerebellar development. *Front Neuroanat*, **7**, 18.

Martini, M., De Santis, M.C., Braccini, L., Gulluni, F. & Hirsch, E. (2014) PI3K/AKT signaling pathway and cancer: an updated review. *Ann Med*, **46**, 372-383.

Matsuda, S., Launey, T., Mikawa, S. & Hirai, H. (2000) Disruption of AMPA receptor GluR2 clusters following long-term depression induction in cerebellar Purkinje neurons. *Embo J*, **19**, 2765-2774.

Matsuda, S., Mikawa, S. & Hirai, H. (1999) Phosphorylation of serine-880 in GluR2 by protein kinase C prevents its C terminus from binding with glutamate receptor-interacting protein. *J Neurochem*, **73**, 1765-1768.

McDonald, B.J. & Moss, S.J. (1997) Conserved phosphorylation of the intracellular domains of GABA(A) receptor beta2 and beta3 subunits by cAMP-dependent protein kinase, cGMP-dependent protein kinase protein kinase C and Ca2+/calmodulin type II-dependent protein kinase. *Neuropharmacology*, **36**, 1377-1385.

Meikle, L., Pollizzi, K., Egnor, A., Kramvis, I., Lane, H., Sahin, M. & Kwiatkowski, D.J. (2008) Response of a neuronal model of tuberous sclerosis to mammalian target of rapamycin (mTOR) inhibitors: effects on mTORC1 and Akt signaling lead to improved survival and function. *J Neurosci*, **28**, 5422-5432.

Meikle, L., Talos, D.M., Onda, H., Pollizzi, K., Rotenberg, A., Sahin, M., Jensen, F.E. & Kwiatkowski, D.J. (2007) A mouse model of tuberous sclerosis: neuronal loss of Tsc1 causes dysplastic and ectopic neurons, reduced myelination, seizure activity, and limited survival. *J Neurosci*, **27**, 5546-5558.

Melotte, V., Qu, X., Ongenaert, M., van Criekinge, W., de Bruine, A.P., Baldwin, H.S. & van Engeland, M. (2010) The N-myc downstream regulated gene (NDRG) family: diverse functions, multiple applications. *Faseb J*, **24**, 4153-4166.

Mendoza, M.C., Er, E.E. & Blenis, J. (2011) The Ras-ERK and PI3K-mTOR pathways: cross-talk and compensation. *Trends Biochem Sci*, **36**, 320-328.

Miale, I.L. & Sidman, R.L. (1961) An autoradiographic analysis of histogenesis in the mouse cerebellum. *Exp Neurol*, **4**, 277-296.

Miles, J.H. (2011) Autism spectrum disorders--a genetics review. *Genet Med*, **13**, 278-294.

Mittmann, W., Koch, U. & Hausser, M. (2005) Feed-forward inhibition shapes the spike output of cerebellar Purkinje cells. *J Physiol*, **563**, 369-378.

Miyata, T., Ono, Y., Okamoto, M., Masaoka, M., Sakakibara, A., Kawaguchi, A., Hashimoto, M. & Ogawa, M. (2010) Migration, early axonogenesis, and Reelin-dependent layer-forming

behavior of early/posterior-born Purkinje cells in the developing mouse lateral cerebellum. *Neural Dev*, **5**, 23.

Morales, D. & Hatten, M.E. (2006) Molecular markers of neuronal progenitors in the embryonic cerebellar anlage. *J Neurosci*, **26**, 12226-12236.

Morara, S., van der Want, J.J., de Weerd, H., Provini, L. & Rosina, A. (2001) Ultrastructural analysis of climbing fiber-Purkinje cell synaptogenesis in the rat cerebellum. *Neuroscience*, **108**, 655-671.

Morel, M.P., Dusart, I. & Sotelo, C. (2002) Sprouting of adult Purkinje cell axons in lesioned mouse cerebellum: "non-permissive" versus "permissive" environment. *J Neurocytol*, **31**, 633-647.

Morton, S.M. & Bastian, A.J. (2004) Cerebellar control of balance and locomotion. *Neuroscientist*, **10**, 247-259.

Moss, S.J. & Smart, T.G. (1996) Modulation of amino acid-gated ion channels by protein phosphorylation. *Int Rev Neurobiol*, **39**, 1-52.

Mugnaini, E., Dino, M.R. & Jaarsma, D. (1997) The unipolar brush cells of the mammalian cerebellum and cochlear nucleus: cytology and microcircuitry. *Prog Brain Res*, **114**, 131-150.

Munton, R.P., Vizi, S. & Mansuy, I.M. (2004) The role of protein phosphatase-1 in the modulation of synaptic and structural plasticity. *FEBS Lett*, **567**, 121-128.

Musumeci, S.A., Bosco, P., Calabrese, G., Bakker, C., De Sarro, G.B., Elia, M., Ferri, R. & Oostra, B.A. (2000) Audiogenic seizures susceptibility in transgenic mice with fragile X syndrome. *Epilepsia*, **41**, 19-23.

Narayanan, U., Nalavadi, V., Nakamoto, M., Thomas, G., Ceman, S., Bassell, G.J. & Warren, S.T. (2008) S6K1 phosphorylates and regulates fragile X mental retardation protein (FMRP) with the neuronal protein synthesis-dependent mammalian target of rapamycin (mTOR) signaling cascade. *J Biol Chem*, **283**, 18478-18482.

Nie, D., Di Nardo, A., Han, J.M., Baharanyi, H., Kramvis, I., Huynh, T., Dabora, S., Codeluppi, S., Pandolfi, P.P., Pasquale, E.B. & Sahin, M. (2010) Tsc2-Rheb signaling regulates EphA-mediated axon guidance. *Nat Neurosci*, **13**, 163-172.

Nopoulos, P.C., Ceilley, J.W., Gailis, E.A. & Andreasen, N.C. (1999) An MRI study of cerebellar vermis morphology in patients with schizophrenia: evidence in support of the cognitive dysmetria concept. *Biol Psychiatry*, **46**, 703-711.

Oberdick, J., Schilling, K., Smeyne, R.J., Corbin, J.G., Bocchiaro, C. & Morgan, J.I. (1993) Control of segment-like patterns of gene expression in the mouse cerebellum. *Neuron*, **10**, 1007-1018.

Offermanns, S., Hashimoto, K., Watanabe, M., Sun, W., Kurihara, H., Thompson, R.F., Inoue, Y., Kano, M. & Simon, M.I. (1997) Impaired motor coordination and persistent multiple climbing fiber innervation of cerebellar Purkinje cells in mice lacking Galphaq. *Proc Natl Acad Sci U S A*, **94**, 14089-14094.

Oh, W.J. & Jacinto, E. (2011) mTOR complex 2 signaling and functions. *Cell Cycle*, **10**, 2305-2316.

Oh, W.J., Wu, C.C., Kim, S.J., Facchinetti, V., Julien, L.A., Finlan, M., Roux, P.P., Su, B. & Jacinto, E. (2010) mTORC2 can associate with ribosomes to promote cotranslational phosphorylation and stability of nascent Akt polypeptide. *Embo J*, **29**, 3939-3951.

Oristaglio, J., Hyman West, S., Ghaffari, M., Lech, M.S., Verma, B.R., Harvey, J.A., Welsh, J.P. & Malone, R.P. (2013) Children with autism spectrum disorders show abnormal conditioned response timing on delay, but not trace, eyeblink conditioning. *Neuroscience*, **248**, 708-718.

Ostroff, L.E., Fiala, J.C., Allwardt, B. & Harris, K.M. (2002) Polyribosomes redistribute from dendritic shafts into spines with enlarged synapses during LTP in developing rat hippocampal slices. *Neuron*, **35**, 535-545.

Pan, T., Rawal, P., Wu, Y., Xie, W., Jankovic, J. & Le, W. (2009) Rapamycin protects against rotenone-induced apoptosis through autophagy induction. *Neuroscience*, **164**, 541-551.

Park, S., Park, J.M., Kim, S., Kim, J.A., Shepherd, J.D., Smith-Hicks, C.L., Chowdhury, S., Kaufmann, W., Kuhl, D., Ryazanov, A.G., Huganir, R.L., Linden, D.J. & Worley, P.F. (2008) Elongation factor 2 and fragile X mental retardation protein control the dynamic translation of Arc/Arg3.1 essential for mGluR-LTD. *Neuron*, **59**, 70-83.

Parker, K.L., Narayanan, N.S. & Andreasen, N.C. (2014) The therapeutic potential of the cerebellum in schizophrenia. *Front Syst Neurosci*, **8**, 163.

Parkinson, J. (2002) An essay on the shaking palsy. 1817. *J Neuropsychiatry Clin Neurosci*, **14**, 223-236; discussion 222.

Pei, J.J. & Hugon, J. (2008) mTOR-dependent signalling in Alzheimer's disease. *J Cell Mol Med*, **12**, 2525-2532.

Peterson, T.R., Sengupta, S.S., Harris, T.E., Carmack, A.E., Kang, S.A., Balderas, E., Guertin, D.A., Madden, K.L., Carpenter, A.E., Finck, B.N. & Sabatini, D.M. (2011) mTOR complex 1 regulates lipin 1 localization to control the SREBP pathway. *Cell*, **146**, 408-420.

Pierce, E.T. (1975) Histogenesis of the deep cerebellar nuclei in the mouse: an autoradiographic study. *Brain Res*, **95**, 503-518.

Pijpers, A., Winkelman, B.H., Bronsing, R. & Ruigrok, T.J. (2008) Selective impairment of the cerebellar C1 module involved in rat hind limb control reduces step-dependent modulation of cutaneous reflexes. *J Neurosci*, **28**, 2179-2189.

Porstmann, T., Santos, C.R., Griffiths, B., Cully, M., Wu, M., Leevers, S., Griffiths, J.R., Chung, Y.L. & Schulze, A. (2008) SREBP activity is regulated by mTORC1 and contributes to Akt-dependent cell growth. *Cell Metab*, **8**, 224-236.

Poulopoulos, A., Aramuni, G., Meyer, G., Soykan, T., Hoon, M., Papadopoulos, T., Zhang, M., Paarmann, I., Fuchs, C., Harvey, K., Jedlicka, P., Schwarzacher, S.W., Betz, H., Harvey, R.J., Brose, N., Zhang, W. & Varoqueaux, F. (2009) Neuroligin 2 drives postsynaptic assembly at perisomatic inhibitory synapses through gephyrin and collybistin. *Neuron*, **63**, 628-642.

Purves, D., Augustine, G.J., Fitzpatrick, D., Hall, W.C., LaMantia, A.-S., McNamara, J.O. & White, L.E. (2008) Neuroscience Fourth Edition.

Raike, R.S., Pizoli, C.E., Weisz, C., van den Maagdenberg, A.M., Jinnah, H.A. & Hess, E.J. (2013) Limited regional cerebellar dysfunction induces focal dystonia in mice. *Neurobiol Dis*, **49**, 200-210.

Ravikumar, B., Duden, R. & Rubinsztein, D.C. (2002) Aggregate-prone proteins with polyglutamine and polyalanine expansions are degraded by autophagy. *Hum Mol Genet*, **11**, 1107-1117.

Ravikumar, B., Vacher, C., Berger, Z., Davies, J.E., Luo, S., Oroz, L.G., Scaravilli, F., Easton, D.F., Duden, R., O'Kane, C.J. & Rubinsztein, D.C. (2004) Inhibition of mTOR induces autophagy and reduces toxicity of polyglutamine expansions in fly and mouse models of Huntington disease. *Nat Genet*, **36**, 585-595.

Raymond, J.L., Lisberger, S.G. & Mauk, M.D. (1996) The cerebellum: a neuronal learning machine? *Science*, **272**, 1126-1131.

Reeber, S.L., Otis, T.S. & Sillitoe, R.V. (2013) New roles for the cerebellum in health and disease. *Front Syst Neurosci*, **7**, 83.

Reith, R.M., McKenna, J., Wu, H., Hashmi, S.S., Cho, S.H., Dash, P.K. & Gambello, M.J. (2013) Loss of Tsc2 in Purkinje cells is associated with autistic-like behavior in a mouse model of tuberous sclerosis complex. *Neurobiol Dis*, **51**, 93-103.

Reith, R.M., Way, S., McKenna, J., 3rd, Haines, K. & Gambello, M.J. (2011) Loss of the tuberous sclerosis complex protein tuberin causes Purkinje cell degeneration. *Neurobiol Dis*, **43**, 113-122.

Reyes, M.G. & Gordon, A. (1981) Cerebellar vermis in schizophrenia. *Lancet*, **2**, 700-701.

Reymann, K.G. & Frey, J.U. (2007) The late maintenance of hippocampal LTP: requirements, phases, 'synaptic tagging', 'late-associativity' and implications. *Neuropharmacology*, **52**, 24-40.

Rizzuto, R., Pinton, P., Carrington, W., Fay, F.S., Fogarty, K.E., Lifshitz, L.M., Tuft, R.A. & Pozzan, T. (1998) Close contacts with the endoplasmic reticulum as determinants of mitochondrial Ca2+ responses. *Science*, **280**, 1763-1766.

Roberson, E.D., English, J.D. & Sweatt, J.D. (1996) A biochemist's view of long-term potentiation. *Learn Mem*, **3**, 1-24.

Robitaille, A.M., Christen, S., Shimobayashi, M., Cornu, M., Fava, L.L., Moes, S., Prescianotto-Baschong, C., Sauer, U., Jenoe, P. & Hall, M.N. (2013) Quantitative phosphoproteomics reveal mTORC1 activates de novo pyrimidine synthesis. *Science*, **339**, 1320-1323.

Rodda, R.A. (1981) Cerebellar atrophy in Huntington's disease. *J Neurol Sci*, **50**, 147-157.

Romanino, K., Mazelin, L., Albert, V., Conjard-Duplany, A., Lin, S., Bentzinger, C.F., Handschin, C., Puigserver, P., Zorzato, F., Schaeffer, L., Gangloff, Y.G. & Ruegg, M.A. (2011) Myopathy caused by mammalian target of rapamycin complex 1 (mTORC1) inactivation is not reversed by restoring mitochondrial function. *Proc Natl Acad Sci U S A*, **108**, 20808-20813.

Roux, P.P., Ballif, B.A., Anjum, R., Gygi, S.P. & Blenis, J. (2004) Tumor-promoting phorbol esters and activated Ras inactivate the tuberous sclerosis tumor suppressor complex via p90 ribosomal S6 kinase. *Proc Natl Acad Sci U S A*, **101**, 13489-13494.

Sabatini, D.M., Barrow, R.K., Blackshaw, S., Burnett, P.E., Lai, M.M., Field, M.E., Bahr, B.A., Kirsch, J., Betz, H. & Snyder, S.H. (1999) Interaction of RAFT1 with gephyrin required for rapamycin-sensitive signaling. *Science*, **284**, 1161-1164.

Sabatini, D.M., Erdjument-Bromage, H., Lui, M., Tempst, P. & Snyder, S.H. (1994) RAFT1: a mammalian protein that binds to FKBP12 in a rapamycin-dependent fashion and is homologous to yeast TORs. *Cell*, **78**, 35-43.

Sabers, C.J., Martin, M.M., Brunn, G.J., Williams, J.M., Dumont, F.J., Wiederrecht, G. & Abraham, R.T. (1995) Isolation of a protein target of the FKBP12-rapamycin complex in mammalian cells. *J Biol Chem*, **270**, 815-822.

Saci, A., Cantley, L.C. & Carpenter, C.L. (2011) Rac1 regulates the activity of mTORC1 and mTORC2 and controls cellular size. *Mol Cell*, **42**, 50-61.

Saito, H., Tsumura, H., Otake, S., Nishida, A., Furukawa, T. & Suzuki, N. (2005) L7/Pcp-2-specific expression of Cre recombinase using knock-in approach. *Biochem Biophys Res Commun*, **331**, 1216-1221.

Saito, N. & Shirai, Y. (2002) Protein kinase C gamma (PKC gamma): function of neuron specific isotype. *J Biochem*, **132**, 683-687.

Sancak, Y., Bar-Peled, L., Zoncu, R., Markhard, A.L., Nada, S. & Sabatini, D.M. (2010) Ragulator-Rag complex targets mTORC1 to the lysosomal surface and is necessary for its activation by amino acids. *Cell*, **141**, 290-303.

Sancak, Y., Peterson, T.R., Shaul, Y.D., Lindquist, R.A., Thoreen, C.C., Bar-Peled, L. & Sabatini, D.M. (2008) The Rag GTPases bind raptor and mediate amino acid signaling to mTORC1. *Science*, **320**, 1496-1501.

Sancak, Y., Thoreen, C.C., Peterson, T.R., Lindquist, R.A., Kang, S.A., Spooner, E., Carr, S.A. & Sabatini, D.M. (2007) PRAS40 is an insulin-regulated inhibitor of the mTORC1 protein kinase. *Mol Cell*, **25**, 903-915.

Santini, E., Huynh, T.N., MacAskill, A.F., Carter, A.G., Pierre, P., Ruggero, D., Kaphzan, H. & Klann, E. (2013) Exaggerated translation causes synaptic and behavioural aberrations associated with autism. *Nature*, **493**, 411-415.

Sarbassov, D.D., Ali, S.M., Kim, D.H., Guertin, D.A., Latek, R.R., Erdjument-Bromage, H., Tempst, P. & Sabatini, D.M. (2004) Rictor, a novel binding partner of mTOR, defines a rapamycin-insensitive and raptor-independent pathway that regulates the cytoskeleton. *Curr Biol*, **14**, 1296-1302.

Sarbassov, D.D., Ali, S.M., Sengupta, S., Sheen, J.H., Hsu, P.P., Bagley, A.F., Markhard, A.L. & Sabatini, D.M. (2006) Prolonged rapamycin treatment inhibits mTORC2 assembly and Akt/PKB. *Mol Cell*, **22**, 159-168.

Sarbassov, D.D., Guertin, D.A., Ali, S.M. & Sabatini, D.M. (2005) Phosphorylation and regulation of Akt/PKB by the rictor-mTOR complex. *Science*, **307**, 1098-1101.

Scelfo, B. & Strata, P. (2005) Correlation between multiple climbing fibre regression and parallel fibre response development in the postnatal mouse cerebellum. *Eur J Neurosci*, **21**, 971-978.

Schieke, S.M., Phillips, D., McCoy, J.P., Jr., Aponte, A.M., Shen, R.F., Balaban, R.S. & Finkel, T. (2006) The mammalian target of rapamycin (mTOR) pathway regulates mitochondrial oxygen consumption and oxidative capacity. *J Biol Chem*, **281**, 27643-27652.

Schmahmann, J.D., Weilburg, J.B. & Sherman, J.C. (2007) The neuropsychiatry of the cerebellum - insights from the clinic. *Cerebellum*, **6**, 254-267.

Schonewille, M., Belmeguenai, A., Koekkoek, S.K., Houtman, S.H., Boele, H.J., van Beugen, B.J., Gao, Z., Badura, A., Ohtsuki, G., Amerika, W.E., Hosy, E., Hoebeek, F.E., Elgersma, Y., Hansel, C. & De Zeeuw, C.I. (2010) Purkinje cell-specific knockout of the protein phosphatase PP2B impairs potentiation and cerebellar motor learning. *Neuron*, **67**, 618-628.

Schonewille, M., Gao, Z., Boele, H.J., Veloz, M.F., Amerika, W.E., Simek, A.A., De Jeu, M.T., Steinberg, J.P., Takamiya, K., Hoebeek, F.E., Linden, D.J., Huganir, R.L. & De Zeeuw, C.I. (2011) Reevaluating the role of LTD in cerebellar motor learning. *Neuron*, **70**, 43-50.

Schonewille, M., Luo, C., Ruigrok, T.J., Voogd, J., Schmolesky, M.T., Rutteman, M., Hoebeek, F.E., De Jeu, M.T. & De Zeeuw, C.I. (2006) Zonal organization of the mouse flocculus: physiology, input, and output. *J Comp Neurol*, **497**, 670-682.

Sears, L.L., Finn, P.R. & Steinmetz, J.E. (1994) Abnormal classical eye-blink conditioning in autism. *J Autism Dev Disord*, **24**, 737-751.

Sengupta, S., Peterson, T.R. & Sabatini, D.M. (2010) Regulation of the mTOR complex 1 pathway by nutrients, growth factors, and stress. *Mol Cell*, **40**, 310-322.

Serra, H.G., Duvick, L., Zu, T., Carlson, K., Stevens, S., Jorgensen, N., Lysholm, A., Burright, E., Zoghbi, H.Y., Clark, H.B., Andresen, J.M. & Orr, H.T. (2006) RORalpha-mediated Purkinje cell development determines disease severity in adult SCA1 mice. *Cell*, **127**, 697-708.

Settembre, C., Zoncu, R., Medina, D.L., Vetrini, F., Erdin, S., Huynh, T., Ferron, M., Karsenty, G., Vellard, M.C., Facchinetti, V., Sabatini, D.M. & Ballabio, A. (2012) A lysosome-to-nucleus signalling mechanism senses and regulates the lysosome via mTOR and TFEB. *Embo J*, **31**, 1095-1108.

Shakkottai, V.G., do Carmo Costa, M., Dell'Orco, J.M., Sankaranarayanan, A., Wulff, H. & Paulson, H.L. (2011) Early changes in cerebellar physiology accompany motor dysfunction in the polyglutamine disease spinocerebellar ataxia type 3. *J Neurosci*, **31**, 13002-13014.

Sharma, A., Hoeffer, C.A., Takayasu, Y., Miyawaki, T., McBride, S.M., Klann, E. & Zukin, R.S. (2010) Dysregulation of mTOR signaling in fragile X syndrome. *J Neurosci*, **30**, 694-702.

Shimobayashi, M. & Hall, M.N. (2014) Making new contacts: the mTOR network in metabolism and signalling crosstalk. *Nat Rev Mol Cell Biol*, **15**, 155-162.

Sillitoe, R.V., Gopal, N. & Joyner, A.L. (2009) Embryonic origins of ZebrinII parasagittal stripes and establishment of topographic Purkinje cell projections. *Neuroscience*, **162**, 574-588.

Sillitoe, R.V. & Joyner, A.L. (2007) Morphology, molecular codes, and circuitry produce the three-dimensional complexity of the cerebellum. *Annu Rev Cell Dev Biol*, **23**, 549-577.

Siuta, M.A., Robertson, S.D., Kocalis, H., Saunders, C., Gresch, P.J., Khatri, V., Shiota, C., Kennedy, J.P., Lindsley, C.W., Daws, L.C., Polley, D.B., Veenstra-Vanderweele, J., Stanwood, G.D., Magnuson, M.A., Niswender, K.D. & Galli, A. (2010) Dysregulation of the norepinephrine transporter sustains cortical hypodopaminergia and schizophrenia-like behaviors in neuronal rictor null mice. *PLoS Biol*, **8**, e1000393.

Smit, A.E., van der Geest, J.N., Vellema, M., Koekkoek, S.K., Willemsen, R., Govaerts, L.C., Oostra, B.A., De Zeeuw, C.I. & VanderWerf, F. (2008) Savings and extinction of conditioned eyeblink responses in fragile X syndrome. *Genes Brain Behav*, **7**, 770-777.

Sotelo, C. (2004) Cellular and genetic regulation of the development of the cerebellar system. *Prog Neurobiol*, **72**, 295-339.

Sotelo, C. & Dusart, I. (2009) Intrinsic versus extrinsic determinants during the development of Purkinje cell dendrites. *Neuroscience*, **162**, 589-600.

Sparks, C.A. & Guertin, D.A. (2010) Targeting mTOR: prospects for mTOR complex 2 inhibitors in cancer therapy. *Oncogene*, **29**, 3733-3744.

Spencer, B., Potkar, R., Trejo, M., Rockenstein, E., Patrick, C., Gindi, R., Adame, A., Wyss-Coray, T. & Masliah, E. (2009) Beclin 1 gene transfer activates autophagy and ameliorates the neurodegenerative pathology in alpha-synuclein models of Parkinson's and Lewy body diseases. *J Neurosci*, **29**, 13578-13588.

Spilman, P., Podlutskaya, N., Hart, M.J., Debnath, J., Gorostiza, O., Bredesen, D., Richardson, A., Strong, R. & Galvan, V. (2010) Inhibition of mTOR by rapamycin abolishes cognitive deficits and reduces amyloid-beta levels in a mouse model of Alzheimer's disease. *PLoS One*, **5**, e9979.

Stoodley, C.J., Valera, E.M. & Schmahmann, J.D. (2012) Functional topography of the cerebellum for motor and cognitive tasks: an fMRI study. *Neuroimage*, **59**, 1560-1570.

Strick, P.L., Dum, R.P. & Fiez, J.A. (2009) Cerebellum and nonmotor function. *Annu Rev Neurosci*, **32**, 413-434.

Sugihara, I. (2006) Organization and remodeling of the olivocerebellar climbing fiber projection. *Cerebellum*, **5**, 15-22.

Sugihara, I., Wu, H.S. & Shinoda, Y. (2001) The entire trajectories of single olivocerebellar axons in the cerebellar cortex and their contribution to Cerebellar compartmentalization. *J Neurosci*, **21**, 7715-7723.

Sun, Y., Fang, Y., Yoon, M.S., Zhang, C., Roccio, M., Zwartkruis, F.J., Armstrong, M., Brown, H.A. & Chen, J. (2008) Phospholipase D1 is an effector of Rheb in the mTOR pathway. *Proc Natl Acad Sci U S A*, **105**, 8286-8291.

Swiech, L., Perycz, M., Malik, A. & Jaworski, J. (2008) Role of mTOR in physiology and pathology of the nervous system. *Biochim Biophys Acta*, **1784**, 116-132.

Takada, M., Sugimoto, T. & Hattori, T. (1993) MPTP neurotoxicity to cerebellar Purkinje cells in mice. *Neurosci Lett*, **150**, 49-52.

Takechi, H., Eilers, J. & Konnerth, A. (1998) A new class of synaptic response involving calcium release in dendritic spines. *Nature*, **396**, 757-760.

Tanaka, S., Kawaguchi, S.Y., Shioi, G. & Hirano, T. (2013) Long-term potentiation of inhibitory synaptic transmission onto cerebellar Purkinje neurons contributes to adaptation of vestibulo-ocular reflex. *J Neurosci*, **33**, 17209-17220.

Tang, G., Gudsnuk, K., Kuo, S.H., Cotrina, M.L., Rosoklija, G., Sosunov, A., Sonders, M.S., Kanter, E., Castagna, C., Yamamoto, A., Yue, Z., Arancio, O., Peterson, B.S., Champagne, F., Dwork, A.J., Goldman, J. & Sulzer, D. (2014) Loss of mTOR-dependent macroautophagy causes autistic-like synaptic pruning deficits. *Neuron*, **83**, 1131-1143.

Tang, S.J., Reis, G., Kang, H., Gingras, A.C., Sonenberg, N. & Schuman, E.M. (2002) A rapamycin-sensitive signaling pathway contributes to long-term synaptic plasticity in the hippocampus. *Proc Natl Acad Sci U S A*, **99**, 467-472.

Tang, S.J. & Schuman, E.M. (2002) Protein synthesis in the dendrite. *Philos Trans R Soc Lond B Biol Sci*, **357**, 521-529.

Tavazoie, S.F., Alvarez, V.A., Ridenour, D.A., Kwiatkowski, D.J. & Sabatini, B.L. (2005) Regulation of neuronal morphology and function by the tumor suppressors Tsc1 and Tsc2. *Nat Neurosci*, **8**, 1727-1734.

Tee, A.R., Fingar, D.C., Manning, B.D., Kwiatkowski, D.J., Cantley, L.C. & Blenis, J. (2002) Tuberous sclerosis complex-1 and -2 gene products function together to inhibit mammalian target of rapamycin (mTOR)-mediated downstream signaling. *Proc Natl Acad Sci U S A*, **99**, 13571-13576.

Tee, A.R., Manning, B.D., Roux, P.P., Cantley, L.C. & Blenis, J. (2003) Tuberous sclerosis complex gene products, Tuberin and Hamartin, control mTOR signaling by acting as a GTPase-activating protein complex toward Rheb. *Curr Biol*, **13**, 1259-1268.

Thomanetz, V., Angliker, N., Cloetta, D., Lustenberger, R.M., Schweighauser, M., Oliveri, F., Suzuki, N. & Ruegg, M.A. (2013) Ablation of the mTORC2 component rictor in brain or Purkinje cells affects size and neuron morphology. *J Cell Biol*, **201**, 293-308.

Thoreen, C.C., Chantranupong, L., Keys, H.R., Wang, T., Gray, N.S. & Sabatini, D.M. (2012) A unifying model for mTORC1-mediated regulation of mRNA translation. *Nature*, **485**, 109-113.

Tobia, M.J. & Woodruff-Pak, D.S. (2009) Delay eyeblink classical conditioning is impaired in Fragile X syndrome. *Behav Neurosci*, **123**, 665-676.

Tran, K.D., Smutzer, G.S., Doty, R.L. & Arnold, S.E. (1998) Reduced Purkinje cell size in the cerebellar vermis of elderly patients with schizophrenia. *Am J Psychiatry*, **155**, 1288-1290.

Treins, C., Warne, P.H., Magnuson, M.A., Pende, M. & Downward, J. (2010) Rictor is a novel target of p70 S6 kinase-1. *Oncogene*, **29**, 1003-1016.

Tsai, P.T., Hull, C., Chu, Y., Greene-Colozzi, E., Sadowski, A.R., Leech, J.M., Steinberg, J., Crawley, J.N., Regehr, W.G. & Sahin, M. (2012) Autistic-like behaviour and cerebellar dysfunction in Purkinje cell Tsc1 mutant mice. *Nature*, **488**, 647-651.

Tsuruno, S. & Hirano, T. (2007) Persistent activation of protein kinase Calpha is not necessary for expression of cerebellar long-term depression. *Mol Cell Neurosci*, **35**, 38-48.

Turmaine, M., Raza, A., Mahal, A., Mangiarini, L., Bates, G.P. & Davies, S.W. (2000) Nonapoptotic neurodegeneration in a transgenic mouse model of Huntington's disease. *Proc Natl Acad Sci U S A*, **97**, 8093-8097.

Tyagarajan, S.K. & Fritschy, J.M. (2014) Gephyrin: a master regulator of neuronal function? *Nat Rev Neurosci*, **15**, 141-156.

Tyagarajan, S.K., Ghosh, H., Yevenes, G.E., Nikonenko, I., Ebeling, C., Schwerdel, C., Sidler, C., Zeilhofer, H.U., Gerrits, B., Muller, D. & Fritschy, J.M. (2011) Regulation of GABAergic synapse formation and plasticity by GSK3beta-dependent phosphorylation of gephyrin. *Proc Natl Acad Sci U S A*, **108**, 379-384.

Tzatsos, A. (2009) Raptor binds the SAIN (Shc and IRS-1 NPXY binding) domain of insulin receptor substrate-1 (IRS-1) and regulates the phosphorylation of IRS-1 at Ser-636/639 by mTOR. *J Biol Chem*, **284**, 22525-22534.

Um, S.H., Frigerio, F., Watanabe, M., Picard, F., Joaquin, M., Sticker, M., Fumagalli, S., Allegrini, P.R., Kozma, S.C., Auwerx, J. & Thomas, G. (2004) Absence of S6K1 protects against age- and diet-induced obesity while enhancing insulin sensitivity. *Nature*, **431**, 200-205.

Urbanska, M., Gozdz, A., Swiech, L.J. & Jaworski, J. (2012) Mammalian target of rapamycin complex 1 (mTORC1) and 2 (mTORC2) control the dendritic arbor morphology of hippocampal neurons. *J Biol Chem*, **287**, 30240-30256.

van den Buuse, M. (2010) Modeling the positive symptoms of schizophrenia in genetically modified mice: pharmacology and methodology aspects. *Schizophr Bull*, **36**, 246-270.

van Woerden, G.M., Hoebeek, F.E., Gao, Z., Nagaraja, R.Y., Hoogenraad, C.C., Kushner, S.A., Hansel, C., De Zeeuw, C.I. & Elgersma, Y. (2009) betaCaMKII controls the direction of plasticity at parallel fiber-Purkinje cell synapses. *Nat Neurosci*, **12**, 823-825.

Vander Haar, E., Lee, S.I., Bandhakavi, S., Griffin, T.J. & Kim, D.H. (2007) Insulin signalling to mTOR mediated by the Akt/PKB substrate PRAS40. *Nat Cell Biol*, **9**, 316-323.

Varoqueaux, F., Jamain, S. & Brose, N. (2004) Neuroligin 2 is exclusively localized to inhibitory synapses. *Eur J Cell Biol*, **83**, 449-456.

Vega-Rubin-de-Celis, S., Abdallah, Z., Kinch, L., Grishin, N.V., Brugarolas, J. & Zhang, X. (2010) Structural analysis and functional implications of the negative mTORC1 regulator REDD1. *Biochemistry*, **49**, 2491-2501.

Viltono, L., Patrizi, A., Fritschy, J.M. & Sassoe-Pognetto, M. (2008) Synaptogenesis in the cerebellar cortex: differential regulation of gephyrin and GABAA receptors at somatic and dendritic synapses of Purkinje cells. *J Comp Neurol*, **508**, 579-591.

Voogd, J. & Glickstein, M. (1998) The anatomy of the cerebellum. *Trends Neurosci*, **21**, 370-375.

Walker, F.O. (2007) Huntington's disease. *Lancet*, **369**, 218-228.

Walther, S. & Strik, W. (2012) Motor symptoms and schizophrenia. *Neuropsychobiology*, **66**, 77-92.

Wang, H., Bedford, F.K., Brandon, N.J., Moss, S.J. & Olsen, R.W. (1999) GABA(A)-receptor-associated protein links GABA(A) receptors and the cytoskeleton. *Nature*, **397**, 69-72.

Wang, Q., Liu, L., Pei, L., Ju, W., Ahmadian, G., Lu, J., Wang, Y., Liu, F. & Wang, Y.T. (2003) Control of synaptic strength, a novel function of Akt. *Neuron*, **38**, 915-928.

Wang, S.S., Denk, W. & Hausser, M. (2000) Coincidence detection in single dendritic spines mediated by calcium release. *Nat Neurosci*, **3**, 1266-1273.

Wang, S.S., Kloth, A.D. & Badura, A. (2014) The Cerebellum, Sensitive Periods, and Autism. *Neuron*, **83**, 518-532.

Wang, V.Y. & Zoghbi, H.Y. (2001) Genetic regulation of cerebellar development. *Nat Rev Neurosci*, **2**, 484-491.

Wang, X., Li, W., Williams, M., Terada, N., Alessi, D.R. & Proud, C.G. (2001) Regulation of elongation factor 2 kinase by p90(RSK1) and p70 S6 kinase. *Embo J*, **20**, 4370-4379.

Wang, Y.T. & Linden, D.J. (2000) Expression of cerebellar long-term depression requires postsynaptic clathrin-mediated endocytosis. *Neuron*, **25**, 635-647.

Wassef, M., Chedotal, A., Cholley, B., Thomasset, M., Heizmann, C.W. & Sotelo, C. (1992) Development of the olivocerebellar projection in the rat: I. Transient biochemical compartmentation of the inferior olive. *J Comp Neurol*, **323**, 519-536.

Webb, J.L., Ravikumar, B., Atkins, J., Skepper, J.N. & Rubinsztein, D.C. (2003) Alpha-Synuclein is degraded by both autophagy and the proteasome. *J Biol Chem*, **278**, 25009-25013.

Weber, A.M., Egelhoff, J.C., McKellop, J.M. & Franz, D.N. (2000) Autism and the cerebellum: evidence from tuberous sclerosis. *J Autism Dev Disord*, **30**, 511-517.

Weiler, I.J., Irwin, S.A., Klintsova, A.Y., Spencer, C.M., Brazelton, A.D., Miyashiro, K., Comery, T.A., Patel, B., Eberwine, J. & Greenough, W.T. (1997) Fragile X mental retardation protein is translated near synapses in response to neurotransmitter activation. *Proc Natl Acad Sci U S A*, **94**, 5395-5400.

Weinberger, D.R., Kleinman, J.E., Luchins, D.J., Bigelow, L.B. & Wyatt, R.J. (1980) Cerebellar pathology in schizophrenia: a controlled postmortem study. *Am J Psychiatry*, **137**, 359-361.

Welker, W.I. (1990) The significance of foliation and fissuration of cerebellar cortex. The cerebellar folium as a fundamental unit of sensorimotor integration. *Arch Ital Biol*, **128**, 87-109.

Welsh, J.P., Yamaguchi, H., Zeng, X.H., Kojo, M., Nakada, Y., Takagi, A., Sugimori, M. & Llinas, R.R. (2005) Normal motor learning during pharmacological prevention of Purkinje cell long-term depression. *Proc Natl Acad Sci U S A*, **102**, 17166-17171.

Weston, M.C., Chen, H. & Swann, J.W. (2014) Loss of mTOR repressors Tsc1 or Pten has divergent effects on excitatory and inhibitory synaptic transmission in single hippocampal neuron cultures. *Front Mol Neurosci*, **7**, 1.

White, J.J. & Sillitoe, R.V. (2013) Development of the cerebellum: from gene expression patterns to circuit maps. *Wiley Interdiscip Rev Dev Biol*, **2**, 149-164.

Whitney, E.R., Kemper, T.L., Bauman, M.L., Rosene, D.L. & Blatt, G.J. (2008) Cerebellar Purkinje cells are reduced in a subpopulation of autistic brains: a stereological experiment using calbindin-D28k. *Cerebellum*, **7**, 406-416.

Whitney, M.L., Jefferson, L.S. & Kimball, S.R. (2009) ATF4 is necessary and sufficient for ER stress-induced upregulation of REDD1 expression. *Biochem Biophys Res Commun*, **379**, 451-455.

Wingate, R.J. & Hatten, M.E. (1999) The role of the rhombic lip in avian cerebellum development. *Development*, **126**, 4395-4404.

Wirth, M., Joachim, J. & Tooze, S.A. (2013) Autophagosome formation--the role of ULK1 and Beclin1-PI3KC3 complexes in setting the stage. *Semin Cancer Biol*, **23**, 301-309.

Woodward, D.J., Hoffer, B.J., Siggins, G.R. & Bloom, F.E. (1971) The ontogenetic development of synaptic junctions, synaptic activation and responsiveness to neurotransmitter substances in rat cerebellar purkinje cells. *Brain Res*, **34**, 73-97.

Wu, T. & Hallett, M. (2013) The cerebellum in Parkinson's disease. *Brain*, **136**, 696-709.

Wuchter, J., Beuter, S., Treindl, F., Herrmann, T., Zeck, G., Templin, M.F. & Volkmer, H. (2012) A comprehensive small interfering RNA screen identifies signaling pathways required for gephyrin clustering. *J Neurosci*, **32**, 14821-14834.

Wullschleger, S., Loewith, R. & Hall, M.N. (2006) TOR signaling in growth and metabolism. *Cell*, **124**, 471-484.

Xia, J., Chung, H.J., Wihler, C., Huganir, R.L. & Linden, D.J. (2000) Cerebellar long-term depression requires PKC-regulated interactions between GluR2/3 and PDZ domain-containing proteins. *Neuron*, **28**, 499-510.

Xia, Z. & Storm, D.R. (2005) The role of calmodulin as a signal integrator for synaptic plasticity. *Nat Rev Neurosci*, **6**, 267-276.

Xie, J. & Proud, C.G. (2013) Crosstalk between mTOR complexes. *Nat Cell Biol*, **15**, 1263-1265.

Yang, S.N., Tang, Y.G. & Zucker, R.S. (1999) Selective induction of LTP and LTD by postsynaptic [Ca2+]i elevation. *J Neurophysiol*, **81**, 781-787.

Yang, Y., Coleman, M., Zhang, L., Zheng, X. & Yue, Z. (2013) Autophagy in axonal and dendritic degeneration. *Trends Neurosci*, **36**, 418-428.

Yecies, J.L., Zhang, H.H., Menon, S., Liu, S., Yecies, D., Lipovsky, A.I., Gorgun, C., Kwiatkowski, D.J., Hotamisligil, G.S., Lee, C.H. & Manning, B.D. (2011) Akt stimulates hepatic SREBP1c and lipogenesis through parallel mTORC1-dependent and independent pathways. *Cell Metab*, **14**, 21-32.

Yokogami, K., Wakisaka, S., Avruch, J. & Reeves, S.A. (2000) Serine phosphorylation and maximal activation of STAT3 during CNTF signaling is mediated by the rapamycin target mTOR. *Curr Biol*, **10**, 47-50.

Yoon, M.S., Sun, Y., Arauz, E., Jiang, Y. & Chen, J. (2011) Phosphatidic acid activates mammalian target of rapamycin complex 1 (mTORC1) kinase by displacing FK506 binding protein 38 (FKBP38) and exerting an allosteric effect. *J Biol Chem*, **286**, 29568-29574.

Young, D.M., Schenk, A.K., Yang, S.B., Jan, Y.N. & Jan, L.Y. (2010) Altered ultrasonic vocalizations in a tuberous sclerosis mouse model of autism. *Proc Natl Acad Sci U S A*, **107**, 11074-11079.

Yu, Y., Yoon, S.O., Poulogiannis, G., Yang, Q., Ma, X.M., Villen, J., Kubica, N., Hoffman, G.R., Cantley, L.C., Gygi, S.P. & Blenis, J. (2011) Phosphoproteomic analysis identifies Grb10 as an mTORC1 substrate that negatively regulates insulin signaling. *Science*, **332**, 1322-1326.

Yuan, H.X., Russell, R.C. & Guan, K.L. (2013) Regulation of PIK3C3/VPS34 complexes by MTOR in nutrient stress-induced autophagy. *Autophagy*, **9**, 1983-1995.

Zalfa, F., Giorgi, M., Primerano, B., Moro, A., Di Penta, A., Reis, S., Oostra, B. & Bagni, C. (2003) The fragile X syndrome protein FMRP associates with BC1 RNA and regulates the translation of specific mRNAs at synapses. *Cell*, **112**, 317-327.

Zarate, C.A., Jr., Singh, J.B., Carlson, P.J., Brutsche, N.E., Ameli, R., Luckenbaugh, D.A., Charney, D.S. & Manji, H.K. (2006) A randomized trial of an N-methyl-D-aspartate antagonist in treatment-resistant major depression. *Arch Gen Psychiatry*, **63**, 856-864.

Zhang, Y., Venkitaramani, D.V., Gladding, C.M., Kurup, P., Molnar, E., Collingridge, G.L. & Lombroso, P.J. (2008) The tyrosine phosphatase STEP mediates AMPA receptor endocytosis after metabotropic glutamate receptor stimulation. *J Neurosci*, **28**, 10561-10566.

Zhao, Z., Ksiezak-Reding, H., Riggio, S., Haroutunian, V. & Pasinetti, G.M. (2006) Insulin receptor deficits in schizophrenia and in cellular and animal models of insulin receptor dysfunction. *Schizophr Res*, **84**, 1-14.

Zinzalla, V., Stracka, D., Oppliger, W. & Hall, M.N. (2011) Activation of mTORC2 by association with the ribosome. *Cell*, **144**, 757-768.

Zoncu, R., Bar-Peled, L., Efeyan, A., Wang, S., Sancak, Y. & Sabatini, D.M. (2011) mTORC1 senses lysosomal amino acids through an inside-out mechanism that requires the vacuolar H(+)-ATPase. *Science*, **334**, 678-683.

8. Appendix

8.1. Publication 3: *In vivo evidence for mTORC2-mediated actin cytoskeleton rearrangement in neurons* Angliker, N. and Rüegg, M.A. (2013) Bioarchitecture, 3(4):113-8.

This publication is a commentary on publication 2 (see section 5) and further outlines how mTORC2 ablation in Purkinje cells may affect their morphology.

BioArchitecture 3:4, 113–118; July/August 2013; © 2013 Landes Bioscience

In vivo evidence for mTORC2-mediated actin cytoskeleton rearrangement in neurons

Nico Angliker and Markus A Rüegg*
Biozentrum; University of Basel; Basel, Switzerland

Keywords: rictor, PKC, GAP-43, MARCKS, Adducin, Tiam1, Rac1, Purkinje cell, synaptic plasticity, dendrite

Abbreviations: CA1, Cornu Ammonis area 1; CA3, Cornu Ammonis area 3; DEPTOR, DEP domain containing mTOR-interacting protein; FDA, Food and Drug Administration; GAP-43, growth-associated protein-43; Hts, Hu-li tai shao; LTP, long-term potentiation; LTD, long-term depression; E-LTP, early phase-LTP; L-LTP, late phase-LTP; mLST8, mammalian lethal with sec-13 protein 8; mSin1, stress-activated map kinase-interacting protein 1; mTOR, mammalian target of rapamycin; mTORC1, mTOR complex 1; mTORC2, mTOR complex 2; MARCKS, myristoylated, alanine-rich C kinase substrate; raptor, regulatory-associated protein of mammalian target of rapamycin; rictor, rapamycin-insensitive companion of mammalian target of rapamycin; S6K, S6 kinase; P, postnatal day; PI3K, phosphatidylinositide 3-kinase; PKC, protein kinase C; PI(4,5)P2, phosphatidylinositol-4,5-diphosphate; PRAS40, proline-rich Akt substrate 40 kDa; Protor1/2, protein observed with rictor 1 and 2; SCA14, spinocerebellar ataxia 14; SGK1, serum- and glucocorticoid-induced protein kinase 1; Tiam1, T-cell-lymphoma invasion and metastasis-1 protein; 4E-BP, eukaryotic translation initiation factor 4E (eIF4E)-binding protein

Submitted: 09/12/13

Accepted: 09/14/13

http://dx.doi.org/10.4161/bioa.26497

*Correspondence to: Markus A. Rüegg;
Email: markus-a.ruegg@unibas.ch

The mammalian target of rapamycin (mTOR) assembles into two distinct multi-protein complexes called mTORC1 and mTORC2. While mTORC1 controls the signaling pathways important for cell growth, the physiological function of mTORC2 is only partially known. Here we comment on recent work on gene-targeted mice lacking mTORC2 in the cerebellum or the hippocampus that provided strong evidence that mTORC2 plays an important role in neuron morphology and synapse function. We discuss that this phenotype might be based on the perturbed regulation of the actin cytoskeleton and the lack of activation of several PKC isoforms. The fact that PKC isoforms and their targets have been implicated in neurological disease including spinocerebellar ataxia and that they have been shown to affect learning and memory, suggests that aberration of mTORC2 signaling might be involved in diseases of the brain.

Introduction

mTOR is a serine/threonine kinase that functions within two distinct protein complexes that are referred to as mTOR complex 1 (mTORC1) and mTOR complex 2 (mTORC2). Differences in protein composition assign these two complexes specific functions. There are shared components, such as mTOR itself, mLST8, DEPTOR and the Tti1/Tel2 complex, but also some that are complex-specific. For mTORC1 this is raptor and PRAS40 and for mTORC2 rictor, mSin1 and Protor1/2.[1] The best described function of mTOR is its role in cell growth, metabolism and aging, functions that all can be inhibited by the name-giving drug rapamycin, a macrolide isolated from a soil sample of Easter Island. Rapamycin and its derivatives, called rapalogs, are FDA approved as immunosuppressants after allograft transplantation, as anti-restenosis drugs in stents and for the treatment of some cancers.[2] Current evidence suggests that the rapalogs act mainly via inhibiting mTORC1. In metazoans, mTORC1 is activated by growth factor signaling and, like in protozoans, by nutrients and the energy status of a cell. The main targets of mTORC1 are S6K and 4E-BP, which both control protein synthesis. Another important function of mTORC1 is the control of autophagy, a process that is essential to clean cells from unfolded proteins, non-functional organelles and to overcome the lack of nutrients during starvation.[3] In summary, mTORC1 appears to be the main hub that controls cell growth and metabolism, which also explains its involvement in cancer. Recent evidence suggests a role of mTORC1 in diseases of the central nervous system, such as Alzheimer disease, autism spectrum disorders or epilepsy.[4-7]

In contrast to mTORC1, the role of mTORC2 has been studied much less and thus its function is not well defined. Rapamycin does not inhibit mTORC2 acutely although long-term treatment affects mTORC2 function.[8] Activation of mTORC2 involves its PI3K-dependent association with ribosomes.[9] Compared with mTORC1, the number of downstream targets of mTORC2 is much lower but includes several members of the AGC

kinase family, among them Akt, PKC and SGK1. Some of these effectors, in particular Akt, are involved in the regulation of cell survival and apoptosis, suggesting that mTORC2 might also contribute to cancerogenesis.[10] Evidence obtained in yeast and in cultured mammalian cells in addition indicates a function of mTORC2 in the regulation of the actin cytoskeleton.[11-13] However, major changes in cell shape and the cytoskeleton were not observed in tissue-specific deletion of *rictor* in skeletal muscle, adipocytes, liver or kidney.[14-17] Only the recent deletion of *rictor* in the central nervous system revealed a role of mTORC2 for the shape of neurons[18] and for synaptic plasticity, an adaptive response of synapses to changes in activity.[19] Both of these functions involve the rearrangement of the actin cytoskeleton. In this commentary, we will briefly summarize those data and then discuss our view of how mTORC2 might regulate actin dynamics to shape neurons during development and of how this activity may contribute to synaptic plasticity in the adult.

mTORC2 Regulates Actin Cytoskeletal Rearrangements in Vivo

In recent work, we conditionally deleted *rictor* in the developing and the adult central nervous system by using mice that express Cre under the control of the *nestin* or the Purkinje cell-specific *L7/Pcp-2* promoter. The two major findings of this work were that the brain was smaller and that the morphology of neurons was strongly affected.[18] The microcephaly was a consequence of a reduction in neuron size but not number, which in turn resulted in an increased cell density. Interestingly, despite lower levels of phosphorylation of the mTORC2 target Akt, the microcephaly was not accompanied by alterations in any of the downstream targets of Akt; in particular, no changes in the mTORC1 targets S6K and 4E-BP were seen. Thus, mTORC2 appears to affect neuron size independently of mTORC1.

Changes in neuronal morphology encompassed the number, the length and the thickness of the neurites. Most notably, Purkinje cells of the cerebellum, which are characterized by expressing only one primary dendrite, contained up to six such primary dendrites. The changes in dendrite number were a cell-autonomous effect of rictor depletion as multiple primary dendrites were also observed when rictor was depleted selectively in Purkinje cells. The particularly strong changes in the morphology of the Purkinje cells were accompanied by an ataxia-like motor phenotype, consistent with the view that Purkinje cells, which provide the sole output of the cerebellum, are important for motor coordination.[20]

The molecular mechanisms involved in the neuronal phenotype observed in the rictor depleted brain were analyzed biochemically. Of all the bona fide targets of mTORC2, the most pronounced changes were observed in the PKC family of proteins. In rictor-deficient brain lysates, the phosphorylation and protein level of all classical PKCs (i.e., PKCα, -β and -γ) and the novel PKC isozyme, PKCε, were strongly reduced. In addition, phosphorylation of the PKC substrates GAP-43 and MARCKS, which are known to be important for the regulation of the actin cytoskeleton was diminished. Such a pronounced effect of mTORC2 ablation on the PKC pathway has so far not been reported in any other tissue. Interestingly, another group also reported on changes in the actin cytoskeleton of neurons in mice where rictor was conditionally deleted in the hippocampus.[19] Those authors did not investigate PKC signaling but provided evidence that rictor depletion affected the Tiam1-Rac1-PAK-cofilin pathway. In summary, both studies provided first in vivo evidence that depletion of rictor specifically affects the actin cytoskeleton in neurons. This is in stark contrast to studies in other organs where little or no cytoskeletal disturbances have been described.

PKC Signaling and Its Downstream Substrates

Among the best-studied PKC substrates in the brain are GAP-43, MARCKS, fascin and adducins.[21] GAP-43 and MARCKS have been proposed to share some function because both are highly hydrophilic and associate with plasma membranes via palmityolation and myristoylation, respectively, and are therefore frequently summed up as GAP-43-like proteins. In their dephosphorylated form, GAP-43 and MARCKS bind to PI(4,5)P2 and are associated with lipid raft-like structures of the plasma membrane.[22] Phosphorylation of GAP-43 or MARCKS by classical or novel PKC isoforms results in their detachment from the plasma membrane. As a consequence, the levels of PI(4,5)P2 are decreased.[22,23] Thus, the phosphorylation state of GAP-43 and MARCKS may directly affect the levels of PI(4,5)P2 in neurons and changes in PI(4,5)P2 have been implicated in the regulation of the actin cytoskeleton.[24] Adducins are a family of three related genes, which encode for either α-, β- or γ-adducin. All of them possess an N-terminal head domain, a neck domain, and a C-terminal tail domain that includes a conserved 22 amino acid MARCKS-related domain, which is necessary for actin binding. Adducins form tetramers composed of either α/β- or α/β-heterodimers and cap the fast growing end of the actin filaments (F-actin) to recruit spectrin to those actin filaments. Phosphorylation of adducin by PKC within the C-terminal MARCKS-related domain reduces F-actin-capping and thereby promotes free-barbed ends that are prone to polymerization/depolymerization.[25] Thus, adducins affect actin cytoskeleton dynamics and this activity is regulated by PKC.

Purkinje Cell Development and the Role of PKC Signaling

Purkinje cell development in rodents largely occurs between P0 and P21 and can roughly be split into three phases.[26] At P0, Purkinje cells have small somata with multiple dendrites that are organized in a multipolar manner. In a first growth phase (P0 to ~P9), the somata of the Purkinje cells are enlarged and all but one primary dendrite are eliminated. This first phase is followed by the stage of rapid growth of the dendritic tree and a third phase of rather slow dendritic growth. Excessive neurite outgrowth

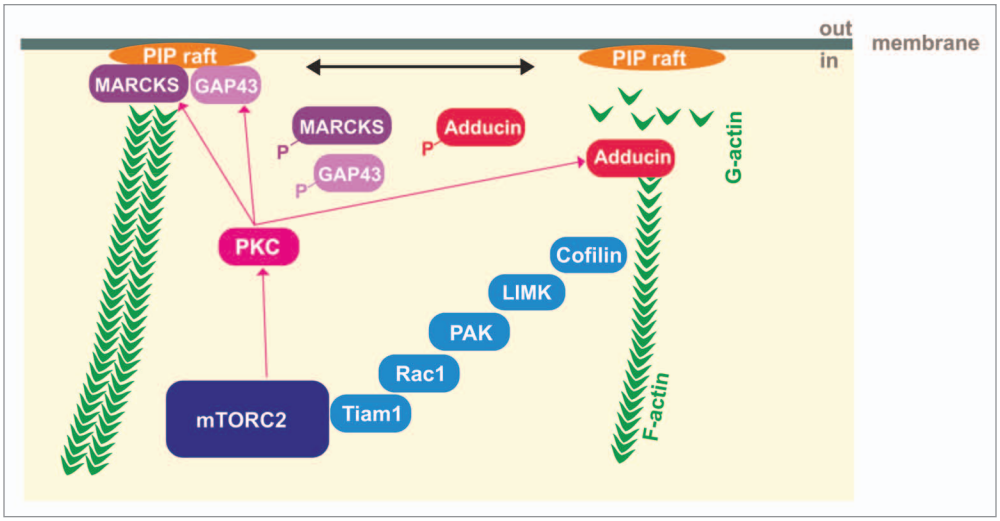

Figure 1. Model for the regulation of actin cytoskeletal dynamics by mTORC2. Activation of PKC by mTORC2 results in a phosphorylation of GAP-43-like proteins, MARCKS and GAP-43, which dissociate from PI(4,5)P2 rafts and make PI(4,5)P2 accessible for other actin cytoskeletal regulating proteins or hydrolysis. In parallel, PKC causes free-barbed actin filament ends by phosphorylating adducin which promotes actin dynamics. Association of mTORC2 with Tiam1 and the regulation of its downstream targets may also contribute to actin filament stabilization. In this model, mTORC2 affects depolymerization and polymerization of actin at different sites by controlling PKC- and Tiam1-signaling.

or improper dendrite retraction during the first developmental stage may result in Purkinje cells with multiple primary dendrites.

As mentioned above, rictor-deficient Purkinje cells have too many primary dendrites. As PKC isoforms are strongly de-regulated in rictor knockout brains, the question arises whether these morphological changes might be based on alterations in PKC signaling. Indeed, there is evidence that PKC activity affects Purkinje cell development and function. For example, mutations in the gene coding for PKCγ, whose expression is strongly reduced in rictor-deficient brain, cause spinocerebellar ataxia 14 (SCA14).[27] Although the exact molecular mechanisms involved in the ontogeny of SCA14 are not well understood, experiments in organotypic slice cultures of the cerebellum indicate that PKC is important for dendrite morphology of Purkinje cells.[28-30] Purkinje cells also express high levels of mRNA encoding the PKC substrate MARCKS both during development and in the adult. In contrast, transcripts for GAP-43 are low in Purkinje cells at both stages,[31] suggesting that GAP-43 is unlikely to be the main effector responsible for the changes observed in the cerebellum of the rictor-deficient brains. The PKC substrate fascin is highly expressed in the developing brain but cannot be detected anymore in adult Purkinje cells.[32,33] In the adult brain, fascin seems rather to be expressed in non-neuronal cells and there is evidence that its expression correlates with morphology, invasiveness and motility of glioma cells.[34] Finally, expression of α- and β-adducin is widespread in the brain while expression of γ-adducin is highest in the hippocampus and in Purkinje cells of the cerebellum.[35,36] Interestingly, phosphorylation of adducin is also significantly diminished in the brain of rictor-deficient mice (Angliker and Rüegg, unpublished observation). Thus, the expression pattern of the PKC substrates in the cerebellum suggests that rictor, by controlling PKC phosphorylation and protein levels, may act in Purkinje cells through MARCKS and adducins but not via GAP-43 or fascin.

The change in the phosphorylation state of MARCKS and adducin in rictor knockout mice will shift the equilibrium between membrane/actin-bound and the cytosolic form of MARCKS and adducin toward membrane and the actin-bound form, respectively (**Fig. 1**). A shift in the relative amount of phosphorylated MARCKS has been implicated in dendrite morphology. For example, hyperactivity of PKC and thus hyperphosphorylation of MARCKS has been shown to contribute to the strongly reduced dendritic arborization observed upon forebrain-specific deletion of the gene cluster encoding the γ-protocadherins.[37] Reduction of dendritic arborization by knockdown of MARCKS or overexpression of a "dominant-negative" (e.g., phosphomimetic) form of MARCKS was also reported in cultured hippocampal neurons.[38] These results argue that the loss of phosphorylation of MARCKS in rictor-depleted neurons would result in exuberant dendritic branching. Indeed, rictor-knockout Purkinje cells show an increased number of primary dendrites.[18]

The Role of PKC and Its Downstream Substrates in Synaptic Plasticity

Changes in neuronal activity are known to affect neural circuits and current evidence suggests that such changes are the basis of learning and memory. On the cellular level, it is well established that neuronal activity can cause the weakening or strengthening of existing synapses and trigger the formation or elimination of synapses. Depending on the frequency of presynaptic neuronal activity (i.e., release of neurotransmitter)

and the synchrony with the postsynaptic elements, synapses are strengthened (long-term potentiation; LTP) or weakened (long-term depression; LTD).

For example, the parallel fiber synapses of a Purkinje cell become depressed when stimulated in conjunction with a postsynaptic depolarization of the Purkinje cell via the innervating climbing fiber. PKC isoforms have been shown to be essential for this form of cerebellar LTD. This has been demonstrated using pharmacological inhibitors or activators of PKC and also by Purkinje cell-specific expression of a peptidic PKC inhibitor.[39,40] Surprisingly, a knockout of PKCγ, the major PKC isoform in Purkinje cells, does not affect cerebellar LTD[41] but more recent evidence indicates that PKCα is the essential isoform for this kind of synaptic plasticity.[42] Although Purkinje cells of PKCγ knockout mice reveal normal cerebellar LTD, they fail to reduce the number of climbing fibers to a single one during their development, which results in adult Purkinje cells innervated by multiple climbing fibers.[43] Interestingly, climbing fiber synapse elimination is also compromised in mice in which rictor is specifically depleted in Purkinje cells (Angliker and Rüegg, unpublished observation). Thus, this provides additional evidence that the neuronal phenotype observed in rictor-deficient neurons might be based on changes in PKC signaling.

Probably the best characterized form of LTP is generated between neurons of CA3 and CA1 region of the hippocampus upon high frequency stimulation of the Schaffer collaterals. The use of PKC inhibitors and activators has provided solid evidence for the notion that PKC isoforms also contribute to synaptic plasticity in the hippocampus.[44] Furthermore, there is evidence that PKC activation and expression is lost in transgenic mouse models that reiterate the memory loss observed in Alzheimer disease. Importantly, treatment of those mice with the PKC activator bryostatin-1 or DCP-LA prevents the loss of memory.[45] In line with this finding, the same activators have been reported to promote LTP in hippocampal slices.[46]

In the hippocampus, one can distinguish an early phase-LTP (E-LTP), which is based on changing the conductance or number of ion channels in the postsynaptic membrane and a late form, called L-LTP, which requires new protein synthesis and involves structural changes of the synapses. Recent work by Huang and colleagues (2013) provided strong evidence that rictor is required for L-LTP. The paper very nicely shows that rictor regulates actin polymerization, which is well known to affect synaptic plasticity, and that the defect in L-LTP results in a learning deficit in the mutant mice. Importantly, both the deficit in L-LTP and the impairment in learning are rescued by the application of jasplakinolide, which directly promotes actin polymerization.[19] While Huang and colleagues provide evidence that the phenotype might be based on the rictor function to affect phosphorylation of Akt and on its regulatory function on the Tiam1-Rac1 pathway, changes in PKC signaling might also contribute to the phenotype as outlined below.

In particular, the PKC downstream target β-adducin has been implicated in synaptic plasticity in the hippocampus as mice deficient for β-adducin show an impairment in CA3-CA1 LTP and LTD and deficits in spatial learning.[47,48] Noteworthy, these knockout mice also show motor coordination deficits, which manifest in a decreased latency to fall off a rotating rod. When β-adducin knockout mice are exposed to an enriched environment, a stimulus that increases synapse formation and turnover, synapses still disassemble but fail to be reformed, which is paralleled by deficits in augmented hippocampus-dependent learning. Enhanced enrichment upregulates phosphorylation of β-adducin in a PKC-sensitive manner and PKC activity was found to be crucial for the disassembly of synapses upon enrichement, a process that is essential for augmented learning as well. Altogether, these findings demonstrate the importance of β-adducin and its PKC-mediated phosphorylation for hippocampal synaptic plasticity that underlies augmented learning.[49] It should be noted that adducins are expressed both pre- and postsynaptically suggesting that perturbation of their function may affect both parts of the synapse. A presynaptic effect seems indeed to dominate over the postsynaptic effect in Drosophila, where it has been shown that the presynaptic expression of adducin (also called Hts) is sufficient to rescue the morphological changes at the neuromuscular junction of adducin-deficient flies.[50] These studies are very strong evidence that adducins can affect actin dynamics and thereby influence synaptic plasticity. Thus, many of the phenotypes observed in mice that are deficient for rictor in neurons might be based on the changes in PKC signaling.

Conclusion

We propose that actin cytoskeleton regulation by mTORC2 occurs in a canonical manner, for example via PKC activation and their downstream targets like GAP-43, MARCKS or adducin. To satisfy the demands of the brain for functional and anatomical plasticity, it might express not only a subset of mTORC2 downstream targets that regulate actin dynamics but a rather large panel of them, thereby possibly generating some redundancy, which in turn also might guarantee stability. The last notion is also reflected in the suggestion that GAP-43-like proteins possibly compensate the knockout of each other. However, usage of different mTORC2 downstream targets likely also varies among different brain regions and during brain development, dependent on their temporal and spatial expression profiles. In general, ablation of rictor in the brain seems to cause dysregulation of several proteins involved in actin cytoskeleton rearrangement and hence result in strong morphological changes. Additionally, the brain is an optimal organ to detect morphological alterations on the cellular level since neurons show elaborate growth and branching of neurites.

Disclosure of Potential Conflicts of Interest

No potential conflict of interest was disclosed.

Acknowledgments

We thank Dr Judith Reinhard for valuable input and careful reading of the

manuscript. This work was supported by a Sinergia grant from the Swiss National Science Foundation and by funds from the Cantons of Basel-Stadt and Basel-Landschaft.

References

1. Laplante M, Sabatini DM. mTOR Signaling. Cold Spring Harb Perspect Biol 2012; 4:4; PMID:22129599; http://dx.doi.org/10.1101/cshperspect.a011593
2. Benjamin D, Colombi M, Moroni C, Hall MN. Rapamycin passes the torch: a new generation of mTOR inhibitors. Nat Rev Drug Discov 2011; 10:868-80; PMID:22037041; http://dx.doi.org/10.1038/nrd3531
3. Choi AM, Ryter SW, Levine B. Autophagy in human health and disease. N Engl J Med 2013; 368:1845-6; PMID:23656658; http://dx.doi.org/10.1056/NEJMra1205406
4. Ehninger D, Silva AJ. Rapamycin for treating Tuberous sclerosis and Autism spectrum disorders. Trends Mol Med 2011; 17:78-87; PMID:21115397; http://dx.doi.org/10.1016/j.molmed.2010.10.002
5. Santini E, Klann E. Dysregulated mTORC1-Dependent Translational Control: From Brain Disorders to Psychoactive Drugs. Front Behav Neurosci 2011; 5:76; PMID:22073033; http://dx.doi.org/10.3389/fnbeh.2011.00076
6. Tsai PT, Hull C, Chu Y, Greene-Colozzi E, Sadowski AR, Leech JM, Steinberg J, Crawley JN, Regehr WG, Sahin M. Autistic-like behaviour and cerebellar dysfunction in Purkinje cell Tsc1 mutant mice. Nature 2012; 488:647-51; PMID:22763451; http://dx.doi.org/10.1038/nature11310
7. Bateup HS, Johnson CA, Denefrio CL, Saulnier JL, Kornacker K, Sabatini BL. Excitatory/inhibitory synaptic imbalance leads to hippocampal hyperexcitability in mouse models of tuberous sclerosis. Neuron 2013; 78:510-22; PMID:23664616; http://dx.doi.org/10.1016/j.neuron.2013.03.017
8. Sarbassov DD, Ali SM, Sengupta S, Sheen JH, Hsu PP, Bagley AF, Markhard AL, Sabatini DM. Prolonged rapamycin treatment inhibits mTORC2 assembly and Akt/PKB. Mol Cell 2006; 22:159-68; PMID:16603397; http://dx.doi.org/10.1016/j.molcel.2006.03.029
9. Zinzalla V, Stracka D, Oppliger W, Hall MN. Activation of mTORC2 by association with the ribosome. Cell 2011; 144:757-68; PMID:21376236; http://dx.doi.org/10.1016/j.cell.2011.02.014
10. Guertin DA, Stevens DM, Saitoh M, Kinkel S, Crosby K, Sheen JH, Mullholland DJ, Magnuson MA, Wu H, Sabatini DM. mTOR complex 2 is required for the development of prostate cancer induced by Pten loss in mice. Cancer Cell 2009; 15:148-59; PMID:19185849; http://dx.doi.org/10.1016/j.ccr.2008.12.017
11. Jacinto E, Loewith R, Schmidt A, Lin S, Rüegg MA, Hall A, Hall MN. Mammalian TOR complex 2 controls the actin cytoskeleton and is rapamycin insensitive. Nat Cell Biol 2004; 6:1122-8; PMID:15467718; http://dx.doi.org/10.1038/ncb1183
12. Loewith R, Jacinto E, Wullschleger S, Lorberg A, Crespo JL, Bonenfant D, Oppliger W, Jenoe P, Hall MN. Two TOR complexes, only one of which is rapamycin sensitive, have distinct roles in cell growth control. Mol Cell 2002; 10:457-68; PMID:12408816; http://dx.doi.org/10.1016/S1097-2765(02)00636-6
13. Sarbassov DD, Ali SM, Kim DH, Guertin DA, Latek RR, Erdjument-Bromage H, Tempst P, Sabatini DM. Rictor, a novel binding partner of mTOR, defines a rapamycin-insensitive and raptor-independent pathway that regulates the cytoskeleton. Curr Biol 2004; 14:1296-302; PMID:15268862; http://dx.doi.org/10.1016/j.cub.2004.06.054
14. Bentzinger CF, Romanino K, Cloëtta D, Lin S, Mascarenhas JB, Oliveri F, Xia J, Casanova E, Costa CF, Brink M, et al. Skeletal muscle-specific ablation of raptor, but not of rictor, causes metabolic changes and results in muscle dystrophy. Cell Metab 2008; 8:411-24; PMID:19046572; http://dx.doi.org/10.1016/j.cmet.2008.10.002
15. Cybulski N, Polak P, Auwerx J, Rüegg MA, Hall MN. mTOR complex 2 in adipose tissue negatively controls whole-body growth. Proc Natl Acad Sci U S A 2009; 106:9902-7; PMID:19497867; http://dx.doi.org/10.1073/pnas.0811321106
16. Gödel M, Hartleben B, Herbach N, Liu S, Zschiedrich S, Lu S, Debreczeni-Mór A, Lindenmeyer MT, Rastaldi MP, Hartleben G, et al. Role of mTOR in podocyte function and diabetic nephropathy in humans and mice. J Clin Invest 2011; 121:2197-209; PMID:21606591; http://dx.doi.org/10.1172/JCI44774
17. Hagiwara A, Cornu M, Cybulski N, Polak P, Betz C, Trapani F, Terracciano L, Heim MH, Rüegg MA, Hall MN. Hepatic mTORC2 activates glycolysis and lipogenesis through Akt, glucokinase, and SREBP1c. Cell Metab 2012; 15:725-38; PMID:22521878; http://dx.doi.org/10.1016/j.cmet.2012.03.015
18. Thomanetz V, Angliker N, Cloëtta D, Lustenberger RM, Schweighauser M, Oliveri F, Suzuki N, Rüegg MA. Ablation of the mTORC2 component rictor in brain or Purkinje cells affects size and neuron morphology. J Cell Biol 2013; 201:293-308; PMID:23569215; http://dx.doi.org/10.1083/jcb.201205030
19. Huang W, Zhu PJ, Zhang S, Zhou H, Stoica L, Galiano M, Krnjević K, Roman G, Costa-Mattioli M. mTORC2 controls actin polymerization required for consolidation of long-term memory. Nat Neurosci 2013; 16:441-8; PMID:23455608; http://dx.doi.org/10.1038/nn.3351
20. Seidel K, Siswanto S, Brunt ER, den Dunnen W, Korf HW, Rüb U. Brain pathology of spinocerebellar ataxias. Acta Neuropathol 2012; 124:1-21; PMID:22684686; http://dx.doi.org/10.1007/s00401-012-1000-x
21. Larsson C. Protein kinase C and the regulation of the actin cytoskeleton. Cell Signal 2006; 18:276-84; PMID:16109477; http://dx.doi.org/10.1016/j.cellsig.2005.07.010
22. Laux T, Fukami K, Thelen M, Golub T, Frey D, Caroni P. GAP43, MARCKS, and CAP23 modulate PI(4,5)P(2) at plasmalemmal rafts, and regulate cell cortex actin dynamics through a common mechanism. J Cell Biol 2000; 149:1455-72; PMID:10871285; http://dx.doi.org/10.1083/jcb.149.7.1455
23. Caroni P. New EMBO members' review: actin cytoskeleton regulation through modulation of PI(4,5)P(2) rafts. EMBO J 2001; 20:4332-6; PMID:11500359; http://dx.doi.org/10.1093/emboj/20.16.4332
24. Janmey PA, Lindberg U. Cytoskeletal regulation: rich in lipids. Nat Rev Mol Cell Biol 2004; 5:658-66; PMID:15366709; http://dx.doi.org/10.1038/nrm1434
25. Matsuoka Y, Li X, Bennett V. Adducin: structure, function and regulation. Cell Mol Life Sci 2000; 57:884-95; PMID:10950304; http://dx.doi.org/10.1007/PL00000731
26. McKay BE, Turner RW. Physiological and morphological development of the rat cerebellar Purkinje cell. J Physiol 2005; 567:829-50; PMID:16002452; http://dx.doi.org/10.1113/jphysiol.2005.089383
27. Chen DH, Brkanac Z, Verlinde CL, Tan XJ, Bylenok L, Nochlin D, Matsushita M, Lipe H, Wolff J, Fernandez M, et al. Missense mutations in the regulatory domain of PKC gamma: a new mechanism for dominant nonepisodic cerebellar ataxia. Am J Hum Genet 2003; 72:839-49; PMID:12644968; http://dx.doi.org/10.1086/373883
28. Metzger F. Molecular and cellular control of dendrite maturation during brain development. Curr Mol Pharmacol 2010; 3:1-11; PMID:20030626
29. Gundlfinger A, Kapfhammer JP, Kruse F, Leitges M, Metzger F. Different regulation of Purkinje cell dendritic development in cerebellar slice cultures by protein kinase Calpha and -beta. J Neurobiol 2003; 57:95-109; PMID:12973831; http://dx.doi.org/10.1002/neu.10259
30. Schrenk K, Kapfhammer JP, Metzger F. Altered dendritic development of cerebellar Purkinje cells in slice cultures from protein kinase Cgamma-deficient mice. Neuroscience 2002; 110:675-89; PMID:11934475; http://dx.doi.org/10.1016/S0306-4522(01)00559-0
31. Higo N, Oishi T, Yamashita A, Matsuda K, Hayashi M. Cell type- and region-specific expression of protein kinase C-substrate mRNAs in the cerebellum of the macaque monkey. J Comp Neurol 2003; 467:135-49; PMID:14595765; http://dx.doi.org/10.1002/cne.10850
32. De Arcangelis A, Georges-Labouesse E, Adams JC. Expression of fascin-1, the gene encoding the actin-bundling protein fascin-1, during mouse embryogenesis. Gene Expr Patterns 2004; 4:637-43; PMID:15465486; http://dx.doi.org/10.1016/j.modgep.2004.04.012
33. Zhang FR, Tao LH, Shen ZY, Lv Z, Xu LY, Li EM. Fascin expression in human embryonic, fetal, and normal adult tissue. J Histochem Cytochem 2008; 56:193-9; PMID:17998567; http://dx.doi.org/10.1369/jhc.7A7353.2007
34. Hwang JH, Smith CA, Salhia B, Rutka JT. The role of fascin in the migration and invasiveness of malignant glioma cells. Neoplasia 2008; 10:149-59; PMID:18283337; http://dx.doi.org/10.1593/neo.07909
35. Seidel B, Zuschratter W, Wex H, Garner CC, Gundelfinger ED. Spatial and sub-cellular localization of the membrane cytoskeleton-associated protein alpha-adducin in the rat brain. Brain Res 1995; 700:13-24; PMID:8624703; http://dx.doi.org/10.1016/0006-8993(95)00962-P
36. Lein ES, Hawrylycz MJ, Ao N, Ayres M, Bensinger A, Bernard A, Boe AF, Boguski MS, Brockway KS, Byrnes EJ, et al. Genome-wide atlas of gene expression in the adult mouse brain. Nature 2007; 445:168-76; PMID:17151600; http://dx.doi.org/10.1038/nature05453
37. Garrett AM, Schreiner D, Lobas MA, Weiner JA. γ-protocadherins control cortical dendrite arborization by regulating the activity of a FAK/PKC/MARCKS signaling pathway. Neuron 2012; 74:269-76; PMID:22542181; http://dx.doi.org/10.1016/j.neuron.2012.01.028
38. Li H, Chen G, Zhou B, Duan S. Actin filament assembly by myristoylated alanine-rich C kinase substrate-phosphatidylinositol-4,5-diphosphate signaling is critical for dendrite branching. Mol Biol Cell 2008; 19:4804-13; PMID:18799624; http://dx.doi.org/10.1091/mbc.E08-03-0294
39. De Zeeuw CI, Hansel C, Bian F, Koekkoek SK, van Alphen AM, Linden DJ, Oberdick J. Expression of a protein kinase C inhibitor in Purkinje cells blocks cerebellar LTD and adaptation of the vestibulo-ocular reflex. Neuron 1998; 20:495-508; PMID:9539124; http://dx.doi.org/10.1016/S0896-6273(00)80990-3
40. Saito N, Shirai Y. Protein kinase C gamma (PKC gamma): function of neuron specific isotype. J Biochem 2002; 132:683-7; PMID:12417016; http://dx.doi.org/10.1093/oxfordjournals.jbchem.a003274

41. Chen C, Kano M, Abeliovich A, Chen L, Bao S, Kim JJ, Hashimoto K, Thompson RF, Tonegawa S. Impaired motor coordination correlates with persistent multiple climbing fiber innervation in PKC gamma mutant mice. Cell 1995; 83:1233-42; PMID:8548809; http://dx.doi.org/10.1016/0092-8674(95)90148-5
42. Leitges M, Kovac J, Plomann M, Linden DJ. A unique PDZ ligand in PKCalpha confers induction of cerebellar long-term synaptic depression. Neuron 2004; 44:585-94; PMID:15541307; http://dx.doi.org/10.1016/j.neuron.2004.10.024
43. Kano M, Hashimoto K, Chen C, Abeliovich A, Aiba A, Kurihara H, Watanabe M, Inoue Y, Tonegawa S. Impaired synapse elimination during cerebellar development in PKC gamma mutant mice. Cell 1995; 83:1223-31; PMID:8548808; http://dx.doi.org/10.1016/0092-8674(95)90147-7
44. Sossin WS. Isoform specificity of protein kinase Cs in synaptic plasticity. Learn Mem 2007; 14:236-46; PMID:17404386; http://dx.doi.org/10.1101/lm.469707
45. Hongpaisan J, Sun MK, Alkon DL. PKC ε activation prevents synaptic loss, Aβ elevation, and cognitive deficits in Alzheimer's disease transgenic mice. J Neurosci 2011; 31:630-43; PMID:21228172; http://dx.doi.org/10.1523/JNEUROSCI.5209-10.2011
46. Kim H, Han SH, Quan HY, Jung YJ, An J, Kang P, Park JB, Yoon BJ, Seol GH, Min SS. Bryostatin-1 promotes long-term potentiation via activation of PKCα and PKCε in the hippocampus. Neuroscience 2012; 226:348-55; PMID:22986161; http://dx.doi.org/10.1016/j.neuroscience.2012.08.055
47. Porro F, Rosato-Siri M, Leone E, Costessi L, Iaconcig A, Tongiorgi E, Muro AF. beta-adducin (Add2) KO mice show synaptic plasticity, motor coordination and behavioral deficits accompanied by changes in the expression and phosphorylation levels of the alpha- and gamma-adducin subunits. Genes Brain Behav 2010; 9:84-96; PMID:19900187; http://dx.doi.org/10.1111/j.1601-183X.2009.00537.x
48. Rabenstein RL, Addy NA, Caldarone BJ, Asaka Y, Gruenbaum LM, Peters LL, Gilligan DM, Fitzsimonds RM, Picciotto MR. Impaired synaptic plasticity and learning in mice lacking beta-adducin, an actin-regulating protein. J Neurosci 2005; 25:2138-45; PMID:15728854; http://dx.doi.org/10.1523/JNEUROSCI.3530-04.2005
49. Bednarek E, Caroni P. β-Adducin is required for stable assembly of new synapses and improved memory upon environmental enrichment. Neuron 2011; 69:1132-46; PMID:21435558; http://dx.doi.org/10.1016/j.neuron.2011.02.034
50. Pielage J, Bulat V, Zuchero JB, Fetter RD, Davis GW. Hts/Adducin controls synaptic elaboration and elimination. Neuron 2011; 69:1114-31; PMID:21435557; http://dx.doi.org/10.1016/j.neuron.2011.02.007

9. Acknowledgements

I would like to thank Markus Rüegg for giving me the opportunity to do my PhD in his laboratory. I always appreciated his honesty and sharp way of thinking, which helped me a lot in my scientific and personal development. Moreover, I enjoyed the freedom he conferred in exploring my ideas.

The project I was working on was financially supported by a Sinergia grant of the Swiss National Science Foundation to Jean-Marc Fritschy and Markus Rüegg. I would to thank Jean-Marc Fritschy and his group, in particular Mariana Zaichuk, for the fruitful and nice collaboration.

I am very happy to have spent four very pleasant years in the Rüegg lab where I made acquaintance with various people who I appreciated very much. Therefore, I would like to thank all the former and current members of this lab including: Shuo Lin, Dimitri Cloetta, Klaas Romanino, Alexander Kriz, Venus Thomanetz, Regula Lustenberger, Manuel Schweighauser, Anny Schäfer, Barbara Kupr, Nathalie Rion, David Hollinger, Lionel Tintignac, Maitea Guridi Ormazabal, Perrine Castets, Pankaj Sharad Shende, Marco Kaiser, Mathieu Rajalu, Geraldine Maier, Gian Moor, Filippo Oliveri, Sarina Meinen, Diana Flores Dominguez, Kathrin Chojnowska, Manuela Von Arx and Jny Wittker.

Most of all, I enjoyed the time sitting and working next to Judith Reinhard to whom I am very grateful for her mental and intellectual support and the pleasant lunch breaks, 3 o'clock coffees and 6 o'clock darvidas!

Many thanks also go to Michael Burri who was master student in our laboratory and made very valuable contributions to the story presented in this thesis.

During my PhD I could count on electrophysiological support from the laboratories of Bernhard Bettler and Kaspar E. Vogt. I would like to thank them and the following members of theirs labs including Riad Seddik, Audrée Pinard, Enrique Pérez-Garci, Julien Gaudias and Sylvia Willadt.

Regarding behavioural experiments I would like to thank Stéphane Baudouin and Harald Witte for their help.

Moreover, I thank all the people working in the animal facility for taking care of the mice needed for this project.

I would like to thank Bernhard Bettler for accepting to be co-referee of this thesis and Martin Spiess for chairing the exam.

Finally, I would like to thank my parents and my two brothers for their unconditional love and support. The nice walks and hikes, including discussions, on weekends were always a perfect source of recreation to me.

Last but not least I am grateful to my band members, Sean Frank Claassen, Nicolas Brügger, Thomas Firmin, Samuel Moser and Fabian von Allmen for the good time and for their tolerance when I neglected the musical part of my life at the expense of my lab life.